The Aryl Hydrocarbon Receptor Plays a Key Role in the Transcriptional Programme of Regulatory B cells

by Christopher James Michael Piper

Supervisors

Prof. Claudia Mauri

Prof. David Isenberg

Dr. Paul Blair

UCL Centre for Rheumatology

The Rayne Institute

5 University Street

London, WC1E 6JF

UCL

Immunology

Submitted for the degree of Doctor of Philosophy

May 2020

Declaration

I, Christopher Piper, confirm that the work presented in this thesis is my own. Where information has been derived from other sources, I confirm that this has been indicated in the thesis.

Christopher Piper
May 2020

Acknowledgements

I would like to express my sincere gratitude to my supervisor Professor Claudia Mauri for all her support, encouragement and mentoring over the years. I feel exceedingly fortunate to have worked in your lab and I have learned so much over the years through your guidance. I would like to thank the Rosetrees Trust for funding my PhD and, in tandem with the Wellcome Trust for making this research possible.

I would like to thank members of the Mauri Lab, both past and present, for their support, advice and friendship and for our philosophical late night chats about science, politics and just general life. To Lizzy - for all your support, career advice and for listening to me moan about RNA-seq and ATAC-seq. It's been a rollercoaster 1.5 years, but we made it! To Merry, with whom I worked closely during the 'JDM years,' I thank you for your all your support and for your positivity. It was a pleasure working with you during this time. To Kiran - for all that you have taught me in the lab and for giving me the necessary tools to succeed in science. In particular, I would like to thank Kristine for all the wonderful memories and friendship over the years, particularly our time 'skiing', and also our time in Davos and Japan. I couldn't have done it without you. Also for giving me the nicknames, ChrisP, PerCP and Crispr; thankfully the latter two haven't caught on! To all my colleagues - Kristine, Amanda, Lizzy, Paul, Diego, Diana and Hannah; you are all amazingly talented individuals and I feel extremely fortunate to have worked with you throughout my time here.

I would also like to thank all of my friends, especially my TA friends Mathu and Harry (London), Roland (Switzerland), Johan (Denmark) and Imtiyaaz (South Africa) for all the good times, general chats and for the daily laughs. It was good to chat to you after many a late night in the lab.

To my family - Mum and Dad and my two sisters Caroline and Victoria. I feel extremely blessed to have you as my family and this journey would not have been possible, if not for your unending love and support over the years. Thanks for all your encouragement and for helping me to realise my potential. I love you all more than you know. This thesis is dedicated to you all.

Abstract

Regulatory B cells (Bregs) play a critical role in the control of autoimmunity and inflammation. IL-10 production is the hallmark for the identification of Bregs. However, the molecular determinants that regulate the transcription of IL-10 and control the Breg developmental program remain unknown. The aryl hydrocarbon receptor (AHR) is an environmental sensor that binds to a variety of ligands, including physiological compounds derived from the digestion of dietary components by commensal microbiota. Here, we demonstrate that AHR regulates the differentiation and function of IL-10-producing $CD19^{+}CD21^{hi}CD24^{hi}$ Bregs and limits their differentiation into B cells that contribute to inflammation. Chromatin profiling and transcriptome analyses show that loss of AHR in B cells reduces expression of IL-10 by skewing the differentiation of $CD19^{+}CD21^{hi}CD24^{hi}$ B cells into a pro-inflammatory program, under Breg-inducing conditions. B cell AHR-deficient mice develop exacerbated arthritis, show significant reductions in IL-10-producing Bregs and regulatory T cells (Tregs), and show an increase in T helper (Th) 1 and Th17 cells compared with B cell AHR-sufficient mice.

The most abundant source of AHR ligands are derived from the diet and the metabolism of dietary tryptophan. We have previously established a link between microbiota-driven signals in the gut and the differentiation of Bregs. Of the gut microbiota-derived metabolites, the short-chain fatty acids (SCFAs) are the most well characterised. More recently, the SCFA butyrate has been demonstrated to act as an AHR ligand in an intestinal epithelial cell line. Given the association of butyrate with AHR activation and the supporting findings showing that butyrate promotes Treg function, these data led us to hypothesise that butyrate acts via AHR to enhance Breg suppression. Here, we demonstrate that mice supplemented with butyrate reduces arthritis severity by inhibiting the differentiation of GC B cells and plasma cells, whilst maintaining Breg numbers and promoting the suppressive function of Bregs. We show that supplementation of mice with butyrate, changes the composition of the microbiota to favour species which metabolise tryptophan; a major source of AHR ligands. Therefore, we hypothesised that butyrate controls the balance between pro-arthritogenic and regulatory B cell differentiation, through the generation of microbiota derived AHR ligands. To date, the AHR ligands which direct Breg function are unknown. We rule out that butyrate acts as a direct ligand of AHR and establish that supplementation with butyrate increases the availability

of 5-Hydroxyindole-3-acetic acid (5-HIAA), a downstream metabolite of serotonin, which we identify as a novel ligand of AHR in B cells. Mice supplemented with 5-HIAA promote Breg function and suppress arthritis severity, only in mice with AHR-sufficient B cells. Thus, we identify AHR as a relevant contributor to the transcriptional regulation of Breg differentiation and show that microbiota in the gut influence Breg differentiation by increasing the availability of AHR ligands.

Impact statement

Regulatory B cells (Bregs) are a potent modulator of immune responses, which prevent excessive inflammation and maintain immune homeostasis after infection or tissue-injury. Abnormalities in Breg number and function are often prevalent in immune-related pathologies such as autoimmune disease, chronic infections, cancer and in the rejection of transplants. Thus, it is of utmost clinical importance to understand the ontogeny of these populations, to phenotypically characterise Breg populations and to understand the cellular signals and the molecular cues which drive Breg differentiation. By better characterising Breg populations and the processes leading to their differentiation, we can potentially identify target molecules/pathways for therapeutic interventions in immune-related pathologies. To address these knowledge gaps in the field of regulatory B cell research, our aim was to identify a unique molecular signature that distinguishes Bregs from effector B cells, as well as identify the molecular signals that drive Breg differentiation. The data presented here identifies the aryl hydrocarbon receptor (AHR) as a key transcription factor involved in defining Breg identity and controlling Breg function. Our data suggests that we can expand or contract Breg numbers through modulating AHR signalling, which could have therapeutic potential in a variety of autoimmune diseases and in cancer.

In recent years, we have started to build a clearer picture of the signals required for Breg differentiation and have previously shown that the microbiota facilitates this process. Here we link microbiota derived signals and AHR-driven Breg differentiation. We show that the short chain fatty acid butyrate, a microbial-derived end product of complex carbohydrate metabolism, changes the composition of the microbiota. This shift promotes the growth of bacterial genera which metabolise tryptophan to generate the metabolite 5 Hydroxyindole-3-acetic acid (5-HIAA), which we show for the first time is a novel AHR ligand. Moreover, we show that the metabolites of tryptophan can influence Breg differentiation in a metabolite-specific manner. Collectively, these data highlight that microbiota and dietary metabolites control the balance between effector and regulatory B cell differentiation and show this process is driven through AHR. Thus, data from these studies implicate an important role of dietary and microbial-derived metabolites in the generation of regulatory B cells and could provide a therapeutic target in the treatment of

autoimmunity, either through manipulation of microbial end-products or through supplementation of AHR ligands.

Table of Contents

List of figures

List of tables

List of abbreviations

3'IgHRR - 3'IgH transcriptional regulatory region

3-MC - 3-methylchoanthrene

5-HIAA - 5-Hydroxyindole-3-acetic acid

5-HT - 5-hydroxytryptamine

α-GalCer - α-galactosylceramide

ABX - antibiotic

AHR - Aryl hydrocarbon receptor

AHRR - aryl hydrocarbon receptor repressor

AIA - antigen-induced arthritis

AID - activation-induced cytidine deaminase

AIP - AHR-interacting protein

ALDH - aldehyde dehydrogenase

AP1 - activator protein 1

APC - antigen-presenting cell

APRIL - a proliferation-inducing ligand

ARE - adenosine-rich elements

ARNT - aryl hydrocarbon nuclear translocator

ATAC-seq - assay for transposase-accessible chromatin using sequencing

BAFF - B cell-activating factor

BAFFR - B cell-activating factor receptor

BATF - basic leucine zipper transcription factor ATF-like

BCL - B cell lymphoma/leukaemia

BCMA - B cell maturation antigen

BCR - B cell receptor

Be - B effector

bHLH - basic helix-loop-helix

BLIMP-1 - B lymphocyte-induced maturation protein 1

Breg - regulatory B cell

BRG1 - Brahma/SWI2-related gene 1

BTK - Bruton's tyrosine kinase

CBFβ - core-binding factor subunit β

CCL - CC chemokine ligand

CCR - CC chemokine receptor

CD - cluster of differentiation

CFA - complete Freund's adjuvant

ChIP - chromatin immunoprecipitation

CHS - contact hypersensitivity

CIA - collagen-induced arthritis

CII - type II collagen

CLP - common lymphoid progenitor

CNS - conserved non-coding sequence

CREB - cyclic adenosine 3,5-monophosphate response element-binding protein

CSR - class-switch recombination

CTLA-4 - cytotoxic T-lymphocyte associated protein 4

CUL4B - cullin 4B ubiquitin ligase complex

CXCL - CXC chemokine ligand

CXCR - CXC chemokine receptor

CYP - cytochrome P

D - diversity in reference to gene rearrangement

DAR - differentially accessible region

DC - dendritic cell

DEG - differentially expressed genes

DIM - 3,3'-diindolylmethane

DL1 - delta-like 1

DNFB - 2,4-dinitrofluorobenzene

DRE - dioxin response element

DSS - dextran sulphate sodium

DTH - delayed type hypersensitivity

DZ - dark zone

EAE - experimental autoimmune encephalomyelitis

EBF1 - early B cell factor 1

EBI2 - Epstein Barr virus induced gene 2

ER - endoplasmic reticulum

ERK - extracellular signal-related kinase

ESR - oestrogen receptor

FDC - follicular dendritic cell

FFAR - free fatty acid receptor

FICZ - 6-formylindolo[3,2-*b*]carbazole

FLT3 - Fms-like tyrosine kinase 3

FO - follicular

FOXO1 - forkhead box O1

FOXP3 - forkhead box P3

GALT - gut associated lymphoid tissue

GATA3 - GATA binding protein 3

GC - germinal centre

GC-RMA - Gene chip robust multi-array average

GFI1 - growth factor independence 1

GIFT15 - GM-CSF and IL-15 fusokine

GLT - germline transcripts

GM-CSF - granulocyte-macrophage colony-stimulating factor

GPCR - G-protein-coupled receptor

H - heavy in reference to Ig chains

H3K27 - histone 3 lysine 27

HAH - halogenated aromatic hydrocarbons

HAT - histone acetyltransferase

HDACi - histone deacetylase inhibitor

HEL- hen egg lysozyme

HIF1α - hypoxia-inducible factor 1α

hs - hypersensitive sites

HSA - heat stable antigen

HSC - hematopoietic stem cell

HSP - heat shock protein

I3C - indole-3-carbinol

IBD - inflammatory bowel disease

ICAM - intracellular adhesion molecule

ICOS - inducible T cell co-stimulator

ICOSL - inducible T cell co-stimulator ligand

ICZ - indolo-[3,2-b]-carbazole

IDO - indoleamine 2,3-dioxygenase

IFA - incomplete Freund's adjuvant

Ig - immunoglobulin

IKKα - IκB kinase α

IL - interleukin

ILC - innate-like lymphoid cell

iNKT - invariant natural killer T

IPA - indolepyruvic acid

ITAM - immunoreceptor tyrosine-based activation motif

ITIM - immunoreceptor tyrosine-based inhibitory motifs

IRF - Interferon regulatory factor

J - joining in reference to gene rearrangement

KLF – Kruppel like factor

KO – knockout

KYNA – kynurenic acid

L - light in reference to Ig chains

LAG3 - lymphocyte activation gene 3

LFA-1 - lymphocyte function associated antigen 1

LLPC - long-lived plasma cell

LMPP - lymphoid-primed multipotent precursor

LPS – lipopolysaccharide

LT - lymphotoxin

LZ – light zone

MADCAM1 - mucosal vascular addressin cell adhesion molecule 1

MAPK - mitogen-activated protein kinase

MBC - memory B cell

mBSA - methylated bovine serum albumin

MCMV - murine cytomegalovirus

mRNA – messenger RNA

MFI - median fluorescence intensity

MHC - major histocompatibility complex

miR - microRNA

MLN - mesenteric lymph node

MOG - myelin oligodendrocyte glycoprotein

mTOR - mammalian target of rapamycin

MyD88 - myeloid differentiation primary-response gene 88

MZ - marginal zone

NFAT - nuclear factor of activated T cells

NF-κB - nuclear factor κB

NHEJ - Non-homologous end-joining factors

NK - natural killer

NOR – norisoboldine

NP-CGG - 4-Hydroxy-3-nitrophenylacetyl-chicken gamma globulin

NRF2 - nuclear factor erythroid 2-related factor

OCT4 - octamer-binding protein

OVA - ovalbumin

PABA-HEA - paraeminobenzoic acid-Hen egg albumin

PAH - polycyclic aromatic hydrocarbons

PALS - periarteriolar lymphoid sheath

PAS - PER-ARNT-SIM

PAX5 - paired box 5

PCA - Principal component analysis

PCPA - L-para-chlorophenylalanine

PDC - plasmacytoid dendritic cell

PER - periodic circadian protein

PI3K - phosphoinositide 3-kinase

PLCγ2 - phospholipase Cγ2

PMA - phorbol 12-myristate 13-acetate

pMHC - peptide MHC

PP - Peyer's patches

Prdm1 - positive-regulatory-domain containing 1

PRR - pattern recognition receptor

PtC - phosphatidylcholine

P-TEFb - positive transcription elongation factor

RA - rheumatoid arthritis

RAG-1/-2 - recombination activating genes-1/-2

RARA - retinoic acid receptor alpha

RB - retinoblastoma protein

RBC - Red blood cells

RBP - RNA binding proteins

RBP - Jκ recombination signal binding protein for Igκ J region

RSS - recombination signal sequences

RUNX - runt-related transcription factor

S1P - sphingosine 1-phosphate

$S1P_1$ - sphingosine 1-phosphate receptor 1

SCFA - Short chain fatty acid

SHM - somatic hypermutation

SHP1 - SH2-domain-containing PTP 1

SIM - single-minded protein

SLAM - signalling lymphocyte activation molecule

SLC - surrogate light chain

SLC5A8 - sodium-coupled monocarboxylate transporter 1

SLE - systemic lupus erythematosus

SLPC - short-lived plasma cell

SP1 - specificity protein 1

SPF - specific pathogen free

SREBF1 - sterol regulatory element-binding protein 1

STAT - signal transducer and activator of transcription

STIM - stromal interaction molecules

SWI/SNF - switching defective/sucrose non-fermenting

T1/T2/T3 – transitional 1/2/3

T2-FP - Transitional 2 follicular precursor

T2-MZP - transitional 2-marginal zone precursor

TACI - transmembrane activator and calcium modulator and cyclophilin-ligand interactor

TCDD - 2,3,7,8-tetrachlorodibenzo-*p*-dioxin

TCR - T cell receptor

TD - T-dependent

TdT - terminal deoxynucleotidyl transferase

TFIIB - transcription factor IIB

Tfh - T follicular helper

Tfr - T follicular regulatory cells

TGF-β1 - transforming growth factor-β1

Th - T helper

TI - T-independent

TIM - T cell Ig and mucin domain

TLR - Toll-like receptor

TNFα - tumour necrosis factor α

Treg - regulatory T cells

TSS - transcription start site

URE - Uridine-rich elements

UTR - untranslated regions

V - variable in reference to gene rearrangement

WT - wild-type

XBP1 - X-box binding protein 1

Xid - X-linked immunodeficiency

XLA - X-linked agammaglobulinemia

XRE - xenobiotic response element

CHAPTER I: Introduction

1.1 B cells

B cells are lymphocytes, which express a unique antigen receptor, which recognises specific antigenic epitopes, and undergo clonal selection and expansion in response to their cognate antigen. Whilst both B and T cells undergo somatic gene rearrangement for their antigen receptors, both receptors differ in a number of key areas. In terms of antigen processing and presentation, the antigen receptor on B cells can recognise protein, lipid or carbohydrate antigens in their native conformation and this process is not major histocompatibility complex (MHC) restricted. This is in contrast to the antigen receptor on T cells, which only recognises MHC-restricted processed peptide antigen, or lipid antigens presented by cluster of differentiation (CD) 1 molecules[1, 2]. One of the key roles of B cells is to provide protective humoral responses through the production of antibodies. However, B cells also coordinate immune responses through antigen presentation and through the production of cytokines and chemokines[1]. In order to understand how B cells modulate and coordinate immune responses, it is important to understand the developmental pathways of B cells and the phenotypical and functional diversity of B cells.

1.1.1 B cell development in the bone marrow

1.1.1.1 Commitment to the B cell lineage

During embryogenesis, haematopoiesis first occurs in the yolk sac[3] and at a later developmental stage in the foetal liver, which is seeded by circulating haematopoietic cells[4]. At birth, haematopoietic stem cells (HSCs) colonise the bone marrow, whilst in the postnatal stages of life the HSC pool is maintained in the bone marrow by HSC self-renewal and differentiation[5]. Indeed, in contrast to the proliferative nature of foetal HSCs, most postnatal HSCs are quiescent and divide only to replenish the pool of HSCs or to regulate the number of differentiated blood cells[6, 7].

For the commitment to the B cell lineage, HSCs first differentiate into lymphoid-primed multipotent precursors (LMPPs)[8] and then into the common lymphoid precursors (CLPs). As HSCs differentiate into CLPs, the expression of Fms-like tyrosine kinase 3 (FLT3) and Interleukin (IL)-7Rα, key factors for the survival and

expansion of both LMPPs[9] and CLPs[10], are increased. LMPPs and CLPs can undergo a differentiation programme to become T or B cells, but also retain myeloid differentiation potential.

T and B cells share a number of developmental commonalities, namely their ability to carry out somatic gene rearrangement of genes for their respective antigen receptor through the recombination activating genes 1 and 2 (RAG1/RAG2)-mediated programme, which results in a large variety of antigen specificities in these receptors, allowing for the recognition of a wide range of antigens. However, these cell populations also share a number of other developmental programmes including cell cycle arrest phases, required for gene rearrangement and the use of positive and negative checkpoints to ensure a fully functional antigen receptor repertoire with limited self-reactivity[11]. The divergence of the T cell-like and B cell-like programmes dates back more than 500 million years[12]. Distinct transcriptional regulatory modules are required for the development of T and B cell precursor subsets.

Differentiation to the CLP stage is dependent on a series of transcription factors, including IKAROS[13], PU.1[14], E2A[15] and B cell lymphoma/leukaemia (BCL)11A[16]. In addition, a second group of transcription factors, including growth factor independence 1 (GFI1)[17], signal transducer and activator of transcription (STAT)5A/STAT5B[18], MYB[19] and runt-related transcription factor (RUNX) family members and binding partner core-binding factor subunit β (CBFβ)[20] are required for the differentiation of CLPs, as well as being indispensable for other haematopoietic programmes. Commitment towards the B cell fate is also partly dependent on increased RAG1 expression, the downregulation of KIT and the expression of a λ5 transgene[21, 22]. However, the two fundamental transcription factors needed for commitment to a B cell fate are early B cell factor 1 (EBF1) and paired box 5 (PAX5)[23], as will be discussed below.

1.1.1.2 Early B cell development

The early B cell precursors can be split into 4 fractions, consisting of pre-pro B cells, pro-B cells, large pre-B cells and small pre-B cells. Development of B cells in the bone marrow is characterised by the sequential rearrangement of the B cell receptor heavy and light chain genes[24]. The transition from the uncommitted pre-

pro B cells to pro-B cells is marked by the upregulation of PAX5[25, 26]. EBF1 in tandem with E2A, creates a distinguishable gene expression profile specific to the B cell lineage. PAX5 is required for the stabilization of this profile, and in addition, plays a key role in the rearrangement of the Ig heavy chain regions, by changing the accessibility of these regions. Both EBF1 and PAX5 interact, and work in tandem, with many other transcription factors important for the pan-haematopoietic lineage, including MYB and IKAROS, which are responsible for contributing to the expression of a large proportion of the B cell lineage specific genes. PAX5 and EBF1 remain expressed throughout the differentiation stages of a B cell, and only in the terminal differentiation stage are these genes silenced[27, 28]. As well as positively directing the B cell lineage transcriptional programme, PAX5 alongside EBF1 has a negative role in reducing the T cell developmental potential. Ectopic expression of PAX5 in HSCs and progenitors favoured B cell development over T cell lymphopoiesis, specifically through its role in inhibiting the expression of *Notch1*[29, 30].

Pro-B cells are identified by the rearrangement of the *Igh* gene locus, with recombination of one of the large arrays of variable (V), diversity (D) and joining (J) gene segments. V(D)J recombination is mediated through recombinase complex containing RAG1/RAG2 and other DNA repair enzymes. The RAG complex has endonuclease activity and introduces double-stranded breaks in the *Igh* locus at recombination signal sequences (RSSs), that flank each gene segment. Non-homologous end-joining factors (NHEJ) join the V, D and J segments together[31]. In pro-B cells, recombination of the D and J gene segments occurs first and is followed by the recombination of the DJ_H segment to one V_H gene segment and then splicing onto one of the adjacent constant μ ($C\mu$) exons to form a complete Igμ heavy chain gene[24]. During the recombination stage, diversification of the BCR repertoire can be achieved by the actions of the terminal deoxynucleotidyl transferase (TDT) enzyme, which adds non-templated nucleotides to the V-D and D-J junctions of the Ig heavy chain, increasing diversity at the complementarity determining region 3 (CDR3) of the Ig heavy chain[32]. Many B cells which undergo somatic recombination produce out-of-frame rearrangements and subsequently initiate apoptosis. Only one of three B cells which undergo recombination of the V(D)J regions occur ‘in frame’[33, 34].

Entry into the pre-B cell stage is marked by the expression of the pre-BCR, which involves the pairing of a complete Igμ heavy chain with the invariant surrogate light chain (SLC) proteins λ5 and VpreB[35, 36]. In addition, Igα and Igβ, both of which contain immunoreceptor tyrosine-based activation motifs (ITAMs), are expressed and mediate downstream signals after activation of the pre-BCR complex. Signals through the pre-BCR are an important step in the differentiation of pre-B cells. However, it is not currently known if this occurs in a ligand-dependent or independent manner[37]. Signals through the pre-BCR promotes the proliferation and expansion of B cells, thus giving rise to the developmental stage known as 'large pre-B cells'; the end result being an expansion of B cells with the same 'in frame' heavy chain. Signals through the pre-BCR halts further V_H to DJ_H rearrangements of the *Igh* locus, in part by a process known as allelic exclusion. This process stops the second allele undergoing V_H to DJ_H recombination, thus ensuring monospecificity of B cells, which is required for efficient antigen-specific antibody responses[38]. Lastly, pre-BCR signals also induce the re-expression of RAG1/RAG2, which leads to the recombination of the V_L to J_L gene segments of the immunoglobulin light chain (firstly the *Igκ* loci, then the *Igλ* loci if unsuccessful), which marks the entry into small pre-B cell stage. The developing B cell has two attempts at rearranging the *Igh* locus and 4 attempts at the Ig light chain rearrangement (both paternal and maternal *Igκ* loci and *Igλ* loci). If successful, a fully functional BCR is synthesized and expressed on the surface of the B cell, marking the IgM^+IgD^- immature B cell stage of development[39, 40]. The different stages of B cell development in the bone marrow are shown in Figure 1.1.

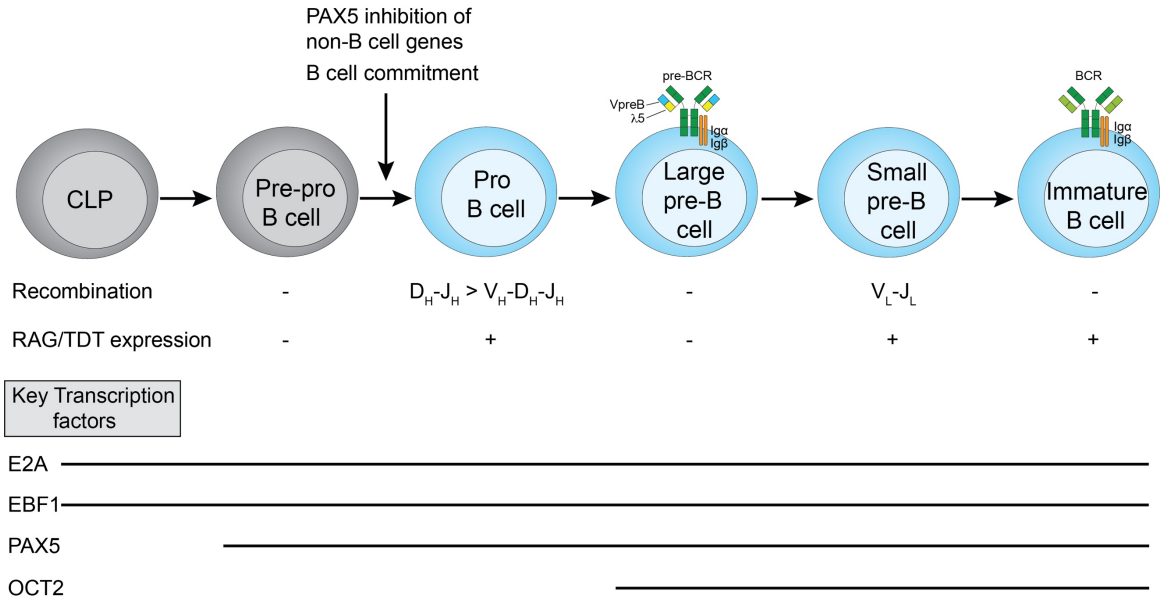

Figure 1.1. B cell development in the bone marrow. Cells commit to the B cell lineage at the Pro-B cell stage, upon which PAX5 directs the transcriptional programme leading to the silencing of other lineage specific transcription networks. The B cell transcriptional programme is strengthened by expression of E2A and EBF1. At the Pro-B cell stage gene arrangement of the *Igh* chain locus occurs. Upon successful V_H-D_H-J_H gene rearrangement, the pre-BCR is expressed upon the cell with the surrogate light chain. After signals through the pre-BCR and rounds of proliferation, small pre-B cells re-upregulate RAG1/2 and rearrange the light chain. Successful rearrangement of both heavy and light chains leads to the expression of a fully functional BCR on immature B cells.

1.1.1.3 Central B cell tolerance

During various stages of a B cells developmental cycle, tolerance checkpoints are used to decrease the numbers of autoreactive B cells from entering the periphery. Central B cell tolerance is the process in the bone marrow by which emerging immature B cells are rendered tolerant to self-antigens and any strongly autoreactive B cells are removed from the pool[41]. Historically, it was thought that any lymphocyte clone that reacted to self-antigen would be eliminated by apoptosis to prevent immune activation to 'self'; a process called clonal deletion[41]. This theory was later examined by using transgenic mice expressing antibodies against H2-k or against hen egg lysozyme (HEL). Results from these studies demonstrated that immature B cells that bound to these antigens with high avidity, failed to differentiate further and entered apoptosis within 1-3 days of ligation[42, 43, 44]. However, it is now thought that only a small fraction of self-reactive B cells undergoes clonal deletion. Indeed, central tolerance primarily takes place through receptor editing and induction of anergy, with clonal deletion occurring only when receptor editing fails[45]. Approximately 50-75% of immature B cells express BCRs that are specific for self-antigens, compared to only 20-40% of transitional and naïve mature B cells[46, 47]. A proportion of autoreactive immature B cells do evade central tolerance, enter the periphery and differentiate into mature B cells[41, 48].

Engagement of the BCR on immature B cells by self-antigen, leads to the downregulation of the BCR and the upregulation of forkhead box O1 (FOXO1), which promotes RAG1/2 expression and receptor editing[49, 50]. Receptor editing is the process by which there is secondary rearrangement of the VJ gene segments of the Ig light chain. Although uncommon, some B cells can undergo receptor editing on the heavy chain[51]. The exact frequency of B cells which undergo receptor editing is difficult to determine[45]. One study has reported that approximately 20% of immature B cells are actively carrying out receptor editing[52]. The process of receptor editing is directional and starts at the κ L-chain loci, before proceeding to the λ L-chain. Receptor editing that results in a kappa-lambda edit rather than a kappa-kappa edit has been suggested to be more effective in silencing natural autoreactive B cells[53]. If receptor editing fails to quench autoreactivity, then self-reactive B cells undergo apoptosis, a process termed clonal deletion.

If an autoreactive lymphocyte bypasses central tolerance and escapes to the periphery, then the cell will be subject to peripheral tolerance mechanisms such as anergy. Anergic B cells in the periphery have a markedly reduced half-life (averaging 3-5 days), when compared to non-autoreactive B cells (averaging 7-8 weeks), and are marked by reduced expression of IgM and increased recruitment of negative regulators of BCR signalling to the BCR[54, 55, 56, 57]. When an immature B cell successfully expresses a non-autoreactive BCR, the B cell enters the transitional 1 (T1) B cell stage and can leave the bone marrow and recirculate to the periphery. Transitional B cells are no longer able to carry out RAG mediated V(D)J or VJ recombination of the heavy and light chains respectively[45].

1.1.2 B cell development in the spleen

1.1.2.1 BCR tonic signalling

Signals through the pre-BCR and mature BCR are essential for the development of B cells in the bone marrow and, in addition, are required for B cells to enter the periphery. Indeed, if a newly developed immature B cell lacks a functional mature BCR these cells do not differentiate any further or egress from the bone marrow[58] [59]. In order for B cells to survive in the periphery, tonic BCR signalling is required. Tonic BCR signalling is the process in which you have functional downstream signalling of the BCR, independent of antigen activation. Tonic BCR signalling differs from that of antigenic activation in that it does not lead to the full activation of B cells, but rather promotes B cell survival and maturation. In the absence of constitutive BCR signalling in immature B cells, light chain rearrangement is reinitiated and immature B cells upregulate a gene expression profile consistent to that of Pro-B cells[60].

Activation of the BCR through tonic signalling or through interaction with antigen, induces the activation of the Igα and Igβ subunits of the BCR complex and leads to the Lyn-mediated phosphorylation of the tyrosine amino acids in their ITAM motifs[61, 62]. BCR activation is finely tuned by a series of co-activatory or inhibitory molecules which modulate BCR signalling. Positive regulators of BCR signalling include CD19[63] and CD45; the latter is a phosphatase which targets an inhibitory tyrosine residue on the SRC-family protein tyrosine kinases for dephosphorylation[64]. BCR signalling is inhibited by the negative co-receptors CD5, CD22 and CD72 and activation of their immunoreceptor tyrosine-based inhibitory

motifs (ITIMs) recruits the protein tyrosine phosphatase SH2-domain-containing PTP 1 (SHP1). SHP1 attenuates BCR signalling by competing with the activatory protein tyrosine kinases like LYN[65]. Activation of the BCR complex induces a complex network of downstream activators including the mitogen-activated protein kinase (MAPK), nuclear factor of activated T cells (NFAT), nuclear factor κB (NF-κB) and phosphoinositide 3-kinase (PI3K) pathways. Inducible deletion of the BCR leads to the loss of mature B cells with the average half-life spanning 3-6 days. Only constitutive PI3K, but not MAPK/extracellular signal-related kinase (ERK), NF-κB or BCL2 (by itself), signalling rescues the survival of mature B cells[66 67]. In contrast, antigen engagement of the BCR, fails to induce T1 B cells to proliferate and they undergo apoptosis. These findings demonstrate that a certain threshold of BCR signalling strength is needed for survival of the early transitional B cells, and that as a B cell matures they acquire the ability to respond to antigenic BCR activation[68].

1.1.2.2 The role of BAFF in B cell maturation

B lymphocyte activating factor (BAFF), a member of the tumour necrosis factor (TNF) family, is a trimeric cytokine which can be found in membrane-bound or soluble forms. The primary source of BAFF expression is mainly from innate immune cells including, but not limited to, neutrophils, macrophages, dendritic cells, monocytes, but can also be produced by bone marrow stromal cells and B cells[69, 70]. BAFF signals through one of three receptors including the B cell activating factor of the TNF-family receptor (BAFFR), the transmembrane activator and calcium modulator and cyclophilin ligand activator (TACI) and through B cell maturation antigen (BCMA)[71]. Activation of the BAFFR promotes survival of B cells through activation of the non-canonical NF-κB2 pathway[72, 73].

For B cells to mature beyond the T1 stage, activation of B cells by BAFF is required in tandem with tonic BCR signalling. Indeed, in BAFF knockout mice there is almost a complete loss of marginal zone (MZ) and follicular (FO) B cells[74, 75]. It is at the early transitional stages, that B cells start to express the BAFFR, at which point they start to receive pro-survival signals. The expression of these receptors varies according to the developmental stage, with the BAFFR being predominantly important for T1 and T2 development, whilst expression of TACI and BCMA is important for mature B cell function and survival[76, 77, 78, 79]. BAFFR expression

directly correlates with the levels of surface IgM. Interestingly, the expression of BAFFR is decreased in autoreactive B cells, suggesting an important role in selectively promoting the survival of non-autoreactive B cells[80]. Highlighting the essential role of BAFF in B cell maturation and survival, BAFF-Tg mice have enlarged T2 and marginal zone (MZ) B cell compartments in the spleen[81]. As well as having an important pro-survival function for B cells at the transitional B cell stages and beyond, signals through TACI and the BAFFR on B cells have been shown to have a role in other B cell functions such as isotype switching, as will be discussed later on[82].

1.1.2.3 B-1 cells

B-1 cells are a subpopulation of B cells which have the capacity to self-renew and are functionally and phenotypically distinct from B-2 cells. The finding that CD5 (also known as Ly-1 in mice and Leu-1 in humans) expression was highly expressed both on many B cell chronic lymphocytic leukaemia cells and in B cell tumours prompted researchers to identify the steady state CD5-expressing B cells[83, 84, 85]. This population was first identified in mice by Hayakawa and colleagues in 1983 and were defined by the expression of CD5[86]. It soon became evident that B-1 cells could be subdivided into two distinct subpopulations; B-1a cells which express CD5 and B-1b cells which are CD5 negative[87, 88]. Each population has distinct immunological functions and developmental pathways, with B-1b cells developing in tandem with B-2 cells[89].

B-1 cells are functionally distinct from B-2 cells and are characterised by their ability to self-renew and to spontaneously produce IgM antibodies. Furthermore, unlike B-2 cells, B-1 cells are mainly found in the peritoneal and pleural cavities (defined as $IgM^{hi}IgD^{lo}CD23^{-}CD11b^{+}CD43^{+}CD5^{+/-}$)[90], with a small population found in the spleen ($IgM^{+}IgD^{lo}CD23^{-}CD11b^{-}CD43^{+}CD5^{+/-}$)[91, 92]. B-1 cells are abundant in young mice and the frequencies of this population decrease into adulthood[86]. In particular, B-1a cells, can produce natural polyreactive IgM antibodies, which tend to have an autoreactive repertoire with reduced junctional diversity, decreased levels of somatic hypermutation and tend to favour V_H12 usage[93]. Around 10% of peritoneal B-1 cells were found to bind phosphatidylcholine (PtC), which is expressed on senescent red blood cells (RBCs)[94]. B-1 cells also recognise a carbohydrate epitope on the thymocyte glycoprotein Thy-1, thereby illustrating the broad self-

reactive BCR repertoire of B-1 cells[95]. Intriguingly, B-1a cells acquire their self-reactive phenotype by bypassing the pre-BCR stage[96]. The SLC is redundant in B-1a cell development as the frequency of this population is unaffected by the absence of the SLC[96, 97]. Indeed, the SLC has a reduced efficiency in binding with autoreactive heavy chains and as such its absence may allow the expression of the autoreactive BCRs that characterise B-1a cells[98, 99]. Natural antibodies produced by B-1 cells can also bind to the phosphocholine epitope on the cell wall polysaccharide of *Streptococcus pneumoniae*, leading to their opsonisation and clearance[100, 101]. Thus B-1 cells are an important source of natural antibodies for clearance of apoptotic cells and in the first line defence against pathogens such as *S. pneumoniae*[89] and *Salmonella typhi*[102], amongst others[103, 104] and participate in T cell independent responses (TI), as opposed to B-2 cells which participate in both T cell dependent (TD) and TI responses[105].

In addition to their role in natural antibody production, B-1 cells are an important source of the anti-inflammatory cytokine IL-10[106] and have been implicated in attenuated responses to Leishmania[107, 108]. In contrast to murine B-1 cells, the existence and phenotype of human B-1 cell orthologues remain inconclusive.

1.1.3 B2 B cells

1.1.3.1 Transitional B cells

T1 B cells migrate out of the central sinus of the bone marrow and enter the periphery via the blood stream. Migration to the spleen occurs through the central arterioles and T1 B cells subsequently migrate to the periarteriolar lymphoid sheaths (PALS)[109]. The migration of T1 B cells directly to the spleen and not to other lymphoid tissue is mediated by their lack of CD62L expression, which is important for entry into other secondary lymphoid tissues[110]. Entry into the T2 stage is marked by the upregulation of IgD and the complement receptor CD21. In addition to the expression of IgM, IgD and CD21, transitional B cell subsets in the murine spleen can be distinguished by the expression of AA4.1, CD23 and heat stable antigen (HSA; also known as CD24)[111].

Loder, Carsetti and their colleagues first proposed that B cell development in the spleen was marked by a series of steps based on signals received through the BCR and identified the phenotype of transitional B cells[112]. This phenotypical

characterisation was further refined in a later study by showing that transitional B cells, rather than being a homogenous population, consisted of two distinct subpopulations defined by their response to BCR engagement and by the levels of expression of CD21, CD23, CD24, IgD and IgM. Importantly, the results from this study, established a timeline of B cell development from immature B cells from the bone marrow to mature B cells in the spleen and reported two key findings. Firstly, T1 B cells ($CD21^{lo}CD24^{hi}IgD^{-/lo}IgM^{hi}$) were established as the progenitors of T2 B cells ($CD21^{int/hi}CD24^{hi}IgD^{hi}IgM^{hi}$) and maturation along this pathway was contingent upon positive selection through the BCR[110]. Secondly, as demonstrated through adoptive transfer experiments of T2 B cells into *Rag2*$^{-/-}$ mice, T2 B cells were demonstrated to develop into mature B cells in the spleen[110].

Allman and colleagues proposed an alternative model that defines the different transitional B cell subpopulations, according to the expression of IgM, CD23 and AA4.1[68]. Two important distinctions arose between the two proposed models. In contrast to T1 and T2 in Loder and Carsetti's model, Allman's model proposed that transitional B cells could be split into three subpopulations; T1 ($AA4^{+}IgM^{high}CD23^{-}$), T2 ($AA4^{+}IgM^{high}CD23^{+}$) and T3 ($AA4^{+}IgM^{low}CD23^{+}$). Importantly, the functional characteristics of T2 B cells also differ. In Allman's model, T1, T2 and T3 B cells are unable to proliferate in response to BCR crosslinking *in vitro*, or *in vivo.* Moreover, they suggested that it is the T3 population, instead of the T2 population, that gives rise to mature B cells. In contrast, in Loder and Carsetti's model, T2 B cells are able to proliferate in response to BCR engagement; a finding which was subsequently confirmed by the Rawlings and Khan groups[113, 114].

More recent studies have called into question the idea that T3 B cells differentiate into mature B cells[115]. Instead, it has been proposed that T3 B cells more resemble anergic B cells, are not part of the typical transitional B cell differentiation pathway and are hyporesponsive to activation through the BCR[115]. This hypothesis was elegantly supported by the finding that in the absence of HEL expression, mice that express a high affinity anti-HEL IgM have very few T3 B cells. In contrast, when HEL was present the T3 population comprised the vast majority of the transitional B cells[116]. Despite the lack of consensus regarding the stages of transitional B cell development, it is generally accepted that transitional B cells can differentiate into mature naïve MZ and FO B cells, dependent on the environmental signals they

receive[117]. The current consensus is that the T2 population described by Loder *et al* is a heterogenous population that contains T2 marginal zone precursor (T2-MZP) and T2- follicular precursor (T2-FP) populations. Whilst T2-FP B cells can be found in all secondary lymphoid organs, T2-MZP B cells are only resident in the spleen[118]. The phenotype of T2-MZP B cells based on the expression of CD21, CD23 and CD24, as described by Loder and Pillai, will be used throughout this thesis.

1.1.3.2 Anatomical features of the spleen

The spleen functions as a filter for both blood-borne pathogens and antigens, as well as having pivotal roles in iron metabolism and the removal of old and faulty erythrocytes from the blood[119]. Broadly speaking, the spleen is structurally organised into two distinct compartments; the red pulp and the white pulp. The red pulp consists of a mesh of fibroblasts and reticular fibres and red pulp macrophages; the latter have a major role in the clearance of RBCs. The spleen has no afferent lymph vessels and, as such, leukocytes can only enter the spleen through the arterial vessels. Arterial blood traverses the cords of Billroth, which are enriched in macrophages, and then moves into the venous sinuses of the spleens. Due to the arrangement of the endothelial cells on the venous sinuses and the connecting stress fibres, aging RBCs are unable to cross into the sinuses due to the rigidity of their membranes. Consequently, the aging RBCs are stuck in the cords of the red pulp and phagocytosed by the red pulp macrophages[120].

The white pulp of the spleen encompasses distinct anatomical compartments which include the periarteriolar lymphocyte sheath (PALS), where there is a predominance of T cells, and the follicle and marginal zone areas, where B cells are located. The marginal zone surrounds both the PALS and B cell follicles[121]. In addition, the marginal zone also contains dendritic cells, marginal zone macrophages (defined as SIGN-RI^{+}MARCO^{+}) and metallophilic macrophages[119, 122]. Marginal zone macrophages have defined roles in pathogen clearance and importantly liver X receptor alpha signalling in MZ macrophages is required for the retention of MZ B cells in the marginal zone[122].

1.1.3.3 Functional characteristics of mature B-2 B cells

After leaving the bone marrow, transitional B cells migrate to the spleen. Whilst residing in the spleen, T2 precursor populations can give rise to both FO and MZ B cells. The maturation of T2 B cells into FO B cells mainly takes place in the spleen, however T2 B cells can also develop into FO B cells in the bone marrow. This was demonstrated by the presence of *in situ* maturation of B cells in the bone marrow of splenectomised lymphotoxin (LT) α deficient mice, which also lack secondary lymph nodes and Peyer's Patches (PP)[123, 124].

FO B cells home to the follicles on a gradient of C-X-C motif chemokine ligand (CXCL)13 and require the expression of C-X-C motif chemokine receptor (CXCR)5 to access and to be retained in the B cell follicles[125]. The close positioning of FO B cells to the T cell zone means these cells are ideally suited for T cell dependent (TD) antibody responses. When a FO B cell encounters an antigen and receives T cell help, it can either differentiate into a short lived plasma cell or can enter into the GC reaction, in which the FO B cell can either become a germinal centre (GC) B cell, long-lived plasma cell or memory B cell[126]. FO B cells are able to migrate to the MZ, but are unable to reside there due to a lack of integrin-mediated adhesion and, therefore, migrate into the red pulp[127]. Why FO B cells migrate to the MZ is not known, but one plausible explanation is that this route is one possible way that FO B cells can exit from the B cell follicles and circulate between the blood, spleen and peripheral lymph nodes.

T2-MZP B cells migrate to the marginal zone of the spleen and differentiate into MZ B cells, where they are retained and acquire the ability to self-renew[126]. The retention of MZ B cells into the MZ is dependent on signals through the sphingosine 1-phosphate receptor 1 ($S1P_1$) and the presence of the ligand sphingosine 1-phosphate (S1P) in the blood. Signals through $S1P_1$ prevent CXCL13-mediated recruitment of MZ B cells to the follicle area of the spleen[128]. The main source of S1P in adults is RBCs and both the vascular and lymphatic endothelial cells, with RBC's accounting for the production of approximately 75% of plasma S1P in mice[129, 130, 131, 132]. Importantly, activation of MZ B cells via the BCR or by lipopolysaccharide (LPS) leads to downregulation of $S1P_1$ and their movement of MZ B cells out of the MZ[128]. In the MZ, retention signals are required to stop the egress of MZ B cells. Integrins play a key role in this process, as combined

inhibition of both $\alpha4\beta1$ and lymphocyte function associated antigen 1 (LFA-1) leads to the migration of MZ B cells out of the MZ[133]. It is important to note the role that mucosal vascular addressin cell adhesion molecule 1 ($MADCAM1^+$) endothelial cells play in the anatomical structure of the spleen and in MZ B cell function. In the absence of $S1P_3$, the single cell endothelial layer that lines the marginal sinus is disrupted and the endothelial cells are dispersed[134]. This loss of barrier function has two main consequences. Firstly, MZ B cell numbers are increased and these cells are more rapidly able to migrate to the B cell follicles. Secondly, MZ B cells in this setting display less effective T cell independent antigen responses[134].

The location of MZ B cells, means that these cells are uniquely adapted to respond to blood-borne antigens and pathogens, such as the encapsulated bacteria. The position of MZ B cells allows for the first wave of humoral immunity against pathogens and they can produce antigen-specific antibodies in a T cell independent (TI) manner and a TD manner (at least in human MZ B cells). TI responses tend to be elicited against polysaccharides on the cell walls of encapsulated bacteria[135]. In addition, MZ B cells are able to rapidly deliver opsonised antigens from the blood, via capture by the complement receptor CD21, and shuttle the antigen between the MZ and the follicles. Whilst in the follicles, MZ B cells can transfer the antigens to follicular dendritic cells (FDCs), promoting T cell dependent FO B cell responses[136]. Indeed, around 20% of MZ B cells transit between the compartments every hour. Moreover, owing to the high expression of CD1d, MZ B cells can orchestrate immune responses via presentation of lipid antigen to invariant natural killer T cells (iNKT). MZ B cells are also a key source of lipid antigen specific antibodies[137].

The functional characteristics of the humoral response vary between MZ and FO B cells. In contrast to FO B cells, MZ B cells can produce natural antibody in the absence of infection and are more likely to recognise self-antigen than FO B cells[138]. In addition, antibodies produced by MZ B cells tend to be of low affinity, have a broader specificity and mostly belong to the IgM class[139]. After interacting with antigen, MZ B cells can rapidly differentiate into plasmablasts either in the follicles or in extrafollicular foci and produce large quantities of IgM within the first 3 days of a primary response[140, 141]. Alternatively, MZ B cells can also produce IgA and IgG after class switch recombination (CSR), which will be discussed later[142].

Whilst FO B cells between mice and humans are functionally very similar, a number of differences exist in MZ B cell phenotype and function between species. One intriguing feature is that in humans, MZ B cells are also found outside of the spleen, suggesting that, unlike in mice where they are sessile, in humans they can recirculate[143]. In particular, in humans, MZ B cells can be found in the subepithelial dome of the Peyer's Patches[144], the epithelium of tonsillar crypts[145] or in the subcapsular sinus of lymph nodes[146]. Interestingly, MZ B cells in humans (defined as $IgM^{hi}IgD^{low}CD1c^{+}CD21^{hi}CD23^{-}CD27^{+}$) are phenotypically similar to memory B cells, in that both populations express CD27 and contain mutated V(D)J genes. Indeed, a proportion of these cells retain a molecular programme that indicates that these cells have previously been in a germinal centre reaction, which suggests they have exited the GC reaction before CSR[147, 148]. However, this population is distinct from memory B cells as they have fewer IgV mutations and fewer past cell divisions than memory B cells, and also express IgD[149]. Mouse MZ B cells express non-mutated IgV mutations, a proportion of which encode for a polyreactive BCR. On the other hand, approximately 90-95% of human MZ B cells have mutated IgV regions[139, 148]. However, the processes governing MZ B cell development in humans remain poorly understood.

1.1.3.4 MZ vs FO B cell fate decisions

The differentiation of a T2 B cell into a MZ or FO B cell is a complex process, which involves the integration of signals though the BCR, BAFFR, NOTCH2, the canonical NF-κB pathway and regulation of these pathways through the expression of microRNA's and RNA-binding proteins (RBPs). The strength of BCR signalling is a crucial component in what determines the differentiation into either a MZ or FO B cell. It is well established that weak BCR signalling favours MZ B cell differentiation, whilst strong BCR signalling favours FO B cells[126]. Absence of functional positive or negative regulators of BCR signalling lead to defects in either MZ or FO B cell development. Bruton's tyrosine kinase (BTK) is a crucial component of the BCR signalling cascade, which promotes activation of the NFAT and NF-κB pathways. Absence of the BTK protein in humans leads to the primary immunodeficiency X-linked agammaglobulinemia (XLA), in which there is a severe block in B cell differentiation in the bone marrow[150]. However, mice with a loss of function mutation in the *Btk* gene present with a milder phenotype, with only an

impairment of mature B cells in the periphery[151, 152]. Activation of BTK phosphorylates and activates phospholipase Cγ2 (PLCγ2)[153]. Loss of function mutations in PLCγ2 also result in a reduction of FO B cells[154, 155]. This phenotype is also observed in mice lacking CD45 (a positive regulator of BCR signalling), which can be reversed upon reciprocal deletion of the negative regulator SHP1[156]. In contrast, deficiency of both AIOLOS and CD22 (two negative regulators of BCR signalling) lead to a reduction in MZ B cells[157, 158, 159]. In both cases BCR signalling was increased, supporting the notion that strong BCR signals favour FO B cell development over MZ B cells. In support of these findings, mice lacking sialic acid esterase (SIAE) and CMP N-acetyl hydroxylase (CMAH), two enzymes which promote the generation of sialic acid ligands for CD22, have increased BCR signalling and reduced numbers of T2-MZP B cells and MZ B cells[160].

Although signals through the BCR are a pre-requisite for survival and for the maturation of B cells, other signals feed into regulating the differentiation potential of a T2 B cell into a MZ or FO B cell. Both tonic BCR signalling and BAFFR signalling promote the survival of B cells up until the FO B cell stage through the non-canonical NF-κB pathway. This process is mediated by increasing the levels of the NF-κB precursor p100 and by promoting the cleavage of p100 to p52 by the IκB kinase α (IKKα)[161, 162]. Although BAFFR mainly signals through the non-canonical NF-κB pathway in transitional B cells, signals through this receptor can also activate the canonical pathway[126]. Mice lacking p50 have a defect in MZ B cell development. This is also true, but to a lesser extent, in the absence of C-REL or RELA, suggesting that the NF-κB complexes are partially involved in marginal zone B cell development[163].

Unlike in FO B cells, NOTCH2 signalling is required for the differentiation of MZ B cells[164, 165]. Both T2-MZP and MZ B cells are absent in mice with a B cell deficiency of NOTCH2, the receptor for delta like-1 (DL1), indicating the importance of this pathway for inducing the differentiation of T1 B cells into T2-MZP and then MZ B cells[165]. Transitional B cells are rendered responsive to NOTCH2 signalling by the BCR-dependent upregulation of ADAM10, which cleaves NOTCH2 and releases the intracellular domain (NICD) to activate downstream gene targets in tandem with other signalling components[166]. Mice lacking NOTCH2, the signalling components of the NOTCH pathway RBP-Jκ and Mastermind-like 1 or the Notch

ligand DL1 have reduced numbers of MZ B cells in the spleen[164, 167, 168, 169]. The exact transcriptional programme initiated by NOTCH2 signalling in MZ B cells is not clear, but is thought to involve the E2A and the ID2/ID3 proteins; the latter promoting MZ B cell differentiation[170].

Recent evidence also points to an increasingly important role of microRNA's and RBPs in the post-transcriptional regulation of gene networks regulating B cell development. The RNA-binding protein ZFP36L1 promotes the maintenance of the MZ B cell compartment by actively limiting the expression of the transcription factors interferon regulatory factor (IRF)8 and Kruppel like factor (KLF)2; two factors known to implement the FO B cell transcriptional programme[171, 172]. In the absence of KLF2, the marginal zone B cell population is expanded[173, 174]. This is in direct contrast to KLF3, which promotes MZ B cell development[175]. Direct binding of microRNA's (miRs) to the 3' complementary untranslated regions (UTR) of target messenger RNA (mRNA's) regulates B cell development. Both miR-146a and miR-142, respectively promote or repress the generation of MZ B cells[176, 177]. Absence of the endonuclease DICER, the enzyme responsible for the generation of small interfering RNA's and miRNA's, also promotes MZ B cell development, suggesting an important role of post-transcriptional regulation in governing mature B cell differentiation[178]. Interestingly, miR-146a is upregulated by NF-κB signalling and targets components of the NOTCH pathway[176, 179].

1.1.3.5 Initiation of the Germinal Centre Response

The GC is the location in which mature B cells undergo affinity maturation and isotype switching. Throughout the maturation process of a B cell, affinity to an antigen, be it 'self' or non-self, and the strength of BCR signalling decides the fate of the B cell, through both negative and positive selection. One of the defining features of a mature B cell and the humoral immune response is the incremental increase in antibody affinity over time through somatic hyper-mutation (SHM), driven by the enzyme activation-induced cytidine deaminase (AID)[180, 181]. This process occurs in the primary response with an antigen and upon secondary challenge to an antigen[182]. These B cell clones are then negatively and positively selected within the GC and compete for signals in an affinity dependent manner. Successful B cell clones then undergo an intense burst of proliferation and maturation either into antibody secreting plasma cells or into memory B cells.

The germinal centre can be split into two distinct anatomical compartments. The region which is closest to the T cell zone and mainly absent of FDCs is the dark zone (DZ). The region which is closest to the MZ in the spleen, which is rich in FDCs and is distal to the T cell zone, is known as the light zone (LZ)[183]. Within the DZ reside the highly proliferative B cells, also known as centroblasts, which express high levels of the chemokine receptor CXCR4[184]. The centroblasts are retained in the DZ by CXCL12-expressing reticular cells[185]. The DZ is considered to be the site of SHM, as the DZ B cells have high expression of AID. In contrast, the LZ contains centrocytes (GC B cells found in the LZ, which are not actively proliferating), and many more FDCs, infiltrating naïve B cells and T follicular helper cells (Tfh) than the DZ[186].

The entire GC process is contingent upon exposure of an antigen-reactive B cell to their cognate antigen in its native conformation[186]. Recognition of antigen primarily takes place in secondary lymphoid organs, where these organs are specialised in filtering blood and lymph. There is also a continual migration of cells to and from these organs. Both these factors combined increase the chances of a B cell to encounter its cognate antigen. The initial capture of antigen is mediated by different cell types, according to the secondary lymphoid organ. In the case of the lymph nodes, antigen capture is carried out by specialised macrophages in the subcapsular region[187]. In the follicular regions in the spleen, FDC's capture and display opsonised antigens on the dendritic processes. These tail processes are in contact with the follicular B cells[188]. Indeed, in B cell follicles which lack GCs, FDCs play a crucial role in organising the B cells into compact clusters[189]. In the GCs of both spleens and lymph nodes, FDCs are key for the survival of GC B cells. In the absence of toll like receptor (TLR)4 signalling in FDCs, both the GC size is reduced and there is a reduction in the affinity of the BCRs, due to impaired SHM. FDC TLR4 responses are driven *in vivo* by endogenous oxidised phospholipids[190]. In addition, FDCs can retain antigen for several weeks. This process is important for testing the affinity of the BCRs on B cells that have undergone SHM[188, 191].

The retention of antigen is critical, as B cells which migrate into the follicles survey the antigen presented by FDCs and subcapsular macrophages. Migration to the follicles is guided by FDC and stromal cell derived CXCL13 and oxysterol 7α25-

hydroxycholesterol production. Production of these two chemoattractants recruit antigen naïve B cells to the outer follicle, through binding to the CXCR5 and Epstein Barr virus induced gene 2 (EBI2) receptors respectively. It is important to note that in GCs EBI2 is strongly downregulated, which prevents migration of GC B cells to the outer follicle[192, 193, 194]. Retention of GC B cells in the centre of the follicle is also maintained by expression of $S1P_2$, which inhibits the migration of GC B cells in response to follicular chemoattractants[195]. Antigen activation induces the upregulation of C-C motif chemokine receptor (CCR)7 and EBI2, which trigger the migration of B cells to the T cell-B cell border, where they receive co-stimulatory signals from $CD4^+$ T cells[196]. Importantly, antigen activation of the BCR leads to the internalisation of the receptor and, ultimately, transfer of the antigen to the lysosomes for proteolytic processing ready for loading to MHC class II molecules. MHC molecules then present the cognate antigen to $CD4^+$ T helper (Th) cells[197]. If a B cell is unsuccessful in encountering an antigen, it will exit the lymphoid tissue in response to S1P, via expression of $S1P_1$[198].

B cell activation by $CD4^+$ T helper cells is a multistep process. Firstly, naïve $CD4^+$ T cells are primed by dendritic cells that present antigen in the context of MHC class II, and express CD80/CD86. The integration of these signals with IL-6, inducible T cell co-stimulator ligand (ICOSL) and IL-2 are required for the initiation of the Tfh cell differentiation programme (pre-Tfh cells)[199, 200]. Key to this process is the upregulation of BCL6 and CXCR5, which allows for the migration of the activated T cells to the T-B cell border[199, 200]. B cells receiving T cell help will either initiate the GC response or differentiate into short-lived plasma cells or GC-independent memory B cells based on the strength of BCR activation[201, 202]. Extrafollicular plasma cells are an important early source of antibodies in the fight against infection, whilst the GC response is being initiated[197].

Cell fate decisions promoting GC B cell differentiation incorporate many cell signals derived from Tfh cells. LFA1 on Tfh cells binds intracellular adhesion molecule (ICAM)1 and ICAM2 on B cells to form long-lasting cognate interactions, which promote B cell clonal expansion and GC seeding[203]. Optimal B-T cell interactions depend on the co-stimulatory molecules CD86:CD28, ICOS:ICOSL and also on homotypic interactions between members of the signalling lymphocyte activation molecule (SLAM) family (namely SLAM, Ly108 and CD84)[197, 204]. SLAM pathway

interactions are important for IL-4 production by Tfh cells, which in turn influence B cell proliferation[200]. IL-4 in tandem with IL-21 produced by Tfh are crucial for promoting B cell proliferation, CSR and ultimately differentiation to memory B cells or plasma cells[199]. Notably, IL-21 signalling seems to be more important for the transition of pre-GC B cells to the intrafollicular GC B cell stage[205]. However, both cytokines are key for the induction of *Bcl6* and *Aicda*, which are both crucial in the GC response[206, 207]. In addition, CD40-CD40L interactions co-operate with IL-4 signalling to induce *Aicda* in B cells[206]. Moreover, activation of CD40 by Tfh CD40L expression can induce ICOSL expression in mouse GC B cells, leading to a positive feedback loop in B-T cell interactions[208]. It is important to note that expression of PDL1 and PDL2 on B cells can negatively regulate the GC response, by inhibiting Tfh recruitment into the follicle[209]. Once B-T cell help interactions are concluded, B cells will migrate to the centre of the follicle and initiate the GC response.

In recent years, a new population of regulatory T cells (Treg) called T follicular regulatory cells (Tfr), which express the *bona fide* Treg transcription factor FOXP3, have been shown to display regulatory properties within the GC response[210, 211]. Tfr cells play an important role throughout the GC process from the initiation of the GC response to the resolution of a GC and also contribute to the inhibition of autoantibody production[212]. The exact mechanism of Tfr cell regulation of the GC response is still being elucidated, however it is believed to involve expression of the co-inhibitory receptor cytotoxic T-lymphocyte associated protein 4 (CTLA-4) and to halt the expansion of both Tfh cells and GC B cells[213, 214].

1.1.3.6 Positive and negative selection of clones within the GC

Following the migration of activated B cells to the dark zone, centroblasts undergo SHM. SHM is the process by which stepwise point mutations are introduced into the Ig V genes. Both SHM and CSR is driven by the expression of AID, which deaminates cytidine residues in the Ig gene[215]. Due to the high rate of mutation and the fact that AID targets single stranded DNA at transcriptionally inactive sites, AID can damage the genome and lead to chromosomal translocations, thereby leading to GC lymphomas[216]. The high mutation rate generates successive BCR clones which change the affinity of the BCR, in a process known as affinity maturation.

After activation, B cells can change the isotype of their BCR through CSR from IgM and IgD to IgA, IgE or IgG, with each Ig isotype having distinct immunological functions. As with SHM, CSR requires the expression of AID. Recent studies have also implicated a role of the aryl hydrocarbon receptor (AHR) in the regulation of CSR, due to its direct binding and negative regulation of the *Aicda* gene[217]. Due to the excision of DNA regions during CSR, a stepwise approach to the induction of different Ig isotypes is maintained such that an IgG^+ B cell can switch to IgE^+, but not vice versa[197]. Selection of the relevant isotype is driven by T cell help[218, 219]. Until recently, GCs have been considered to be the main site where CSR takes place[220]. Using immunisation models and examining first germline transcripts (GLTs), a marker of CSR, Vinuesa and colleagues have recently shown that CSR takes place before GC or extrafollicular B cell differentiation stages at the B-T cell border. The authors suggest that this mechanism occurs as a way to restrict and prevent the long-term survival of B cell clones with pathogenic double-strand breaks[221].

Typically, proliferation and hypermutation of GC B cells occurs in the DZ. The B cell clones are then tested for affinity in the LZ, in a competitive manner, for antigen presented by FDCs[186]. Dependent on the mutations generated, B cell clones will undergo positive and negative selection events within the germinal centre. The germinal centre reaction is a dynamic process with a constant migration of GC B cells between the LZ and DZ compartments. All the meanwhile, GC B cells undergo successive cycles of SHM and proliferation and are prone to selective pressures within the GC. This holds true for clonal populations of cells, which will undergo contraction or expansion based on the relative fitness of the population[186]. The process of migration between the LZ to the DZ is known as cyclic re-entry and is required for a greater degree of affinity against an antigen[222]. Subsequent studies have provided experimental evidence for this process, using *in vivo* imaging to illustrate the bi-directional nature of GC B cells[223]. The transition into the LZ is contingent upon GC B cells undergoing a set number of cell divisions, and the downregulation of CXCR4 alone is not enough for migration to the LZ[185, 224]. It is estimated that 10-30% of B cells in the LZ re-enter the DZ after positive selection in the LZ[225].

In recent years, the mechanism of positive selection has been elucidated and confirmed by a number of *in vivo* studies. Antigen presented by FDCs in the LZ is retrieved by BCRs expressed by GC B cells in an affinity-dependent manner. GC B cells with a higher affinity BCR are more likely to retrieve the antigen than a GC B cell with a lower affinity BCR[226]. Antigen retrieved in this manner is presented to Tfh cells. By limiting the number of Tfh cells present in the LZ, GC B cell clones undergo selective pressure and compete for T cell help. The number of antigen loaded MHC class II molecules vary between different GC B cell clones, with GC B cells with high affinity BCRs taking up and processing more antigen on MHC class II molecules. A competitive advantage exists for GC B cells with increasing amounts of peptide MHC (pMHC) concentrations on their surface and it is these cells that have strong interactions with Tfh cells and receive signals for cyclic re-entry[227]. Contact duration of GC B cells with Tfh cells is increased in those cells with higher levels of pMHC[228]. This mechanism allows for an indirect sensing by Tfh of BCR affinity and shows that T cell help is required for the cyclic re-entry of GC B cells to the DZ[224, 229]. It is important to note, that the strength of T cell help will determine the number of cell divisions a GC B cell will undergo in the DZ and promotes the survival of a clonal population based on their 'fitness', by accumulating increased numbers of the same B cell clone[229]. Tfh production of IL-4, IL-21, BAFF and expression of CD40L are all key essential survival signals for GC B cells, with GC B cells exposed to increasing amounts of these signals based on the levels of surface pMHC[228, 230].

Re-entry into the DZ leads to the downregulation of pMHC on GC B cells, thus ensuring that any newly generated BCR can undergo successive cycles of selection and prevent any autoreactivity to self-antigen[231]. In addition, it has recently been discovered that soluble antibodies can compete with newly generated B cell clones for antigen expressed on FDCs, thus ensuring the survival of the clone with the highest affinity and preventing BCRs with overlapping specificities[232].

Due to the random nature of SHM, deleterious effects of hypermutation may also occur in the IgV gene leading to the recognition of 'self'. A number of checkpoints exist to regulate and eliminate any self-reactive B cell clones. An elegant study by Chan *et al* showed that self-reactive GC B cells are only eliminated if the self-

antigen is present in the GC microenvironment. GC B cells which recognise other tissue specific antigens were not subject to negative selection[233]. Complementing the elimination of self-reactive GC B cells, under certain conditions, anergic self-reactive $IgM^{lo}IgD^{+}$ GC B cells could re-enter the DZ to undergo SHM thereby eliminating autoreactivity in these clones[234].

It was previously thought that only a few clones could inhabit a single GC[235]. However, in recent years this view has been challenged. The number of clones inhabiting a single GC in the early stages of GC formation vary greatly, but can exceed more than 100. GCs can lose clonal diversity at varying rates dependent on a host of factors, including the strength of T cell help and based on the antigen-related properties. However, clonal bursts (rapid proliferation) of high affinity SHM variants can lead to loss of clonal diversity[236]. GC lifespan varies greatly, dependent on the type of immune stimulus. Certain vaccines or chronic viral infections, or indeed inflammation in autoimmune disease, can lead to GCs which remain active for long periods of time[237]. However, the requirements needed for long-term GC maintenance are not very well defined.

1.1.3.7 Mature B cell fate decisions

The cell fate decision for a mature B cell to either differentiate into a memory B cell or plasma cell occurs at two distinct stages, either at the T-B cell border when the mature B cell receives T cell help or after positive selection in the LZ[186]. B cells that are differentiating towards plasma cells are called plasmablasts and are defined by their continued proliferation, which ceases when a cell terminally differentiates to a plasma cell[238]. What determines this cell fate decision is still under intense study. Two key determinants in this response are the affinity and isotype of the BCR. As is the case for both at the B-T cell border and after positive selection in the GC, B cells with a higher affinity for antigen will preferentially differentiate into plasma cells. Antigen receptor signals are required for the initiation of this process, but T cell help is essential for the completion of differentiation[239]. Depending on the stage of activation of B cells in the GC process by their cognate antigen, these cells can either differentiate into short-lived or long-lived plasma cells (SLPCs or LLPCs). B cells which differentiate at the B-T cell border tend to be short-lived and remain in the peripheral lymphoid tissue. In contrast, GC B cells in the LZ can give rise to LLPCs and live for several months[238]. The isotype of the BCR also

influences plasma cell differentiation. Intriguingly, B cells with the IgE subclass favour differentiation into non-GC derived SLPC, and not MBCs or LLPCs[240].

The differentiation into plasma cells requires the induction of a transcriptional programme that enables the plasma cell to secrete large amounts of immunoglobulin, to relocate to different niches and to support the long-term survival of the cell. This programme is primarily driven by the expression of B lymphocyte-induced maturation protein 1 (BLIMP-1), encoded by PR domain zinc finger protein 1 (*Prdm1*), X-box binding protein 1 (XBP1) and IRF4 and through the silencing of the B cell transcriptional programme[238]. Due to the high immunoglobulin turnover, PCs are prone to ER stress from the accumulation of unfolded proteins. XBP1 is induced by endoplasmic reticulum (ER) stress and plays a particularly vital role in regulating the rate of immunoglobulin secretion, processing of *Igh* mRNA and in promoting an organised ER morphology in plasma cells[241, 242].

BLIMP-1 is essential for the differentiation programme of a mature B cell into a plasma cell. Rapidly dividing plasmablasts can be distinguished from PCs by their intermediate expression of BLIMP-1, in contrast to the high expression in plasma cells[243]. Although essential for the formation of mature plasma cells, BLIMP-1 is not required for the initiation of plasma cell differentiation, as shown by the generation of a pre-plasmablast population in its absence[244]. BLIMP-1 is primarily thought to suppress key regulators of the B cell programme. However, it has since been shown to have a multifactorial role in regulating the developmental programme of plasma cells[245]. As well as suppressing both *Aicda* and other B cell programme specific transcription factors, BLIMP-1 induces the transcription of the immunoglobulin genes, regulates the post-translational switch mechanism responsible for the production of a secretory form of immunoglobulin and recruits chromatin remodelling complexes to its target genes. BLIMP-1 is required for the induction of IRF4, another key transcription factor involved in the plasma cell differentiation programme, thus illustrating the essential role of BLIMP-1 in orchestrating an interconnected transcriptional programme[245]. IRF4 itself is important in the induction of *Prdm1* and is essential for the differentiation of plasma cells and for promoting their survival[246]. In the absence of IRF4, plasma cells fail to survive[247, 248]. Despite the notable functional and phenotypical differences

between SLPCs and LLPCs, the transcriptional programme governing the fate decision between these two populations remains largely unknown. A recent study has illustrated the role of the zinc finger protein ZBTB20 in establishing a pool of LLPCs in response to some immunisations, but not others[249].

Once a cell differentiates into a plasma cell, it migrates from the GC and homes primarily to the bone marrow niche. However, other tissue-specific niches have been described within the spleen and lymph nodes[250]. Exit from the lymphoid tissue requires the upregulation of $S1P_1$[197]. Plasma cells upregulate different chemokine receptors required for homing to their respective niches. For migration to the bone marrow CXCR4 expression is required, whilst homing to the gut requires expression of CCR9 and CCR10[197]. Whilst in their respective niches LLPCs receive survival signals that promotes their survival. The extent to which their longevity is down to survival signals in the niches versus the intrinsic features of the LLPCs is not clear[197].

In contrast to plasma cells, the cell derived signals and transcription factors controlling memory B cell (MBC) differentiation are much less well characterised. Much like in plasma cells, MBC differentiation is influenced by the BCR isotype, as well as by signals through CD40 and cytokines. IL-9, for instance, promotes the generation of memory B cells[251]. Unlike the defined transcriptional programme of plasma cells, no unique transcription factor of MBC differentiation has been identified. However, GC B cells which express higher levels of BACH2 have the propensity to seed the MBC pool[252].

Historically, it was thought that all MBCs had undergone CSR and were derived from GC B cells. Later this notion was revised, as BCL6 deficient B cells, which can't form GC, differentiated into IgM and IgG1 MBCs in the spleen, suggesting that not all MBCs go through the GC reaction[253]. However, GC B cells still give rise to a large proportion of the MBC pool[254]. For the most part MBCs are a recirculating population of cells, but they can also be tissue resident[255]. MBCs found in the lymph nodes, are located in the subcapsular niche, which predisposes MBCs to rapid exposure to antigen[256]. Shlomchik and colleagues showed that the MBC pool in mice can be divided into 5 populations based on their expression of PD-L2, CD80 and CD73, with these populations differing in their ontogeny and

selection[257]. It has since been shown that $CD80^{-}PD\text{-}L2^{-}$ MBCs mainly seed the GCs, whilst $CD80^{+}PD\text{-}L2^{+}$ MBCs rapidly differentiate into plasma cells, upon rechallenge with a TD antigen[258].

Upon re-exposure to antigen, MBCs can migrate to the bone marrow and rapidly differentiate into LLPCs[254]. The predisposition of MBCs to differentiate into LLPCs upon antigen exposure, seems partially dependent on the downregulation of BACH2[252]. The notion that MBCs, in a secondary response to antigen, are the main source of B cells to enter the GC has recently been challenged. Instead, naïve B cells without prior GC exposure appear to be the main source of cells which repopulate the GCs (over 90%) in a secondary response to an antigen[259]. B cell maturation in the spleen and the signals and transcription factors which define these processes are summarised in Figure 1.2.

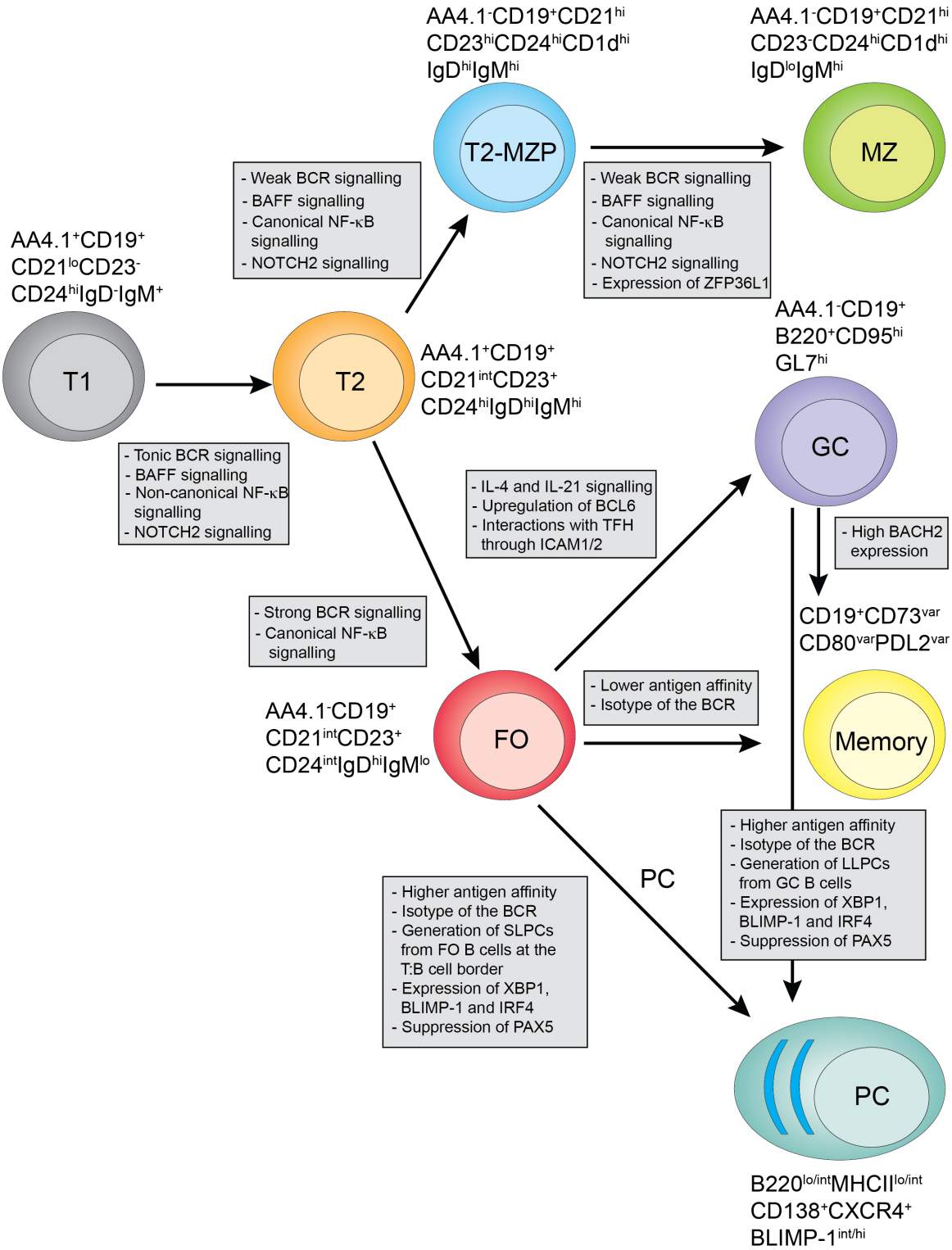

Figure 1.2. B cell differentiation in the spleen. Transitional 1 B cells in the periphery migrate to the spleen, upon where they differentiate into T2 precursors seeding both the MZ and FO B cell pools. FO B cells, upon encounter with antigen, can directly differentiate into SLPC, memory B cells or GC B cells. GC B cells can either reseed the GC, give rise to LLPCs or memory B cells, dependent on the strength of BCR signalling and on the isotype of the BCR.

1.1.4 B cells as orchestrators of the immune response

Although B cells are primarily recognised for their role in producing antibodies, B cells can also co-ordinate immune responses through antigen presentation and through co-stimulatory signals[1]. One of the features of B cells is their ability to act as an antigen presenting cells (APC). Native antigen captured by the BCR can be endocytosed, loaded onto MHCII molecules and presented to CD4 and CD8 T cells. Alternative means of access to antigen for presentation by MHC molecules include fluid phase pinocytosis and macroautophagy[260]. However, BCR mediated presentation is by far the most efficient mechanism of antigen presentation[261]. Multiple factors contribute to the efficiency of BCR-mediated antigen presentation. Firstly, the high affinity of the BCR allows for the efficient capture of antigens, even at very low concentrations. Secondly, B cells can retain their antigen-BCR complexes for extended periods of time allowing time for the cognate recognition of the antigen by T cells[262]. The locale of mature B cells and their ability to survey the secondary lymphoid tissue makes encounter with their specific antigen much more likely. Lastly, antigen-specific MHCII activate their cognate T cell and leads to the upregulation of co-stimulatory molecules on both B and T cells. Antigen activation of the BCR leads to the upregulation of CD80 and CD86, alongside MHC class II, which interact with CD28 and the T cell receptor (TCR) on T cells respectively[260]. B cells are also important for the presentation of lipid antigens to iNKT cells, leading to iNKT activation and suppression of excessive inflammation[263, 264].

Cytokine production by B cells is important for shaping the immune response and the development of lymphoid tissue, both positively and negatively regulating immune cell activation[265]. Harris *et al* showed that cytokine secreting B cells could be divided into two distinct effector populations, B effector 1 (Be1) and Be2, based on the microenvironmental cues that the B cells receive. Be1 cells produce interferon-γ (IFNγ) and TNFα, whilst Be2 produce IL-4, IL-6 and IL-13 *in vitro*, which could subsequently influence the differentiation of naïve $CD4^+$ T cells into Th1 or Th2 cells respectively. In addition, the authors identified that Be1 were increased in *Toxoplasma gondii* infected mice, whilst Be2 cells were the predominant cytokine producing B cells in *Heligomosomoides polygyrus* infected mice; two microorganisms known to induce Th1 and Th2 type responses respectively[266].

Since this seminal study, the reported list of cytokines produced by B cells have grown, with demonstrated roles in shaping T helper cell and innate immune responses. EBV transformed mouse B cells produce IL-5, which promotes the proliferation of eosinophil precursors[267]. Moreover, B cell expression of lymphotoxin and tumour necrosis factor α (TNFα) are required for the formation of B cell follicles in the spleen and in the development of follicular dendritic cells[268, 269, 270].

Cytokines produced by B cells can also shape T helper cell differentiation into Th1, Th2, Th17 or Tfh cells. B cells produce IL-2 in response to *H polygyrus* and *T gondii*. In turn, IL-2 produced by B cells promotes the polarisation of naïve $CD4^+$ T cells to Th2 cells and the formation of memory T cells[271]. The cytokine granulocyte-macrophage colony-stimulating factor (GM-CSF) activates DCs that promote Th1 differentiation[272]. GM-CSF production by B-1a cells is important for the survival of mice from *Escherichia coli* and *Streptococcus pneumoniae*. GM-CSF produced by these cells acts in an autocrine manner and promotes the rapid production of natural polyclonal IgM[273]. Furthermore, GM-CSF production by $CD138^{hi}IgM^{hi}B220^+CD21^-CD23^-CD43^{hi}VLA4^{hi}$ plasma cells expands the numbers of classical dendritic cells that promote Th1 responses and increases inflammation in atherosclerosis[274]. Another important cytokine produced by B cells with pleiotropic functions is IL-6. Production of IL-6 leads to the expression of IL-21 in $CD4^+$ T cells and influences Tfh differentiation[275]. Furthermore, IL-6 activates both Th1 and Th17 cells in experimental autoimmune encephalomyelitis (EAE)[276, 277]. Lastly, B cells are also able to secrete IL-17A and IL-17F. Modification of CD45 by *T. cruzi* trans-sialidase leads to the induction of IL-17 in mouse extrafollicular IgM^{hi} plasmablasts and in human B cells[278].

B cells are also known to produce chemokines including CCL3, CCL4, CCL17 and CCL22, which are important for the recruitment of immune cells in infection and play a role in the pathogenesis of autoimmune diseases. CCL3 is a chemoattractant that binds to the chemokine receptors CCR1, CCR3 and CCR5 on a wide variety of cell types, including T cells[279]. B cell derived CCL3 in *T. gondii* infection recruits $CD4^+$ T cells and enhances $CD4^+$ T cell IFN-γ production[280]. On the other hand, recruitment of Tregs to B cells or other APCs is facilitated by the expression of CCL4[281]. Both the closely related chemokines CCL17 and CCL22

are expressed by B cells and are important in the recruitment of activated T cells, primarily Th2 cells and $CD4^{+}CD25^{+}$ Tregs[282, 283, 284, 285].

B cells are also a crucial source of anti-inflammatory cytokine mediators important for the resolution of inflammation. Dependent on the inflammatory context, B cells can produce IL-35, transforming growth factor beta (TGF-β1) and IL-10, which will be discussed in depth in the next section.

1.2 Regulatory B cells

1.2.1 Introduction to the field

Regulatory B cells (Bregs) is a collective term given to B cells that suppress or regulate inflammation and promote tolerance through a variety of mechanisms. Historically, Breg function has been identified by their role in regulating pathogenic T cell responses, but this has been expanded to show that Bregs can influence a wide variety of other cell types, including conventional dendritic cells (DCs), iNKT cells and monocytes, amongst others[286].

The suppressive function of B cells was first proposed in the 1970's in studies examining delayed type hypersensitivity (DTH) reactions using either 2,4 dinitrofluorobenzene (DNFB) or ovalbumin (OVA) in incomplete Freud's adjuvant (IFA) or paraeminobenzoic acid-Hen egg albumin conjugate (PABA-HEA) in guinea pigs. Increased intensity and prolonged DTH reactions were observed in B cell depleted DNFB sensitised guinea pigs[287]. Later studies showed that adoptive transfer of lymphocytes or total splenocytes suppressed the intensity of the DTH response[288, 289]. These cells were dubbed "suppressor B cells". However, the mechanisms behind the suppressive response were never investigated and the study of B cell regulation was not renewed until the 1990's, when it was observed that B cell deficient mice developed an exacerbated form of EAE[290]. After these initial observations, three key studies identified that B cell mediated suppression was dependent on the expression of IL-10 in mouse models of colitis, EAE and collagen induced arthritis (CIA), as will be discussed throughout this section[291, 292, 293]. IL-10-expressing B cells were coined as regulatory B cells; a term which now encompasses a wide variety of subsets and mechanisms of suppression.

1.2.2 Signals required for Breg differentiation

Evidence in the literature shows that Bregs increase in response to inflammatory signals. Although far away from having identified all the signals that induce their differentiation, it appears that Bregs differentiate in response to a combination of pro-inflammatory cytokines and in response to activated T cells and plasmacytoid dendritic cells (pDCs). The current extent of our knowledge is hampered by the lack of a transcription factor unique to Bregs, and the reliance on looking at IL-10 expression and suppressive capacity to define and identify Bregs. In the context of this thesis, I define Breg differentiation as the ability of a precursor population to

acquire the ability to start producing IL-10 and to become suppressive. The stimuli known to be involved in the differentiation of murine Bregs are summarised in Figure 1.3.

1.2.2.1 BCR and antigen specificity

Although the role of antigen specificity in the function of Bregs remains to be fully elucidated, there are several lines of evidence suggesting that antigen specificity plays a role in the differentiation of Bregs. EAE is the most commonly used experimental model to examine autoimmune inflammatory disease of the central nervous system and shares some of the clinical features associated with multiple sclerosis in humans. To induce EAE, mice are immunised with the myelin oligodendrocyte glycoprotein (MOG) antigen in complete Freund's adjuvant (CFA)[294]. Chimeric mice reconstituted with MD4 B cells that carry the IghelMD4 transgene and therefore specifically recognise the HEL antigen[295], developed a more severe course of EAE disease, compared to mice reconstituted with wild type (WT) B6 B cells[292]. These results suggest that in EAE, B cells require activation through the BCR by the MOG antigen to elicit suppressive function. Supporting this data, MD4 mice have reduced frequencies of splenic IL-10-producing $CD1d^{+}CD5^{+}$ B cells (B10); a population previously ascribed with regulatory capacity[296]. In CIA, type II collagen (CII) antigen activation of the BCR enhances CD40-induced IL-10 production in total B cells and in T2-MZP B cells[293, 297]. Moreover, adoptive transfer of T2-MZP B cells isolated from mice immunised with MOG in CFA, failed to suppress the development of arthritis (unpublished data). It is important to note that in this experiment mice were immunised with CII in CFA following the adoptive transfer of T2-MZP B cells. A role of self-antigen in the differentiation of Bregs has also been proposed. TgV_H3B4 mice which have polyreactive natural antibodies against self-antigens such as actin and keratin, have increased numbers of B10 cells. Indeed, immunisation with actin increased the numbers of B10 cells in these mice, suggesting that positive selection of B10 cells occurs through self-antigen activation of the BCR[298].

Both the strength of BCR activation and activation of its downstream signals are involved in the induction of IL-10. Mice with a loss-of-function point mutation in p110δ, a PI3K subunit downstream of the BCR, develop spontaneous inflammatory bowel disease (IBD), implicating that BCR activation plays an important part in the

differentiation of Bregs[299]. Although no link was made in this study, it could be that BCR driven IL-10 production was reduced in these mice, as *Il10*$^{-/-}$ mice develop a similar spontaneous form of colitis[300]. B cell expression of stromal interaction molecules (STIM) 1/2 is required for BCR driven IL-10 production in B10 cells[301]. BCR activation triggers store-operated Ca^{2+} influx and this process requires the endoplasmic reticulum calcium sensors STIM1/2[302]. B10 cells from mice lacking expression of STIM1/2 exclusively on B cells (*Stim1*$^{f/f}$*Stim2*$^{f/f}$*Mb1*$^{cre/+}$) have a marked reduction of secreted IL-10, following stimulation with LPS+anti-IgM compared to B10 cells from *Mb1*$^{cre/+}$ controls, due to decreased activation of NFAT. As a result of the reduced IL-10 production by B cells, these mice developed a more severe EAE compared to WT mice. Adoptive transfer of IL-10-IRES-GFP transduced *Stim1*$^{f/f}$*Stim2*$^{f/f}$*Mb1*$^{cre/+}$ B cells into μMT recipient mice, reduced the severity of EAE, corroborating the role of the BCR in the suppressive function of Bregs[301].

The BCR co-receptors are also involved in the differentiation of Bregs. Mice lacking the co-receptor CD19, develop exacerbated inflammation in a number of models of inflammation including contact hypersensitivity (CHS), spontaneous models of lupus and dextran sulfate sodium (DSS) induced colitis, whilst overexpression of CD19 increases Breg number and reduces inflammation in CHS[303, 304, 305, 306].

1.2.2.2 CD40 and other cognate interactions with T cells

CD40 is a co-stimulatory transmembrane receptor, expressed on B cells, DCs, macrophages, monocytes and in some non-haematopoietic cells such as endothelial cells. Expression of CD40 is required for a wide range of B cell functions including, but not limited to, formation of GCs, CSR, induction of cytokines, lowering the threshold required for BCR signalling and for upregulating the expression of MHCII and other co-stimulatory receptors[307]. CD40 activation is a key inducer of cytokines in B cells, with known roles in promoting the expression of IL-6, IL-10, IL-12, LTα, TGF-β and TNFα[308].

Ever since the first studies identifying and characterising Bregs, CD40 has been linked to the differentiation of Bregs. Mizoguchi and colleagues were the first to identify a role of CD40, CD80 and CD86 in B cell mediated suppression, using adoptive transfer of B cells into *Tcrα*$^{-/-}$*μMT* mice. *Tcrα*$^{-/-}$ mice develop a

spontaneous form of chronic colitis resembling ulcerative colitis in humans. Unlike untreated B cells, B cells treated with blocking anti-CD40, anti-CD80 or anti-CD86 antibodies before adoptive transfer to $\alpha\mu^{-/-}$ mice were unable to limit the pathogenic function of $\alpha^{-}\beta^{low}$ T cells in colitis[309]. A regulatory role of B cell CD40 was further demonstrated in EAE and CIA models. Activation with antigen (either MOG 35-55 or CII respectively), in combination with agonistic anti-CD40 increased IL-10 expression in B cells[292]. Chimeric mice lacking CD40 on B cells developed a severe course of EAE[292]. Similarly, in CIA, adoptive transfer of collagen and agonistic anti-CD40 stimulated B cells suppressed induction of disease[293].

MRL/*lpr* mice develop a spontaneous form of autoimmune disease characterised by anti-double stranded DNA antibodies and immune complex-associated disease of the kidney and is one of the experimental models used to determine the aetiology of systemic lupus erythematosus (SLE)[310]. Disease progression in MRL/*lpr* mice is characterised by a marked decrease in T2-MZP B cell numbers. Moreover, adoptive transfer of T2-MZP B cells from MRL/*lpr* mice, unlike control T2-MZP B cells as described above, failed to improve the mortality rate of recipient MRL/*lpr* mice[311]. Suppressive capacity was restored to MRL/*lpr* T2-MZP B cells after activation with an agonistic anti-CD40[311]. The requirement for CD40 is not limited to T2-MZP derived Bregs, as adoptive transfer of B10 cells from *Cd40*$^{-/-}$ mice fail to confer protection from EAE in WT recipient mice[312].

CD80 and CD86 (historically known as B7.1 and B7.2) are two co-stimulatory molecules which are expressed on B cells, bind to CD28 or CTLA-4 on T cells and regulate T cell activation[313]. As mentioned earlier, CD80/86 are key for B cell suppression of colitis[309]. Furthermore, in EAE, mice lacking CD80/86 on B cells failed to enter the remission phase of disease, suggesting that B cell expression of CD80/86 is required for the resolution of EAE[314].

1.2.2.3 Toll like receptors

TLRs are pattern recognition receptors (PRRs), which respond to signals from infection and cellular/tissue damage, via the recognition of pathogen-associated molecular patterns and damage-associated molecular patterns respectively. TLRs are one class of a bigger family of PRR receptors, including retinoic acid inducible gene 1-like receptors, nucleotide oligomerization domain-like receptors and C-type

lectin receptors. Following engagement of TLRs, downstream signals are mediated either by myeloid differentiation primary-response protein 88 (MYD88) or TIR domain-containing adaptor protein inducing IFNβ (TRIF). Activation of TLRs initiates signalling cascades that leads to downstream activation of NF-κB, IRFs and the MAP kinases. TLR activation promotes B cell differentiation and initiation of cytokine production[315]. Murine B cells express varying levels of TLR1-9, and even between B cell subsets there are marked differences in expression patterns of TLRs. B cells are particularly responsive to TLR2, TLR4, TLR7 and TLR9 agonists, with selective agonists preferentially inducing more IL-10, IL-6 or IL-12p40. Of note, TLR2 agonist peptidoglycan, TLR4 agonist lipopolysaccharide (LPS) and TLR9 agonist CpG-B induces the most IL-10 production by B cells[316]. B cells can upregulate IL-10 in a TLR2-dependent manner, upon administration of tumour cell-released autophagosomes or upon activation with *Helicobacter pylori* sonicate[317 318].

The role of TLR4 in Breg function has been extensively studied in multiple Breg subsets. LPS activation of B cells increases the expression of IL-10, TGF-β1 and FASL, which promotes Breg-mediated suppression of pro-diabetogenic Th1 responses in NOD mice[319]. In addition, TGF-β1 expression by B cells can induce anergy in $CD8^+$ T cells[320]. Subsequent reports have extended these findings to show that TLR4 promotes Breg function in autoimmunity and infection models. Intraperitoneal injection of LPS delays the onset of EAE[321]. Although the authors never addressed the mechanism of action, considering the wealth of evidence linking TLR4 activation to B cell IL-10 production, it is tempting to speculate that the delayed onset could be due to the initial burst of IL-10 production by B cells[321]. Indeed, supporting this idea, LPS administration to mice before the induction of cerebral ischemia, reduced infarct volumes and protected mice from neuronal apoptosis. LPS pre-conditioned mice had elevated levels of IL-10 in the brain and increased numbers of $IL\text{-}10^+CD19^+$ cells in the spleen[322]. LPS, either alone or in combination with other inflammatory signals, supports the differentiation of T2-MZP, B10, $CD138^+$ plasma cells and $LAG3^+CD138^{hi}$ plasma cell Breg subsets[303, 323].

Central to both TLR2 and TLR4 is the signalling through the adaptor protein MYD88. Deletion of MYD88 in B cells lead to the prolonged survival of mice

infected with *S. typhimurium*, and this was associated with a reduction in IL-10 production by $CD138^+$ plasmablast cells[324]. Moreover, chimeric mice lacking MYD88 in B cells developed an exacerbated EAE, compared to WT mice[325]. Furthermore, in WT mice infected with *Leishmania donavani*, signals through MYD88 are important for differentiation of Bregs. MZ B cells from infected mice suppressed $CD4^+$ and $CD8^+$ T cell responses through expression of IL-10 and suppressed the protective T cell responses during *L. donavani* infection[326]. Thus, these studies show a central role of MYD88 in TLR mediated Breg differentiation.

Although much less characterised, signals through TLR7 have also been implicated in the generation of Bregs. Both *in vivo* and *in vitro* activation of B cells with the TLR7 agonists imiquimod or R848 induce the expression of IL-10 in B cells, with the highest proportion of IL-10 being expressed by $CD19^+CD1d^{hi}$ B cells. Adoptive transfer of $CD19^+CD1d^{hi}$ B cells protects recipient mice from developing allergic lung inflammation by promoting the differentiation of naïve $CD4^+$ T cells into Tregs in an IL-10 dependent manner[327]. Several studies have also shown that R848 induces IL-10 production in human mature ($CD19^+CD27^+$) and immature ($CD19^+CD27^-$) B cells, suggesting a role of TLR7 in the differentiation of both human and murine Bregs[327, 328, 329].

Disentangling the role of TLR9 in Breg differentiation has been harder to establish. Although, TLR9 activation is a potent inducer of IL-10 in both mouse and human B cells, there have been conflicting reports as to the role of TLR9 in Breg induction *in vivo*[316, 330, 331]. Chimeric mice reconstituted with *Tlr9*$^{-/-}$ B cells did not develop a worse course of EAE compared to B-WT controls, implicating a functional redundancy of the TLR9 pathway in Breg mediated suppression, at least in the context of EAE[325]. In contrast, several studies have shown that TLR9 activated Bregs limit inflammation in models of autoimmunity and sepsis. TLR9 activated $CD5^+CD23^-$ B cells inhibited pro-inflammatory cytokine production by pDCs and conventional DCs *in vitro*, through the production of IL-10. Moreover, mice given CpG-B are protected from D-galactosamine induced endotoxic shock; a process driven through TLR9-induced IL-10 production by $CD5^+CD23^-$ B cells. In support of this data, adoptive transfer of *Tlr9*$^{-/-}$ B cells failed to promote the survival of *Il10*$^{-/-}$ recipient mice, unlike in *Il10*$^{-/-}$ mice receiving WT B cells, which prevented endotoxic shock[332]. TLR9 activation also induces IL-10 expression in neonatal

$CD5^+$ B cells, which in turn inhibits DC driven Th1 priming[333]. Lastly, two studies by Gray and colleagues showed that apoptotic cells (ACs), through activation of TLR9, increased IL-10 production by MZ B cells and B-1a cells. Mice receiving AC stimulated B cells reduced CIA and EAE disease severity[330, 334]. Thus, the role of TLR9 in Breg differentiation and function seems to be disease and cell type specific.

1.2.2.4 Cytokines as inducers of Breg differentiation

It is now well established that inflammatory signals can promote the differentiation of Bregs. To date, numerous cytokines from different cellular sources have been shown to facilitate the induction and expansion of Breg populations in a variety of models of autoimmunity, infection and transplantation. Of particular note, it has been shown that the composition of the microbiota can provide signals for the differentiation of Bregs[323]. Adoptive transfer of T2-MZP B cells from antibiotic (ABX) treated mice to recipient WT mice, failed to alleviate antigen induced arthritis (AIA) in recipient mice, due to a reduction in T2-MZP B cell IL-10 production[323]. In addition, T2-MZP B cells isolated from specific-pathogen free (SPF) housed mice, present with a marked reduction in IL-10^+Bregs compared to conventionally housed mice, implicating that microbiota is required for the induction of IL-10^+Bregs. Of note, both in ABX treated mice and in SPF housed mice, there was a significant reduction of the frequency and numbers of splenic IL-1β and IL-6 producing macrophages ($CD11b^+CD11c^-$). Stimulation of T2-MZP B cells with a combination of these two cytokines and agonistic anti-CD40 increased the frequencies of IL-10^+Bregs (T2-MZP, B10 and TIM-1^+ subsets). Chimeric mice lacking the IL-1R1 or IL-6R specifically on B cells (*B-Il1r1*$^{-/-}$ or *B-Il-6r*$^{-/-}$) developed an exacerbated arthritis, further linking these two inflammatory cytokines to Breg differentiation and function. Importantly, 70% of splenic T2-MZP B cells expressed the integrin $\alpha4\beta7$; a marker which indicates that lymphocytes have previously recirculated via the gut[335]. The $\alpha4\beta7^+$ T2-MZP B cells displayed enhanced suppressive capacity, compared to $\alpha4\beta7^-$ T2-MZP B cells[323]. Collectively, this data suggests that the precursors of Bregs may be primed initially in the gut and upon exposure to inflammatory stimuli in the spleen, then differentiate into IL-10^+Bregs[323].

IL-21 is a versatile cytokine with broad functions in the innate and adaptive immune response and is mainly produced by Tfh, Th17, $CD8^+$ and NKT cells. In B cells, IL-21 has a role in plasma cell differentiation, IgG1 production and more recently has been identified to be important in Breg differentiation[336]. B10 cell differentiation requires both IL-21 and CD40:CD40L interactions with T cells[312]. Adoptive transfer of B10 B cells from *Il21r*$^{-/-}$, *Cd40*$^{-/-}$ and *Mhc-II*$^{-/-}$ mice failed to alleviate EAE in recipient mice, unlike their WT counterparts, further suggesting a role of IL-21 in the differentiation and function of B10 cells[312]. Moreover, addition of IL-21 to anti-IgM and anti-TIM-1 cultured B cells further increased IL-10 production in TIM-1^+Bregs[337]. These findings have been translated to human Breg populations, with IL-21 in combination with signals through the BCR or with TLR9 and CD40, inducing IL-10 and/or Granzyme B expression in B cells, depending on the co-stimuli used[338 339].

Interestingly, both BAFF and APRIL, two key cytokines involved in B cell maturation and survival, are important inducers of IL-10 production in both mouse and human B cells[76]. Administration of BAFF *in vivo* and *in vitro*, induced IL-10 in MZ B cells[340]. In addition, BAFF increased IL-35 expression, another immunoregulatory cytokine expressed by Bregs, mainly in a population exhibiting a MZ B cell phenotype in *MRL/lpr* mice[341]. Likewise, addition of BAFF to CpG-B stimulated B cells also induced human Breg differentiation in healthy controls (HC) and in chronic lymphocytic leukaemia (CLL) patients. Importantly though, this seems to be in part, an indirect effect of the pro-survival function of BAFF on these cells[342].

APRIL can also confer immunosuppressive function to B cells, primarily through inducing IL-10 expression in B-1a cells. Mice overexpressing APRIL (APRIL-tg) are protected from EAE and oxalazone induced CHS reactions[343]. APRIL-tg mice depleted of peritoneal B-1a cells negated the protective effect of APRIL in EAE[344]. Similarly, APRIL can increase IL-10 expression in both HC and rheumatoid arthritis (RA) B cells[343] and induces naïve human B cells to differentiate into IL-10-secreting IgA^+PD-$L1^+$ Bregs[344].

A number of cytokines share the ability to promote both Treg and Breg differentiation in mice. IL-33 for instance, induces a novel form of Breg defined as

$CD19^+CD25^+CD1d^{hi}IgM^{hi}CD5^-CD23^-TIM1^-$ (subsequently coined Breg-IL-33). Injection of IL-33 into WT mice increases the frequencies of IL-10^+Bregs found in the blood. Adoptive transfer of the Breg-IL-33 precursor population ($CD19^+CD23^-$ B cells) from IL-33 treated mice into *Il10*$^{-/-}$ mice, markedly delayed onset of IBD in these mice and reduced gut histopathological signs associated with IBD. Moreover, adoptive transfer of $CD19^+CD23^-$B cells from IL-33 treated *Il10*$^{-/-}$ mice failed to confer protection from IBD, suggesting that IL-33 primes Breg function by increasing the expression of IL-10[345]. These findings were confirmed in DSS colitis, where IL-33 induced IL-10^+Breg differentiation in the mesenteric lymph nodes (MLNs) of mice[346]. In addition, IL-35 expands an IL-10^+IL-35^+Breg population in both mice and humans, as will be discussed later[347]. Lastly, IL-5 has been shown to promote the function of killer B cells; a population which mediates cell death through the expression of FASL[348]. IL-5 in tandem with CD40L signalling, induces IL-10 expression in B cells and promotes the antigen-specific killing of $CD4^+$ T cells[349].

Whilst no study to date has implicated a role of IFNα in driving Breg IL-10 in mice, pDC driven IFNα expression expands human IL-$10^+CD24^{hi}CD38^{hi}$ Bregs in healthy controls, in a dose dependent response. In healthy controls, low levels of IFNα expands IL-$10^+CD24^{hi}CD38^{hi}$ Breg numbers, and Bregs in turn suppress pDC driven IFNα production. In contrast, high levels of IFNα produced by pDCs in SLE patients induces the differentiation of plasmablasts and fails to expand Breg numbers, suggesting that the strength and dose of inflammatory stimuli is important for determining regulatory versus effector B cell fate decisions[350].

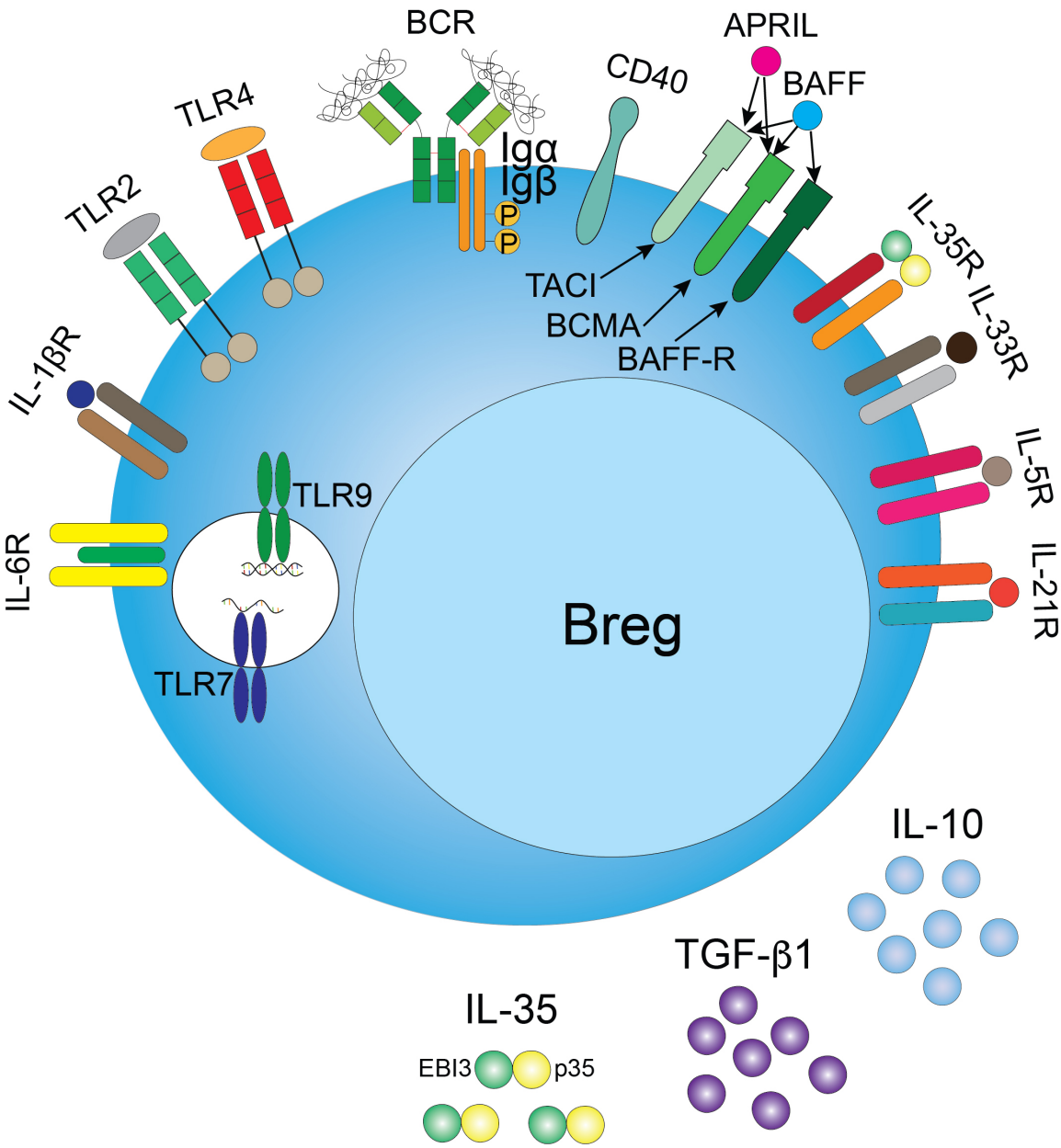

Figure 1.3. Stimuli that induce murine Breg differentiation. The expanding list of inflammatory stimuli which induce Breg differentiation includes signals through the BCR, TLR and CD40 ligation and activation through various cytokine receptors. Activation of Bregs induces the expression of IL-10, IL-35 and TGF-β1.

1.2.3 Regulatory B cell Phenotype and Mechanisms of suppression

Bregs are defined by the ability to suppress inflammation primarily through the production of IL-10, but also through alternative means of suppression such as TGF-β1 or IL-35 and by contact-dependent mechanisms. The ontogeny of Bregs and their relation to conventional B cell development remains elusive. However, it is becoming increasingly clear that Bregs can arise at various stages of B cell development and that the common denominator in Breg differentiation at different stages, as described above, is the presence of inflammatory signals. Murine Breg subsets and mechanisms of immune suppression are summarised in Figure 1.4. In disease settings, Breg numbers and their function can be perturbed. In the case of autoimmunity, the numbers and function of Bregs are often diminished[351], whilst Breg IL-10 often promotes cancer progression[352]. What pre-determines the Breg vs Beffector cell fate decision is unknown and remains an important relevant question to address in the clinical setting.

1.2.3.1 Transitional-2 Marginal Zone Precursor Cells

Building on previous findings showing that anti-CD40 stimulated B cells suppressed CIA through the provision of IL-10[293], further characterisation of Bregs revealed that T2-MZP B cells (defined as $CD19^{+}CD21^{hi}CD23^{hi}CD24^{hi}IgM^{hi}IgD^{hi}CD1d^{hi}AA4^{+}$) were the main producers of IL-10 in CIA[297]. Importantly, the frequency of IL-10^{+}T2-MZP B cells were increased in the remission phase of CIA and displayed greater suppressive capacity upon adoptive transfer than their antigen naïve counterparts, suggesting inflammatory signals were needed for Breg differentiation. No suppression was observed after the adoptive transfer of MZ and FO B cells[297]. T2-MZP reduced disease severity by decreasing the levels of CII specific IgG2a antibodies in the serum and by inhibiting $CD4^{+}IFN\gamma$ production. Importantly, only IL-10-sufficient T2-MZP B cells could suppress CIA, upon adoptive transfer highlighting Breg suppressive function was contingent upon IL-10 expression[297]. The importance of T2-MZP Bregs in autoimmunity, was also confirmed in MLR/*lpr* mice, which develop a spontaneous severe systemic lupus-like autoimmune disease[311], as described in section 1.2.2.2.

Further mechanistic insight into IL-10^{+}T2-MZP Breg function was elucidated in AIA, a T-cell driven DTH model which mimics some of the pathological characteristics seen in RA[353]. IL-10^{+}Bregs were shown to be important for the induction of

forkhead box P3 (FOXP3) Tregs and Tr1 cells[354]. Indeed, *Il10*$^{-/-}$ B cell chimeric mice had reduced numbers of FOXP3 Tregs in the inguinal draining lymph nodes (dLN) and in the synovia of the joint, mirrored by an increased frequency of IFN-γ^+ and IL-17$^+$ CD4$^+$ T cells, implicating IL-10$^+$Bregs in the differentiation fates of naïve CD4$^+$ T cells in this model. *Il10*$^{-/-}$ B cells displayed reduced contact times with WT CD4$^+$ T cells, in comparison to WT B cells, suggesting that, in addition to IL-10, Bregs can regulate immune responses by cell-contact dependent mechanisms. Suppressive function of T2-MZP Bregs or T2-like Bregs has also been shown to be important in infection, cancer and transplantation models and in allergic hypersensitivity reactions. In the latter, infection of WT mice with *Schistosoma mansoni* conferred protection from anaphylaxis reactions and chronic airway hyperresponsiveness, due to parasite driven upregulation of IL-10 by B cells[355, 356, 357].

Whilst IL-10 production is still considered a hallmark of Breg identity and function, IL-10 independent mechanisms are also a big part of the Breg 'arsenal' in restraining inflammation in a variety of settings and diseases. CD1d is an MHC class I-like antigen presenting molecule, which presents glycosphingolipid and phospholipid antigens to iNKT cells. Within the B cell populations, CD1d is highly expressed on MZ and T2-MZP B cells[358]. High expression of CD1d is commonly expressed by different Breg subsets[286]. T2-MZP Bregs have been shown to confer immunosuppressive function to iNKT cells, in an IL-10 independent manner, through the expression of CD1d[264]. Chimeric mice lacking CD1d on B cells develop an exacerbated arthritis compared to WT mice. Moreover, whereas adoptive transfer of WT T2-MZP B cells was able to ameliorate arthritis in recipient mice, adoptive transfer of *Cd1d*$^{-/-}$ T2-MZP B cells failed to suppress AIA. T2-MZP B cells from α-galactosylceramide (α-GalCer) treated WT mice, presented α-GalCer on CD1d and enhanced iNKT suppression of CD4$^+$ IFN-γ and IL-17 production, implicating a crucial role of B cell CD1d expression in the amelioration of arthritis in this setting. It is important to note that even though MZ B cells express the highest level of CD1d amongst the B cell subpopulations, MZ B cell depletion did not impact α-GalCer mediated suppression in this study[264].

1.2.3.2 MZ B cells

MZ B cells can also produce IL-10 in response to a wide range of TLR agonists, including LPS and CpG[316]. Injection of mice with ACs ameliorates CIA disease, through the production of B cell IL-10. In this setting, MZ B cells secreted the most IL-10 in response to AC driven TLR9 activation. Although not directly demonstrated experimentally in this study, the authors reasoned that MZ B cells were the subset responsible for AC-induced protection from CIA[334]. Subsequent research by the Gray group has later shown that B-1a cells are the main cells which carry out immune tolerance to apoptotic cells[359]. MZ B cells have also been shown to be detrimental to survival of mice with *Listeria monocytogenes,* due to their production of IL-10. Adoptive transfer of MZ B cells into *Il10*$^{-/-}$ mice increased bacterial load in the spleen of recipient mice. Importantly, MZ B cell deficient mice (*Rbpj* conditional KO) developed resistance to *L. monocytogenes* infection and prolonged the survival of infected mice[360].

In addition to IL-10, a subset of MZ B cells can also produce TGF-β1. Adoptive transfer of activated B cells producing TGF-β1 have been shown to suppress diabetes incidence, through reducing T cell IFN-γ expression in pre-diabetic NOD mice and leading to the apoptosis of diabetogenic T cells. Although not directly attributed to MZ B cells, increased levels of apoptosis were seen in the MZ area of the spleen of mice adoptively transferred with activated B cells, suggesting these cells were the likely source of TGF-β1[319]. TGF-β1 expressing B cells have since been shown to control Treg induction and to promote immune tolerance. Whilst the exact phenotype of TGF-β1 expressing B cells remains to be elucidated, it is not thought to be included in the T2-MZP, B10 or CD138^{+} plasma cell Bregs[361].

1.2.3.3 B10 cells

Shortly after the discovery that T2-MZP B cells were a source of IL-10^{+}Bregs, a new subset of Bregs defined as CD1d^{hi}CD5^{+}, known as B10 cells were identified to have regulatory capacity in an oxazolone-driven model of CHS[303]. B10 cells were identified based on their expression of IL-10 after 5h stimulation with phorbol 12-myristate 13-acetate (PMA) and ionomycin. Mice expressing the human CD19 transgene (hCD19tg) were more resistant to CHS than WT mice, due to increased numbers of B10 cells. Conversely, *Cd19*$^{-/-}$ mice developed an exacerbated CHS reaction, suggesting B10 cell generation is dependent on the BCR signalling[303].

Adoptive transfer of *Il10*$^{-/-}$CD1d^{hi}CD5^{+} B cells failed to suppress CHS in recipient mice, showing that B10 cells suppress via the provision of IL-10. Importantly, only antigen-specific B10 cells were able to suppress disease, as evidenced by the fact that adoptive transfer of CD1d^{hi}CD5^{+} B cells from mice sensitized to a different antigen (DFNB), failed to resolve CHS in *Cd19*$^{-/-}$ recipient mice[303].

It is important to note that the B10 cells are defined as CD19^{hi}CD24^{hi}CD21^{+}CD23^{-} IgM^{hi}CD1d^{hi}CD5^{+} and therefore share overlapping markers with that of CD5^{+}B-1a cells, MZ and T2-MZP B cells, but do not exclusively fit into one population of cells. Nevertheless, there are many degrees of similarity between T2-MZP B cells and CD1d^{hi}CD5^{+}-derived Bregs. Both populations need 'priming' through inflammation before suppressive capacity is seen. Antigen naïve T2-MZP B cells and B10 cells fail to ameliorate disease severity in AIA and CHS respectively. This feature could be due to the kinetics of Breg differentiation in both models, requiring several days for Breg differentiation *in vivo*. Both B10 cells and T2-MZP B cells require T-cell help to become fully functional Bregs, with both CD40L expression on T cells and MHC class II expression on B cells being important for the generation of Bregs[311]. Interestingly, B10 cells retain the ability to differentiate into plasma cells and induce the expression of *Blimp-1* and *Irf4*. Moreover, B10 cells are able to produce antigen-specific IgG in response to immunizations and also polyreactive IgM which recognises both self and foreign antigens[362]. Data from these studies supports the notion that B10 cells are derived from multiple subpopulations and do not define a distinct B cell lineage.

Since their initial characterisation in CHS reactions, B10 cells have also been reported to have functional roles in a number of models of autoimmunity and infection. Adoptive transfer of B10 cells reduced the severity of EAE in WT recipient mice and suppressed CD4^{+} T cell IFN-γ expression, in an IL-10 dependent manner[305, 363]. Adoptive transfer of B10 cells also ameliorated the symptoms of lupus in NZB/W mice and reduced intestinal inflammation in DSS induced colitis[304, 306]. In the context of infection, B10 cells play a deleterious role in the survival of mice infected with *Leishmaniasis major* and *Listeria monocytogenes*[364 365]. Mice infected with *L. monocytogenes* have increased numbers of B10 cells *in vivo*, which suppress macrophage TNFα, IFN-γ and nitric oxide production. Additionally, B10

cells impaired the ability of macrophages to phagocytose the pathogen, leading to increased bacterial load[365].

1.2.3.4 B-1 cells

B-1a cells with suppressive capacity have been described in autoimmune and infection models and in recognition to self-antigens found on ACs[355]. B-1a cells are a major source of natural polyreactive IgM which is important for the clearance of ACs and play a key role in the first line defence against pathogens[105]. In addition B-1a cells are a potent source of IL-10[106].

TLR9 engagement with DNA complexes from ACs drives the expression of IL-10 in MZ and B-1a cells. Indeed, *Tlr9*$^{-/-}$ peritoneal cavity B-1a B cells are unable to increase IL-10 upon stimulation with ACs, unlike their WT counterparts[330]. IL-10 secretion by B-1a cells can dampen macrophage phagocytosis and reduce secreted levels of nitric oxide and hydrogen peroxide[366].

Numerous other studies have implicated an important role of IL-10^{+}B-1a cells in models of infection and autoimmunity. IL-10 expression by B-1a cells can be induced by lacto-N-fucopentaose III, a sugar found on *Schistosoma mansoni* eggs. Infection with *S. mansoni* increased numbers of B-1a cells within 2-4 weeks of infection in multiple strains of mice, namely in the CBA/J, C3H/HeJ and BALB/c, but not in C57BL/6 and BALB/c.Xid mice, which could account for the differing degrees of pathology reported between the strains[367]. Interestingly, BALB/c.Xid mice which have reduced numbers of CD5^{+} B-1a cells are more susceptible to *Litomosoides sigmodontis* infection, due to the relative paucity of natural IgM and IL-10 secreted in these mice[367]. Alongside IL-10 production, B-1a cells upon infection with *S. mansoni*, upregulate FASL and have increased capacity to induce the apoptosis of CD4^{+} T cells. These cells were later termed 'Killer B cells'[368].

In CHS, suppression of disease is dependent on IL-10^{+}CD22-expressing B-1a cells[369]. CD22 is a transmembrane receptor which binds to sialic acids and negatively regulates signals through the BCR[370]. *Cd22*$^{-/-}$ mice develop a more severe CHS reaction. Adoptive transfer of peritoneal B-1a, and not B-1b cells, reduced the severity of the CHS reaction. Although no differences were observed in the amount of IL-10 produced by splenic or peritoneal B-1a B cells between WT

and *Cd22*$^{-/-}$ mice, adoptive transfer of peritoneal B-1a cells from both mice into recipient WT mice revealed distinct migratory patterns. *Cd22*$^{-/-}$ B-1a cells migrated less to the spleen and LN's in the CHS reaction and therefore were less able to suppress disease in an IL-10-dependent manner[369]. Similarly to T2-MZP B cells and B10 cells, adoptive transfer of B-1a cells also conferred protection in EAE[359]. B-1a B cells can also exert tolerogenic function in an IL-10 independent fashion. In colitis, *Tcr*$\alpha^{-/-}$ mice which were housed in a SPF environment developed a more severe form of colitis than conventionally housed mice. Colitis severity correlated to the amount of B-1a derived natural IgM. Indeed, when mice which lacked B cells and the TCRα chain ($\alpha\mu$ double knockout mice [DKO]) were conventionally housed, they developed a worse course of disease than SPF housed *Tcr*$\alpha^{-/-}$ mice, implicating that B-1a B cells play a key role in suppression of disease; a finding which was confirmed by suppression of colitis upon adoptive transfer of peritoneal of B-1a cells into $\alpha\mu$ DKO mice[371]. The mechanism as to how natural IgM suppressed colitis induction was not addressed in this study.

1.2.3.5 Plasmablasts and plasma cells

The first indication Breg subsets could be contained within plasma cells and plasmablasts came from examining the transcription of *Il10 in vivo*, by using an *Il10*eGFP transcriptional reporter strain (known as Vert-X mice)[372]. After challenging these mice with LPS, CpG, goat anti-IgD or murine cytomegalovirus, it was identified that CD19$^+$ B cells comprised the biggest population within the IL-10$^+$GFP$^+$ population. Remarkably, CD19$^+$CD138$^+$ plasmablasts after anti-IgD or murine cytomegalovirus (MCMV) challenge made up around 60% and 30% of the GFP$^+$ leukocytes in the dLNs respectively. However, the relative frequencies of splenic B cell subpopulations constituting the GFP$^+$ population in the spleen was not reported[372]. IL-10 producing CD19$^+$CD138$^+$ plasmablasts were also shown to be increased *in vivo*, after 1 day of infection with *Salmonella typhimurium*[324]. IL-10 secretion by CD19$^+$CD138$^+$ cells had a detrimental effect in the survival of mice infected with Salmonella. Indeed, B-*Il10*$^{-/-}$ chimeric mice were protected from *S. typhimurium* infection due to increased numbers of IFN-γ secreting natural killer (NK) and CD4$^+$ T cells and TNFα producing neutrophils; two key cell types in protective immunity against Salmonella infection[324, 373, 374].

A protective effect of plasmablast derived Bregs have also been demonstrated in EAE, where IL-10$^+$ plasmablasts (defined here as CD138$^+$CD44$^+$) are important for the suppression of disease[375]. Importantly, suppression of EAE is dependent on the homing of IL-10$^+$ plasmablasts to the lymph nodes; a process which is mediated by the expression of CD62L (aka as SELL)[376]. Adoptive transfer of *Sell*$^{-/-}$ B cells to B cell deficient recipients (μMT) failed to suppress disease, unlike adoptive transfer of WT B cells. Interestingly, the generation of CD138$^+$CD44^{hi} Bregs is independent of the GC reaction, as mice lacking functional copies of BCL6 still had comparable numbers of plasmablasts compared to the WT controls[375].

The role of plasma cell derived Bregs has also recently been demonstrated in restricting tumour-directed cytotoxic T cell functions. IgA$^+$PD-L1$^+$IL-10-expressing plasma cells inhibit cytotoxic T cell function after oxaliplatin treatment; an immunogenic cytotoxic chemotherapeutic agent[377]. More recently, a subset of natural regulatory plasma cells has been identified, which suppress immune responses via the production of IL-10[378]. These cells express lymphocyte activation gene 3 (LAG3), which is an important receptor for enhancing Treg mediated suppression[379]. This population was shown to be mainly IgM$^+$ and are present in naïve mice, suggesting these cells do not go through the GC reaction. LAG3$^+$ plasma cells differentiate into IL-10$^+$Bregs upon activation with LPS or LPS+anti-IgM or upon infection of mice with *S. typhimurium*[378].

In addition to regulation of IL-10, plasma cells also produce IL-35, which is a heterodimeric cytokine consisting of the IL-12 family members p35 and EBI3[380]. IL-35 has previously been shown to contribute to Treg function in IBD and in CIA[381, 382]. Chimeric mice with B cells lacking either p35 or EBI3 develop a more severe course of EAE, due to enhanced effector T cell IFN-γ and IL-17 production. Reciprocally, the lack of B cell p35 or EBI3 in *S. typhimurium* infection prolonged survival of these mice by expanding the numbers of mononuclear phagocytes and increasing CD4$^+$ IFN-γ production. The main source of IL-35-expressing B cells during *S. typhimurium* infection were CD138^{hi} plasma cells. It is important to note that CD138^{hi} plasma cells are also able to co-express IL-10[380]. IL-35 can also act in an autocrine manner to promote the expansion of IL-10$^+$IL-35$^+$Bregs. Moreover, treatment of mice with IL-35 protected mice from experimental autoimmune uveitis [347]. Whether plasmablast and plasma cell derived Bregs functionally mature from

Bregs that arise from previous stages of B cell maturation, or whether they represent a *de novo* form of Bregs remains unclear.

1.2.3.6 Other Breg subsets

A growing number of Breg subsets are identified based on their differing phenotype and function. These subsets share expression of core B cell markers, but also express distinct markers from the subsets discussed above. Amongst these, GM-CSF and IL-15 fusokine (GIFT15) generated Bregs appear phenotypically similar to T2-MZP Bregs as they also express CD21, CD23, CD24, CD1d, IgD and IgM. However, in contrast to T2-MZP Bregs, GIFT15 Bregs express very lows levels of CD19 and high levels of CD138; a phenotype reminiscent of plasma cells. Intravenous injection of GIFT15 Bregs ameliorates EAE disease, through the upregulation of IL-10 and MHC class II on B cells[383].

Another well described Breg subset is defined by the expression of T-cell Ig domain-1 (TIM-1); a marker which is associated with immune regulation[384]. In T cells, activation with a low affinity anti-TIM-1 antibody (RMT1-10) inhibits EAE and can promote long-term allograft acceptance by promoting skewing towards Th2 and Tregs[385, 386]. TIM-1 expression is widely reported to be expressed across a majority of IL-10$^+$Breg subsets, including B10 cells, CD138$^+$IgA$^+$ plasma cells and CD138$^+$ plasmablasts[377, 380, 387]. The role of TIM-1$^+$Bregs has been well characterised in transplantation studies and in models of autoimmunity.

The expression of TIM-1 on B cells was first identified by work from the Rothstein group[387]. Data from this study showed that upon allogeneic islet transplantation, B cells in the spleen upregulated the expression of TIM-1. Importantly, in chemically-induced diabetic BALB/c mice receiving a transplantation of B6 islets, treatment with RMT1-10 promoted tolerance to the allograft and survival of these mice, through upregulation of B cell IL-4 and IL-10 expression[387]. Furthermore, generation of mice which lack the mucin domain of TIM-1 (TIM-1$^{\Delta MUCIN}$), showed decreased binding to phosphatidylserine on ACs and were unable to induce IL-10 upon activation with ACs. Activation of TIM-1 by RMT1-10 in TIM-1$^{\Delta MUCIN}$ mice failed to promote survival in these mice[388]. TIM-1$^{\Delta MUCIN}$ mice also developed spontaneous autoimmunity with increased production of IFN-γ by CD4$^+$ T cells and had elevated serum levels of IgG and dsDNA IgG[389]. The loss of B cell TIM-1

expression also promotes age-related tissue inflammation and splenomegaly. Moreover, *Tim1*$^{-/-}$ B cells produced less IL-10 and more pro-inflammatory IL-12 and IL-6 upon BCR ligation. Indeed, the severity of EAE disease is worse in *Tim1*$^{-/-}$ mice and can be ameliorated by the adoptive transfer of WT TIM-1^{+} B cells[337].

Recently, a novel subset of Breg defined as CD39^{+}CD73^{+} have been shown to exert immunosuppressive function by the production of adenosine. CD39 expression is common on B cells, but CD73 expression is limited to certain populations. Roughly 30-50% of B-1 cells and IL-10 expressing B10 cells are CD73^{+}. Specifically, CD73^{+}B-1 cells can produce adenosine in the presence of 5'-adenosine monophosphate (AMP). *Cd73*$^{-/-}$ mice develop a more severe course of DSS colitis compared to WT mice, which can be partially resolved upon adoptive transfer of CD73^{+}B-1 cells. Interestingly, *Il10*$^{-/-}$ B-1 cells produce less adenosine and express less CD73, suggesting a proportion of these cells have dual functions producing adenosine and IL-10[390].

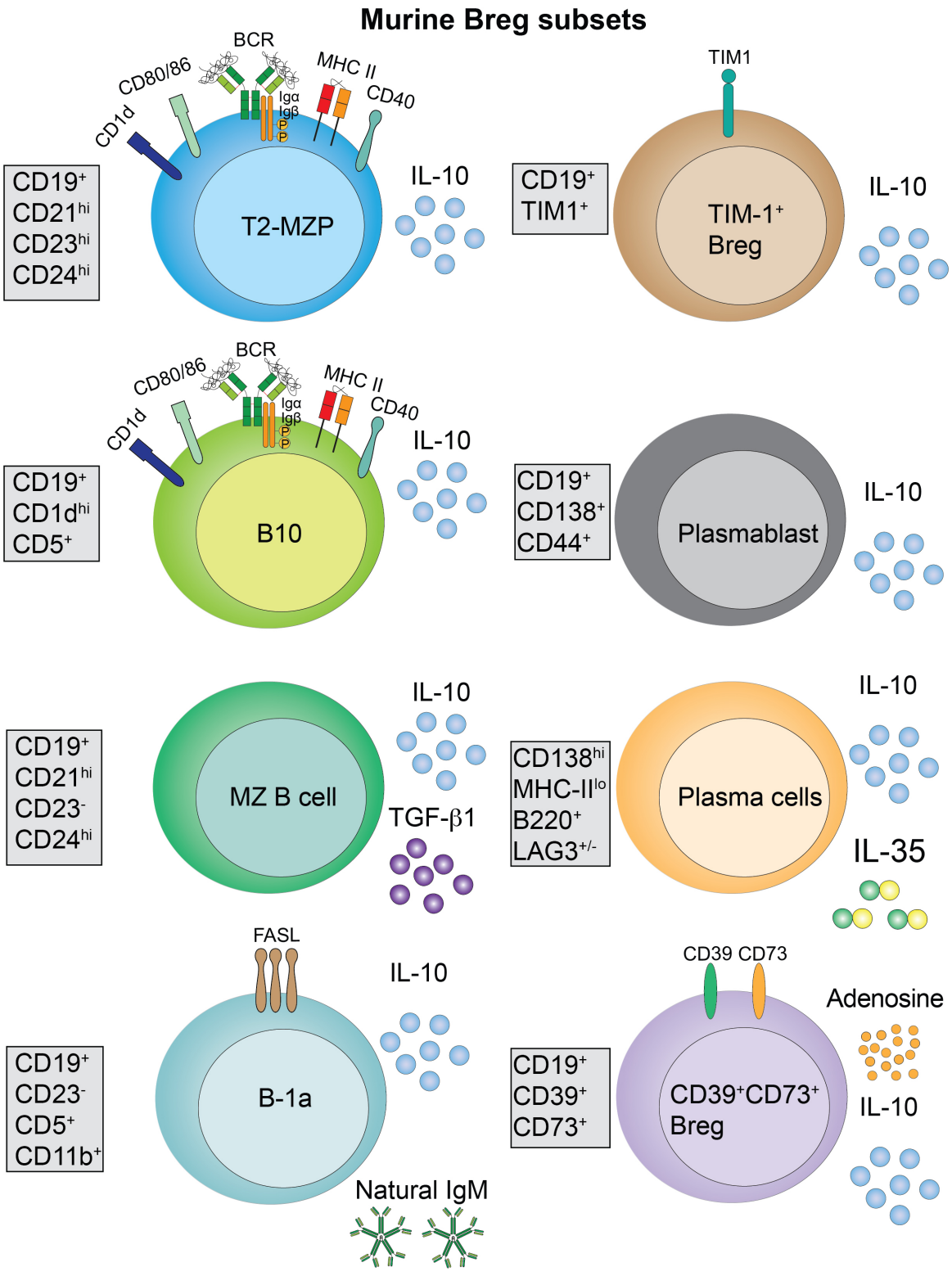

Figure 1.4. Breg subsets and mechanisms of suppression in mouse. Breg subsets in mouse arise from multiple stages of B cell differentiation. Mechanisms of suppression include secreted cytokines (IL-10, IL-35 and TGF-β1), cell-contact dependent mechanisms (CD1d, MHCII, CD80/86, CD40, FASL and TIM-1) and modulation of metabolic processes (i.e adenosine production by CD39 and CD73).

1.2.4 Human Breg populations

Due to the comparative lack of tools and technologies in the isolation and tracking of IL-10$^+$ cells in human B cells, less is known about Breg ontogeny and their role *in vivo*. As is the case with mouse Bregs, human Bregs are defined by the expression of IL-10, or indeed by expression of other markers that exert suppressive functions. Although there are numerous phenotypical differences between mouse and human Breg subsets, the mechanisms of suppression are largely conserved between species. Bregs are known to be functionally impaired or have reduced numbers in multiple autoimmune diseases, including, but not limited to, SLE[350, 391], systemic sclerosis[392], RA[393], ANCA-associated vasculitis[394] and multiple sclerosis[395]. Moreover, the function and phenotypes of human Bregs in infection, transplantation, allergy and cancer are starting to be unraveled.

Breg identification and function in humans was first attributed to CD19$^+$CD24^{hi}CD38^{hi} transitional (or immature) B cells in the blood, with the CD19$^+$CD24^{hi}CD38^{hi} transitional B cell population identified as the main IL-10-expressing B cell population. Analogous to murine Bregs[311], the IL-10$^+$Breg population could be expanded upon ligation of CD40 on B cells and suppressed CD4$^+$ T cell IFN-γ and TNFα expression[391]. Similar to T2-MZP B cells in MRL/*lpr* mice, CD19$^+$CD24^{hi}CD38^{hi} B cells from SLE patients produce less IL-10 after stimulation with CD40 and fail to suppress T cell IFN-γ and TNFα[391]. Moreover, CD19$^+$CD24^{hi}CD38^{hi} B cells from SLE patients are also defective in maintaining iNKT cell homeostasis, due to a defect of CD1d recycling in this population[263].

Similarly to T2-MZP Bregs in mouse, in addition to inhibiting Th1 and Th17 differentiation, human CD19$^+$CD24^{hi}CD38^{hi} Bregs also promote the generation of FOXP3$^+$ Tregs. In RA, CD19$^+$CD24^{hi}CD38^{hi} Bregs are unable to convert naïve CD4$^+$CD25$^-$ T cells into Tregs, or to suppress the differentiation into Th17 cells, but maintain the ability to suppress Th1 differentiation[393]. Since these initial findings, there have been many reports showing reduced Breg function or numbers in autoimmune diseases[351]. These findings have recently been extended to studies of Breg function in cancer. In gastric cancer, intratumoural CD19$^+$CD24^{hi}CD38^{hi}CD1d^{hi}CD5$^+$ B cells produce more IL-10 than B cells from the blood or B cells from the peritumoural area. Bregs in gastric cancer promote the

differentiation of $CD4^+FOXP3^+$ Tregs and reduce the frequencies of $CD4^+IFN\text{-}\gamma^+$ T cells in the blood. Thus, in this setting, Bregs promote tumour evasion[396].

Although the phenotypical markers vary between mouse and human Breg populations, a number of other human Breg subsets share functional similarities to, and are derived from the same precursor populations as, their mouse counterparts. B10 cells have also been identified in the peripheral blood of HCs, and are readily available to produce IL-10 after activation with LPS, PMA and Ionomycin[397]. Interestingly B10 cells share a cell surface phenotype resembling that of memory B cells, with a reported phenotype of $CD24^{hi}CD27^+CD38^{lo}CD48^{hi}CD148^{hi}$. B10 cells were reported to suppress monocyte-derived TNFα production[397]. In addition, a human orthologue of the mouse plasmablast Breg population ($IL\text{-}10^+CD138^+CD44^{hi}$) has been identified in the peripheral blood, defined as $IL\text{-}10^+CD27^{int}CD38^{hi}$. Lastly, both adenosine triphosphate-hydrolysing ($CD39^+CD73^+CD25^+$) and Granzyme-B^+ Breg populations have been identified in human blood. Both Breg populations suppress the proliferation of $CD4^+$ T cells, whilst Granzyme-B^+ Bregs additionally induce $CD4^+$ T cell apoptosis[338, 398, 399].

The only human Breg subset so far discovered with no mouse analogue are BR1 cells, which are enriched after allergen immunotherapy. Uniquely these cells produce IgG4, which is not expressed by murine B cells[400]. Bee keepers tolerised to bee venom allergen phospholipase A_2, have increased frequencies of $IL\text{-}10^+IgG4^+CD25^{hi}CD71^{hi}CD73^-$ Bregs compared to HCs. Remarkably, allergic patients have increased numbers of BR1 cells after receiving specific immunotherapy, thus linking BR1 cells to the maintenance of tolerance against bee venom allergens[401].

1.3 AIA as a model to study Breg function

AIA is a T cell driven DTH reaction driven by the injection of antigen into the knee joint of a pre-immunised animal[353]. AIA was first described in the 1960s, where AIA was induced in rabbits[402]. AIA can be induced by a variety of antigens, including fibrin, ovalbumin and methylated bovine serum albumin (mBSA). In mice, however, cationic antigens must be used for the retention of the antigen in the anionic cartilage of the joints of the animals[353]. Our work is based on the mBSA induced AIA model, which was first described in 1977[403].

The pathogenesis of AIA is thought to be mediated primarily by $CD4^+$ T cells. Initial experiments in this model, showed that transfer of splenocytes enriched in $CD4^+$ T cells exacerbated the severity of disease in recipient mice[404]. Depletion of B cells further accentuated the clinical severity of the disease, implicating a role of B cells in the immunoregulation of the disease[404]. Determination that it was $CD4^+$ and not $CD8^+$ T cells which were pathogenic was delineated by Petrow *et al*, who showed that the depletion of $CD4^+$, and not $CD8^+$, T cells before transfer prevented the development of arthritis in SCID recipient mice[405]. Flare mediated destruction of the joint is T cell driven and antigen specific[406, 407, 408]. Moreover, CD4 depletion ameliorates disease by reducing inflammatory macrophage production of IL-1β and IL-6 in the joints of AIA mice[409]. IL-1β drives joint pathology by promoting joint inflammation and cartilage degradation[410].

A number of features of the AIA model make it ideal to study the function of Bregs. Firstly, the disease course is well defined; that is to say peak swelling is achieved at days 1-3, and remission from disease occurs at days 5-7. This allows for study of Bregs and their differentiation during both the inflammatory and resolution stages of disease. Secondly, arthritis is restricted to one joint, so we can determine disease swelling relative to the unaffected joint and examine the degree of severity of swelling in conditional and global knockout mice. Lastly, the incidence rate of AIA is 100%, with no sex bias[353].

1.4 The transcriptional regulation of IL-10

IL-10 is an anti-inflammatory cytokine which targets both innate and adaptive immune responses. It exerts its immunosuppressive function and reduces tissue damage by curbing excessive inflammation caused by effector cells during the resolution phase of infection and inflammation[411]. Although originally associated as a Th2-associated cytokine[412], IL-10 has since been shown to be a critical regulator of anti-inflammatory responses, initiated in cell types of both the adaptive and innate immune system[413]. IL-10 transcriptional regulation is a complex process, often dictated by the type of stimuli inducing IL-10, and is regulated in a cell-context dependent manner by several transcription factors and by epigenetic regulation. In macrophages, IL-10 is regulated by c-MAF[414], cyclic adenosine 3,5-monophosphate response element-binding protein (CREB)[415], NF-κB[416], specificity protein 1 (SP1)[417] and several others[418]. In Th2, GATA binding protein 3 (GATA3)[419] and c-JUN[420] are important for induction of IL-10. In Treg, IRF1 and basic leucine zipper transcriptional factor ATF-like (BATF) are critical in acting as pioneering transcription factors for opening the *Il10* locus and initiating the transcription of IL-10[421], allowing c-MAF and AHR to bind and regulate IL-10[422].

1.4.1 Transcriptional control of Il10 in B cells

The transcription factors which regulate *Il10* expression in macrophages, DCs, $CD4^+$ T cells and other cell types have been well described[418]. However, unlike in other immune cells the molecular determinants that regulate the transcription of IL-10 in B cells remains relatively unknown. B cell expression of IL-10 is indispensable for regulatory function and its expression is tightly regulated. Recently, hypoxia-inducible factor 1α (HIF1α) has been linked to IL-10 expression in B cells[423]. HIF1α responds to hypoxia and initiates the metabolic rewiring of a cell, by altering the gene expression profile to help the cell adapt to hypoxic conditions[424]. *Hif1a* expression is increased in B cells upon activation with LPS or anti-IgM stimulation. In B cell conditional knockout mice (*Hif1a*$^{f/f}$*Mb1*^{cre}), both the frequencies of B-1a cells in the peritoneal cavity and IL-10^+B-1a cells in the spleen are reduced compared to WT controls, suggesting an important role of HIF1α in the generation of IL-10^+Bregs[423]. This seems to be, in part, due to the role of HIF1α in regulating glycolysis. Splenic B cells cultured in hypoxic conditions make more *Il10* and this is dependent on HIF1α and STAT3 co-operatively transactivating the *Il10* locus.

Hif1a$^{f/f}$*Mb1*^{cre} mice develop exacerbated courses of CIA and EAE compared to WT controls, due to the skewing of T cells towards a Th1 and Th17 phenotype[423].

C-MAF is a member of the activator protein 1 (AP1) transcription factor family, which has previously been shown to increase the expression of IL-10 in Tr1 cells and in macrophages[418]. More recently, the expression of c-MAF has also been associated with IL-10 production by B cells[425]. LPS activated B cells upregulate the expression of IL-10 and cMAF. Total splenic B cells have reduced levels of IL-10, after C-MAF is silenced by short hairpin RNA, thereby implicating this transcription factor in the regulation of IL-10. Whether c-MAF binds to the *Il10* locus has not been determined in B cells[425]. However, it is feasible that c-MAF binds to the *Il10* locus in B cells, as this has been demonstrated in Tr1 cells[422].

As discussed earlier, NFATc1 is a component of the BCR signalling pathway and is important in regulating the expression of IL-10 in B cells. However, there have been conflicting reports as to whether NFATc1 acts as a positive or negative regulator of IL-10 expression in B cells. Mice with B cell specific deficiency of NFATc1 developed a significantly ameliorated course of EAE[426]. *Nfatc1*$^{f/f}$*Mb1cre* developed an attenuated psoriasis, due to the increased numbers of IL-10^{+}CD1d^{hi}CD5^{+} and IL-10^{+}CD138^{+} B cells, compared to WT mice[427]. In contrast, Matsumoto *et al* report that the calcium sensors STIM1/2 and NFATc1 are required for BCR driven IL-10 production[301].

More recently, BLIMP-1 and IRF4 have been linked to the transcription of *Il10* by plasmablasts, with IRF4 directly binding to the conserved non-coding sequence (CNS)9 region of the *Il10* locus in BLIMP-1^{+} B cells[375]. Of interest, IRF1 and BATF bind to the same region in Tregs[421]. After TLR and BCR activation, B cells deficient in IRF4 secreted less IL-10. B cell IRF4 deficient mice developed an exacerbated EAE disease compared to their WT counterparts[375]. Moreover, ectopic expression of IRF4 in a B cell lymphoma line enhanced IL-10 secretion, thus suggesting a direct role of IRF4 in the regulation of IL-10 in B cells[428].

In human B cells, very little is known regarding the transcription of *Il10*. Using a luciferase reporter downstream of the *Il10* locus in human B cell lines, Ziegler-Heitbrock *et al* showed that STAT3 was required for the induction of IL-10. Mutated

STAT3, but not IRF1, binding sites prevented the transcription of *Il10*[429]. Less phosphorylation of STAT3 was also associated to reduced IL-10 in $CD19^{+}CD24^{hi}CD38^{hi}$ B cells from SLE patients[391]. Moreover, inhibition of ERK1/2 or STAT3 with inhibitory peptides abrogated IL-10 production from TLR7/8 and TLR9 stimulated human B cells, suggesting a role of these pathways in the regulation of B cell IL-10[328]. It should be noted, that although individually these transcription factors are important for the induction of IL-10, it is far more likely that these transcription factors interact and act in tandem with each other as part of a transcriptional complex for the induction of IL-10.

1.4.2 The post-translational and epigenetic regulation of Il10 expression in B cells

The expression of cytokines needs to be tightly regulated to prevent hypo-/hyper-activation of the immune system. In the absence of IL-10, mice develop chronic transmural enterocolitis, a condition which bears a resemblance to Crohn's disease in humans[430]. Equally, excess IL-10 can have pro-tumourigenic effects. Indeed, it has been shown that IL-10 promotes an escape mechanism for cancerous cells to avoid immune surveillance[431, 432]. However, this remains a highly debatable topic, with evidence both supporting and contradicting this hypothesis. It is likely to be a context-specific phenomenon, where multiple factors such as the hosts genetics, the inflammatory milieu and the type of cancer interplay.

To prevent dysregulation of immune responses, as well as being regulated at the transcriptional level, cytokines can be controlled through post-translational modifications. Cytokine mRNAs are often unstable and are subjected to rapid degradation after their synthesis, due to the presence of adenosine- and uridine-rich elements (ARE/URE) in the 3'UTR[418]. Several pro-inflammatory and anti-inflammatory cytokines/chemokines have ARE elements, including IL-10[433], IL-27[434], GM-CSF[435] (the first cytokine identified to contain ARE) and TNF[436]. IL-10 contains 6 AUUUA pentamers, which facilitates the binding of the tristetraprolin (also known as ZFP36)[433]. ZFP36 belongs to a family of RNA-binding proteins, which targets mRNA by binding to AREs on mRNA and recruiting deadenylation and degradation factors[437]. Although no study to date has defined the role of ZFP36 in IL-10 expression in B cells, it is highly likely to play a role in regulating the amount of IL-10 produced. Recent evidence has pointed towards a role of other ZFP36

family member's in the regulation of B cell differentiation. ZFP36L1 maintains MZ B cell identity by promoting the degradation of KLF2 and IRF8; two transcription factors known to enforce a FO B cell phenotype[171].

In addition to RBPs, miRNAs play a crucial role in the post-translational regulation of mRNA expression in B cells. MiRNAs are small endogenous RNAs of 21-25 nucleotides in length and direct their target mRNAs for degradation[438]. Of the known miRNAs, both miR-15/16-1 and miR-21 play a direct inhibitory role in the regulation of IL-10 in B cells. Intriguingly, both $CD1d^{hi}CD5^{+}$ and $TIM\text{-}1^{+}$B cells express lower levels of miR-21 than their $CD1d^{-}CD5^{-}$ and $TIM\text{-}1^{-}$ counterparts. Blocking miR-21 with a specific antagomir, in LPS and CD40 stimulated B cells increased IL-10 production by B cells. In addition, mimics of miR-21 also inhibit IL-10 production. Treatment of mice with the antagomir of miR-21 (antagomir-21) or adoptive transfer of antagomir-21 treated B cells partially ameliorated EAE severity, suggesting a contributing role for post-translational regulation of IL-10 in B cells *in vivo*[439]. In addition, aged (15-18 month old) miR-15a/16-1 KO mice have increased $IL\text{-}10^{+}$B cells compared to age-matched WT controls[440]. However, this is not the case in young adult mice (8-12 weeks). The reason for the increased IL-10, specifically in the aged miR-15a/16-1 KO mice, was due to increased tumour burden and the corresponding increase in $TIM\text{-}1^{+}$B cells in the aged miR-15a/16-1 KO mice. These data suggest that, in addition to inhibiting IL-10 production, miR-15a/16-1 also are important in suppressing the development of $TIM\text{-}1^{+}$ B cells[440]. Unlike other MiRs, miR-155 and its mimics increase IL-10 expression in human B cells, by increasing the phosphorylated levels of STAT3. MiR-155 acts indirectly on IL-10, by downregulating the expression of JARID2; the epigenetic negative regulator of IL-10[441]. JARID2 silences gene expression by recruiting polycomb repressive complex 2 to target sites, which leads to histone 3 lysine 27 (H3K27) trimethylation[442].

Epigenetic modulation and chromatin remodelling of loci represent an important step in the initiation, maintenance and cessation of transcription. Epigenetic imprinting and chromatin accessibility of any given locus, varies according to the cell type, activation status of a cell and on the type of external stimuli a cell receives. Broadly speaking, DNA methylation inhibits gene expression, whilst acetylation promotes gene transcription, by making the chromatin more

accessible[418]. In mouse splenic B cells, and human peripheral blood B cells, the methylation status of the *Il10* locus differs between IL-10^{+} and IL-10^{-} subsets. Specifically, within the CNS -9, -4.5kb and +1.6kb regions on the mouse *Il10* locus, IL-10^{+} B cells have less CpG island methylation, indicating these sites are more accessible in cells actively producing IL-10.

The human *Il10* locus also has less methylation in IL-10^{+} B cells, when compared to IL-10^{-} B cells specifically at the CNS -12.5kb region (which corresponds to the CNS -9kb region in mice). These data indicate that there is species specific epigenetic regulation of the *Il10* locus. CLL cells, which produce more IL-10 than healthy B cells, also have a lower degree of methylation at the -12.5kb region[443]. Of interest both IRF1 and BATF, two pioneering transcription factors, involved in opening the *Il10* locus in Tr1 cells bind to CNS -9 region[421]. In Tr1 cells opening of the chromatin facilitates the binding of c-MAF and AHR to MAF recognition element and xenobiotic response element (XRE) sites on the *Il10* locus, closer to the transcription start site (TSS)[422]. Determining the pioneering transcription factors which bind to these sites in B cells remains to be determined.

1.5 The AHR pathway

1.5.1 General introduction

The aryl hydrocarbon receptor is an evolutionary conserved transcription factor,[444] belonging to the basic helix-loop-helix (bHLH) periodic circadian protein (PER)-AHR nuclear translocator (ARNT)-single-minded protein (SIM) superfamily of transcription factors. Typically, these transcription factors are involved in sensing changes in the environment, such as oxygen gradients or circadian rhythms. Recognition of endogenous factors by AHR is achieved through the PER-ARNT-SIM (PAS) domains[445]. In addition, AHR contains an (N-)terminal bHLH domain required for DNA binding[446] and a Q-rich carboxy (C-)terminal transcriptional activation domain. Like other members of the large bHLH family, the bHLH domains in AHR can homodimerise in the absence, or heterodimerise, in the presence of its binding partner ARNT[446]. The heterodimeric bHLH domains of AHR:ARNT bind to the AHR-specific consensus sequence (5'-NGCGTG-3') known as the xenobiotic or dioxin response element (XRE/DRE)[447, 448] and initiates gene transcription of AHR target genes[449], with AHR and ARNT binding the T(N)GC (5'-half sites) and GTG (3'-half sites) sequences respectively[447]. PAS domains of AHR are linked to the binding of the bHLH regions to DNA, as proteins lacking the PAS domains fail to show XRE binding activity, suggesting a role of the PAS domains in regulating the conformational activity of the bHLH domains[446].

In the absence of ligands, AHR is maintained in an inactive state in the cytoplasm of the cell, bound to actin filaments[450] as part of a chaperone complex with AHR-interacting protein (AIP; also known as XAP2)[451, 452], a dimer of heat shock protein (HSP)90[453], the SRC protein kinase[454, 455] and p23[456, 457]. The chaperone complex serves to regulate AHR activity and signalling in multiple ways. One HSP90 molecule binds to the bHLH region of AHR, whilst the second binds to both the bHLH region and the ligand binding region contained within the PAS-B domain of AHR[458, 459], which prevents constitutive AHR binding to DNA and maintains AHR in a conformational shape suited for high ligand-binding affinity[460]. The chaperone AIP and co-chaperone p23 are important for maintaining the cytoplasmic localisation of AHR before ligand binding[461, 462] and, in addition, prevents the ubiquitination and subsequent degradation of AHR[463, 464].

Binding of a ligand to AHR causes the dissociation of AIP from the complex[465], but not HSP90, which leads to a conformational change exposing a nuclear localisation signal in the bHLH region of AHR, allowing the translocation of AHR to the nucleus through interaction of the AHR complex with β-importin[461, 466, 467]. Interaction of AHR with ARNT in the nucleus leads to the dissociation of the chaperone machinery[467], and subsequent recruitment of the AHR-ARNT complex to the XRE regions[468] to regulate gene expression, as shown in Figure 1.5.

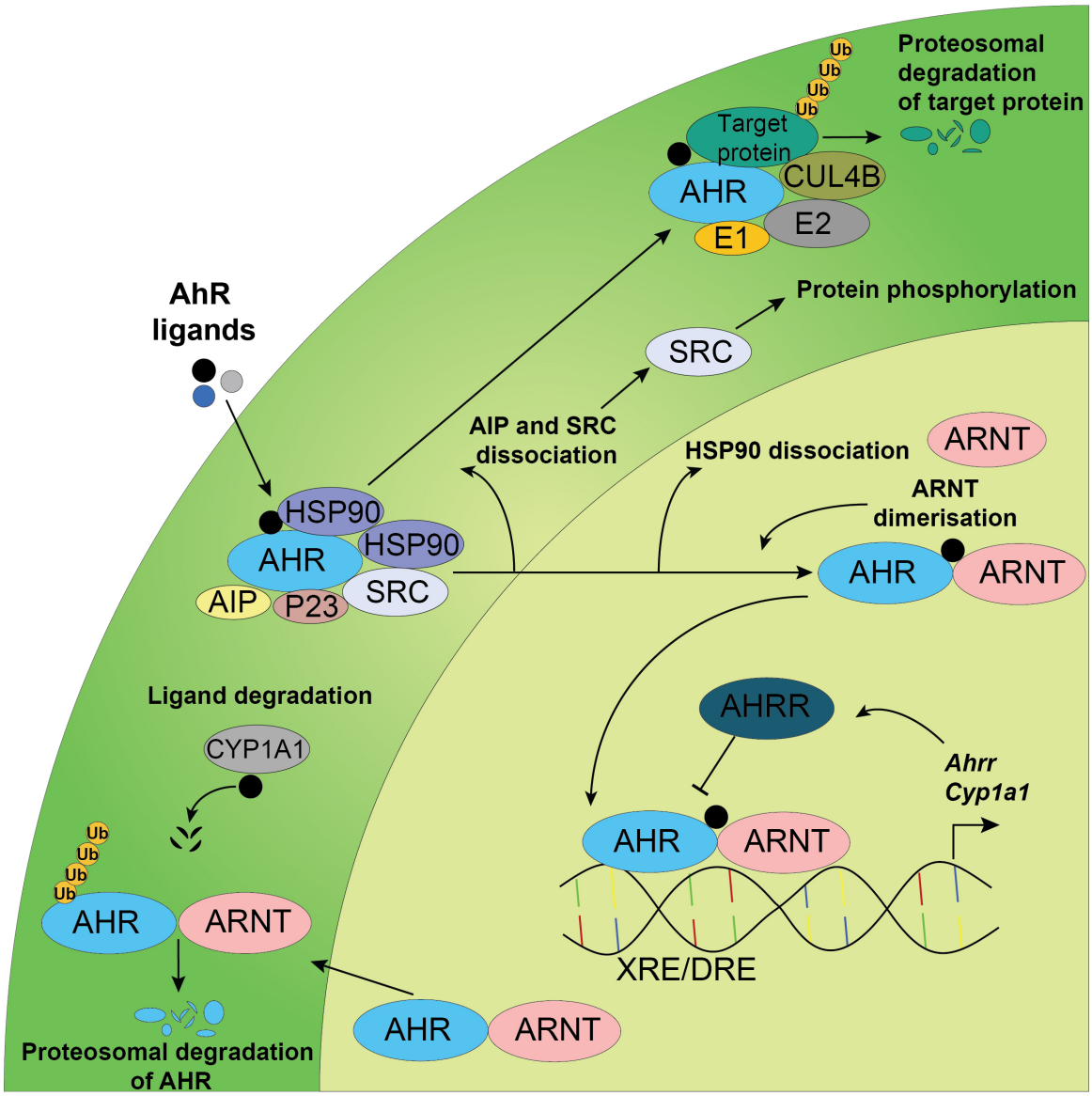

Figure 1.5. AHR signalling pathway. AHR ligands from the diet, microbiota, host metabolism or the environment activate AHR, inducing a conformational change in AHR, allowing for the nuclear translocation of the ligand-AHR complex. Whilst in the nucleus, AHR binds to ARNT and the complex binds to XRE/DRE sites on DNA and initiates gene transcription. Two direct gene targets include *Ahrr* and *Cyp1a1* which act to curtail AHR signalling through displacement of AHR from ARNT, or through AHR ligand metabolism. AHR activation can also trigger phosphorylation cascades, through the release of SRC. Target proteins can also be directed for proteosomal degradation through the E3 ubiquitin ligase activity of AHR. Lastly, AHR can also regulate gene transcription, by binding to different transcription factor response elements through interaction with other transcription factors.

1.5.2 Other mechanisms of gene regulation by AHR

In addition to the role of AHR in regulating its target genes, through binding to XRE regions, AHR can also regulate gene expression by other direct and indirect mechanisms. AHR can directly interact with the transcription machinery including transcription factor IIB (TFIIB)[469] and the mediator complex[470], enhancing the transcription of its target genes. In particular, AHR has been shown to interact with the positive transcription elongation factor (P-TEFb)[471]; a cyclin-dependent kinase controlling elongation by RNA polymerase II[472].

One emerging role of AHR is its ability to regulate the local chromatin architecture. Of note, AHR interacts with Brahma/SWI2-related gene 1 (BRG1), part of the switching defective/sucrose non-fermenting (SWI/SNF) chromatin-remodelling complex, and direct interaction with this complex regulates AHR target gene expression[473]. AHR can positively regulate the epigenetic landscape by modifying histone acetylation and methylation, through displacement of histone deacetylase (HDAC) complexes by AHR[474, 475]. In addition, AHR can recruit the steroid receptor coactivator-1 complex, which has histone acetyltransferase (HAT) activity[476].

In addition to the regulation of gene expression by the classical canonical pathway, AHR can also crosstalk with other pathways by binding to other DNA-responsive elements in combination with other transcription factors to modulate their downstream gene targets[445, 477]. AHR has been shown to interact with members of the NF-κB pathway, most notably RELA and RELB. AHR/RELB complexes bind NF-κB response elements in the *IL8*[478], *BAFF*, *CCL1*, *CXCL13* and *IRF3* promoters[479] in human macrophages. Similarly, AHR binding to RELA has been shown to regulate *CMYC* in human mammary cells[480] and *IL6* in human lung adenocarcinoma cells[481]. AHR can interact with STAT1, downregulating murine macrophage IL-6 expression, highlighting a central role of the crosstalk between these pathways in the regulation of immune responses[482]. AHR can be recruited to different transcription factor binding sites through interactions with KLF6[483], retinoic acid receptor alpha (RARA), retinoblastoma protein (RB)[484], oestrogen receptor (ESR)[485], sterol regulatory element-binding protein 1 (SREBF1)[486] and nuclear factor erythroid 2-related factor (NRF2)[487], amongst others[488]. Given AHR primarily functions as an environmental sensor, the fact that it can bind to and

regulate other transcription factor responses suggests a crucial role of AHR as a molecular rheostat in the fine-tuning of cellular responses.

AHR can also negatively regulate the activity of these transcription factors by reducing their half-life by functioning as an E3 ubiquitin ligase, targeting these proteins for proteosomal degradation. One well characterised example is the ESR, where AHR forms a part of the cullin 4B ubiquitin ligase complex (CUL4B) which targets the ESR for degradation[489]. Formation of the $CUL4B^{AHR}$ complex is dependent on the presence of an AHR ligand and on the readily available levels of ARNT. ARNT competes with CUL4B to bind to AHR, with low levels of ARNT leading to increased E3 ubiquitin ligase activity by AHR[490]. Similar processes also dictate the degradation of other transcription factors by AHR including HIF1α, MYC, FOS, octamer-binding protein (OCT4)[491, 492], RELA[493] and β-catenin; the latter of which is implicated in the suppression of intestinal carcinogenesis[494].

1.5.3. AHR Ligands

AHR acts as an environmental sensor, linking external environmental signals to internal cellular processes, therefore its primary function is to sense both exogenous and endogenous chemical mediators and modulate downstream target genes. Broadly speaking, AHR agonists can be split into two main categories with those that are synthetic (exogenous) in nature (i.e formed from municipal waste products or other anthropogenic activity) and endogenous ligands which are naturally occurring in nature and which can be further subdivided into many different categories. Due to the large number of AHR ligands described in the literature, these have been summarised in Table 1.1.

1.5.3.1 Exogenous ligands

Extensive research has been conducted on exogenous AHR ligands, in particular on the environmental contaminants such as the halogenated aromatic hydrocarbons (HAH) and the non-halogenated polycyclic aromatic hydrocarbons (PAH)[495]. The HAH's are more metabolically stable and have a higher binding affinity to AHR (pM to nM range), compared to the PAH's (in the nM to μM range). The HAH's include the polyhalogenated dibenzo-p-dioxins, biphenyls and dibenzofurans[496]. The most well characterised and potent HAH in terms of its binding affinity is 2,3,7,8-tetrachlorodibenzo-*p*-dioxin (TCDD), which is a by-

product of industrial organic synthesis of herbicides. TCDD exposure leads to chloracne outbreaks, in addition to more life-threatening clinical symptoms including emphysema, progressive liver and renal failure and myocardial degeneration[445]. Due to its acute toxicity and spate of accidental exposures, primarily the Seveso accident north of Milan in 1976[497], early studies examined the mechanism of toxicity behind TCDD, which eventually led to the discovery of the receptor which bound TCDD in 1976[498]. Even today, activation of AHR through TCDD remains well studied in multiple fields of biology including toxicology and immunology.

In contrast, the PAHs are generated through incomplete combustion of fossil fuels, or other anthropogenic activity such as petroleum refining, coke and asphalt production and wood treatment[499]. The most well studied PAH AHR agonists include the benzoflavones, 3-methylchoanthrene (3-MC) and benzo(a)pyrene. In addition, a number of 'non-classical' synthetic AHR ligands exist, which are structurally diverse and whose physiochemical properties are very different from the classical synthetic AHR agonists, highlighting the structural diversity of AHR ligands.

1.5.3.2 Endogenous AHR ligands

Since the generation of synthetic AHR ligands is dependent on anthropogenic activity, the evolutionary pressure of synthetic ligands on the function of AHR in vertebrate systems is a relatively new event. Instead, the exposure to endogenous AHR ligands are more likely to have driven the evolution of AHR structure and function. The vast majority of AHR ligands are provided through the diet, either through naturally occurring dietary ligands, such as the indoles and flavonoids or through the metabolism of tryptophan[500]. One of the prototypic endogenous AHR ligands is indole-3-carbinol (I3C), a metabolite of glucobrassicin, which is naturally present in cruciferous vegetables including broccoli and Brussels sprouts[501]. Under acidic conditions in the stomach, I3C is further enzymatically degraded to the higher affinity AHR ligands 3,3'-diindolylmethane (DIM) and indolo-[3,2-b]-carbazole (ICZ)[502]. Another abundant source of dietary AHR ligands is flavonoids, which are ubiquitously found in fruits and vegetables and represent the most abundant class of plant polyphenols. Activators of AHR have been identified in

three of the six major subgroups of flavonoids including flavonols, isoflavones and flavones[503].

The most likely source of endogenous agonists of AHR are the derivatives of tryptophan metabolism, due to the aromaticity of tryptophan. Dietary tryptophan is metabolised through four main pathways: through hydroxylation (serotonin and melatonin), transamination (indolepyruvic acid [IPA]), decarboxylation (tryptamine) and lastly through the kynurenine pathway, which accounts for 95% of all dietary tryptophan metabolism[504]. However, AHR ligands can arise from all 4 pathways of tryptophan metabolism. Indeed, IPA can activate AHR and suppress experimental colitis in mice[505] and tryptamine is a pro-ligand for AHR[506]. The downstream metabolite of tryptamine which activates AHR has so far evaded discovery. Other groups have shown that serotonin (5-hydroxytryptamine; 5-HT) is an endogenous activator of AHR in intestinal epithelial cells[507] and we demonstrate here that one of serotonin's downstream metabolites, 5-hydroxyindoleacetic acid (5-HIAA), can induce *Cyp1a1* and *Il10* expression in murine B cells. Kynurenine has been suggested to be an AHR ligand, but its physiological relevance as an AHR ligand has cast doubt due to the comparative concentration needed to elicit reporter activity in a hepatoma cell line, in comparison to the well-established AHR ligand 6-formylindolo[3,2-*b*]carbazole (FICZ)[508]. Instead, it is more likely that kynurenine, like tryptamine, serves as a pro-ligand for AHR. In support of this, downstream metabolites of kynurenine such as cinnabarinic acid have been shown to be more potent AHR agonists[509].

Amongst non-haematopoietic tissues, AHR expression is highest in liver, kidney, lung, skin and in the gut; all of which are exposed to high concentrations of endogenous AHR ligands[510]. Although the majority of AHR ligands are derived from the diet, site specific ligands can exist in high concentrations in other organs. FICZ is present in the skin and can activate AHR at picomolar concentrations[511] and is formed through the photolysis of L-tryptophan by ultraviolet light[512]. It is perhaps unsurprising that AHR expression is ubiquitously expressed in all cell types in the dermal[513] and epidermal[514, 515] layers of the skin, as a mechanism to respond to oxidative stress caused by UV light and to prevent excessive inflammation in response to the build-up of oxygen reactive species[516]. Given the ubiquitous expression of AHR in the body, especially at barrier sites, ligand

promiscuity is crucial to AHR's role as an environmental sensor and allows for detection of diverse metabolites present at different barrier sites in the body and the regulation of cellular responses at these sites.

Compound	Type of metabolite or compound	Source
Exogenous ligands		
2,3,7,8-Tetrachloro-ρ-dioxin (TCDD)[498]	Polycyclic/halogenated aromatic hydrocarbons	Industrial pollutants
2,3,7,8-Tetrachlorodibenzofuran[517]	Polycyclic/halogenated aromatic hydrocarbons	
3,4,3,4'-Tetrachloroazoxybenzene[518]	Polycyclic/halogenated aromatic hydrocarbon	
3,4,3,4'-Tetrachloroazobenzene[518]	Polycyclic/halogenated aromatic hydrocarbon	
2,3,6,7-Tetrachloronaphthalene[519]	Polycyclic/halogenated aromatic hydrocarbon	
3-Methylcholanthrene (3-MC)[520]	Polycyclic/halogenated aromatic hydrocarbon	
3,3',4,4',5-pentachlorobiphenyl[521]	Polycyclic/halogenated aromatic hydrocarbon	
Benzo[a]pyrene[522]	Polycyclic/halogenated aromatic hydrocarbon	
7,12-dimethylbenz [a]anthracene[523]	Polycyclic/halogenated aromatic hydrocarbon	
β-naphthoflavone[524]	Polycyclic/halogenated aromatic hydrocarbon	
Omeprazole[524]	Benzimidazole	Synthetic
VAF347[525]	Pyrimidinylphenylamine	
4-hydroxy-tamoxifen (4OHT)[526]	Triphenylethylene	
6-Methyl-1,3,8-trichlorodibenzofuran (6-MCDF)[527]	Alkyl polychlorinated dibenzofuran	
Laquinimod[528]	Carboxamide	
IMA-06201[529]	N.D	
IMA-08401[530]		
10-chloro-7H-benzimidazo[2,1-a]benzo[de]Iso-quinolin-7-one (10-Cl-BBQ)[531]	Benzimidazoisoquinoline	
Leflunomide[532]	N.D	
(2'*Z*,3'*E*)-6-Bromo-1-methylindirubin-3'-oxime (MeBIO)[533]		
Pifithrin-α hydrobromide[534]		
Endogenous ligands		
Malassezin[535]	Indole alkaloid	Yeast and/or fungi
Trypthantrin[536]	Alkaloid tryptophan derivative	Yeast and Plants
Bilirubin[537]	Haem metabolites	Host metabolism
Biliverdin[537]		
Lipoxin A4[538]	Arachidonic acid metabolites	Host metabolism
Prostaglandin G2 (PGG2)[539]		

Leukotriene A4[540]		
Hydroxyeicosatraenoic acid ([12(R)-HETE])[541]		
Indirubin[542]	Phytochemicals	Plants
Indigo[542]		
Indirubin-3'oxime[533]		
Gallic acid[543]	Phenolic acid	
Norisolboldine[544]	Alkaloid	
Indole[545]	Indole metabolites	Dietary metabolite and microbiota metabolism
2-1(1'H-indole-3'-carbonyl)-thiazole-4-carboxylic acid methyl ester (ITE)[546]		Endogenous/chemical process
Indolo[3,2-b]carbazole (ICZ)[547]		Dietary metabolite
2-(indol-3-ylmethyl)-3,3'-diindolylmethane (Ltr-1)[547]		
3,3'-diindolylmethane (DIM)[547]		
Indole-3-acetonitrile[547]		
Indole-3-carbinol (I3C)[547]		
Curcumin[548]	Polyphenol	
Diosmin[549]	Flavonoids	
Flavipin[550]		Fungi
Chrysin[551]		Plants
Galangin[552]		
Genistein[553]		
Baicalein[553]		
Daidzein[553]		
Apigenin[553]		
Kynurenine[508]	Tryptophan metabolites	Microbiome and/or host metabolism
Kynurenic acid[554]		
Xanthurenic acid[554]		
Cinnabarinic acid (CA)[509]		
6-formylindolo[3,2-b]carbazole (FICZ)[512]		
5-Hydroxy-tryptophan (5-HT)[555]		
5-Hydroxyindole-3-acetic acid (5-HIAA)**		
Tryptamine[556]		
Indole-3-acetic acid (IAA)[545]		
3-methylindole (Skatole)[557]	Tryptophan metabolites	Microbiome and/or host metabolism
Indole-3-carboxaldehyde (I3A)[558]		
3-indoxyl sulfate (I3S)[559]		
Tapinarof[560]	Stilbenoid	Bacterial derived
Butyrate[561]	Short chain fatty acids	Microbiome
Propionate[561]		
Iso-valerate[561]		

AHR antagonists		
Kaempferol[562]	Flavonoids	Plants
Quercertin[562]		
Myricetin[553]		
Leuteolin[553]		
Resveratrol[563]	Stilbenoid polyphenol	
CH-223191[564]	N.D.	Synthetic
Stemregenin 1 (SR1)[565]	Purine derivative	
GNF351[566]		
3'-methoxy-4'-nitroflavone (MNF)[567]	Flavonoids	
3',4'-Dimethoxyflavone (DMF)[568]		

Table 1.1. List of known endogenous and exogenous AHR agonists and antagonists. All agonists listed are defined by their ability to induce the expression of *Cyp1a1* or their ability to induce AHR driven XRE luciferase reporter activity in transfected cell lines. N.D. Not determined. **Novel AHR agonist in B cells identified by this group. Kynurenine is controversially listed as a ligand, as the concentration needed to elicit XRE driven luciferase reporter activity is higher than the physiological concentration in the body.

1.5.4 Regulatory feedback loops

Unabated AHR signalling often leads to pathological responses[569], so AHR expression and activity need to be tightly regulated. Central to this process are several autoregulatory feedback loops, for example those involving the expression of the cytochrome P (CYP)450 group of enzymes. The CYP450 family are drug metabolising enzymes, expressed in many different cell types, which play a critical role in the oxidative metabolism of lipophilic compounds[570]. One of these enzymes, CYP1A1, is expressed as a consequence of AHR binding to XRE upstream of the *Cyp1a1* gene[571]. CYP1A1 metabolises AHR ligands, thus negatively regulating AHR signalling. Certain AHR ligands, like the dietary phytochemicals and FICZ are more readily metabolised by CYP1A1[511, 572, 573]. Other ligands like TCDD are more resistant to degradation and persist in the cytoplasm and nucleus (bound to AHR) of the cell[574]. As a way to combat AHR ligands which persist and induce constitutive signalling, AHR induces the expression of the aryl hydrocarbon receptor repressor (AHRR). AHRR has a higher binding affinity for ARNT and can displace AHR from ARNT[575]. Finally, AHR is degraded through the ubiquitin-proteasome pathway after activation[576, 577].

1.5.5 The function of AHR in immunity

A link between AHR and the immune system was originally established after it was observed that TCDD given at increasing dosages in rodents, induced thymic involution and reduced lymphocyte counts[445]. Reduced frequencies of circulating lymphocytes were also noted in humans accidently exposed to TCDD and related chemicals[578]. AHR is expressed in most cells of the immune system, including, but not limited to, monocytes, DCs, mast cells, $\gamma\delta$ T cells, innate-like lymphoid cells (ILCs), NK cells, Th17 cells, FOXP3$^+$ Tregs, Tr1 cells and B cells[579]. Furthermore, DREs are found in a multitude of genes important in orchestrating immune responses, highlighting the importance of AHR in regulating cellular and humoral mediated immune responses[580].

1.5.5.1 The role of AHR in T cell differentiation and function

Within the T cell subsets, AHR is highly expressed within the Th17 and Treg populations (both FOXP3$^+$ Tregs and Tr1 cells). In Th1 and Th2 cells, AHR expression is restricted[445]. AHR is known to promote the generation of Th17 cells and expression of IL-17 and IL-22[581, 582]. Administration of FICZ to mice leads to a

more severe course of EAE, with a reduction in FOXP3$^+$ Tregs and an increase in Th17 cells[581]. In fact, FICZ and other natural agonists of AHR found in culture medium promote the differentiation of Th17 cells. Furthermore, blocking AHR inhibits Th17 differentiation[583]. Similarly, FICZ activation of AHR supports the generation of Th17 and Th22 cells in humans[584, 585]. AHR expression in Th17 cells is driven through IL-6 and IL-21 induced STAT3 expression[586]. AHR can then bind to the *Il17* and *Il22* loci and co-ordinate IL-22 expression by facilitating the recruitment of RORγt to the *Il22* promoter in IL-21 stimulated CD4$^+$ T cells[486, 587]. It is worth noting that although Th17 cells are thought to be pathogenic in a variety of autoimmune diseases[588], Th17 differentiation induced in response to TGFβ and IL-6 can be anti-inflammatory in certain contexts[589]. This is in direct contrast to Th17 cells generated in the presence of IL-23, or in the presence of IL-1β, IL-6 and IL-23, which promote pathogenicity[590, 591].

As well as promoting Th17 differentiation, AHR can contribute to the transdifferentiation of T cells by skewing Th17 cells towards the anti-inflammatory Tr1 cells; a process driven by TGF-β and SMAD3 signalling. Upon secondary infection with helminths, the number of Tr1 ex-Th17 cells are significantly increased. Tr1 ex-Th17 cells were also enriched in antigen specific MOG$^+$CD4$^+$ T cells, compared to MOG$^-$CD4$^+$ T cells in EAE. Intriguingly, in Tr1 ex-Th17, addition of FICZ increased IL-10[592]. The AHR agonist bilirubin also promotes immunosuppression by upregulating CD39 expression on Th17 cells and leads to the downregulation of IL-17 and upregulation of IL-10 in both mouse and human Th17 cells. Mice treated with bilirubin develop a less severe form of DSS colitis[593]. Collectively, these findings suggest that AHR contributes to the differentiation of Th17 cells, however does not determine whether the Th17 cell exerts pathogenic or suppressive function. Dependent on the cytokine mileau e.g. TGFβ or IL-23, AHR plays a supportive role in the function of Th17 cells. The role of AHR in the transdifferentiation of Th17 to Tr1 cells, would seem to support the notion that AHR primarily acts as an immunosuppressive agent. However, how AHR dictates this process is unknown and it is likely that the dose of AHR ligands, the chronicity of AHR ligation and co-stimuli all play a part in this process.

The role of AHR in regulating IL-10 production by T cells is well defined. Initial studies demonstrated that AHR activation by TCDD could mediate suppression of

T cell responses[594]. Recently, it has been reported that TCDD induces functional Tregs, which suppresses acute graft-versus-host disease[595] and EAE[581]. In addition, the AHR ligand norisoboldine (NOR) expanded $CD4^+CD25^+FOXP3^+$ Tregs under hypoxic conditions, by inhibiting glycolysis in an AHR-dependent manner. NOR treatment of mice, much like TCDD, alleviated colitis[596]. Culture of naïve $CD4^+CD25^-$ T cells with kynurenine can also increase the frequencies of $CD4^+CD25^+FOXP3^+$ Tregs[508].

Upregulation of AHR in Tr1 occurs through IL-27 signalling. Mechanistically, AHR forms part of a transcriptional complex with c-MAF and transactivates both the *Il10* and *Il21* promoters in Tr1 cells. Interestingly, in this study, both FICZ and TCDD led to the upregulation of IL-10. Optimal IL-10 and IL-21 production was achieved by culturing naïve T cells with TGFβ, IL-27 and FICZ. MOG (35-55) peptide and IL-27 activated $CD4^+$ T cells, were able to suppress EAE disease upon adoptive transfer into recipient mice. However, this was not the case in mice receiving MOG (35-55) peptide and IL-27 activated donor $Ahr^{d/d}$ (non-responsive allele) $CD4^+$ T cells, suggesting Tr1 cell mediated suppression was dependent on the expression of functional AHR[422]. Concordantly, in human $CD4^+$ T cells, activation of AHR through TCDD, drove the differentiation of $CD4^+FOXP3^-$ Tr1 cells and the upregulation of IL-10. Granzyme B was also upregulated and required for $CD4^+FOXP3^-$ Tr1 cells to suppress effector T cells. Addition of TGF-β1 and TCDD to naïve $CD4^+$ T cells induced $FOXP3^+$ Tregs, which suppressed effector T cells through expression of CD39[597]. More recently, it has been shown that the cytokine Activin-A induces the differentiation of human Tr1 cells. Activin-A signalling induced the expression of AHR, IRF4 and MAF. These transcription factors co-operated as a part of a transcriptional complex which bound to the *Il10* locus and upregulated the expression of IL-10[598].

In addition to enhancing IL-10 production by $FOXP3^+$ Tregs and Tr1 cells, AHR also maintains Tr1 function by metabolic reprogramming. HIF1α controls the early metabolic programming of Tr1 cells and is required for the initial production of IL-10. However, long term production of IL-10 is dependent on AHR signalling and the role of AHR in supporting the degradation of HIF1α[586]. AHR also controls cellular processes of Tregs by modulating the chromatin remodelling of these cells. In $CD4^+$ T cells stimulated with anti-CD3 and anti-CD28, addition of TCDD reduced

the methylation of the *Foxp3* locus, whilst simultaneously increasing the methylation of the *Il17* locus[599]. The *Foxp3* gene needs to be in its unmethylated state to be transcribed[600]. Whether AHR causes displacement of HDACs, or recruits chromatin remodelling complexes to the *Foxp3* locus is not known.

1.5.5.2 AHR in the regulation of B cell responses

In contrast to the wealth of knowledge available in the literature describing the role of AHR in T cells, the function of AHR in B cell biology is less well characterised[601]. Through work on the prototypical ligand TCDD, initial studies identified three key roles of AHR on B cells, which laid down foundations for further study characterising these processes. AHR influences the activation and proliferation of B cells, B cell development and antibody production[445]. Although TCDD has been instrumental in determining much of the knowledge we know regarding the role of AHR in B cells, it is a persistent activator of AHR and is resistant to degradation, so does not reflect the physiological role of AHR activity in B cells. Equally, different ligands can induce tissue specific and cell specific outcomes in a context dependent manner. As such, it is important to identify the role of endogenous ligands in AHR-driven regulation of B cell responses. Both the endogenous ligands of AHR in B cells and their role in shaping B cell responses remain very poorly characterised. Nevertheless, the role of TCDD and other HAH and PAH ligands in shaping these processes will be summarised below.

Initial work characterising the antibody response after TCDD treatment, revealed that guinea pigs receiving tetanus toxoid reduced the serum levels of anti-tetanus toxin antibodies in a dose dependent response to TCDD treatment[594]. Later studies confirmed these findings by showing TCDD treated mice had reduced numbers of antibody secreting cells to both a series of TD and TI antigens[602, 603, 604]. Treatment of mice with TCDD and sensitisation of mice *in vivo* to TD antigens (sheep RBC's), TI antigens (dinitrophenyl–ficoll, trinitrophenyl-lipopolysaccharide) or polyclonal activators of B cells (anti-Ig or LPS) revealed equivalent suppression of the IgM response regardless of the type of antigen used. More importantly, the addition of TCDD to LPS activated B cells *in vitro*, suppressed the IgM response, demonstrating a direct effect of TCDD on B cells[605, 606]. Morris *et al* showed that it was the highly proliferative B cells in the G1 phase of the cell cycle that were more susceptible to the refractory effects of TCDD[607]. The immunotoxic role of TCDD

was first directly demonstrated by direct binding of TCDD-bound AHR to the XRE regions of the 3'IgH transcriptional regulatory region (3'IgHRR) in the mouse B cell lymphoma derived cell line CH12.LX and purified mouse splenic B cells, which led to the downregulation of secreted IgM[608, 609]. The 3'IgHRR region is a 40k region upstream of the constant α region, and contains four enhancers called DNaseI hypersensitive sites (hs) 3, hs1,2, hs3b and hs4[610]. In tandem, TCDD treatment of LPS activated CH12.LX B cells, also led to downregulation of Igκ, the J chain and XBP1[611]. Importantly, deletion of this regulatory region leads to the cessation of Ig heavy chain production[612]. This region also plays a crucial role as deletion of the two 3' enhancers hs3b and hs4, impairs class switching[613].

The addition of TCDD and its timing, either prior to or post-antigen sensitisation is also important. Adding TCDD prior to, or at the time of, antigen sensitisation marks a large suppression of the IgM response. TCDD added post antigen sensitisation (1-5 days) saw a marked decrease in the strength of this response[604, 606]. Data from these studies suggested that AHR affected B cell development, as TCDD only inhibited the IgM response during a narrow time frame around antigen activation. Data from these studies prompted research into the role of TCDD-driven AHR activation on B cell development.

Activation of AHR occurs throughout the B cell maturation process, occurring from the HSC stage right through to the terminal differentiation of B cells. As such the expression of AHR is tightly regulated throughout the maturation process and is highly expressed at certain stages to exert its function as an environmental sensor. We know for instance that AHR is highly expressed in MZ B cells, peritoneal B-1 cells and in Peyer's patches B cells; all sites at which these cells carry out immunosurveillance for pathogens and their associated antigens. Indeed, BCR signals are key for driving the induction of AHR expression, which could explain why both pro- and pre-B cells express very low levels of AHR[614, 615]. Since developing B cells in the bone marrow are more susceptible to environmental stressors and to clonal deletion by the binding of self-antigen, it was hypothesised that bone marrow B cells would be more susceptible to signals through AHR[614]. Indirect activation of AHR in bone marrow cultures with the AHR agonist 7,12-dimethylbenz [a]anthracene rapidly induced apoptosis in pre-B cells at very low doses (10nM)[616]. Activation of AHR in bone marrow stromal cells was responsible

for the apoptosis of pro- and pre-B cells, as co-culture of *Ahr*$^{-/-}$ stromal cells with a bone marrow-derived preB cell line (BU-11) in the presence of PAHs, failed to induce apoptosis of preB cells. Conversely, co-culture of *Ahr*$^{+/+}$ stromal cells with preB cells was able to induce apoptosis[617]. These data suggested that AHR could influence early B cell development, indirectly through altering the bone marrow milieu. Very little is known regarding AHR function from the transitional B cell to mature B cell stages.

In contrast, the role of AHR in terminal differentiation has been extensively studied. AHR is important for inhibiting the terminal differentiation of B cells. In humans, *in vitro* CD40L-induced differentiation of B cells into plasma cells is inhibited by the addition of the PAH benzo[a]pyrene[618]. In addition to its role in regulating Ig production, follow-up studies in mice have shown that AHR acts as a critical overseer in managing the transcriptional network governing mature B cell differentiation and function (summarised in Figure 1.6). As eluded to earlier, BLIMP-1 is essential in driving the differentiation of mature FO B cells to plasmablasts and then plasma cells. BLIMP-1 suppresses the induction of *Aicda* and promotes the expression of *Irf4*, two key events in the terminal differentiation of B cells[245]. Of note, AHR inhibits the expression of BLIMP-1 through transrepression of the *Prdm1* gene. This involves two separate processes; 1) AHR suppression of AP1 and 2) AHR induction of *Bach2* expression. TCDD activated AHR inhibits AP-1 expression and reduced AP-1 binding to the *Prdm1* promoter, thereby inhibiting BLIMP-1 expression[619]. Suppression of BLIMP-1 also occurs through AHR-mediated upregulation of BACH2, a transcription factor important in memory B cell development and for the repression of BLIMP-1[620,621]. Activation of B cells with TCDD, leads to AHR binding to the first intron of the *Bach2* gene, thereby facilitating its expression and indirectly repressing BLIMP-1 by BACH2 mediated binding of the *Prdm1* gene[620].

Furthermore, TCDD activation of AHR led to a reduction in BLIMP-1 binding of the *Pax5* promoter[619]. In normal B cell development, BLIMP-1 expression and the loss of PAX5 expression is required for plasma cell differentiation[622]. It is important to note that no direct binding of AHR to the *Prdm1* gene in B cells has been reported. Further highlighting the ligand and cell-context specific role of AHR activation, methylcolanthrene bound AHR, either directly or indirectly, increases BLIMP-1

expression in epidermal keratinocytes[623]. Using mathematical modelling, Zhang *et al* showed that TCDD mediated repression of terminal B cell differentiation occurred in a binary fashion. That is to say that TCDD reduced the number of IgM-secreting cells in a dose-dependent manner, rather than proportionally reducing the individual plasma cell amount of secreted IgM. The authors hypothesised that TCDD might delay B cell differentiation and increase the chances of class switching[624]. In fact, the converse is true, as we now know that AHR plays a crucial role in CSR[217]. TCDD treated mice infected with influenza have a reduction in the virus-specific IgG, compared to the vehicle control group[625]. More recently, Vaidyanathan *et al* show that AHR can negatively regulate CSR in the absence of any infection, through binding of AHR to the *Aicda* gene and negatively regulating its expression. Moreover, addition of TCDD to B cells cultured with LPS and anti-IgD dextran reduced the frequencies of $IgG3^+$ and IgA^+ B cells. Mixed bone marrow chimeras containing WT CD45.1 and $Ahr^{-/-}$ CD45.2 B cells revealed that in mice immunised with 4-Hydroxy-3-nitrophenylacetyl-chicken gamma globulin (NP-CGG), a TD antigen, $Ahr^{-/-}$ mice contributed to a greater proportion of the NP-specific $IgG1^+$B cell pool. Moreover, chimeric mice infected with the PR8 strain of influenza, revealed that no differences in the frequencies of GC B cells were observed between the WT B cells and $Ahr^{-/-}$ B cells. However, within the $B220^+GL7^+IgG1^+$ GC B cell population, $Ahr^{-/-}$ B cells accounted for over 80% of the haemagglutinin antigen specific B cells. In parallel, more $B220^{lo}CD138^+$ plasma cells were also derived from $Ahr^{-/-}$ B cells, thus highlighting the critical role of B cell AHR expression in restraining both CSR and terminal differentiation of B cells[217].

In addition to regulating B cell maturation, AHR also controls the activation and proliferation of B cells. Stimulation of B cells with IL-4, LPS or activation through the BCR can all induce the expression of AHR in B cells and can act in synergy to further increase AHR expression[217, 615, 626]. In human B cells, both TLR9 activation through CpG-B and CD40 activation can induce AHR expression[627]. Unlike STAT3 in T cells, the transcription factors which upregulate AHR in B cells remains unknown, although the NF-κB pathway has been ruled out[615]. Resting B cells express low levels of AHR, which is then increased upon activation[601]. This is in direct contrast to naïve T cells, who *per se* do not induce AHR expression upon activation[445]. It is tempting to speculate that B cells, after activation, upregulate AHR to respond to environmental cues and regulate their responses in a ligand

dose-dependent manner. Recently, Villa and colleagues have shown that AHR deficiency in B cells, impairs their ability to proliferate in response to anti-IgM. Moreover, the proliferation of antigen specific B cells are impaired in AHR deficient B cells. AHR increased the proliferative capacity of splenic B cells after BCR ligation, through interaction with the cell cycle regulator cyclin O[615].

In conclusion, whilst TCDD has given researchers an insight into the role of AHR in directing B cell responses, these processes *in vivo* are likely to be more transient and much more complex, due to rapid turnover and metabolism of endogenous ligands. Thus, to obtain a more physiological readout of AHR in B cell function, we opted to use the potent endogenous AHR activator FICZ and also to utilise both global and B cell specific AHR knockout mice. We report a role of AHR in the differentiation and maintenance of IL-10^{+}Bregs and identify a novel AHR ligand 5-HIAA, which promotes Breg function.

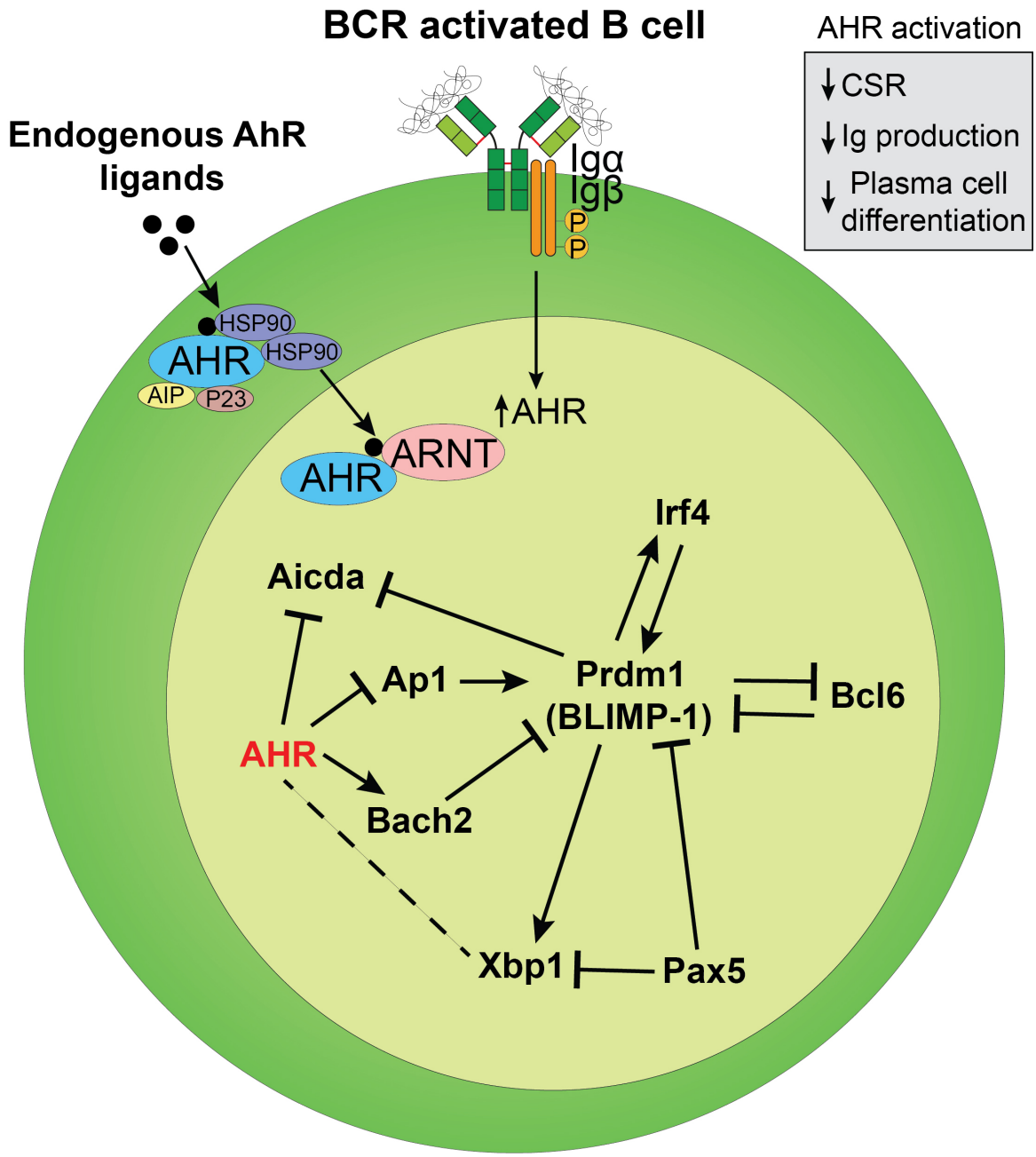

Figure 1.6. AHR regulates the transcriptional network governing terminal B cell differentiation. AHR inhibits the differentiation of activated B cells into plasma cells via transrepression of *Prdm1*, through the upregulation of *Bach2*. XRE sites have been reported in the *Xbp1* locus, but no direct regulation has been observed.

1.6 The role of short chain fatty acids in the immune system

Short chain fatty acids (SCFAs) are a metabolic by-product produced by the fermentation of dietary fibre by anaerobic bacteria[628, 629]. Whilst SCFAs can be produced naturally by host metabolism in the liver, the major site of production is in the colon, where anaerobic bacteria thrive[630]. Acetate, propionate and butyrate are the main SCFAs produced and the concentrations of these metabolites vary according to the diet, host genetics and importantly, the composition of the microbiota. Members of the *Bacteroidetes* phylum are primary producers of acetate and propionate, whilst the *Firmicutes* phylum are the predominant source of butyrate[631]. SCFAs can activate at least 4 known G-protein-coupled receptors (GPCRs); the free fatty acid receptors (FFAR)2 and FFAR3 (also known as GPR43 and GPR41), the olfactory receptor-78 and the niacin/butyrate receptor GPR109a[632]. Although GPR43 and GPR41 can bind to propionate, acetate, butyrate and other SCFAs, both receptors primarily bind to acetate and propionate[628, 633]. In contrast, GPR109a selectively binds to butyrate and niacin[634]. Additionally, SCFAs can enter a cell through the sodium-coupled monocarboxylate transporter 1 (SLC5A8) and can exert their epigenetic modulatory function once inside a cell[635].

SCFAs can exert distinct functions on colonocytes and on immune cells through several distinct mechanisms, which include their direct role as histone deacetylase inhibitors (HDACi), activation of histone acetyltransferase, stabilisation of hypoxia inducible factors or signalling by the GPCRs,[636, 637, 638, 639]. More recently, butyrate has been shown to enhance histone crotonylation which, like acetylation, occurs at the lysine residues[640]. The effects of histone crotonylation on gene expression are unclear, as this epigenetic modification can both activate and inhibit gene expression[640, 641]. Lastly, butyrate has been shown to induce other epigenetic modifications including histone methylation, inhibition of histone phosphorylation, DNA methylation and hyperacetylation of non-histone proteins[642, 643, 644, 645]. These data highlight the diverse functions of SCFAs in the epigenetic regulation of gene expression.

SCFAs can induce a pro-inflammatory or tolerogenic profile in immune cells, depending on the cell type, type of stimulation, the environment and on the type of SCFA. Of the SCFAs, butyrate has been shown to have an anti-inflammatory role

in multiple cell types[632]. Butyrate suppresses the production of nitric oxide, IL-6 and IL-12p40 by murine bone marrow derived macrophages and colonic lamina propria macrophages upon culture with LPS. However, no suppression was seen with acetate and propionate, suggesting SCFA specific effects on the regulation of immune responses. Suppression of pro-inflammatory cytokine expression in these cells is mediated by butyrate's role as a HDACi, and the resulting increase in histone 3 lysine 9 acetylation at the promoter regions of *Il2*, *Il12b* and *Nos2* genes[646]. Indeed, through its role as a HDACi, butyrate drives monocyte to macrophage differentiation and increases macrophage antimicrobial activity. Mice given butyrate have increased resistance to enteropathogens[647].

The role of SCFA's in T cell differentiation and function have been well characterised. SCFAs regulate T cell differentiation, both through direct activation of T cells or indirectly by modulating DC function[629]. Mice lacking the SCFA transporter SLC5A8, do not induce the expression of indoleamine 2,3-dioxygenase (IDO)1 or aldehyde dehydrogenase (ALDH)1A2 upon exposure to butyrate. Unlike the WT counterparts, *Slc5a8*$^{-/-}$ DCs are unable to convert naïve Tregs to FOXP3^{+} Tregs and do not inhibit the generation of IFN-γ expressing T cells in a model of colitis[648]. In addition, butyrate can promote tolerogenic macrophage and DC generation through activation of the butyrate receptor GPR109A, which induces the expression of IL-10 and ALDH1A1 in colonic DCs and macrophages from WT mice. GPR109A-activated DCs promote the differentiation of naïve CD4^{+} T cells to FOXP3^{+} Tregs and provide protection against DSS colitis[649].

Butyrate can also act directly on CD4^{+} T cells through increasing the acetylation of the non-coding sequence regions of the *Foxp3* locus, thereby promoting the differentiation of naïve CD4^{+} T cells to FOXP3^{+} Tregs[650, 651]. SCFAs can also impact the differentiation of other T helper cell subsets. Mice treated with propionate are protected from allergic airway inflammation, due to an impairment in DCs to induce Th2 differentiation[652]. Similarly, acetate influences the generation of Th17 and IL-10^{+} T cells, through increasing the acetylation of p70 S6 kinase; a downstream target of the mammalian target of rapamycin (mTOR) pathway[653]. The mTOR pathway is required for the generation of effector and regulatory cytokine production by T cells, including IFN-γ, IL-10 and IL-17[654].

1.6.1 The regulation of B cell responses by SCFAs - a proposed role for AHR?

To date, elucidating the role of SCFAs on B cell responses have been limited to the effects of SCFAs on the humoral response. Initial studies revealed that mice fed a high fibre diet had increased numbers of IgA^+ plasma cells in the lamina propria and IgA^+ GC B cells in the Peyer's patches (PP), which was attributed to the effect of propionate. Mice fed a high fibre diet or a low fibre diet supplemented with propionate increased the expression of *Aicda* in PP B cells and class switching towards IgA^+ expressing cells. Importantly, both the CNS regions and the class switch regions of the *Aicda* and *Igha* loci respectively, had increased acetylation, suggesting that SCFAs regulated this response through its role as an HDACi[655]. The increase in intestinal IgA was later suggested to be driven by SCFA sensing by the GPR43 receptor, as GPR43 KO mice had reduced levels of faecal IgA^+ and reduced frequencies of IgA^+ expressing B cells in the lamina propria. Furthermore, unlike in control WT mice, treatment of *Gpr43*$^{-/-}$ mice with acetate failed to increase faecal IgA levels. Acetate driven IgA production was shown to be partially dependent on GPR43-induced retinoic acid production by DCs. It is important to note that butyrate did not increase IgA levels in this study, thus reinforcing the idea that each SCFA can exert different functional roles in the regulation of B cell responses[656].

In direct contrast to the previous studies, Sanchez *et al* reported that administration of butyrate and propionate together reduced the levels of IgM, IgG and IgA-expressing B cells in the lamina propria, PPs and MLNs. After challenge with both TD (NP-CGG) and TI antigens (NP-LPS), mice receiving butyrate and propionate had reduced serum levels of IgM, IgG1 and IgA. Importantly, administration of SCFAs to WT mice decreased CSR, by reducing the expression of *Aicda* and also reduced terminal differentiation of B cells to plasma cells by inhibiting *Prdm1*. These effects were attributed to the role of butyrate and propionate as HDAC inhibitors, as the selective GPR43 antagonist GLPG0974 did not affect the suppression of *Aicda* or *Prdm1* by butyrate or propionate[657]. Whilst the reasons for contrasting results between the studies are not entirely explained, it is likely that the type and dose of SCFA affect the outcome of SCFAs on CSR and terminal differentiation.

As detailed in the previous sections, there are notable functional similarities between the role of AHR and SCFAs in the regulation of B cell responses. Notably, both AHR and SCFAs reduce CSR by inhibiting *Aicda* expression, halt the terminal differentiation of B cells and reduce the levels of secreted immunoglobulin. Indeed, several lines of evidence link the effects of SCFAs to AHR activation. Butyrate has been shown to be a direct AHR ligand in an intestinal epithelial cell line[561]. In addition, butyrate can also enhance TCDD-driven AHR activation in mouse colonocytes[658]. These data combined led us to hypothesise that SCFAs regulate B cell responses in an AHR-dependent manner.

CHAPTER II: Materials and Methods

2.1. Mice

2.1.1 Mouse strains

All mice were generated on a C57BL/6 background. C57BL/6 WT mice were purchased from Envigo, UK; B6.129S2-*Ighm*^{tm1Cgn}*/J* (μMT) mice were purchased from Jackson, USA. IL-10eGFP mice were as described[659], courtesy of Prof Karp; 129(B6)-*Il10*^{tm1Cgn}*/J* (*Il10*$^{-/-}$) mice were kindly given courtesy of Professor Fiona Powrie (Kennedy Institute of Rheumatology Oxford University); B6.SJL-Ptprc^{a} Pepc^{b}/BoyJ (CD45.1) mice were kindly given courtesy of Professor Derek Gilroy (University College London). *Ahr*$^{-/-}$, *Ahr*$^{+/-}$, *Mb1*$^{cre/cre}$, *Ahr*$^{fl/fl}$*R26R*$^{fl/fl}$ (courtesy of Prof Reth) and *Ahr*$^{-/-}$*Mb1*$^{cre/cre}$ mice were kindly provided by Prof. Brigitta Stockinger. *Ahr*$^{fl/-}$*Mb1*$^{cre/+}$ were generated by crossing male *Ahr*$^{-/-}$*Mb1*$^{cre/cre}$ with female *Ahr*$^{fl/fl}$*R26R*$^{fl/fl}$ mice. Mice were used at 6–12 weeks of age and were age- and sex-matched. All mice were bred and maintained at the animal facility, University College London. All experiments were approved by the Animal Welfare and Ethical Review Body of University College London and authorized by the United Kingdom Home Office.

2.1.2 Genotyping of mouse strains

Ear clips were taken from mice and processed using a KAPA HotStart mouse genotyping kit (Sigma-Aldrich), according to manufacturer's instructions. Briefly, ear clips ~2mm in diameter were incubated in 100μl lysis buffer containing 88μl H_2O, 10μl 10x KAPA express extract buffer and 2μl KAPA express extract enzyme (20,000 U/ml). Ear tissue was incubated at 75°C for 10 mins, followed by 95°C for 5 minutes. Extracts were diluted 10-fold in Tris-HCL (pH 8.0-8.5).

PCR was carried out on the diluted DNA extracts in a volume of 25μl, consisting of 1μl of DNA extract or H_2O (no template control), 12.5μl of 2x KAPA2G Fast (Hotstart) genotyping mix with dye, 1.25μl of each primer and topped up with H_2O to 25μl. Primers were used at a final concentration of 0.5μM. Primer sequences against genomic DNA were custom designed using Primer-BLAST or using the previously described sequences on the Jax website. Primers for *Mb1* were designed to span exons 2+3; the deleted segments in *Mb1cre* mice. The following

primer sequences were used for genotyping: *Ahr* common forward (5'-AACTAGGTAAGTCACTCAGCATTACA-3'), *Ahr* wild type reverse (5'CCCCTCTACTATACTGCTACCCAAC-3'), *Ahr* mutant reverse (5'CTAAAGCGCATGCTCCAGAC-3'), *Mb1* forward (5'-GTACGGCTCCACTCCTGATG-3'), *Mb1* reverse (5'-GGAAGAAAGAGGGAGCAGGG-3'). PCR reactions were run with using the following cycling parameters in Table 2.1, using a TGradient (Biometra) thermocycler.

Step Number	Temp (°C)	Time	Notes
1	94	2 mins	
2	94	20 sec	
3	65	15 sec	0.5°C decrease per cycle
4	68	10 sec	
5	Various	Various	Repeat steps 2-4 for 10 cycles (Touchdown)
6	94	15 sec	
7	60	15 sec	
8	72	10 sec	
9	Various	Various	Repeat steps 6-8 for 28 cycles for genotyping *Ahr* and 25 cycles for *Mb1*.
10	72	2 mins	

Table 2.1. PCR cycling parameters used for genotyping.

Amplicon lengths were assessed by using a 1% w/v agarose gel (1% agarose, 1x Tris-Acetate-EDTA; Sigma-Aldrich). SYBR™ Safe DNA stain (ThermoFisher Scientific) was included in the gel mix at a 1/10,000 dilution. 15μl of the PCR product (dye already intercalated) or 5μl of Hyperladder™ 1kb (Bioline) DNA ladder were loaded into a well and the gel was run at 90v for 40 minutes. The gel was assessed by UV light for DNA bands, using the ChemiDoc™ XRS imager and Quantity One software (BioRad).

2.2 Induction of antigen-induced arthritis (AIA)

AIA was induced by injecting mice subcutaneously at the tail base with 200μg of methylated BSA (mBSA; Sigma-Aldrich) emulsified in 100μl Complete Freund's Adjuvant (CFA). CFA was made by mixing 3mg/ml of *Mycobacterium tuberculosis* (Difco) in Incomplete Freund's Adjuvant (IFA; Sigma-Aldrich). After 7 days, mice

received an intra-articular (IA) injection of 10μl of PBS containing 200μg mBSA in the right knee and 10μl PBS alone in the left knee as a control. Joint size was measured using callipers (POCO 2T; Kroeplin GmbH) at daily intervals and swelling was calculated as a percentage increase in size between the inflamed and control knee. All experiments, unless stated otherwise, were carried out at day 7 post-IA injection.

2.3. Short-chain fatty acid supplementation

1 week prior to the induction of arthritis the drinking water of mice was supplemented with sodium acetate, sodium propionate or sodium butyrate (all 150mM; Sigma-Aldrich) and changed every 3 days as previously described[660]. The control group received sodium chloride. Mice were maintained on SCFAs throughout the duration of the experiment. For RNA-seq and ATAC-seq analysis, mice were gavaged daily with 500mg/kg of sodium butyrate to reduce variation caused by individual differences in daily water intake. Control mice received a gavage of 500mg/kg of sodium chloride. For antibiotic-treated experiments, one week prior to induction of arthritis, vancomycin (500mg/L; Sigma-Aldrich), Neomycin (1g/L; Sigma-Aldrich), and Metronidazole (1g/L; Sigma-Aldrich) were added to drinking water as previously described[323]. Untreated and treated mice were then gavaged daily with 500mg/kg of sodium butyrate or sodium chloride as a control. Mice were maintained on antibiotics throughout the duration of the experiment. For L-para-chlorophenylalanine (PCPA) experiments, mice were supplemented with butyrate as described above and gavaged daily with PCPA (4mg per mouse) in a suspension of 0.5% methyl cellulose and 0.01% Tween 80. Control mice received vehicle alone.

2.4 Gavage with 5-hydroxyindole-3-acetic acid and kynurenic Acid

Mice were gavaged daily from 1 week prior to the induction of arthritis and throughout the experiment with either 5-Hydroxyindole-3-acetic acid (5-HIAA, 0.5mg per mouse) or kynurenic acid (KYNA, 0.125mg per mouse) dissolved in oil. Control mice received vehicle alone.

2.5 Histology

Affected joints from *Ahr*$^{fl/-}$*Mb1*$^{cre/+}$ and *Mb1*$^{cre/+}$ mice were removed post-mortem, fixed in 5% (w/v) buffered formalin, and decalcified in 5% EDTA. The joints were

subsequently embedded in paraffin, sectioned, and stained with hematoxylin and eosin Y (H&E). Briefly, the sections were rehydrated in PBS, stained with hematoxylin, washed, counterstained with eosin Y, then washed and dehydrated in sequentially higher concentrations of ethanol from 75% to 100%. The sections were scanned using the NDP NanoZoomer (Hamamatsu) at 20x magnification and analyzed with the NDP view software.

2.6 Generation of chimeric mice

Recipient WT mice received 800cGy gamma-irradiation via a caesium source. 5 h following irradiation, recipients received $10x10^6$ donor bone marrow cells. To generate $CD45.2^+$*Ahr*$^{-/-}$$CD45.1^+$ congenic chimeric mice, WT mice were reconstituted with $10x10^6$ donor bone marrow cells containing 50% from $CD45.1^+$ WT mice and 50% from $CD45.2^+$ *Ahr*$^{-/-}$ mice. To generate mice in which the absence of IL-10 was exclusively restricted to B cells, WT mice were reconstituted with mixture of bone marrow consisting of 80% from μMT (B cell deficient) with 20% from *Il10*$^{-/-}$ mice. Control mice received 80% from μMT and 20% bone marrow from WT mice (to give a normal B cell compartment). Chimeras were left to fully reconstitute at least 8 weeks before use in AIA experiments.

2.7 Murine cell isolation and preparation of single cell suspensions

To make complete RPMI-1640, media was supplemented with 10% fetal calf serum, 1% penicillin/streptomycin (P/S; 100U/ml Penicillin + 100μg/ml streptomycin; Sigma-Aldrich). In addition, 50μM 2-mercaptoethanol (ThermoFisher Scientific) was added to the media. All FCS was heat inactivated before use in culture. All wash steps were carried out by adding 30ml complete RPMI media to the cell suspension and included a centrifugation step at 500xg for 10 minutes, unless otherwise stated.

2.7.1 Preparation of cell suspensions from lymphoid organs

Spleens, draining lymph nodes (DLNs) and MLNs were dissected post-mortem from mice and collected in complete RPMI, on ice. For splenocyte and lymph node cell preparation, organs were mashed through a 70μM cell strainer (BD Biosciences) into a 50ml centrifuge tube, using the plunger of a sterile 5ml syringe. Collected splenic cell pellets were lysed using 1ml of Red Cell Lysis Buffer (Sigma-Aldrich) per spleen. The cell pellet was resuspended with 1ml RBC lysis buffer and

left for 1 min at room temperature. The cell suspension was then washed and resuspended in 10ml complete RPMI for cell counting.

2.7.2 Isolation of lymphocytes from bone marrow

Femur bones from mice were collected post-mortem and stored in complete RPMI on ice. The bone marrow cells were flushed from the femur bones with 1x PBS (Sigma-Aldrich), using a 0.5ml syringe (29G). The resulting tissue was mashed through a 70μM cell strainer and the cells were washed with complete RPMI, before counting.

2.8 Isolation of murine B cell subsets

2.8.1 Isolation of murine CD43$^-$ B cells using magnetic beads

Total splenocytes or cells isolated from lymph nodes were resuspended in MACS buffer (2% FCS, 2mM EDTA), before labelling cells with beads targeting CD43. A column based negative selection kit for the isolation of CD43$^-$ cells (Miltenyi Biotec) was used for the isolation of untouched resting B cells, as per manufacturer instructions. B cell purity was routinely >90% (Figure 2.1).

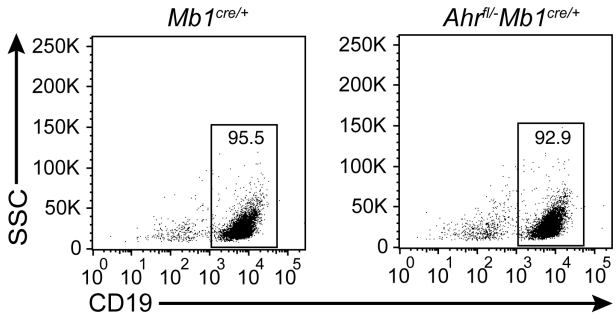

Figure 2.1. Splenic B cell purity plots. Representative flow cytometry plots showing the frequency of CD19$^+$ B cells from *Mb1$^{cre/+}$* and *Ahr$^{fl/-}$Mb1$^{cre/+}$* mice, following negative selection.

2.8.2 Isolation of murine lymphocyte subsets by FACS sorting

For isolation of murine B cell subsets from the spleen, total B cells were initially isolated by CD43-based negative selection and then were washed twice with MACS buffer, prior to staining. Cells were stained at 50M/ml for 30 minutes at 4°C with the following antibodies: CD19 BV785 (6D5), CD21 APC (7E9), CD23 FITC (B3B4) and CD24 PE-Cy7 (M1/69). B cell subsets were sorted using a cell sorter (FACSAria; BD Pharmingen). Dead cells were excluded by the use of 4,6-diamidino-2-phenylindole at 0.5μg/ml (DAPI; Sigma). For RNA-seq, ATAC-seq and

microarray data sets the addition of BV605 dump channel antibodies against CD3 (17A2), CD4 (RM4-5), CD8a (53-6.7), CD11b (M1/70), CD11c (N418), F4/80 (BM8), LY6C/G (RB6-8C5), erythroid cells (TER-119) and TCRβ (H57-597) were incorporated (Biolegend). For isolation of T cell subpopulations, cells were stained with CD3 BV605 (17A2), CD4 BV711 (RM4-5) and CD25 APC (PC61).

For both murine B cell subpopulations, sort purity of B cell subpopulations was routinely >90% (Figure 2.2). Cells were collected into 1xPBS (50% FCS) in polypropylene FACS tubes and washed with complete RPMI media.

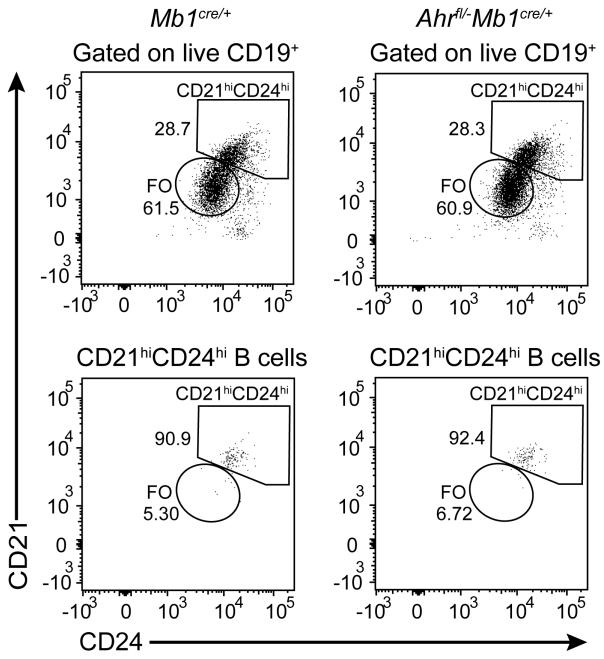

Figure 2.2. Gating strategy and purity plots for CD19^{+}CD21^{hi}CD24^{hi} B cells. Representative flow cytometry plots showing CD19^{+}CD21^{hi}CD24^{hi} B cells from *Mb1$^{cre/+}$* (left plots) and *Ahr$^{fl/-}$Mb1$^{cre/+}$* (right plots) mice prior to sorting (top plots) and purity of CD19^{+}CD21^{hi}CD24^{hi} B cells after sorting (bottom plots).

2.9 Adoptive transfer of CD19^{+}CD21^{hi}CD24^{hi} B cells from *Ahr$^{fl/-}$Mb1$^{cre/+}$* and control *Mb1$^{cre/+}$* mice

CD19^{+}CD21^{hi}CD24^{hi} B cells were FACS-sorted from spleens of *Ahr$^{fl/-}$Mb1$^{cre/+}$* and control *Mb1$^{cre/+}$* mice after remission from AIA and 5x10^{6} were transferred into recipient wild-type mice on the day of intra-articular injection. The control group (no transfer) received a PBS injection.

2.10 Congenic adoptive transfer of CD19^{+}CD21^{hi}CD24^{hi} B cells from *Ahr*$^{fl/-}$*Mb1*$^{cre/+}$ and control *Mb1*$^{cre/+}$ mice

CD45.2^{+}CD19^{+}CD21^{hi}CD24^{hi} B cells (0.75x10^{6}) were isolated from control and butyrate supplemented WT and *Ahr*$^{-/-}$ mice seven days' post-disease onset and adoptively transferred into recipient CD45.1^{+} mice on the day of intra-articular injection.

2.11 Adoptive transfer of IL-10eGFP^{+}CD19^{+}CD21^{hi}CD24^{hi}Bregs

IL-10eGFP^{+}CD19^{+}CD21^{hi}CD24^{hi} Bregs (2.3×10^{5}) were isolated from control or butyrate treated IL-10eGFP (Vert-X) reporter mice seven days' post-disease onset and adoptively transferred intravenously into recipient WT mice on the day of intra-articular injection.

2.12 Adoptive transfer of Tregs

CD3^{+}CD4^{+}CD25^{+} Tregs were isolated from butyrate-supplemented and control *Mb1*$^{cre/+}$ and *Ahr*$^{fl/-}$*Mb1*$^{cre/+}$ mice seven days' post-disease onset and CD3^{+}CD4^{+}CD25^{+} Tregs (2x10^{5}) were transferred intravenously into recipient WT mice on the day of intra-articular injection. The control group (no transfer) received a PBS injection.

2.13 Cell culture

Cells were cultured at 37°C with 5% CO_2 with either RPMI-1640 (Sigma-Aldrich) containing L-glutamine and $NAHCO_3$ or Iscove's Modified Dulbecco's Medium (IMDM; Pan Biotech; murine cultures only), enriched in AHR agonists[583], supplemented with L-Glutamine and 25mM HEPES. Both media were supplemented with 10% fetal calf serum (LabTech), 1% penicillin/streptomycin (100U/ml Penicillin+100μg/ml streptomycin; Sigma-Aldrich) and, for murine culture, 50μM 2-Mercaptoethanol (ThermoFisher Scientific) was added. Cells were cultured at 2.5x10^{6}/ml in a 96 well round-bottom plate. For intracellular cytokine staining, phorbal 12-myristate 13-acetate (PMA; 50ng/ml; Sigma-Aldrich), Ionomycin (250ng/ml; Sigma-Aldrich) and Brefeldin A (5μg/ml; Sigma-Aldrich) were added to culture 4.5h before flow cytometry staining.

Total lymphocytes, B cells and B cell subsets were cultured for 48h with CpGb ODN1826 (1μM; Invivogen), LPS (1μg/ml; Sigma-Aldrich) ± anti-mouse IgM

(10μg/ml; Jackson ImmunoResearch) or anti-CD40 (10μg/ml; BioXcell) ± mBSA (10μg/ml; Sigma-Aldrich). In addition, the AHR agonists FICZ (100nM; Enzo LifeSciences), 5-HIAA (10μM; Sigma-Aldrich), KYNA (50μM; Sigma-Aldrich) or the AHR antagonist CH-223191 (3μM; Sigma-Aldrich) were added to culture. For 48h culture, anti-IgM ± AHR agonists/antagonist were added 24h into culture. For PCR (6 and 24h cultures), AHR agonists/antagonist were added at the start of culture.

2.14 Detection of cytokine and antibody concentrations by ELISA

Supernatants were collected from cell cultures, prior to the addition of PMA, Ionomycin and Brefeldin A to the culture. Cytokine concentrations were calculated using a polynomial (4^{th} order) standard curve. For B cells and B cell subpopulations, cells were cultured at a concentration of 2.5M/ml. For the detection of IL-2, IL-6, IL-10, IL-17 and TNF-α duoset ELISA kits from R&D were used, according to manufacturer's instructions. Serum was collected from *Mb1*$^{cre/+}$ and *Ahr*$^{fl/-}$*Mb1*$^{cre/+}$ day 7 post AIA and was analyzed for total IgA, IgG and IgM (ThermoFisher Scientific).

2.15 Flow cytometry

Anti-rat and anti-hamster Igκ compensation particles kits (BD Biosciences) were used for singles for flow cytometry, according to manufacturer's instructions. LIVE/DEAD singles were made using ArC™ Amine Reactive Compensation Bead Kit (ThermoFisher Scientific), according to manufacturer's instructions. Flow cytometric data were collected on an LSRII or LSR Fortessa (BD Pharmingen) using FACS Diva software. Data were analyzed using Flowjo (Tree Star).

2.15.1 Surface staining and analysis of reporter expression

For multi-color flow cytometric surface staining, $1x10^6$ mouse cells were first centrifuged at 800xg for 3 minutes. All wash steps included a centrifugation step at 800xg for 3 minutes. Cells were washed once with 200μl of 1xPBS. Cells were stained with LIVE/DEAD™ Fixable Blue Dead cell stain (ThermoFisher Scientific) at a final concentration of 1/500, diluted in 1xPBS for 20 minutes at room temperature, in the dark. Cells were then topped up to 200μl with FACS buffer (1xPBS, 1%FCS, 0.005% Sodium azide) and washed once more with FACS buffer. Antibodies targeting cell surface antigens were diluted in FACS buffer or Brilliant

stain buffer (if two or more antibodies contained Brilliant violet conjugates; BD Biosciences) at the optimised concentration (Table 2.2) and added to cells in a 50μl staining volume and were left to incubate at 4°C for 25 minutes in the dark. Cells were washed twice with FACS buffer and then resuspended with 100μl 2% paraformaldehyde and left to incubate at 4°C for 20 minutes in the dark. Cells were then washed twice with FACS buffer and then resuspended in 220μl FACS buffer, prior to acquisition. For the detection of eGFP and FP635 reporter expression, cells were stained as described above, but without the fixation step. Cells were run live, within 2h of staining. To calculate absolute numbers, the total cell count was multiplied by the fraction of lymphocytes in the live gate.

Antigen	Fluorochrome	Clone	Isotype	Concentration	Company
CD1d	PerCP/Cy5.5	1B1	Rat IgG2b, κ	1μg/ml	Biolegend
CD3	BV605	17A2	Rat IgG2b, κ	1μg/ml	Biolegend
CD4	BV605	RM4-5	Rat IgG2a, κ	1μg/ml	Biolegend
CD4	FITC	RM4-5	Rat IgG2a, κ	2.5μg/ml	Biolegend
CD5	AF647	53-7.3	Rat IgG2a, κ	2.5μg/ml	Biolegend
CD8a	BV605	53-6.7	Rat IgG2a, κ	1μg/ml	Biolegend
CD8a	PE	53-6.7	Rat IgG2a, κ	1μg/ml	Biolegend
CD9	AF647	MZ3	Rat IgG2a, κ	2.5μg/ml	Biolegend
CD11b	APC	M1/70	Rat IgG2b, κ	1μg/ml	Thermo Fisher Scientific
CD11b	BV605	M1/70	Rat IgG2b, κ	1μg/ml	Biolegend
CD11c	BV605	N418	Armenian Hamster IgG	1μg/ml	Biolegend
CD11c	FITC	N418	Armenian Hamster IgG	2.5μg/ml	Biolegend
CD11c	PE	HL3	Armenian Hamster IgG2	1μg/ml	BD Biosciences
CD19	BV785	6D5	Rat IgG2a, κ	1μg/ml	Biolegend
CD21	APC	7E9	Rat IgG2a, κ	1μg/ml	Biolegend
CD21	BV421	7E9	Rat IgG2a, κ	1μg/ml	Biolegend
CD21	FITC	7E9	Rat IgG2a, κ	2.5μg/ml	Biolegend
CD23	BV711	B3B4	Rat IgG2a, κ	1μg/ml	BD Biosciences
CD23	FITC	B3B4	Rat IgG2a, κ	2.5μg/ml	Biolegend
CD23	PE/Cy7	B3B4	Rat IgG2a, κ	1μg/ml	Biolegend
CD24	APC	M1/69	Rat IgG2b, κ	1μg/ml	Biolegend

CD24	BV421	M1/69	Rat IgG2b, κ	1μg/ml	Biolegend
CD24	PE/Cy7	M1/69	Rat IgG2b, κ	1μg/ml	Biolegend
CD25	PE	PC61	Rat IgG1, λ	1μg/ml	Biolegend
CD38	PE/Cy7	90	Rat IgG2a, κ	1μg/ml	Biolegend
CD39	PE	Duha59	Rat IgG2a, κ	1μg/ml	Biolegend
CD43	PE-Cy7	S7	Rat IgG2a, κ	1μg/ml	BD Biosciences
CD45.2	BUV737	104	Mouse IgG2a, κ	1μg/ml	BD Biosciences
CD45R (B220)	BUV395	RA3-6B2	Rat IgG2a, κ	1μg/ml	BD Biosciences
CD73	APC	TY/11.8	Rat IgG1, κ	1μg/ml	Biolegend
CD93	PE/Cy7	AA4.1	Rat IgG2b, κ	1μg/ml	Biolegend
CD95	PE/Cy7	Jo2	Hamster IgG2, λ2	1μg/ml	BD Biosciences
CD103	BV421	2E7	Armenian Hamster IgG	1μg/ml	Biolegend
CD138	BV711	281-2	Rat IgG2a, κ	1μg/ml	Biolegend
CD138	BV605	281-2	Rat IgG2a, κ	1μg/ml	Biolegend
CD184 (CXCR4)	APC	L276F12	Rat IgG2b, κ	1μg/ml	Biolegend
CD185 (CXCR5)	PerCP/Cy5.5	L138D7	Rat IgG2b, κ	1μg/ml	Biolegend
CD196 (CCR6)	BV605	29-2L17	Armenian Hamster IgG	1μg/ml	Biolegend
CD199 (CCR9)	PE/Cy7	CW-1.2	Mouse IgG2a, κ	1μg/ml	Biolegend
CD249	PE	BP-1	Mouse IgG2a, κ	1μg/ml	BD Biosciences
CD273 (PD-L2)	PE	TY25	Rat IgG2a, κ	1μg/ml	Biolegend
CD317 (PDCA-1)	PE	129C1	Rat IgG2b, κ	1μg/ml	Biolegend
CD326 (EpCAM)	FITC	G8.8	Rat IgG2a, κ	2.5μg/ml	Biolegend
CD365 (TIM-1)	PE	RMT1-4	Rat IgG2b, κ	1μg/ml	Biolegend
F4/80	BV605	BM8	Rat IgG2a, κ	1μg/ml	Biolegend

GL7	PerCP/Cy5.5	GL7	Rat IgM, κ	2μg/ml	Biolegend
IgD	PerCP/Cy5.5	11-26c.2a	Rat IgG2a, κ	2μg/ml	Biolegend
IgM	APC/Cy7	RMM-1	Rat IgG2a, κ	1μg/ml	Biolegend
Ly6C/G	BV605	RB6-8C5	Rat IgG2b, κ	1μg/ml	Biolegend
TER-119 (Erythroid)	BV605	TER-119	Rat IgG2b, κ	1μg/ml	Biolegend
TCRβ	BV605	H57-597	Armenian Hamster IgG	1μg/ml	Biolegend

Table 2.2. Mouse flow cytometry antibodies for extracellular antigens.

2.15.2 Intracellular staining for the detection of murine cytokines and nuclear transcription factors

For the detection of intracellular cytokines and intra-nuclear transcription factors, cells were stained as above in 2.15.1, up until the fixation step. Cells were then washed twice with 200μl FACS buffer and then fixed with either 100μl intracellular fixation buffer or 100μl FOXP3/Transcription factor staining kit, for cytokines and transcription factors respectively (ThermoFisher Scientific). Cells were fixed at 4°C, for 25 minutes in the dark. Cells were washed twice with 1x Permeabilisation buffer (10x Permeabilisation buffer diluted in FACS buffer; ThermoFisher Scientific). Antibodies targeting intracellular/nuclear antigens were diluted in 1x permeabilisation buffer at the optimised concentration (Table 2.3) and added to cells in a 50μl staining volume and were left to incubate at 4°C for 40 minutes in the dark. Cells were washed twice with 1x permeabilisation buffer, followed by one wash with FACS buffer. Cells were then resuspended in 220μl FACS buffer, prior to acquisition.

Antigen	Fluorochrome	Clone	Isotype	Concentration	Company
BLIMP-1	AF647	5E7	Rat IgG2a, κ	2μg/ml	Biolegend
FOXP3	APC	FJK-16s	Rat IgG2a, κ	2μg/ml	Thermo Fisher Scientific
IFN-γ	PE	XMG1.2	Rat IgG1, κ	2μg/ml	BD Biosciences
IL-6	AF488	MP5-20F3	Rat IgG1	4μg/ml	BD Biosciences
IL-6	V450	MP5-20F3	Rat IgG1	2μg/ml	BD Biosciences
IL-10	PE	JES5-16E3	Rat IgG2b, κ	4μg/ml	Biolegend
IL-17A	eFluor 450	eBio17B7	Rat IgG2a, κ	2μg/ml	Thermo Fisher Scientific
IL-17A	PE	eBio17B7	Rat IgG2a, κ	2μg/ml	Thermo Fisher Scientific
Ki-67	BV421	16A8	Rat IgG2a, κ	1μg/ml	Biolegend
TNFα	BV510	MP6-XT22	Rat IgG1, κ	2μg/ml	Biolegend

Table 2.3 Mouse flow cytometry antibodies for intracellular antigens.

2.16 Immunofluorescence

Spleens were dissected and embedded into optimal cutting temperature compound (OCT, Tissue-Tek) and snap-frozen for cryo-sectioning (6μm). Slides were incubated in 100% ethanol to fix for 5-10min (4°C), followed by rehydration in PBS for 5min (4°C). The sections were blocked with 10% normal goat serum and 0.3% TX-100 (20 min at RT) and then incubated with primary antibodies for 2hr at RT. Primary antibodies: rat anti-mouse GL7 (Thermo Fisher), B220-PE (BD). Secondary antibody: AF647 – conjugated anti-rat IgM (1hr at RT). The slides were mounted in Vectashield with DAPI (Vector Labs). Whole slide fluorescent images (20x) were taken on a Zeiss Axio Scan Z1 microscope using the 365 nm LED to detect DAPI staining in the nuclei, the 470 nm LED for GFP detection (IL-10), the 555 nm LED for PE detection (B220) and the 625 nm LED for the detection of Alexa fluor 647 (GL7). Scans were analyzed using Leica Software and Fiji (ImageJ).

2.17 *In vitro* suppression assay

Splenic B cell subsets from *Ahr*$^{-/-}$ and *Ahr*$^{+/-}$ mice were FACS sorted at day 7 post IA injection and stimulated with CpG-B (ODN2006) for 6 hours. Cells were washed and then co-cultured with 0.5μg/ml plate-bound anti-CD3 (145-2C11, BD Biosciences) for 72 hours with CD4^{+}CD25^{-} FACS sorted T cells from *Ahr*$^{+/-}$ mice. Following stimulation, cells were analyzed for CD4^{+} IFN-γ expression. The percentage suppression of IFN-γ was calculated as a percentage reduction in IFN-γ from CD4^{+} cells cultured alone, compared to when B cell subsets were added to culture.

2.18 Gene expression analysis

2.18.1 Column-based RNA extraction

Total murine B cells or B cell subsets (0.2-1.5 x10^{6} cells) from either ex-vivo or after culture were transferred to a 15ml centrifuge tube, washed with MACS buffer and centrifuged at 500xg for 10 minutes. All centrifugation steps were at 4°C. Cells were resuspended in 1ml MACS buffer and transferred to a 1.5ml Eppendorf and centrifuged at 1000xg for 10 minutes. The supernatant was aspirated and cells were resuspended in 100μl of the extraction buffer and mixed thoroughly. The cell extract was incubated at 42°C for 30 minutes on a heat block and stored at -80°C, until further use. RNA from isolated B cells/subsets was extracted using Arcturus Picopure RNA isolation kit (ThermoFisher Scientific), according to manufacturer's instructions. Briefly, columns were washed for 5 minutes with 250μl conditioning buffer and centrifuged at 16,000xg for 1 minute. The cell extract was diluted 1:1 with 70% ethanol and mixed thoroughly. The mixture was transferred to the column and centrifuged for 2 minutes at 100xg, to allow the RNA to bind to the column. The column was then centrifuged for 30 seconds at 16,000xg, to remove flow-through. Columns were washed once with wash buffer 1 (WB1) and centrifuged at 8000xg for 1 minute. 40μl of DNase, diluted in RDD buffer, (350 Kunitz/ml; Qiagen) was added to the column and left to incubate for 20 minutes at room temperature. The column was washed 1x WB1 and twice with WB2, before a final centrifugation step of 16,000xg for 2 minutes. RNA was eluted in 16μl elution buffer at 1000xg for one minute, followed by 16,000xg for one minute into a 0.5ml Eppendorf. RNA concentration was analysed by Nanodrop-1000 (ThermoFisher Scientific).

2.18.2 cDNA synthesis

Depending on cell number, either 500ng or 1μg of RNA template was used to generate cDNA. The amount of RNA template was standardised between samples and experiments. RNA was reverse transcribed using an iScript cDNA synthesis kit (Bio-Rad), according to manufacturer's instructions. Briefly, 15μl of RNA/H_20 solution was mixed with 4μl of 5x reverse-transcription mix and 1μl reverse transcriptase (RT), to make a final volume of 20μl. The solution was left at room temperature for 5 minutes, before transferring to a heat block for 20 minutes at 46°C. The mixture was incubated for 1 minute at 95°C, for reverse transcriptase inactivation. Samples were topped up to 100μl with molecular biology grade H_2O.

2.18.3 Quantitative polymerase chain reaction (qPCR)

qPCR was carried out on the cDNA samples using iQ™ SYBR® Green Supermix (Bio-Rad), according to manufacturer's instructions. All PCR reactions were carried out in a volume of 20μl, consisting of 5μl of cDNA or H_2O (no template control), 10μl of 2x iQ SYBR® Green, 1μl each of forward and reverse primers (or 2μl of Quantitect primer mix) and 3μl H_2O. Primers were used at a concentration of 10μM, with a final concentration in the reaction of 0.5μM. Primer sequences were custom designed using Primer-BLAST or taken from the literature. Primers were designed with an amplicon length of <200bp. The primers are summarised in Table 2.4. Quantitect primers for murine *Arnt*, *Ahrr* and *Cyp1a1* were purchased from Qiagen. All primers were initially assessed by agarose gel electrophoresis to check amplicon length.

All qPCR reactions were performed on the OPTICON™ instrument (BioRad). The following cycling parameters were used: an initial denaturation step of 3 minutes at 95°C, followed by 41 three-step cycles of 95°C, 60°C and 72°C, for 30 seconds each. Melt curve analysis was incorporated at the end of the cycles, starting at 55°C, with reads every 0.2°C (held for 1 second between reads) up till 95°C. PCR products were tested for amplicon lengths by an agarose gel (1% w/v), to check the specificity of primer pairs. qPCR data were calculated as the ratio of gene to *β-Actin* expression by the relative quantification method ($\Delta\Delta C_t$; means±s.e.m. of triplicate determination).

Target gene	Forward primer	Reverse primer
Ahr	5-AGGATCGGGGTACCAGTTCA-3'	5'-CTCCAGCGACTGTGTTTTGC-3'
β-actin	5'-AGATGACCCAGATCATGTTTGAG-3'	5'-AGGTCCAGACGCAGGATG-3'
Ccl3[661]	5'-TGAGAGTCTTGGAGGCAGCGA-3'	5'-TGTGGGTACTTGGCAGCAAACA-3'
Ccl22[662]	5'-CAGGCAGGTCTGGGTGAA-3'	5'-TAAAGGTGGCGTCGTTGG-3'
Ebi3[380]	5'-CGGTGCCCTACATGCTAAAT-3'	5'-GCGGAGTCGGTACTTGAGAG-3'
Il6	5'-GCCTTCTTGGGACTGATGCT-3'	5'-TGCCATTGCACAACTCTTTTC-3'
Il10[296]	5'-GGTTGCCAAGCCTTATCGGA-3'	5'-ACCTGCTCCACTGCCTTGCT-3'
p35[380]	5'-CATCGATGAGCTGATGCAGT-3'	5'-CAGATAGCCCATCACCCTGT-3'
Tnf[661]	5'-AATGGCCTCCCTCTCATCAGTT-3'	5'-CCACTTGGTGGTTTGCTACGA-3'

Table 2.4. Murine qRT-PCR primers.

2.19 Chromatin Immunoprecipitation

Total Vert-X splenic B cells were bead cell sorted and cultured for 24h with LPS, followed by addition of anti-IgM (10μg/ml) and FICZ (100nM) at 24h into culture. After 48h, total B cells were FACS sorted based on eGFP for IL-10^+ and IL-10^- populations. Cells were fixed for 10 minutes with 1% (vol/vol) formaldehyde and quenched with 400mM Tris. Fixed cells were lysed with 120μl lysis buffer (1% (wt/vol) SDS, 10mM EDTA and 50mM Tris-HCl, pH 8.1, 1 × protease inhibitor 'cocktail' (Roche), 1mM PMSF) per $5x10^6$ cells. Chromatin was sheared to 200-500bp fragments and 10% of the initial chromatin material was kept as input. The chromatin was diluted 5-fold in Dilution Buffer (1% (vol/vol) Triton X-100, 2mM EDTA, 150mM NaCl and 20mM Tris-HCl, pH 8.1) and incubated overnight, after preclearing, with 1μg/10^6 cells of a polyclonal AHR-specific antibody (BML-SA210; Enzo Life Sciences). Immunoprecipitation took place by incubation with protein G Dynal magnetic beads (Invitrogen), held for at least 3 hours at 4ºC. Immunoprecipitated chromatin complexes were washed with High Salt Wash Buffer (2x), Low Salt Wash Buffer (2x), LiCl Wash Buffer (2x) and TE Buffer (2x).

Immunoprecipitated chromatin was eluted from the magnetic beads with Proteinase K Digestion Buffer and heated at 65°C for at least 6h for reverse crosslinking. DNA fragments were purified with NucleoMag beads kit (MN) and were analyzed by SYBR Green Quantitative Real-time PCR. The primers used for the ChIP qPCR are summarised in Table 2.5.

Target region	**Forward primer**	**Reverse primer**
Cyp1a1 -3.6kb	5'-GCTCTTTCTCTGCCAGGTTG-3'	5'-GGCTAAGGGTCACAATGGAA-3'
Cyp1a1 Promoter	5'-AAGCATCACCCTTTGTAGCC-3'	5'-CAGGCAACACAGAGAAGTCG-3'
Gapdh Promoter	5'-GCGCGAAAGTAAAGAAAGAAGCCC-3'	5'-AGCGGCCCGGAGTCTTAAGTATTAG-3'
Il10 -3.5kb	5'-AGGGCTTGATAACGTGTGAGT-3'	5'-TGAACTTCACACCCAGCTTGAG-3'
Il10 -2kb	5-TAAGAGGTGCTGCTTCTCCTG-3'	5-TGGCACTGGACAGTTCTATGA-3'
Il10 -0.5kb	5'-AGGGAGGAGGAGCCTGAATAA-3'	5'-CCTGTTCTTGGTCCCCCTTTT-3'
Il10 +2kb	5'-GCCACATGCATCCAGAGACAC-3'	5'-GTGCCTCAAAGTCACTCCCAC-3'

Table 2.5. ChIP qPCR primers.

2.20 Western Blot

$5x10^6$ cells $CD19^+CD21^{hi}CD24^{hi}$ and FO B cells were FACS sorted from arthritic WT mice and lysed for 15 minutes at 4°C with cell lysis buffer (Cell signaling technology) for extraction of whole cell lysate. Additionally, total B cells ($10x10^6$) cells were negatively purified from WT mice and cultured for 18 h with 500μM of butyrate (Sigma-Aldrich) or in the presence of a vehicle control. B cells were lysed and protein was resolved by SDS-PAGE, transferred to polyvinylidene fluoride (PVDF) membranes (Amersham; for detection of total H3K27 and H3K27ac) or nitrocellulose membranes (for detection of AHR and β-ACTIN), and blotted using

anti-H3K27ac (1/1000; Abcam) and anti-pan-H3 (1/1000; Abcam) or anti-AHR (1/1000; Enzo Life sciences) and anti-β-ACTIN (1/1000; Cell Signaling Technology). Bound antibodies were revealed with HRP-conjugated species-specific secondary antibodies using ECL substrate (Amersham).

2.21 High performance liquid chromatography

2.21.1 Extraction and derivation of short-chain fatty acids from mouse stool pellets

Individual stool pellets were weighed into clean Eppendorf tubes and homogenised in 1ml of 50% methanol. After centrifugation at 13,000xg for 5mins to remove particulate matter, 200μl of the clear supernatants were derivatized as previously reported [663]. Briefly, the clear supernatants were spiked with 2-ethylbutyric acid as an internal standard and the mixture incubated with 2-Nitrophenylhydrazine hydrochloride (NPH) at 60°C for 20mins, with 1-Ethyl-3-(3-dimethylaminopropyl) carbodiimide (EDC) in pyridine as catalysts. The reaction was then terminated and colour allowed to develop by the addition of potassium hydroxide in methanol, followed by incubation at 60°C for a further 20mins. After cooling, the mixture was acidified by the addition of phosphoric acid and the derivatized fatty acids extracted into diethyl ether. After drying down the ether extracts under a gentle stream of nitrogen gas, the resulting fatty acid hydrazides were dissolved in methanol for high performance liquid chromatography (HPLC) analysis.

2.21.2 Analysis of short-chain fatty acid hydrazides by high performance liquid chromatography

Separation of short-chain fatty acid (SCFA) hydrazides was performed by injecting 25μl onto a C8 Hypersil MOS2 column (250 x 4.6mm, 5μm particle size) and eluting using a linear gradient of 20-90% acetonitrile against water over 17min at a flow rate of 1.5ml/min. Compounds eluting from the column were monitored by UV/Vis absorption using a measurement wavelength of 400nm, and quantitated by integration of peak area. Standard curves (20.0-0.1μM) were constructed using pure compounds as follows: Succinic acid (R_t 3.92 min), Lactic acid (R_t 4.72 min), Acetic acid (R_t 5.067 min), propionic acid (R_t 6.173 min), iso-butyric acid (R_t 7.387 min), butyric acid (R_t 7.587 min), 2-methylbutyric acid (R_t 8.733 min), isovaleric acid (R_t 8.947 min), n-valeric acid (R_t 9.24 min), hexonoic acid (R_t 10.707 min), 2-

ethylbutyric acid (R_t 9.88 min) hexanoic acid (R_t 10.707 min), Pyruvic acid (R_t 12.773).

2.21.3 Extraction of indoles, kynurenine and kynurenic acid from mouse faecal pellets

Individual faecal pellets were weighed into clean Eppendorf tubes and homogenized in 200μL of methanol. After centrifuging at 13,000xg for 5min to remove particulate matter, the clear supernatants were diluted 1 in 10 in methanol and subject to high performance liquid chromatography (HPLC) analysis.

2.21.4 Analysis of indoles

Separation of indoles was performed by injecting 20μL onto on an ODS Hypersil column (150 x 4.6mm, 3μm particle size) and eluting using a linear gradient of 5%–100% acetonitrile in 10mM ammonium formate buffer, pH 3.5 over 20min at a flow rate of 0.8ml/min. Compounds eluting from the column were monitored by both fluorescence detection (λ_{ex}: 275nm, λ_{em}: 352nm) as well as by UV/Vis absorption using an online PDA detector (scanning 200-650nm), and quantitated by integration of peak area. Standard curves (20.0 - 0.1μM) were constructed using pure compounds as follows: tryptophan (R_t 6.97 min), tryptamine (R_t 13.04 min), indole (R_t 14.41 min), indole-3-acetic acid (R_t 11.42 min), indole-3-propionic acid (R_t 13.7), 3-methylindole (R_t 15.87 min), indole 3-carboxaldehyde (R_t 10.96 min), 5-Hydroxyindole-3-acetic acid (R_t 8.09 min).

2.21.5 Analysis of L-kynurenine and kynurenic acid

Separation of L-Kynurenine and Kynurenic Acid was performed by injecting 25μL onto on an ODS Hypersil column (150 x 4.6mm, 3 μm particle size) and eluting using a linear gradient of 1%–10% acetonitrile in 10mM ammonium formate buffer, pH 3.5 over 17min at a flow rate of 0.8ml/min. Compounds eluting from the column were monitored by both fluorescence detection (λ_{em}: 364nm, λ_{em}: 480nm for 7.5 min followed by λ_{em}: 330nm, λ_{em}: 390nm for the remainder of the run) as well as by UV/Vis absorption using an online PDA detector (scanning 200-650nm), and quantitated by integration of peak area. Standard curves were constructed using pure compounds as follows: L-Kynurenine (R_t 5.97 min) and Kynurenic Acid (R_t 10.6 min).

2.22 16s rDNA sequencing

20-50mg of faecal material was extracted using the QIAmp DNA mini kit (Qiagen). Extraction was carried out as per the manufacturer's protocol with an additional cell disruption step by bead beating using lysing matrix E (MP Biolmedicals) at 50 Hz for 1min (Tissuelyser LT, Qiagen). Two negative extraction controls were included. Barcoded primers spanning the V3-V4 region of the 16S rRNA gene were designed as described previously[664] to include an Illumina adapter, an 8 nucleotide barcode sequence, a 10 nucleotide pad sequence, a 2 nucleotide linker, and a gene-specific primer: 341F-CCTACGGGNGGCWGCAG or 805R-GACTACHVGGGTATCTAATCC. (Sigma-Aldrich, Dorset, UK). Extracted DNA samples were amplified with different barcode combinations using the Taq Core PCR kit (Qiagen) as per manufacturer's instructions with forward and reverse primers at 0.5μM each. A Microbial Community Standard (Zymo Research) of known bacterial composition was also amplified to assess any bias and error rates. The PCR cycling conditions were as follows: initial denaturation at 95°C for 3min, 30 cycles of 95°C for 30sec, 54°C for 30sec, 72°C for 10min and a final extension at 72°C for 10min. PCR products were purified with AMPure beads (0.7x, Beckman Coulter) and quantified using the Qubit dsDNA High Sensitivity Assay Kit (ThermoFisher). Samples were then pooled to create libraries with approximately equal concentrations of 16S rRNA amplicons from each sample. The pooled library was quality and quantity checked using the High Sensitivity D1000 ScreenTape assay (Agilent Technologies) and a NEBNEXT library quantification kit (New England Biolabs). The pooled library was spiked with 10% PhiX (Illumina) and sequenced on an Illumina MiSeq using the Reagent Kit V2 with 500 cycles (Illumina) and custom primers as previously described[664]. The open-source software Mothur V1.35.13 was used for initial bioinformatic analysis of the sequencing data[664]. Raw sequencing data was demultiplexed and processed according to the online Mothur SOP[665]. Sequences were trimmed and those with ambiguous bases were discarded. Suspected chimeric sequences were identified using VSEARCH[666] and removed. Phylogenetic identification of each OTU was achieved by aligning sequences to the SILVA 16S alignment database (v128)[667]. Sequences that did not meet a 97% similarity threshold were discarded of. Sample reads were rarefied to 50,000 reads prior to further analysis. OTU values generated

by Mothur were further analyzed using R-studio (phyloseq) or GraphPad Prism (la Jolla, USA) v. 400 Software for Apple Mac.

2.23 Microarray

Splenic murine B cell subsets were sorted and RNA extracted using columns (Picopure, Life Technologies) and hybridised to murine mogene 2.0 ST arrays (Affymetrix). Raw CEL files were processed using the online GeneProfiler tool (accessible at www.beringresearch.com). The GeneProfiler pipeline consists of present/absent call detection,[668] Robust Microarray Average (RMA) normalization, and outlier detection[669]. Differential expression analysis was performed using the *limma* package[670]. Heatmaps generated from the microarray data show z scores, based on normalised GeneChip Robust Multiarray Averaging (GC-RMA) values. z scores were generated using the following equation.

$$z_i = \frac{x_i - \mu}{\sigma}$$

z_i is the zeta score of a given sample; x is the GC-RMA value of a given sample; μ is the sample mean of all GC-RMA for a given gene and σ is the standard deviation of all samples.

2.24 RNA sequencing

2.24.1 Sample preparation and sequencing of the transcriptome

Splenic $CD19^{+}CD21^{hi}CD24^{hi}$ B cells were isolated from butyrate supplemented and control *Mb1*^{cre} and *Ahr*$^{fl/-}$*Mb1*^{cre} mice in the remission phase of arthritis, at day 7 post-IA injection. Sorted cells were either left untouched (*ex-vivo*) or stimulated with LPS+anti-IgM for 6h in IMDM media ($CD19^{+}CD21^{hi}CD24^{hi}$ B cells only). Dead cells were excluded using DAPI. Total RNA was isolated from these populations using the Picopure RNA isolation kit (ThermoFisher Scientific), according to manufacturer's instructions. 60bp single reads were sequenced on 3 lanes of an Illumina hiseq. 130-500ng of total RNA was fragmented followed by reverse transcription and second strand cDNA synthesis. The double strand cDNA was subjected to end repair, A base addition, adapter ligation and PCR amplification to create libraries. Libraries were evaluated by Qubit and TapeStation. Sequencing libraries were constructed with barcodes to allow multiplexing of samples in 3

lanes. The libraries were sequenced at the Weizmann Institute of Science on an Illumina HiSeq 2500 V4 instrument. Around 23-43 million single-end 60-bp reads were sequenced per sample. Poly-A/T stretches and Illumina adapters were trimmed from the reads using cutadapt. Resulting reads <30bp were discarded. Reads were mapped to the Mus Musculus GRCm38 reference genome using STAR[671]. Gene annotations were applied from Ensembl (EndToEnd option and outFilterMismatchNoverLmax was set to 0.04). Gene expression levels were quantified using htseq-count ("HTSeq," n.d.)[672], using the gtf above. Transcripts per million (TPM) values were estimated independently using Kallisto[673].

2.24.2 Bioinformatic analysis of RNA-seq data

Differential expression analysis was carried out using the default settings of the edgeR algorithm[674]. p-values reflect two-sided p-values obtained using the exact test proposed by Robinson and Smyth[675] for a difference in means, between two groups of negative binomial random variables (implemented in edgeR package). Signalling Pathway Impact Analysis (SPIA)[676] was used to detect significantly over-represented pathways, with the Kyoto Encyclopedia of Genes and Genomes (KEGG) Pathways database[677] employed as a reference. The full mouse genome was used as background for enrichment. For gene network analysis mouse protein-protein interactions were obtained from the STRING database (PMID: 25352553). An undirected graph representation was used to visualise all interacting protein pairs, whereby each node in a graph corresponds to a protein, whilst each edge corresponds to an interaction (STRING confidence score > 0.5). Differentially expressed subnetworks were extracted by overlying all significantly expressed genes with their corresponding protein names in the network. Heatmaps generated from the RNA-seq data show *z* scores using the same equation in 2.20, but instead using normalised logged counts per million (CPM).

2.25 Assay for transposable accessible chromatin with high-throughput sequencing (ATAC-seq)

2.25.1 Sample preparation and sequencing

Splenic $CD19^{+}CD21^{hi}CD24^{hi}$ B cells were isolated as above for RNA-seq from $Mb1^{cre/+}$ and $Ahr^{fl/-}Mb1^{cre/+}$ mice. Cells were either left untouched (ex-vivo) or stimulated with LPS+anti-IgM for 6h in IMDM media (splenic $CD19^{+}CD21^{hi}CD24^{hi}$

B cells only). After sorting, 40,000 cells were washed with 1xPBS (10% FCS). The cell pellet was prepped for sequencing by using the Nextera DNA library preparation kit (Illumina). Briefly, 10.5μl nuclease free water, 12.5μl 2x Transposase buffer, 2μl transposase and 0.25μl digitonin (0.05%) per reaction were added to the cell pellets. Cells were incubated at 37°C for 30 minutes. DNA was then purified using a MinElute PCR purification kit (Qiagen), according to manufacturer's instructions. Following DNA purification, 1μl of eluted DNA was used in a qPCR reaction to estimate the optimum number of amplification cycles. Library amplification was followed by solid phase reversible immobilization (SPRI) size selection to exclude fragments larger than 1,200bp. DNA concentration was measured with a Qubit fluorometer (Life Technologies). Library amplification was performed using custom Nextera primers. The libraries were sequenced by the Biomedical Sequencing Facility at CeMM using the Illumina HiSeq4000 platform and the 50bp single-end configuration.

2.25.2 Bioinformatic analysis of ATAC-seq data

Bioinformatic analysis was carried out as previously described[678]. Briefly, Illumina Casava1.7 software was used for basecalling. Sequenced reads were trimmed for adaptor and Nextera sequences and reads were mapped to mm10 reference genome using bowtie2 v2.2.4 with the "–very-sensitive" parameter. Duplicate reads were marked and removed with picard tools version 1.118. Reads were extended to the average fragment size and bigWig files containing counts of reads per basepair created. Peaks for ATAC-seq samples were called with MACS2 version 2.1.1.20160309 using the "–nomodel" and "–extsize 147" parameters. Peaks were assigned to genes by proximity. If a peak overlapped the gene body or promoter ± 2500bp of the transcription start site (TSS) the peak was assigned to that gene. If a peak did not fall into these criteria, the peak was assigned to the closest TSS. If the nearest TSS to the peak was further than 100kb away, no gene was assigned. *DESeq2* was used to compare either the effect of genotype or butyrate treatment on the chromatin landscape, and for visualization we created a normalized chromatin accessibility matrix by normalizing for the regulatory elements' length and GC content using the R package *cqn*. To assess transcription factor activity, we employed *ChromVar* by fixing a 500bp window on the center of the regulatory elements and using the JASPAR2016 database, computing deviations and their scores, followed by differential variability for genotype and treatment with default

parameters. For visualisation of representative tracks, track heights between samples were normalised through group autoscaling.

2.26. Data and code availability

The microarray, RNA-seq and ATAC-seq datasets generated during this study are available at ArrayExpress: E-MTAB-7345,E-MTAB-7375, E-MTAB-7525 and E-MTAB-8393. The 16S datasets generated during this study are available at NCBI Sequence Read Archive (accession number PRJNA603680).

2.27 Statistical analysis

Heatmap analyses for microarray, RNA-seq and ATAC-seq datasets were carried out using Multiple Experiment Viewer (MeV_4_8) software[679]. Hierarchical clustering was applied to genes using average linking clustering with the Euclidean distance metric. Venn diagrams were generated using Venny 2.1. All data are expressed as mean±s.e.m, unless stated otherwise. For *in vivo* studies, power calculations were performed on data showing mean maximum wild-type arthritic knee swelling of 2 mm with a s.d. of 0.39 mm, and an expected test group (transferred T2-MZPs) arthritic knee swelling of 1.4 mm. Group sizes of three mice or above were sufficient to reach a statistical power of at least 80% (http://www.statisticalsolutions.net/pss_calc.php). Mice were assigned at random to treatment groups for all mouse studies and, where possible, mixed among cages. Clinical scoring was performed in a blinded fashion. Mice that developed adverse reactions to protocols were excluded from data sets. Statistical significance was determined using unpaired t tests (comparison of two groups), Mann-Whitney tests (comparison of two groups, non-parametric data), Spearmans correlation, one-way ANOVA (comparison of three or more groups) or two-way ANOVA (comparison of two or more groups with 2 independent variables). All data met the assumption of statistical tests and had a normal distribution and variance was similar between groups that were statistically compared. Results were considered significant at $p \leq 0.05$. Statistical tests were carried out using GraphPad Prism (La Jolla, CA, USA) v.6, Software for Apple Mac.

Chapter III: Results I

Although there is some consensus regarding the effector function of Bregs, there is no unified view of Breg phenotype, with an ever-growing list of Breg subsets being reported in almost all stages of B cell differentiation. Bregs are characterised by their expression of IL-10, in addition to *in vivo* or *in vitro* assays assessing their suppressive capacity. However, a conserved transcription factor which controls Breg function that is expressed by all Breg subsets, has so far evaded discovery. Unlike in murine T cells, where it is well established that IL-10 expression is controlled by several transcription factors, including CMAF, AHR, BATF and IRF1, there is limited knowledge of the transcriptional control of IL-10 production by Bregs. Studies of the molecular control of murine B cell IL-10 production have been limited to the examination of NFATC1, IRF4, CMAF and HIF1α[375, 423, 425, 426]. Of these transcription factors, only IRF4 has been demonstrated to directly bind to the *Il10* locus in B cells. Moreover, binding to the *Il10* locus was only demonstrated in BLIMP-1-GFP$^+$ plasmablasts and not in other B cell populations[375]. Thus, the aim of this work was to compare the gene expression profiles between Bregs and non-Bregs and identify a transcription factor which is uniquely expressed by IL-10$^+$CD19$^+$CD21^{hi}CD24^{hi} Bregs (a population of cells which contain virtually all splenic IL-10$^+$ B cells[296, 297, 319, 680]).

In this chapter, I compare gene expression profiles between IL-10$^+$ Bregs (IL-10$^+$CD19$^+$CD21^{hi}CD24^{hi}) and IL-10$^-$ B cell subsets (IL-10$^-$CD19$^+$CD21^{hi}CD24^{hi} and IL-10$^-$ FO B cells) and show that IL-10$^+$ Bregs have a unique transcriptional profile with limited cytokine and chemokine expression, when compared to the IL-10$^-$ B cell counterparts. We identify AHR as being highly expressed in IL-10$^+$ Bregs, with CD19$^+$CD21^{hi}CD24^{hi} B cells poised to become high AHR-expressing B cells. Activation of CD19$^+$CD21^{hi}CD24^{hi} B cells with LPS+anti-IgM induced both the expression of AHR and IL-10. Based on three key findings, we identify that the induction of IL-10 in B cells is AHR-dependent. Firstly, we demonstrate that *Ahr*$^{-/-}$ CD19$^+$CD21^{hi}CD24^{hi} B cells secrete less IL-10 in response to activation with LPS+anti-IgM and fail to inhibit IFN-γ production by CD4$^+$ T cells *in vitro*. Secondly, we show that the addition of AHR agonists augment IL-10 production by CD19$^+$CD21^{hi}CD24^{hi} B cells. Lastly, we show that AHR directly binds to the *Il10* locus in IL-10$^+$ Bregs.

The bioinformatics analysis for the microarray (which involved the count matrix generation, normalisation and differential gene expression analysis) was performed by Ignat Drozdov (Bering Ltd). Similarly, the ATAC-seq bioinformatics analysis (quality control, read trimming, mapping to the genome and peak calling) was carried out by Andre Rendeiro and Thomas Krausgruber (CeMM, Austria). The ChIP qPCR was performed in collaboration with Aggelos Banos (BRFAA, Greece). Where data analysis or experiments were carried out in collaboration, the respective authors are listed in the figure legends.

3.1 IL-10$^+$ Bregs present a restricted cytokine and chemokine gene expression profile

To identify candidate genes that regulate the transcription of *Il10* in Bregs, arthritis was induced in IL-10eGFP reporter mice (Vert-X)[659]. We sorted splenic IL-10eGFP$^+$CD19$^+$CD21^{hi}CD24^{hi} Bregs, IL-10eGFP$^-$CD19$^+$CD21^{hi}CD24^{hi} B cells and IL-10eGFP$^-$ FO B cells (the two GFP$^-$ populations are hereafter referred to as IL-10eGFP$^-$ B cell subsets) and profiled these cells by gene expression microarray (Figures 3.1A-B). This sorting strategy was chosen to capture the majority of described Breg subsets, including IL-10$^+$T2-MZP, IL-10$^+$MZ, and IL-10$^+$CD1d^{hi}CD5$^+$ B cells, which have been shown to exert suppressive capacity via IL-10 in this model of arthritis, and in other models of autoimmunity[296, 297, 319, 680]. Of note, very few IL-10-producing Bregs were present in the joints or DLNs of arthritic mice (Figure 3.1C). Virtually no IL-10-expressing plasma cells or plasmablasts (LAG3$^+$ plasma cells[378], and CD138$^+$CD44$^+$ plasmablasts[375]) were detected in the spleen or DLNs following the induction of arthritis (Figures 3.1D-J).

The purity of sorted IL-10eGFP$^+$ and IL-10eGFP$^-$ subsets isolated for the microarray was over 98% (Figure 3.2A). Principal component analysis (PCA) revealed 3 distinct groups along the first dimension, with the IL-10eGFP$^+$CD19$^+$CD21^{hi}CD24^{hi} Breg population clustered separately away from both IL-10eGFP$^-$ B cell subsets (Figure 3.2B). Analysis of gene expression revealed 1073 differentially expressed genes between IL-10eGFP$^+$CD19$^+$CD21^{hi}CD24^{hi} Bregs and IL-10eGFP$^-$CD19$^+$CD21^{hi}CD24^{hi} B cells, and 1267 genes that were differentially expressed between IL-10eGFP$^+$CD19$^+$CD21^{hi}CD24^{hi} Bregs and IL-10eGFP$^-$ FO B cells (fold change >1.5 and adjusted *p*-value <0.05) (Figure 3.2C-D).

In the context of arthritis, splenic Bregs have been shown to mainly produce IL-10[286]. Of the cytokine genes upregulated in IL-10eGFP$^+$CD19$^+$CD21^{hi}CD24^{hi} Bregs, only *Il10* and *Ebi3* reached an adjusted *p* value of <0.05, compared to both IL-10eGFP$^-$ B cell subsets. However, since *Il12a* was not found to be upregulated in IL-10eGFP$^+$CD19$^+$CD21^{hi}CD24^{hi} Bregs, we excluded a role of IL-35 in these cells. Although a trend in the increase of transcripts for pro-inflammatory genes such as *Il1a*, *Il12b*, *Il15* and *Il18* was noted, the expression of these genes was not

significantly different from the IL-10eGFP^{-} B cell subsets (Figure 3.3A). IL-10eGFP^{-} FO B cells, which unlike CD19^{+}CD21^{hi}CD24^{hi} B cells do not suppress inflammation on adoptive transfer[297], express a different transcriptional profile, characterized by a higher expression of cytokines and cytokine receptors known to mediate inflammatory responses, compared to IL-10eGFP^{+}CD19^{+}CD21^{hi}CD24^{hi} Bregs (Figures 3.3A-B). The transcripts that were significantly differentially expressed in IL-10eGFP^{+}CD19^{+}CD21^{hi}CD24^{hi} Bregs versus IL-10eGFP^{-} B cell subsets are summarised in (Figure 3.3C). In keeping with the anti-inflammatory role of Bregs, we found that the Th2 attracting chemokines *Ccl17* and *Ccl22*[285, 681], and the chemokine receptor *Cxcr3*, important for the trafficking of lymphocytes to the synovium in arthritis[682], were upregulated in IL-10eGFP^{+}CD19^{+}CD21^{hi}CD24^{hi} Bregs compared to IL-10eGFP^{-} B cell subsets (Figures 3.3A-C). These results showed that in the context of arthritis, splenic Bregs displayed a distinct anti-inflammatory transcriptional profile compared to IL-10eGFP^{-} B cell subsets.

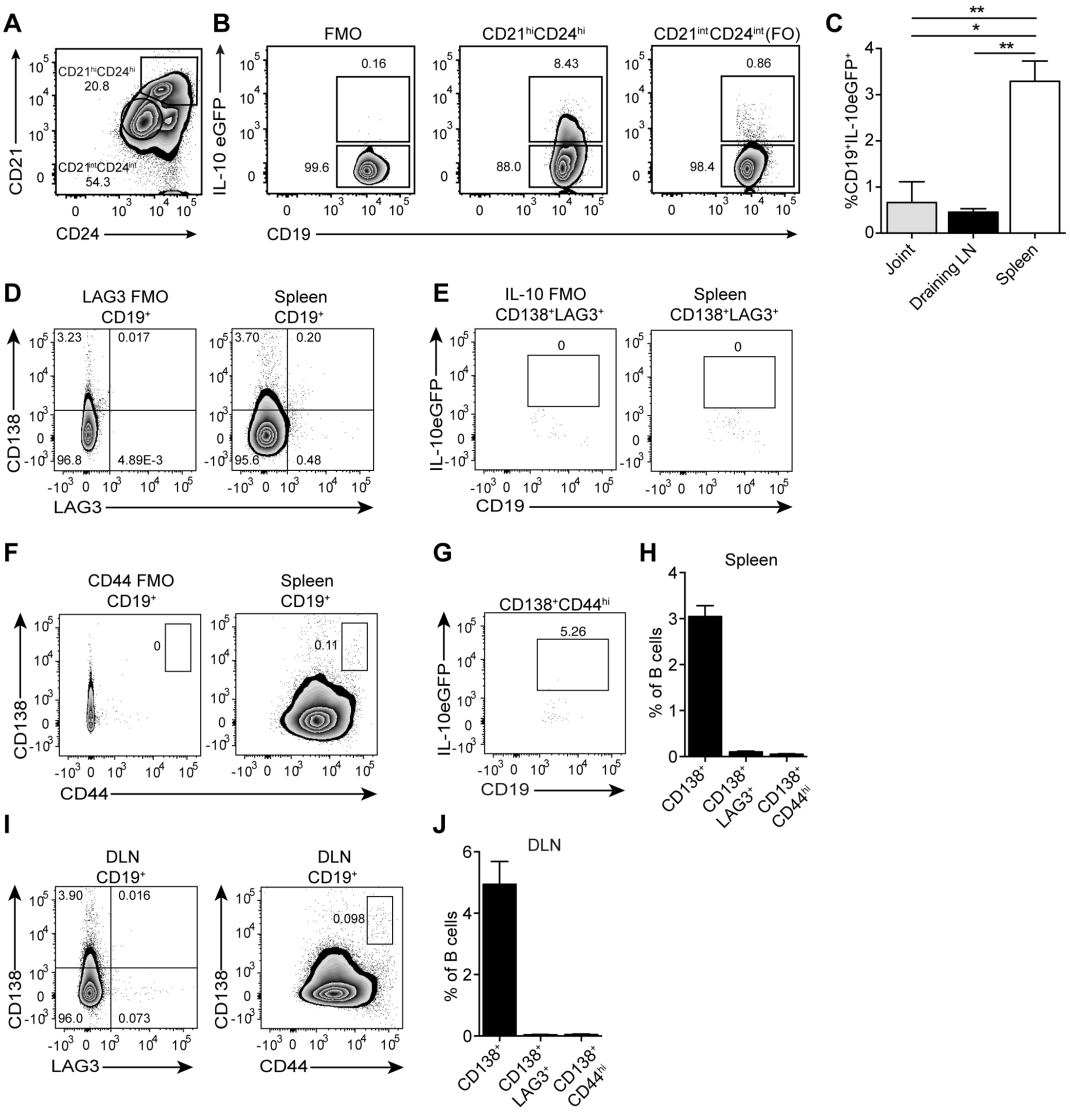

Figure 3.1. IL-10$^+$ Bregs are predominantly found in the CD19$^+$CD21^{hi}CD24^{hi} B cell population in the spleen in AIA. Antigen-induced arthritis (AIA) was induced in IL-10eGFP reporter (Vert-X) mice. (**A**) Representative flow cytometry plots showing the frequency of CD19$^+$CD21^{hi}CD24^{hi} and CD19$^+$CD21^{int}CD24^{int} (FO) B cells. (**B**) Representative flow cytometry plots showing the frequency of IL-10eGFP$^+$ CD19$^+$CD21^{hi}CD24^{hi} and IL-10eGFP$^+$ FO B cell subsets. (**C**) Bar chart showing the frequencies of IL-10$^+$CD19$^+$ B cells in the joint, draining LNs and spleens of Vert-X mice (n=3). **D-G,** Representative flow cytometry plots showing respectively the frequencies of (**D**) CD138$^+$LAG3$^+$ plasma cells, (**E**) IL-10$^+$CD138$^+$LAG3$^+$ plasma cells, (**F**) CD138$^+$CD44^{hi} plasmablasts and (**G**) IL-10$^+$CD138$^+$CD44^{hi} plasmablasts in the spleen. (**H**) Bar chart showing the percentages of CD19$^+$CD138$^+$, CD19$^+$CD138$^+$LAG3$^+$ and CD19$^+$CD138$^+$CD44^{hi} plasmablasts in the spleens of Vert-X mice, as shown gated in **D+F** (n=5). (**I**) Representative flow cytometry plots showing respectively the frequencies of (left) CD138$^+$LAG3$^+$ and (right) CD138$^+$CD44^{hi} plasmablasts in the DLNs of Vert-X mice. (**J**) Bar chart showing the percentages of CD19$^+$CD138$^+$, CD19$^+$CD138$^+$LAG3$^+$ and CD19$^+$CD138$^+$CD44^{hi} plasmablasts/plasma cells in the DLNs of in Vert-X mice, as shown gated in **I** (n=5). All experiments were carried out at day 7 post IA-injection. Figures **A-B,** data are representative of at least 5 independent experiments. For figures **D-J**, data representative of 2 independent experiments. Figures **C, H and J**, data are expressed as mean±sem. *p<0.05, **p<0.01. **C, H and J,** one-way ANOVA. Figure **C** was generated by Elizabeth Rosser.

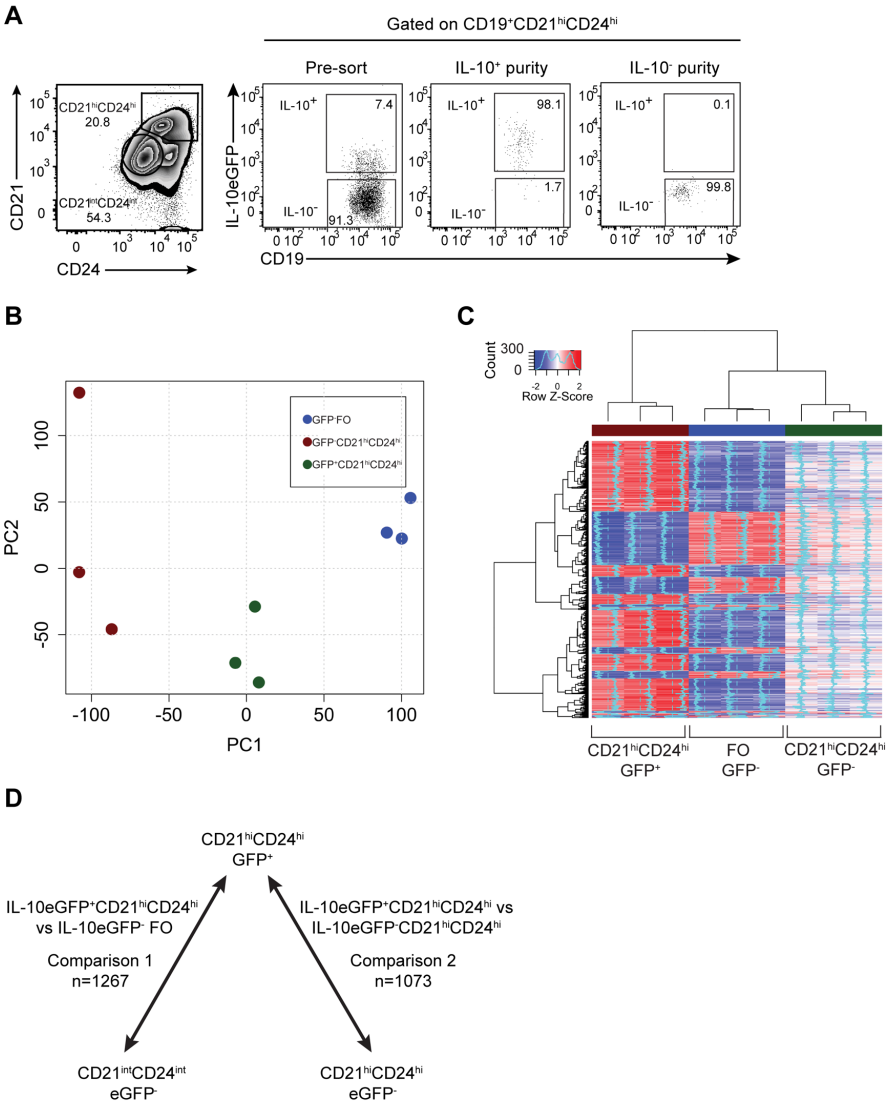

Figure 3.2. IL-10^{+} Bregs have a unique transcriptional profile. Antigen-induced arthritis (AIA) was induced in IL-10eGFP reporter (Vert-X) mice. (**A**) Representative flow cytometry plots showing purity of IL-10eGFP^{+}CD19^{+}CD21^{hi}CD24^{hi} and IL-10eGFP^{-} CD19^{+}CD21^{hi}CD24^{hi} B cells. (**B**) Principal Component Analysis of transcripts in IL-10eGFP^{+}CD19^{+}CD21^{hi}CD24^{hi} , IL-10eGFP^{-}CD19^{+}CD21^{hi}CD24^{hi} and IL-10eGFP^{-} FO B cell subsets (*n*=3). (**C**) Heat map showing the expression of genes by IL-10eGFP^{+}CD19^{+}CD21^{hi}CD24^{hi}, IL-10eGFP^{-}CD19^{+}CD21^{hi}CD24^{hi} and IL-10eGFP^{-} FO B cells. Blue dashed line represents a standard deviation of 0. (**D**) Total number of differentially expressed genes between IL-10eGFP^{+}CD19^{+}CD21^{hi}CD24^{hi} and IL-10eGFP^{-} subsets (>1.5 fold change, adjusted *p* value <0.05). For figure **C,** heat map shows *z* scores based on normalized GC-RMA values. All experiments were performed at day 7 post IA-injection. For figures **B-C**, analysis was performed in collaboration with Ignat Drozdov.

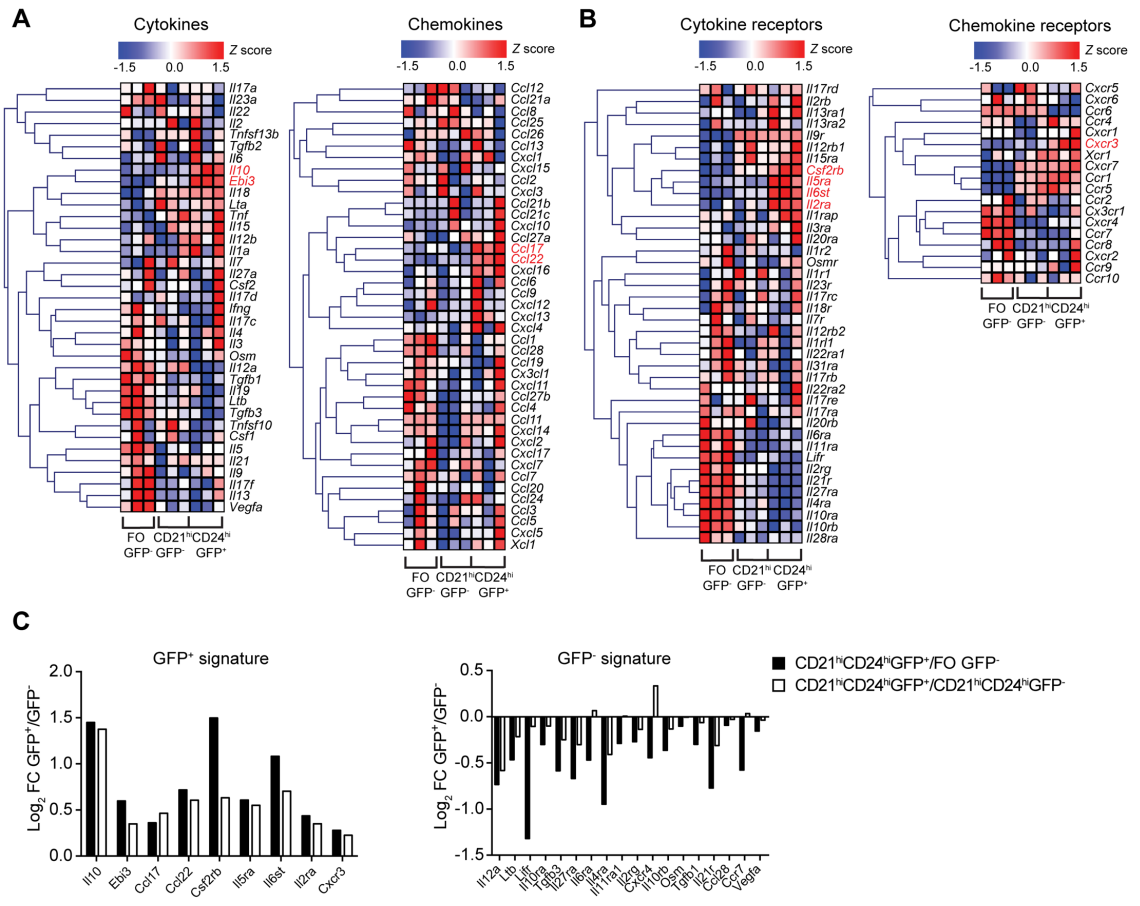

Figure 3.3. Bregs have a restricted cytokine and chemokine transcriptional profile. Antigen-induced arthritis (AIA) was induced in IL-10eGFP reporter (Vert-X) mice. (**A**) Heat maps showing the expression of cytokine (left) and chemokine (right) genes, in the respective subsets. (**B**) Heat maps of cytokine receptor (left) and chemokine receptor (right) expression profiles, in the respective subsets (n=3). (**C**) Log_2 fold changes of all significant genes identified in **A-B** for the GFP^+ (left graph) and GFP^- signatures (right graph). Log_2 fold changes are highlighted for GFP^+ vs both GFP^- populations. All experiments were performed at day 7 post IA-injection. For figures **A-B,** heat maps show z scores based on normalized GC-RMA values. Listed genes highlighted in red are upregulated in the IL-10eGFP$^+$CD19$^+$CD21^{hi}CD24^{hi} population compared to both IL-10eGFP$^-$ populations (adjusted p value <0.05).

3.2 AHR is highly expressed in IL-10-producing Bregs

To screen for molecules involved in IL-10 transcription and Breg function, genes concordant for comparisons 1 (between IL-10eGFP^{+}CD19^{+}CD21^{hi}CD24^{hi} Bregs and IL-10eGFP^{-} FO B cells) and comparison 2 (between IL-10eGFP^{+}CD19^{+}CD21^{hi}CD24^{hi} Bregs and IL-10eGFP^{-}CD19^{+}CD21^{hi}CD24^{hi} B cells) (Figure 3.4A) were filtered based on the transcription factor gene ontology term, resulting in 23 candidates (Figure 3.4B and Appendix I). Pathway analyses showed that AHR represented a central network hub (Figure 3.4C) and was the most significantly enriched candidate in IL-10eGFP^{+}CD19^{+}CD21^{hi}CD24^{hi} Bregs (adjusted *p* value $<3.34\text{x}10^{-5}$; Figure 3.4D). Analysis of transcription factors previously shown to be associated with the transcriptional regulation of *Il10* in other lymphocyte subsets, including Tregs[418], revealed that AHR was the most significantly upregulated IL-10-related transcription factor in IL-10eGFP^{+}CD19^{+}CD21^{hi}CD24^{hi} Bregs, in comparison to IL-10eGFP^{-} B cell subsets (Figure 3.4E). Microarray signal intensities for *Il10* and *Ahr* were higher in IL-10eGFP^{+}CD19^{+}CD21^{hi}CD24^{hi} Bregs compared to IL-10eGFP^{-} B cell subsets (Figure 3.4F). qPCR analysis confirmed that *Il10* and *Ahr* mRNA expression was higher in IL-10eGFP^{+}CD19^{+}CD21^{hi}CD24^{hi} Bregs, than in both IL-10eGFP^{-} B cell subsets (Figures 3.4G-H). Corroborating the results in Figures 3.4G-H, assay for Transposase-Accessible Chromatin using sequencing (ATAC-seq), showed increased accessibility in both the *Il10* and *Ahr* loci in IL-10eGFP^{+}CD19^{+}CD21^{hi}CD24^{hi} Bregs, in comparison to both IL-10eGFP^{-} B cell subsets (Figure 3.5). These data demonstrate that, amongst the previously described IL-10 associated transcription factors, only AHR is significantly upregulated in IL-10eGFP^{+}CD19^{+}CD21^{hi}CD24^{hi} Bregs compared to both IL-10eGFP^{-} B cell subsets.

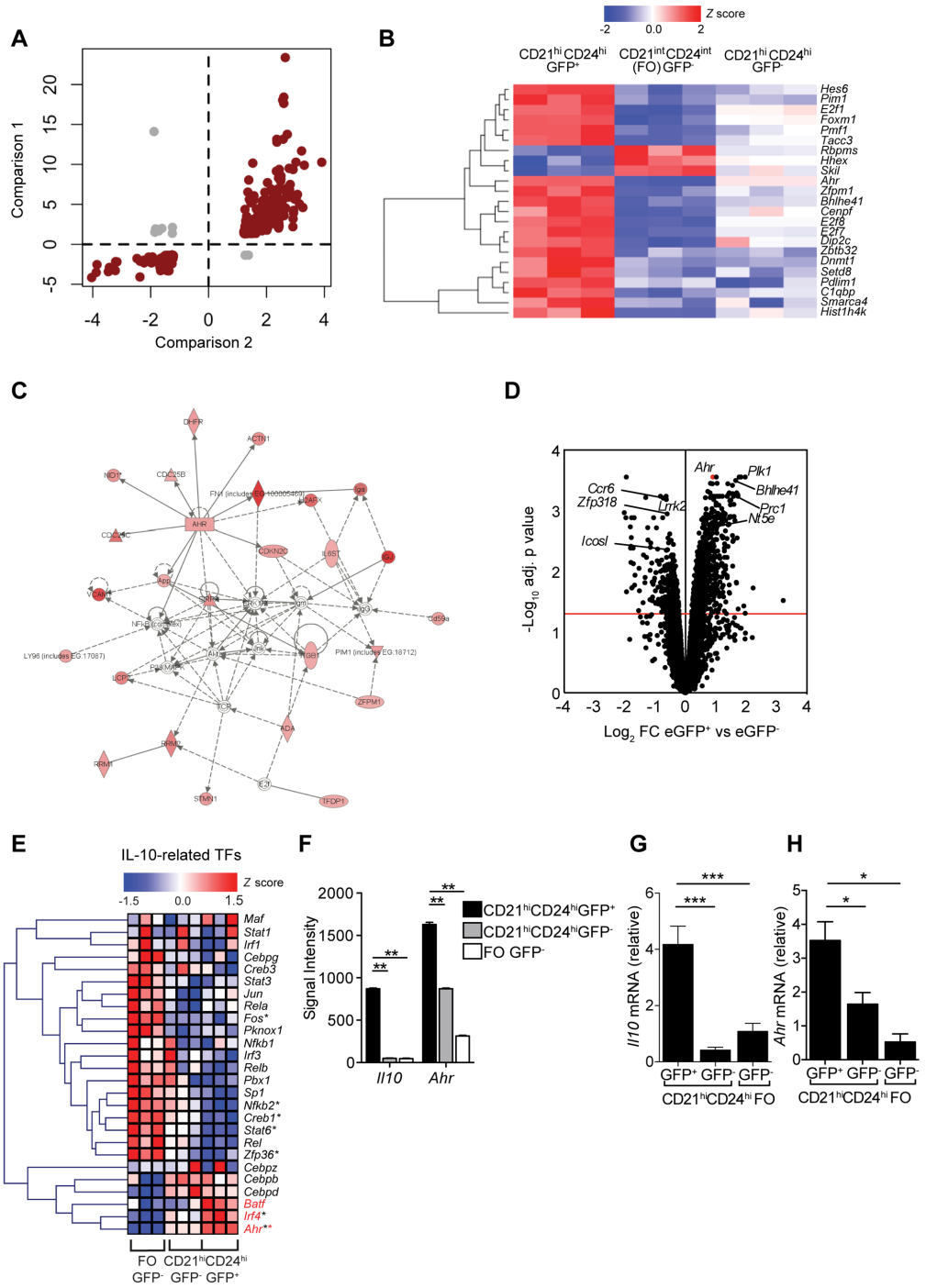

Figure 3.4. Identification of AHR as a key IL-10-associated transcription factor in Bregs. Antigen-induced arthritis (AIA) was induced in IL-10eGFP reporter mice. (**A**) Scatter plot showing fold changes of differentially expressed genes from the two comparisons (n=660). Concordant changes for both comparisons are shown in red, and discordant changes in grey. (**B**) Heat map showing z scores of significantly differentially expressed genes (n=23, adj. p value p<0.05) based on normalized GC-RMA values, filtered on the transcription factor activity gene ontology term in sorted IL-10eGFP^{+}CD19^{+}CD21^{hi}CD24^{hi}, IL-10eGFP^{-}CD19^{+}CD21^{hi}CD24^{hi} and IL-10eGFP^{-}FO B cells. (**C**) Ingenuity pathway network analysis identifies a cluster of genes with AHR as central hub. The lines between genes represent known interactions (solid lines represent direct interactions; dashed lines represent indirect interactions). (**D**) Volcano plot analysis showing log_2 fold changes between IL-10eGFP^{+}CD19^{+}CD21^{hi}CD24^{hi} Bregs versus IL-10eGFP^{-}CD19^{+}CD21^{hi}CD24^{hi} B cells, plotted against -log_{10} adjusted p value. *Ahr* is highlighted in red (adjusted p value of 3.4E-05). (**E**) Heat map of z scores of transcription factors regulating IL-10, expressed by IL-10eGFP^{+}CD19^{+}CD21^{hi}CD24^{hi}, IL-10eGFP^{-}

$CD19^{+}CD21^{hi}CD24^{hi}$ and IL-10eGFP^{-}FO B cells. Genes highlighted in red are upregulated in the IL-10eGFP$^{+}CD19^{+}CD21^{hi}CD24^{hi}$ population compared to IL-10eGFP^{-} populations. Black asterisks - *p*-adjusted values <0.05 for the IL-$10^{+}CD19^{+}CD21^{hi}CD24^{hi}$ Breg vs IL-10eGFP^{-} FO B cell comparison. Red asterisks - *p*- adjusted values <0.05 for the IL-10eGFP$^{+}CD19^{+}CD21^{hi}CD24^{hi}$ Breg vs IL-10eGFP$^{-}CD19^{+}CD21^{hi}CD24^{hi}$ B cell comparison. (**F**) Microarray signal intensities of *Il10* and *Ahr* (*n*=3). Validation of (**G**) *Il10* and (**H**) *Ahr* mRNA expression in the indicated B cell subsets by qPCR (*n*=3). For qPCR, gene expression was calculated normalizing to *β-Actin*. All experiments were performed at day 7 post IA-injection. Figures **F-H,** data are expressed as mean±sem. Figures **F-H,** data representative of 3 independent experiments with biological replicates. **p*<0.05, ***p*<0.01, ****p*<0.001. **F,** two-way ANOVA; **G-H,** one-way ANOVA. For figures **A-C**, analysis was performed in collaboration with Ignat Drozdov.

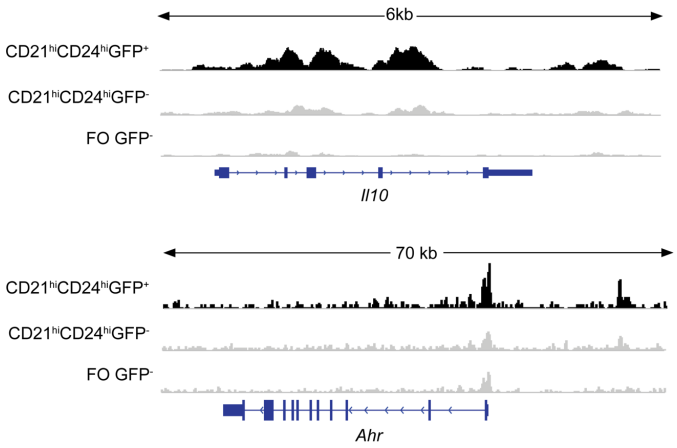

Figure 3.5. The *Il10* and *Ahr* loci are more accessible in IL-10^{+}CD19^{+}CD21^{hi}CD24^{hi} Bregs. Representative ATAC-seq tracks for the *Il10* (top) and *Ahr* (bottom) loci in IL-10eGFP^{+}CD19^{+}CD21^{hi}CD24^{hi} Bregs, IL-10eGFP^{-}CD19^{+}CD21^{hi}CD24^{hi} and IL-10eGFP^{-} FO B cells (*n*=3). Track heights between samples are normalised through group autoscaling.

3.3 AHR upregulation promotes the generation of IL-10^{+}CD19^{+}CD21^{hi}CD24^{hi} Bregs

We and others have recently shown that BCR signals combined with TLR stimulation induce a substantial upregulation of AHR in B cells[217, 615]. As BCR signals together with TLR engagement are known to be pivotal in the generation of Bregs[286], next we investigated whether the differentiation of Bregs, 'marked' by the induction of IL-10 expression by these stimuli, was AHR-dependent. For this purpose, CD19^{+}CD21^{hi}CD24^{hi} B cells were sorted from the spleens of arthritic mice and stimulated with LPS±anti-IgM. An 11-fold increase in the frequency of IL-10^{+}CD19^{+}CD21^{hi}CD24^{hi} Bregs and a 200-fold increase in the production of IL-10 by CD19^{+}CD21^{hi}CD24^{hi} Bregs, was observed upon LPS+anti-IgM stimulation compared to unstimulated (Figures 3.6A-C). We established the kinetics of AHR and AHR pathway associated gene expression in relation to *Il10* transcription, after activation with Breg-polarizing stimuli. We observed a peak in the expression of *Ahr* and *Cyp1a1* (the gene encoding the AHR-dependent cytochrome P4501A1) at 6hrs post stimulation with LPS+anti-IgM, followed by an upregulation of the AHR repressor (*Ahrr*) and *Il10* at 24hr. No significant changes in the expression of the AHR binding partner, the aryl hydrocarbon receptor nuclear translocator (*Arnt*) were observed (Figures 3.6D-H). After activation with LPS+anti-IgM, increased levels of AHR expression were observed in IL-10^{+}CD19^{+}CD21^{hi}CD24^{hi} Bregs compared to IL-10^{-} FO and IL-10^{-}CD19^{+}CD21^{hi}CD24^{hi} B cells (Figure 3.7). Of note, *ex vivo* CD19^{+}CD21^{hi}CD24^{hi} B cells display higher expression of *Ahr* (confirmed at protein level by flow cytometry and western blotting)*, Il10, Cyp1a1*, *Ahrr* and *Arnt* compared to FO B cells (Figures 3.8A-H). Together these data show that IL-10^{+}CD19^{+}CD21^{hi}CD24^{hi} Bregs express the highest levels of AHR compared to the IL-10^{-}CD19^{+}CD21^{hi}CD24^{hi} and IL-10^{-} FO B cells and that in CD19^{+}CD21^{hi}CD24^{hi} B cells, AHR upregulation precedes the production of IL-10.

To understand the role of AHR in the regulation and function of IL-10 expression in CD19^{+}CD21^{hi}CD24^{hi} Bregs, we isolated CD19^{+}CD21^{hi}CD24^{hi} B cells and FO B cells from *Ahr*$^{+/-}$ and *Ahr*$^{-/-}$ mice and stimulated them *in vitro* with LPS+anti-IgM. The absence of AHR significantly reduced the ability of CD19^{+}CD21^{hi}CD24^{hi} B cells to differentiate into IL-10-producing CD19^{+}CD21^{hi}CD24^{hi} Bregs compared to AHR competent CD19^{+}CD21^{hi}CD24^{hi} B cells (Figure 3.9A). In addition, *Ahr*$^{-/-}$ CD19^{+}CD21^{hi}CD24^{hi} B cells presented a reduced capacity to inhibit IFN-γ

production by $CD4^+$ T cells *in vitro* compared to *Ahr*$^{+/-}$ $CD19^+CD21^{hi}CD24^{hi}$ B cells (Figures 3.9B-C). FO B cells failed to produce IL-10 and to suppress IFN-γ production by $CD4^+$ T cells, irrespective of AHR expression (Figures 3.9B-C).

To assess if activation of AHR with endogenous ligands directly promotes the differentiation of $CD19^+CD21^{hi}CD24^{hi}$ B cells into IL-$10^+CD19^+CD21^{hi}CD24^{hi}$ Bregs, we stimulated sorted $CD19^+CD21^{hi}CD24^{hi}$ B cells or FO B cells with the AHR ligand 6-formylindolo(3,2-b) carbazole (FICZ). AHR activation significantly upregulated the expression of *Cyp1a1* and *Il10* in the $CD19^+CD21^{hi}CD24^{hi}$ B cell subset but not in FO B cells, compared to the vehicle control (Figures 3.10A-B). Secretion of IL-10 was further enhanced by the addition of FICZ to LPS+anti-IgM stimulated $CD19^+CD21^{hi}CD24^{hi}$ B cells, compared to LPS+anti-IgM alone (Figure 3.10C). An increase in Breg IL-10 expression was observed when $CD19^+CD21^{hi}CD24^{hi}$ B cells were cultured in Iscove's Modified Dulbecco's Medium (IMDM; enriched in aromatic amino acids which give rise to AHR ligands[583, 683]), compared to RPMI media (Figure 3.10D).

We next investigated whether AHR regulates IL-10 expression in IL-$10eGFP^+CD19^+CD21^{hi}CD24^{hi}$ Bregs by directly binding to the *Il10* locus. To address this, we took advantage of the JASPAR tool[684] and identified putative AHR binding sites in 500bp regions up to -5kb upstream and +5kb downstream of the *Il10* transcription start site (TSS), and designed primer probes to span these regions (Figure 3.11A). We sorted IL-$10eGFP^+$ and IL-$10eGFP^-$ B cells, after stimulation with LPS+anti-IgM+FICZ (the combination of stimuli was used to maximise AHR activation and translocation to the nucleus) and performed chromatin immunoprecipitation (ChIP) qPCR on AHR bound DNA (Figure 3.11B). Significantly enriched AHR binding was observed at -3.5kb upstream of the *Il10* transcription start site in the IL-$10eGFP^+$ population. Minimal binding of AHR was observed in other regions of the *Il10* locus. As a positive control, we confirmed that, under these experimental conditions, there was an enriched binding of AHR to the promoter of *Cyp1a1*, but no binding to *Gapdh*; an AHR-independent housekeeping gene (Figure 3.11C). These results demonstrate that AHR can directly regulate IL-10 expression in Bregs by binding to the *Il10* locus.

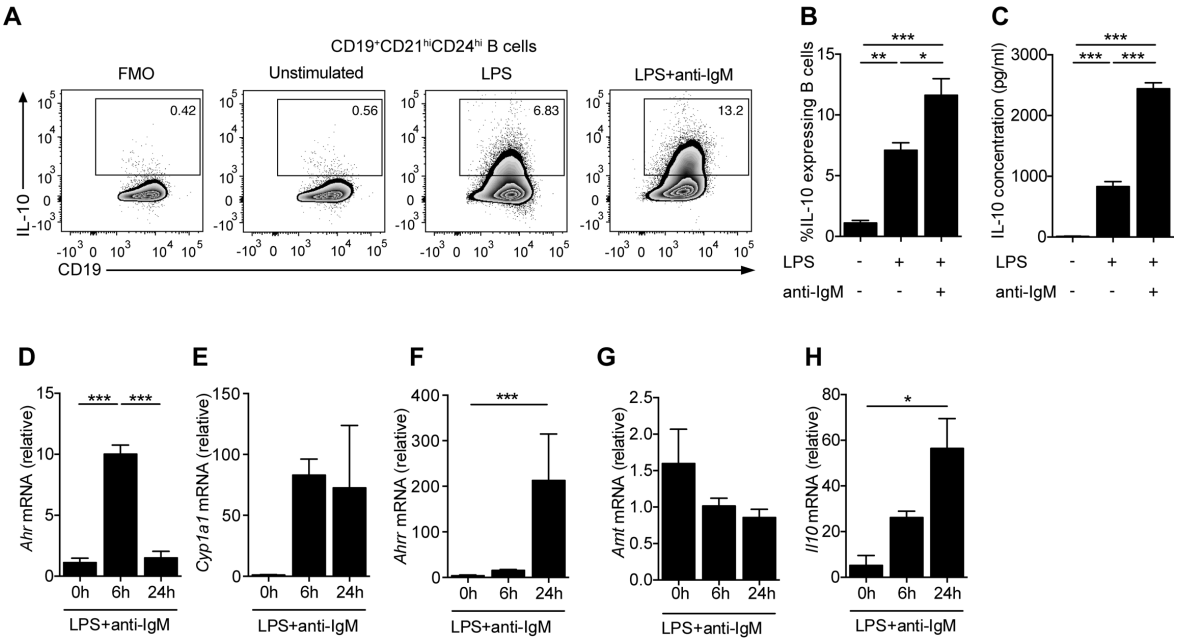

Figure 3.6. LPS+anti-IgM induce *Ahr* and *Il10* expression in CD19^{+}CD21^{hi}CD24^{hi} B cells. Antigen-induced arthritis (AIA) was induced in IL-10eGFP reporter or C57BL/6 mice. **A-B,** (**A**) Representative flow cytometry plots and (**B**) bar chart showing the percentage of IL-10 expression in CD19^{+}CD21^{hi}CD24^{hi} B cells (n=5). In these experiments CD19^{+}CD21^{hi}CD24^{hi} B cells were stimulated for 24h with LPS followed by an additional 24h with anti-IgM. (**C**) IL-10 production, as measured by ELISA (n=7). **D-H,** CD19^{+}CD21^{hi}CD24^{hi} B cells were isolated from WT C57BL/6 mice and stimulated for 6h or 24h with LPS+anti-IgM. The mRNA levels of (**D**) *Ahr*, (**E**) *Cyp1a1*, (**F**) *Ahrr*, (**G**) *Arnt* and (**H**) *Il10* were analyzed *ex-vivo* and after stimulation (n=3). For qPCR, gene expression was calculated normalizing to *β-Actin*. All experiments were performed at day 7 post IA-injection. Data representative of at least 3 independent experiments with biological replicates. Figures **B-H**, data are expressed as mean±sem. *p<0.05, **p<0.01, ***p<0.001. **B-H,** one-way ANOVA.

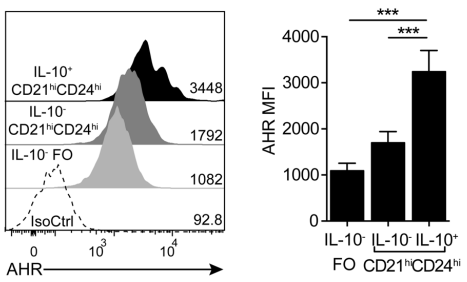

Figure 3.7. AHR is most highly expressed in IL-10^{+}CD19^{+}CD21^{hi}CD24^{hi} B cells after stimulation with LPS+anti-IgM. Representative histogram and bar chart showing the MFI of AHR expression in IL-10^{+}CD19^{+}CD21^{hi}CD24^{hi}, IL-10^{-}CD19^{+}CD21^{hi}CD24^{hi} and IL-10^{-} FO B cells after 48h stimulation with LPS+anti-IgM (n=4). All experiments were carried out at day 7 post IA-injection. Data representative of at least 2 independent experiments with biological replicates. Data are expressed as mean±sem. ***p<0.001, one-way ANOVA.

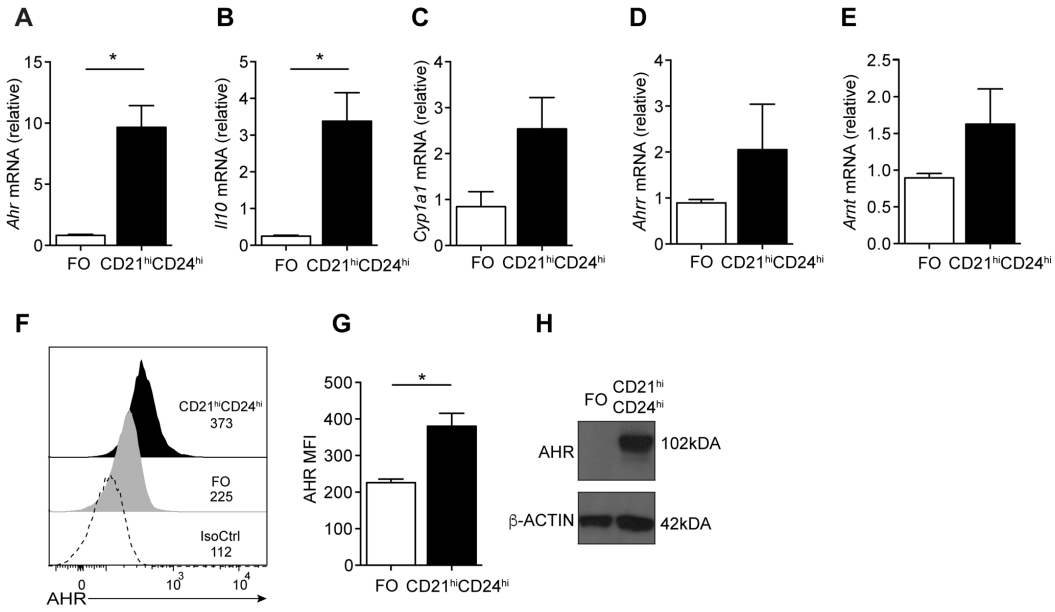

Figure 3.8. Increased levels of *Ahr* and downstream pathway in *ex vivo* CD19^{+}CD21^{hi}CD24^{hi} B cells compared to FO B cells. CD19^{+}CD21^{hi}CD24^{hi} and FO B cells were isolated from WT mice and the mRNA levels of (**A**) *Ahr*, (**B**) *Il10*, (**C**) *Cyp1a1*, (**D**) *Ahrr* and (**E**) *Arnt* were analysed ex-vivo (n=3). (**F**) Representative histogram and (**G**) bar chart showing the median fluorescent intensity (MFI) of AHR expression in CD19^{+}CD21^{hi}CD24^{hi} and FO B cells *ex vivo* (n=4). (**H**) Western blot showing the expression of AHR in CD19^{+}CD21^{hi}CD24^{hi} and FO B cells isolated from arthritic WT mice. β-ACTIN was used as a loading control. The numbers indicate the size of the protein bands in kDA. For qPCR, gene expression was calculated normalizing to *β-Actin*. All experiments were carried out at day 7 post IA-injection. Data representative of at least 2 independent experiments with biological replicates. Figures **A-E** and **G,** data are expressed as mean±sem. *p<0.05. **A-E and G,** Student's t test.

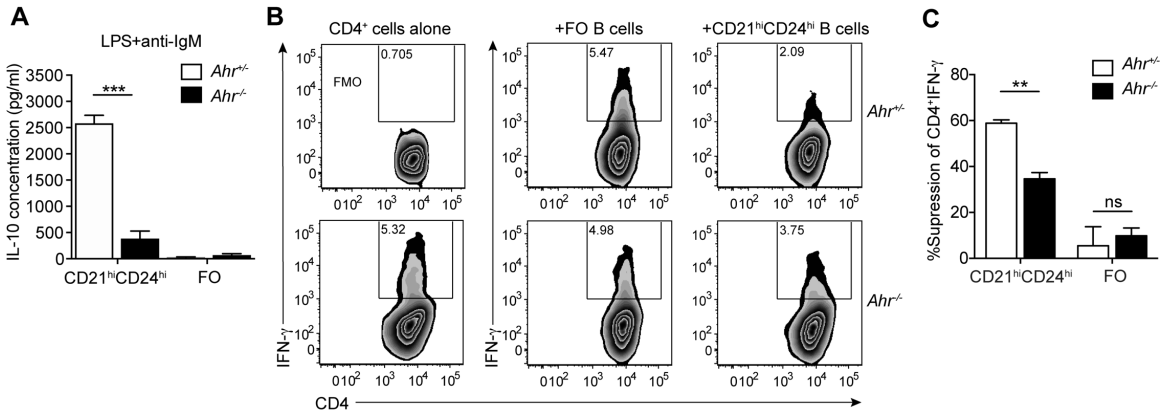

Figure 3.9. AHR controls the differentiation of CD19^{+}CD21^{hi}CD24^{hi} B cells into Bregs. Antigen-induced arthritis (AIA) was induced in *Ahr*$^{+/-}$ and *Ahr*$^{-/-}$ mice (**A**) IL-10 production measured by ELISA in LPS+anti-IgM stimulated CD19^{+}CD21^{hi}CD24^{hi} B cells and FO B cells from *Ahr*$^{+/-}$ and *Ahr*$^{-/-}$ mice (n=4 per group). (**B**) CpG-B-stimulated CD19^{+}CD21^{hi}CD24^{hi} and FO B cells from *Ahr*$^{+/-}$ and *Ahr*$^{-/-}$ mice co-cultured for 72 hours with anti-CD3 stimulated autologous CD4^{+} T cells from *Ahr*$^{+/-}$ mice. Representative flow cytometry plots showing the frequency of IFN-γ^{+}CD4^{+} T cells. (**C**) Bar chart showing percentage suppression of IFN-γ^{+}CD4^{+} T cells by splenic CD19^{+}CD21^{hi}CD24^{hi} B cells or FO B cells, following stimulation with anti-CD3 (n=3). All experiments were performed at day 7 post IA-injection. Data representative of at least 3 independent experiments with biological replicates. Figures **A and C**, data are expressed as mean±sem. **p<0.01, ***p<0.001. **A and C,** two-way ANOVA.

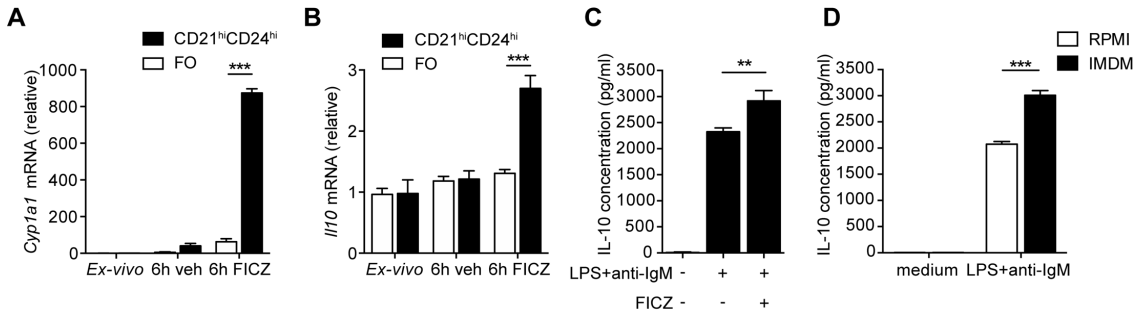

Figure 3.10. AHR agonists induce IL-10 in CD19^{+}CD21^{hi}CD24^{hi} B cells. Antigen-induced arthritis (AIA) was induced in WT C57BL/6 mice. CD19^{+}CD21^{hi}CD24^{hi} and FO B cells were stimulated for 6h with either vehicle alone (DMSO) or with the AHR agonist FICZ and the expression of (**A**) *Cyp1a1* and (**B**) *Il10* was measured by qPCR (*n*=3). (**C**) CD19^{+}CD21^{hi}CD24^{hi} B cells were cultured in RPMI media for 48h with LPS+anti-IgM±FICZ and IL-10 was measured in the supernatant (n=4). (**D**) CD19^{+}CD21^{hi}CD24^{hi} B cells were cultured in LPS+anti-IgM for 48h in RPMI or IMDM media and IL-10 was measured in the supernatant (n=5). For qPCR, gene expression was calculated normalizing to *β-Actin*. All experiments were performed at day 7 post IA-injection. Data representative of at least 3 independent experiments with biological replicates. Figures **A-D**, data are expressed as mean±sem. **p<0.01, ***p<0.001. **A, B and D,** two-way ANOVA; **C,** one-way ANOVA.

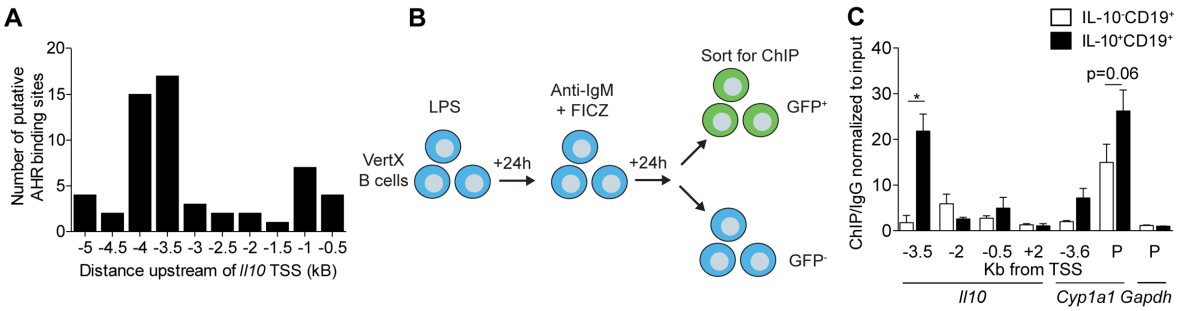

Figure 3.11. AHR binds to the *Il10* locus in IL-10$^+$ Bregs. Antigen-induced arthritis (AIA) was induced in IL-10eGFP reporter or C57BL/6 mice. (**A**) Jaspar binding motif analysis of putative AHR binding sites (XRE sites) in 500bp regions of DNA, upstream of the *Il10* transcription start site (TSS). (**B**) Schematic representing the experimental design for the ChIP-qPCR assay. Briefly, we isolated splenic B cells from IL-10eGFP reporter mice, stimulated them for 24h with LPS followed by 24h with anti-IgM+FICZ. (**C**) ChIP analysis of AHR binding to the *Il10* locus was performed in IL-10eGFP$^+$CD19$^+$ and IL-10eGFP$^-$ CD19$^+$ B cells. Bar chart showing the relative enrichment of AHR binding to regions upstream/downstream, or in the promoters (labeled as P), of the *Il10, Cyp1a1 and Gapdh* loci (*n*=3). All experiments were performed at day 7 post IA-injection. Data representative of at least 3 independent experiments with biological replicates. Figure **C**, data are expressed as mean±sem. **p*<0.05. **C,** multiple unpaired t tests. For Figure **C**, experiment was performed in collaboration with Aggelos Banos (ChIP assay post-fixation of cells).

Chapter IV: Results II

We have so far identified that AHR was highly expressed in IL-10^{+} Bregs and that AHR controlled IL-10 production in these cells via direct binding to the *Il10* locus. Furthermore, we demonstrated that Bregs have a tightly restricted gene expression profile with limited expression of cytokines, chemokines and their related receptors, compared to effector B cells. AHR has previously been shown to downregulate pro-inflammatory cytokines such as IFN-γ, IL-1β, IL-6, IL-17, IL-23a and TNFα in a variety of immune cells[482, 685, 686]. We hypothesised that AHR, in addition to regulating IL-10 expression, also limited inflammatory gene expression in Bregs. Using a combination of chromatin profiling and transcriptome analyses we show that loss of AHR in B cells reduces the expression of IL-10 by skewing the differentiation of CD19^{+}CD21^{hi}CD24^{hi} B cells into a pro-inflammatory programme, even under Breg-polarising conditions. We go on to show that inhibition of AHR increases *Il6*, *Tnf* and *Il2* transcription in CD19^{+}CD21^{hi}CD24^{hi} B cells and rule out that these cytokines are increased in *Ahr*$^{fl/-}$*Mb1*$^{cre/+}$ CD19^{+}CD21^{hi}CD24^{hi} B cells, as a consequence of reduced IL-10 signalling. This data suggests that these genes are direct targets of AHR. Thus, we highlight an important role of AHR in defining the identity of IL-10^{+} Bregs. The combined results in chapter III and this chapter, show that AHR acts as a transcriptional regulator of Breg differentiation by implementing a molecular programme that controls B cell IL-10 production and represses pro-inflammatory cytokine production.

The bioinformatic pipeline analysis for the RNA-seq (mapping to the mouse genome, normalisation and differential gene expression analysis) was carried out by Ignat Drozdov (Bering Ltd). Likewise, the bioinformatic pipeline for the ATAC-seq (read trimming, mapping to genome and peak calling) was carried out by Andre Rendeiro and Thomas Krausgruber (CeMM, Austria). Where data analysis was carried out in collaboration, the respective authors are listed in the figure legends.

4.1 AHR controls the Breg transcriptional programme by suppressing pro-inflammatory gene expression

To examine the role of AHR in controlling the differentiation of CD19^{+}CD21^{hi}CD24^{hi} B cells into Bregs, and to ascertain the relative contribution of AHR in establishing the restricted Breg phenotype identified in the microarray (Figure 3.3), in addition to its role in regulating IL-10 production, we took advantage of mice with a B cell-specific deficiency of AHR (*Ahr$^{fl/-}$Mb1$^{cre/+}$*)[615] (Figures 4.1A-C). The use of these mice avoids any cell extrinsic effects of AHR that could indirectly influence Breg differentiation[445, 477]. CD19^{+}CD21^{hi}CD24^{hi} B cells were sorted from immunised *Mb1$^{cre/+}$* and *Ahr$^{fl/-}$Mb1$^{cre/+}$* mice and the transcriptional profile of sorted CD19^{+}CD21^{hi}CD24^{hi} B cells was compared before and after stimulation under Breg polarising conditions (LPS+anti-IgM). Both the normalized counts for *Ahr* and the accessibility of the *Ahr* locus, measured by ATAC-seq increased in LPS+anti-IgM stimulated *Mb1$^{cre/+}$* CD19^{+}CD21^{hi}CD24^{hi} B cells, compared to *ex-vivo Mb1$^{cre/+}$* CD19^{+}CD21^{hi}CD24^{hi} B cells (Figures 4.2A-B). Signaling pathway impact analysis (SPIA) of differentially expressed genes (DEG) revealed overrepresented pathways relating to cytokine-cytokine receptor interactions and chemokine signalling, in stimulated *Mb1$^{cre/+}$* CD19^{+}CD21^{hi}CD24^{hi} B cells versus *ex vivo Mb1$^{cre/+}$* CD19^{+}CD21^{hi}CD24^{hi} B cells (Figure 4.3A). Analysis of the genes differentially expressed within this pathway, confirmed that under Breg polarising conditions, several genes identified in the IL-10eGFP^{+} signature (as shown in Figure 3.3C) including *Il10*, *Ccl22* and *Il2ra* were upregulated, whilst those associated to the IL-10eGFP^{-} signature including *Il12a, Il10ra and Ltb* were downregulated, under Breg-polarising conditions (Figure 4.3B-C).

A signature of genes related to cytokine-cytokine receptor interaction was upregulated in *Ahr$^{fl/-}$Mb1$^{cre/+}$* CD19^{+}CD21^{hi}CD24^{hi} B cells under LPS+anti-IgM stimulation compared to *Mb1$^{cre/+}$* CD19^{+}CD21^{hi}CD24^{hi} B cells (Figure 4.4A). 44 of 102 genes in this pathway were significantly differentially expressed between *Ahr$^{fl/-}$Mb1$^{cre/+}$* and *Mb1$^{cre/+}$* CD19^{+}CD21^{hi}CD24^{hi} B cells (Figures 4.4B). Of the genes that were differentially expressed under Breg polarising conditions (Figure 4.3B), pro-inflammatory cytokines including *Il6*, *Tnf*, *Il2,* and chemokines such as *Ccl3, Ccl5* and *Cxcl16*, known to recruit lymphocytes to the inflamed synovia in models of arthritis[687, 688, 689, 690], were upregulated in the absence of AHR (Figure 4.4B). The absence of AHR expression, led to the downregulation of the *Il5ra* gene, previously

associated with Breg function[349], and *Ccl22* and *Il18*, which we have identified as Breg-associated genes in the microarray. Testing key arthritogenic pro-inflammatory transcripts[691, 692, 693] by qPCR confirmed that *Il2*, *Il6* and *Tnf* were increased in *Ahr*$^{fl/-}$*Mb1*$^{cre/+}$ CD19^{+}CD21^{hi}CD24^{hi} B cells, and the Breg-associated transcripts *Ccl22* and *Il5ra* were decreased, compared to *Mb1*$^{cre/+}$ CD19^{+}CD21^{hi}CD24^{hi}B cells. The increase in pro-inflammatory cytokines in *Ahr*$^{fl/-}$ *Mb1*$^{cre/+}$ CD19^{+}CD21^{hi}CD24^{hi} B cells was confirmed by ELISA (Figures 4.4C-D). To confirm that AHR suppresses pro-inflammatory gene expression during the development of Bregs, we blocked AHR signaling *in vitro* with CH-223191. Concordant to the results identified with the RNA-seq, blocking AHR signaling resulted in the upregulation of *Il6* and *Tnf*, and the downregulation of *Il10* and *Ccl22* mRNA (Figure 4.5).

Our data suggests that AHR contributes to the Breg transcriptional programme by suppressing pro-inflammatory gene expression. To rule out whether this effect is secondary to the decrease of IL-10, we cultured WT and *Il10r*$^{-/-}$ CD19^{+}CD21^{hi}CD24^{hi} B cells with LPS+anti-IgM in the presence or absence of the selective AHR antagonist CH-223191. The expression of *Il6* and *Tnf* was significantly increased in both WT and *Il10r*$^{-/-}$ CD19^{+}CD21^{hi}CD24^{hi} B cells cultured with the AHR antagonist, suggesting a direct effect of AHR in the suppression of pro-inflammatory gene expression (Figure 4.6). Collectively, these data show that under Breg-polarizing conditions, AHR acts as a molecular switch that 'turns off' a number of pro-inflammatory cytokines and chemokines in CD19^{+}CD21^{hi}CD24^{hi} B cells, whilst promoting the expression of IL-10^{+}CD19^{+}CD21^{hi}CD24^{hi} Breg-associated cytokines and receptors.

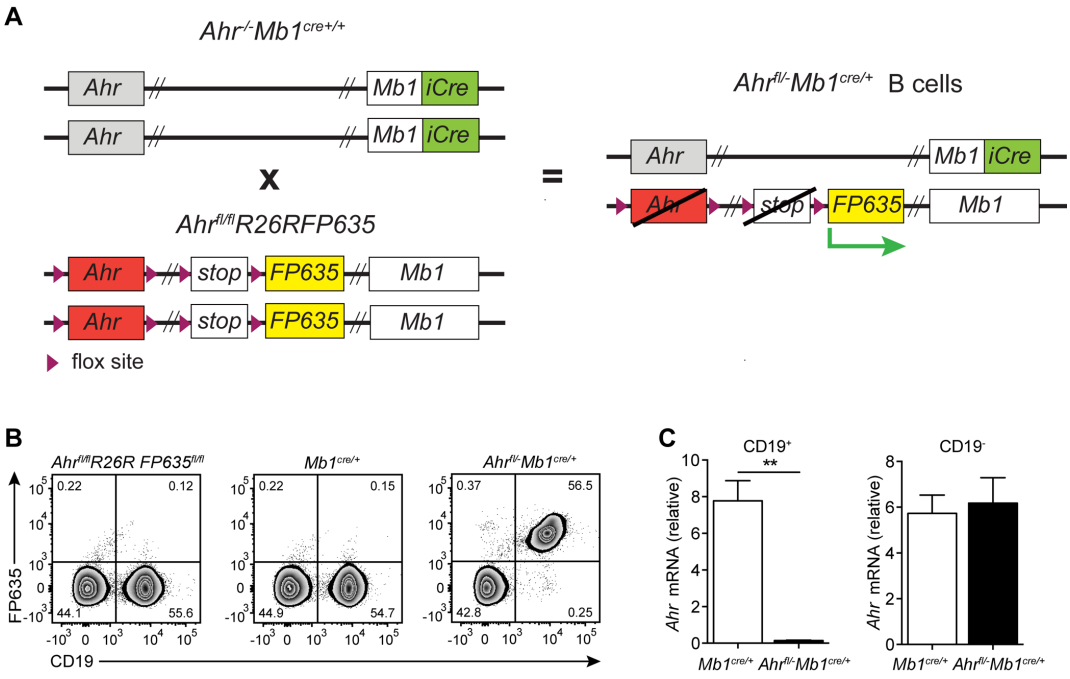

Figure 4.1. Validation of B cell AHR deficient (*Ahr*$^{fl/-}$*Mb1*$^{cre/+}$) mice. (**A**) Schematic showing breeding strategy for the generation of *Ahr*$^{fl/-}$*Mb1*$^{cre/+}$ mice. *Ahr*$^{fl/-}$*Mb1*$^{cre/+}$ mice lack AHR in MB1-expressing cells and report Cre activity via FP635 expression. (**B**) Representative flow cytometry plots of FP635 expression in the parental *Ahr*$^{fl/fl}$*R26R FP635*$^{fl/fl}$ strain, *Mb1*$^{cre/+}$ control mice and *Ahr*$^{fl/-}$*Mb1*$^{cre/+}$ mice. (**C**) Splenocytes from *Ahr*$^{fl/-}$*Mb1*$^{cre/+}$ mice and *Mb1*$^{cre/+}$ controls were sorted into CD19^{+}B220^{+} and CD19^{-}B220^{-} fractions and the levels of *Ahr* mRNA were analysed *ex vivo* (n=3). For qPCR, gene expression was calculated normalizing to β-*Actin*. All experiments were carried out at day 7 post IA-injection. Data representative of at least 2 independent experiments with biological replicates. Figure **C**, data are expressed as mean±sem. **p<0.01. **C,** unpaired t test.

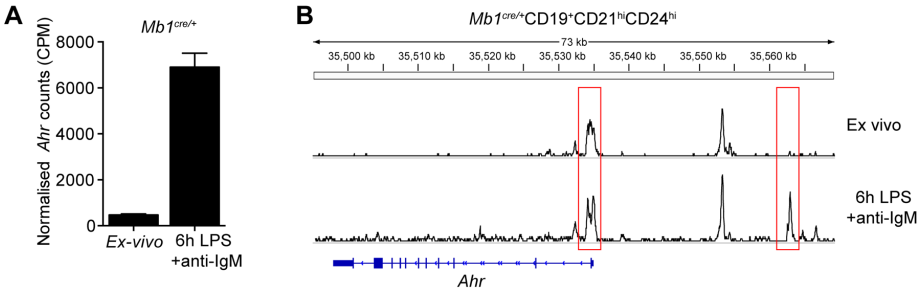

Figure 4.2. Activation of CD19^{+}CD21^{hi}CD24^{hi} B cells under Breg polarising conditions increases *Ahr* expression and the accessibility of the *Ahr* locus. (**A**) Normalised counts (CPM) of *Ahr* expression in *Mb1*$^{cre/+}$ mice *ex vivo* and after activation for 6h with LPS+anti-IgM. (**B**) Representative tracks of the *Ahr* locus before and after stimulation with LPS+anti-IgM in *Mb1*$^{cre/+}$ CD19^{+}CD21^{hi}CD24^{hi} B cells. Red box indicates one significantly differentially accessible region. All experiments were carried out at day 7 post IA-injection. For RNA-seq data, n=3 per condition and genotype. For ATAC-seq data, n=3 for *Mb1*$^{cre/+}$ mice and n=2 for *Ahr*$^{fl/-}$*Mb1*$^{cre/+}$ mice. Figure **A**, data expressed as mean±sem.

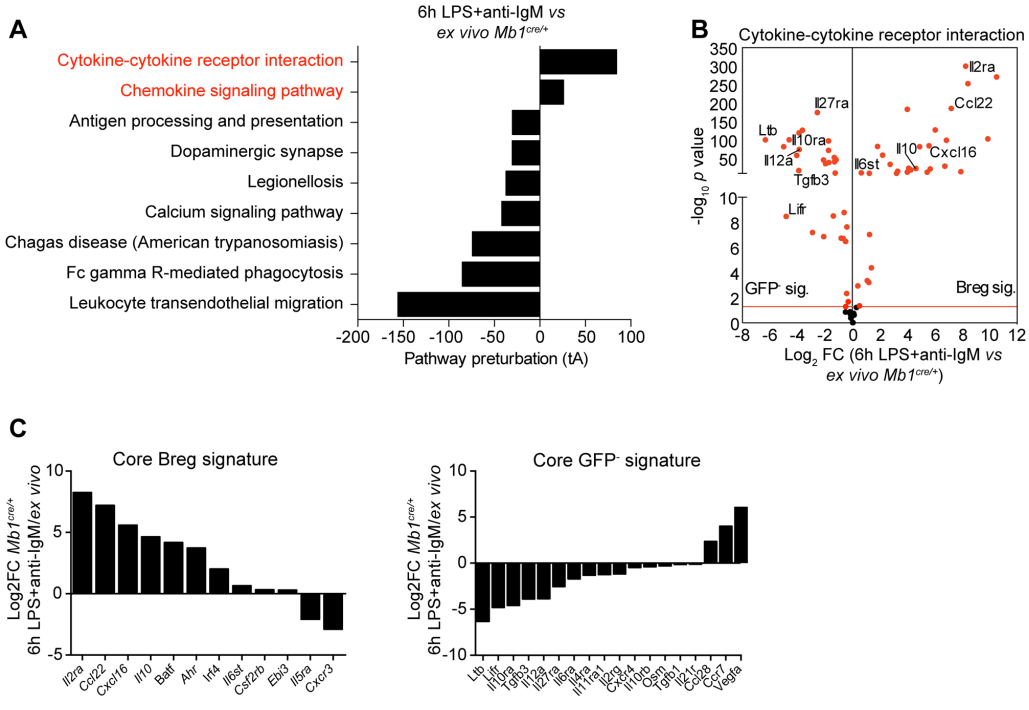

Figure 4.3. AHR increases Breg associated gene expression upon activation with LPS+anti-IgM. AIA was induced in *Mb1*$^{cre/+}$ and *Ahr*$^{fl/-}$*Mb1*$^{cre/+}$ mice. (**A**) Signalling pathway impact analysis (SPIA) showing the top significant (p<0.05) over-represented and under-represented pathways in LPS+anti-IgM stimulated compared to *ex vivo* CD19^{+}CD21^{hi}CD24^{hi} B cells from *Mb1*$^{cre/+}$ mice. The total perturbation accumulation of these pathways (tA) score is represented on the *x*-axis. (**B**) Volcano plot of RNA-seq analysis showing $\log_2$ fold changes between LPS+anti-IgM stimulated compared to *ex vivo* CD19^{+}CD21^{hi}CD24^{hi} B cells from *Mb1*$^{cre/+}$ mice, plotted against $-\log_{10}$ p value for the cytokine-cytokine receptor interaction pathway. Red dots represent significantly differentially expressed genes with the red line denoting a cut-off p value of <0.05. (**C**) Log_2 fold changes for core GFP^{+} and GFP^{-} gene signatures (identified from Figure 3.3C) comparing 6h LPS+anti-IgM vs *ex vivo* *Mb1*$^{cre/+}$ CD19^{+}CD21^{hi}CD24^{hi} B cells. All experiments were performed at day 7 post IA-injection. For RNA-seq data, n=3 per condition and genotype.

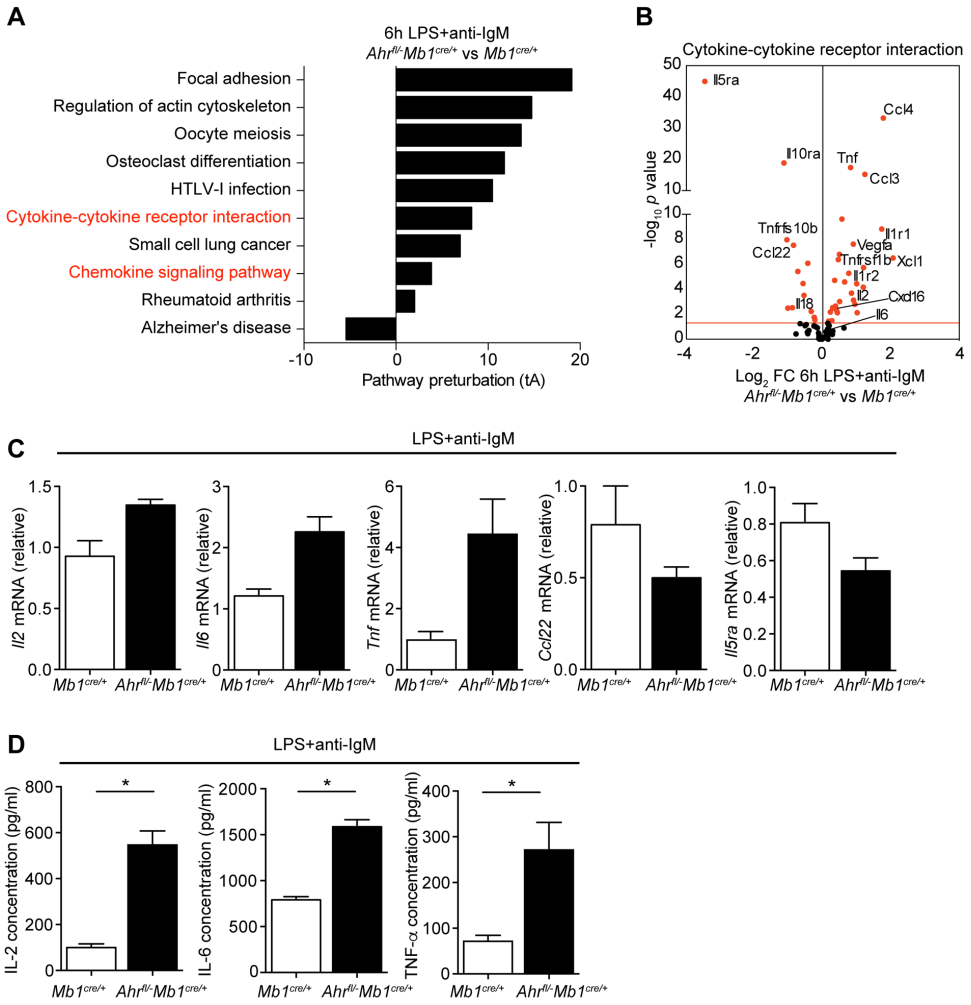

Figure 4.4. AHR suppresses pro-inflammatory gene expression during the differentiation of Bregs. AIA was induced in *Mb1*$^{cre/+}$ and *Ahr*$^{fl/-}$*Mb1*$^{cre/+}$ mice. (**A**) Signalling pathway impact analysis (SPIA) showing the top significant (p<0.05) over-represented and under-represented pathways in 6h LPS+anti-IgM stimulated CD19^{+}CD21^{hi}CD24^{hi} B cells from *Ahr*$^{fl/-}$*Mb1*$^{cre/+}$ mice compared to *Mb1*$^{cre/+}$ mice. (**B**) Volcano plot of RNA-seq analysis showing $\log_2$ fold changes between LPS+anti-IgM stimulated CD19^{+}CD21^{hi}CD24^{hi} B cells from *Ahr*$^{fl/-}$*Mb1*$^{cre/+}$ vs *Mb1*$^{cre/+}$ mice, plotted against $-\log_{10}$ p value for the cytokine-cytokine receptor interaction pathway. (**C**) CD19^{+}CD21^{hi}CD24^{hi} B cells were isolated from *Mb1*$^{cre/+}$ mice and *Ahr*$^{fl/-}$*Mb1*$^{cre/+}$ mice, stimulated for 6h with LPS+anti-IgM and assessed for mRNA levels of *Il2*, *Il6*, *Tnf*, *Ccl22* and *Il5ra* (n=4). (**D**) IL-2, IL-6 and TNFα concentrations from 48h LPS+anti-IgM stimulated CD19^{+}CD21^{hi}CD24^{hi} B cells from *Mb1*$^{cre/+}$ mice and *Ahr*$^{fl/-}$*Mb1*$^{cre/+}$ mice (n=4). For qPCR, gene expression was calculated normalizing to *β-Actin*. All experiments were performed at day 7 post IA-injection. For RNA-seq data, n=3 per condition and genotype. For ATAC-seq data, n=3 for *Mb1*$^{cre/+}$ mice and n=2 for *Ahr*$^{fl/-}$*Mb1*$^{cre/+}$ mice. For figures **C-D**, data representative of 2 independent experiments with biological replicates and data are expressed as mean±sem. *p<0.05. **C-D,** Mann-Whitney test.

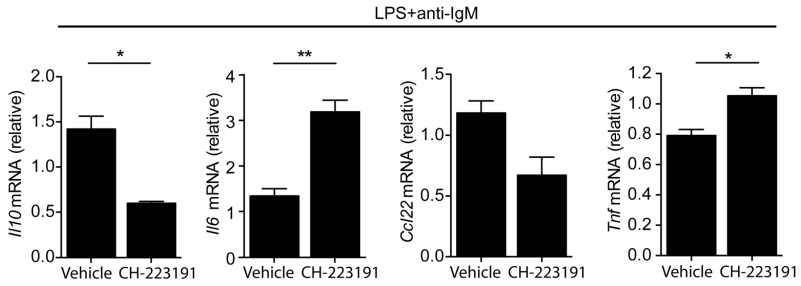

Figure 4.5. Blocking AHR affects the cytokine and chemokine gene expression of LPS+anti-IgM stimulated CD19^{+}CD21^{hi}CD24^{hi} B cells. CD19^{+}CD21^{hi}CD24^{hi} B cells were isolated from WT mice and stimulated for 24h with LPS+anti-IgM in the presence of the AHR antagonist CH-223191 or a vehicle control and *Il10*, *Ccl22*, *Il6* and *Tnf* mRNA levels were analyzed (n=5). For qPCR, gene expression was calculated normalizing to *β-Actin*. All experiments were carried out at day 7 post IA-injection. Data representative of two independent experiments with biological replicates. Data expressed as mean±sem. *p<0.05, **p<0.01, Mann-whitney test.

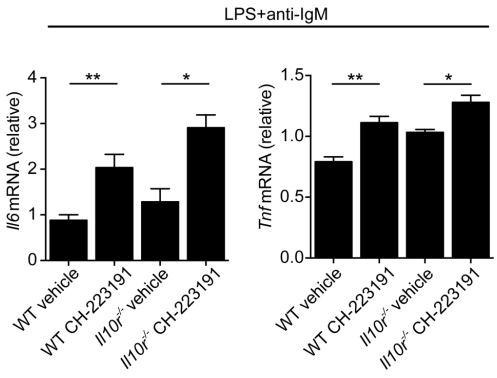

Figure 4.6. *Il6* and *Tnf* are direct targets of AHR and are not affected in the absence of IL-10 signalling. WT or *Il10r*$^{-/-}$ CD19^{+}CD21^{hi}CD24^{hi} B cells were cultured with LPS+anti-IgM±CH-223191 for 24h and *Il6* and *Tnf* mRNA levels were analyzed (n=5). For qPCR, gene expression was calculated normalizing to *β-Actin*. All experiments were carried out at day 7 post IA-injection. Data representative of two independent experiments with biological replicates. Data expressed as mean±sem. *p<0.05, **p<0.01, two-way ANOVA.

4.2 AHR regulates chromatin accessibility of cytokine and chemokine gene loci In B cells

Xenobiotic response elements (XRE), which are specific sites for AHR binding, have been reported in many genes involved in immune function[580]. Comparison of the genome-wide footprint density of up- and down-stream XRE sites, using a previously reported XRE consensus sequence in B cells[694], revealed increased chromatin accessibility of these regions in *Mb1*$^{cre/+}$CD19^{+}CD21^{hi}CD24^{hi} B cells after activation of with LPS+anti-IgM (Figure 4.7A). No increase was seen in *Ahr*$^{fl/-}$ *Mb1*$^{cre/+}$ CD19^{+}CD21^{hi}CD24^{hi} B cells after activation with LPS+anti-IgM. Specific interrogation of differentially accessible regions (DAR) in loci encoding genes from the cytokine-cytokine receptor interaction pathway, revealed an overall decrease in chromatin accessibility in these genes in *Ahr*$^{fl/-}$*Mb1*$^{cre/+}$ CD19^{+}CD21^{hi}CD24^{hi} B cells. 78 DARs (p value <0.05) were identified amongst the genes regulated by AHR at the transcriptional level, including *Il2*, *Il6*, *Ccl3*, *Ccl5, Il5ra, Ccl22* and *Il10* between LPS+anti-IgM polarised *Ahr*$^{fl/-}$*Mb1*$^{cre/+}$ and *Mb1*$^{cre/+}$ CD19^{+}CD21^{hi}CD24^{hi} B cells (Figure 4.7B). These data indicate that AHR binds to the XRE regions and regulates the chromatin accessibility of a number of genes within the cytokine-cytokine receptor interaction pathway.

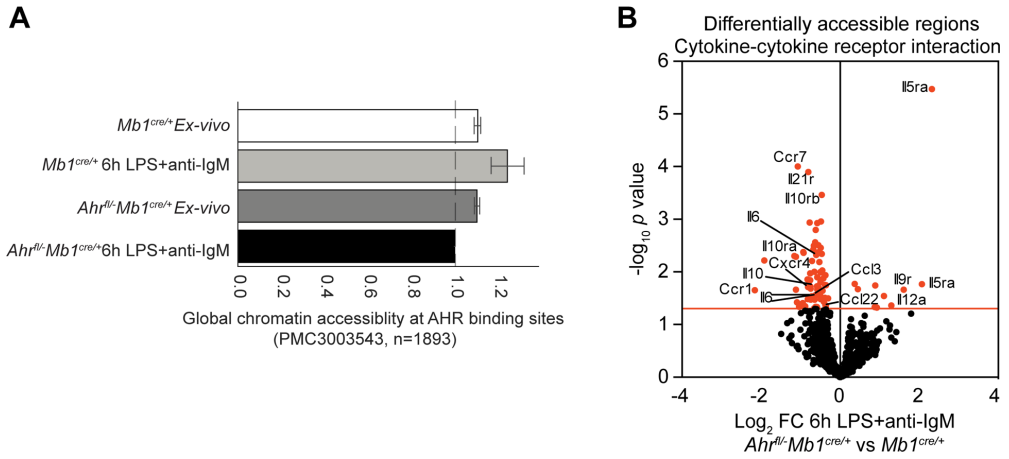

Figure 4.7. AHR increases chromatin accessibility of CD19^{+}CD21^{hi}CD24^{hi} B cells under Breg polarising conditions. AIA was induced in *Mb1*$^{cre/+}$ and *Ahr*$^{fl/-}$*Mb1*$^{cre/+}$ mice. (**A**) Bar chart showing the ratio of mean normalized accessibility in all AHR binding sites (XRE regions) over the normalized mean accessibility of other regulatory elements (mean±95% confidence intervals). (**B**) Volcano plot of ATAC-seq DARs in genes taken from the cytokine-cytokine receptor interaction pathway, comparing chromatin accessibility at these sites between *Ahr*$^{fl/-}$*Mb1*$^{cre/+}$ and *Mb1*^{cre} CD19^{+}CD21^{hi}CD24^{hi} B cells after 6h LPS+anti-IgM. All experiments were performed at day 7 post IA-injection. For ATAC-seq data, *n*=3 for *Mb1*$^{cre/+}$ mice and *n*=2 for *Ahr*$^{fl/-}$*Mb1*$^{cre/+}$ mice.

Chapter V: Results III

The results in chapters III and IV show that AHR is a key transcription factor in the differentiation of $CD19^{+}CD21^{hi}CD24^{hi}$ B cells into IL-10^{+}Bregs, and maintains Breg identity by suppressing pro-inflammatory cytokines otherwise seen in effector B cell populations. In this chapter, we show that AHR is required for Breg suppressive function *in vivo* in a model of arthritis.

We show that B cell-specific AHR deficient mice ($Ahr^{fl/-}Mb1^{cre/+}$) develop a worse disease course of AIA compared to control $Mb1^{cre/+}$ mice, with increased numbers of pathogenic IL-17 and IFN-γ expressing $CD4^{+}$ T cells. As highlighted in the introduction, Breg-derived IL-10 is important for inhibiting the expression of IL-17 and IFN-γ by $CD4^{+}$ T cells[354]. Unlike the adoptive transfer of control $Mb1^{cre/+}$ $CD19^{+}CD21^{hi}CD24^{hi}$ B cells, transfer of $Ahr^{fl/-}Mb1^{cre/+}$ $CD19^{+}CD21^{hi}CD24^{hi}$ B cells failed to suppress AIA disease and inhibit pathogenic $CD4^{+}$ T cell responses. This is due to a marked reduction of IL-10 production by $CD19^{+}CD21^{hi}CD24^{hi}$ B cells in $Ahr^{fl/-}Mb1^{cre/+}$ mice. Importantly, using a series of *in vivo* experiments, we show that the impairment in Breg differentiation in AHR deficient $CD19^{+}CD21^{hi}CD24^{hi}$ B cells is a cell intrinsic defect and not a consequence of impaired survival or proliferation of these cells. Moreover, we demonstrate that in the same inflammatory environment, using a mixed bone marrow chimera, only AHR-sufficient $CD19^{+}CD21^{hi}CD24^{hi}$ B cells differentiate in IL-10^{+} Bregs.

Where experiments were carried out in collaboration, the respective authors are listed in the figure legends.

5.1 B cell specific AHR deficiency causes exacerbated arthritis and increased T cell-driven arthritogenic responses

Having confirmed the contribution of AHR in the programming of the IL-10^{+}CD19^{+}CD21^{hi}CD24^{hi} Breg transcriptional profile, we explored the impact of AHR deficiency specifically in B cells on the immune response associated with arthritis. *Ahr$^{fl/-}$Mb1$^{cre/+}$* mice developed exacerbated arthritis compared to control *Mb1$^{cre/+}$* mice (Figure 5.1A). Histological analysis of joint tissue showed an increase in immune cell infiltration in the synovia and hyper-vascularization in *Ahr$^{fl/-}$Mb1$^{cre/+}$* compared to control *Mb1$^{cre/+}$* mice (Figure 5.1B). The enhanced inflammation was associated with a significant increase in the frequency and number of IFN-γ and IL-17-expressing CD4^{+} T cells in the spleen and DLN in *Ahr$^{fl/-}$Mb1$^{cre/+}$* mice (Figures 5.2A-D). Increased levels of IL-17 were also observed in the synovium of inflamed joints of *Ahr$^{fl/-}$Mb1$^{cre/+}$* compared to control group, whereas IFN-γ levels were undetectable (Figure 5.2E). *Ahr$^{fl/-}$Mb1$^{cre/+}$* mice had an increased frequency and number of IL-17^{+}CD4^{+} T cells and a reduction in the frequency and total number of FOXP3^{+} Tregs in the inguinal DLN, compared to the control mice (Figures 5.2C-D and Figures 5.3A-B).

Adoptive transfer of *Mb1$^{cre/+}$* or *Ahr$^{fl/-}$Mb1$^{cre/+}$* CD19^{+}CD21^{hi}CD24^{hi} B cells into syngeneic mice showed that only CD19^{+}CD21^{hi}CD24^{hi} B cells from *Mb1$^{cre/+}$,* but not from *Ahr$^{fl/-}$Mb1$^{cre/+}$* mice, significantly inhibited disease and Th1/Th17 differentiation in the recipient mice (Figures 5.4A-C), confirming that CD19^{+}CD21^{hi}CD24^{hi} B cells were less effective at suppressing inflammation in the absence of AHR.

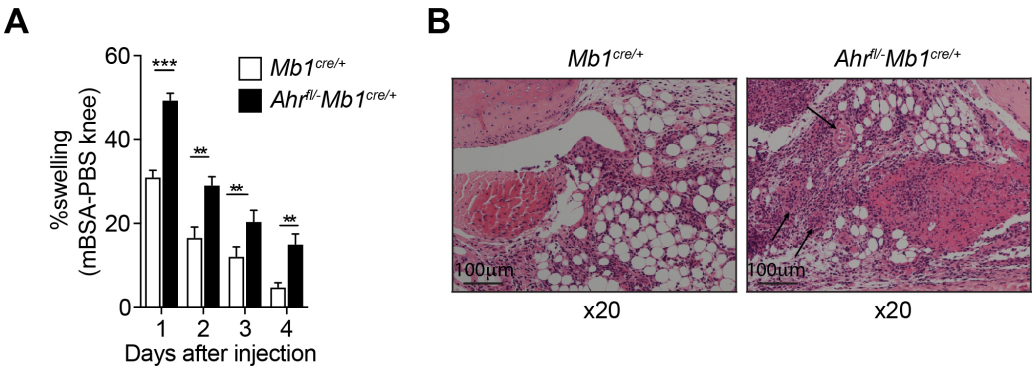

Figure 5.1. B cell AHR deficiency exacerbates antigen induced arthritis. (**A**) Mean clinical score of *Mb1*$^{cre/+}$ and *Ahr*$^{fl/-}$*Mb1*$^{cre/+}$ mice following induction of arthritis; y axis shows percentage swelling in antigen-injected knee compared to control knee (*n*=12 per group). (**B**) Representative H&E staining of arthritic joints from *Mb1*$^{cre/+}$ and *Ahr*$^{fl/-}$*Mb1*$^{cre/+}$ mice (*n*=3; original magnification of 20×). Arrows indicate hyper-vascularisation. Scale bar = 100 μM. All experiments were performed at day 7 post IA-injection. Data representative of at least 3 independent experiments with biological replicates. For figure **A,** data are expressed as mean±sem. ***p*<0.01, ****p*<0.001, two-way ANOVA.

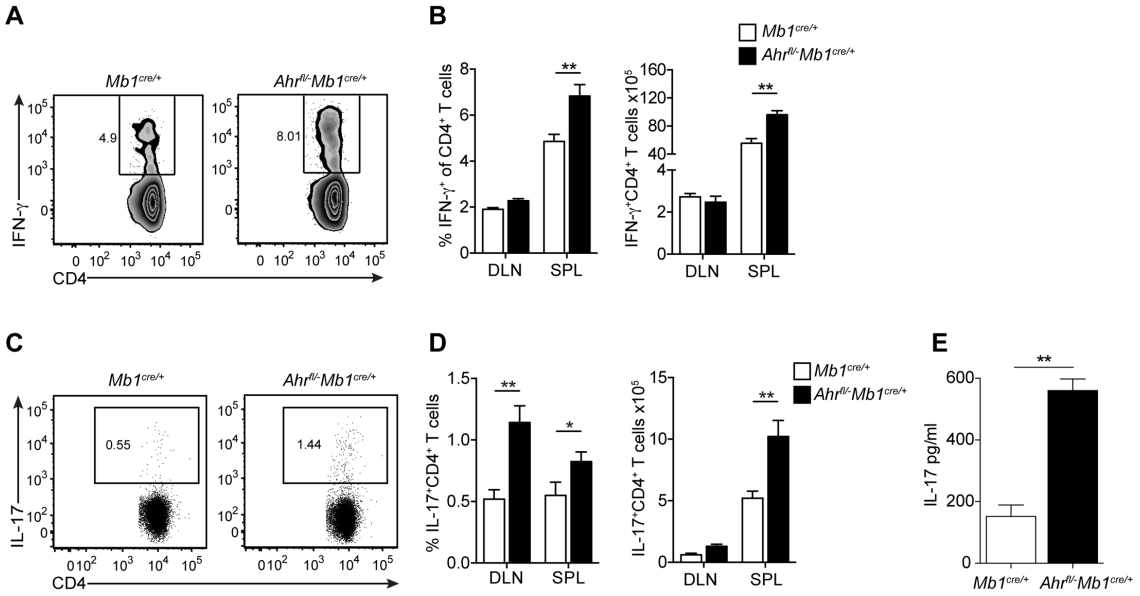

Figure 5.2. *Ahr$^{fl/-}$Mb1$^{cre/+}$* mice have increased IFN-γ and IL-17 expressing CD4$^+$ T cells. A-D, Representative flow cytometry plots and bar charts showing respectively the percentage and number of (**A,B**) IFN-γ$^+$CD4$^+$ T cells and (**C,D**) IL-17$^+$CD4$^+$ T cells in the spleens and DLNs of *Mb1$^{cre/+}$* and *Ahr$^{fl/-}$Mb1$^{cre/+}$* mice (*n*=7). (**E**) IL-17 concentration as measured in the synovial fluid of *Mb1$^{cre/+}$* and *Ahr$^{fl/-}$Mb1$^{cre/+}$* mice (*n*=6). All experiments were performed at day 7 post IA-injection. Data representative of at least 3 independent experiments with biological replicates. Figures **B and D-E,** data are expressed as mean±sem. *p<0.05, **p<0.01. **B and D,** two-way ANOVA; **E,** and Mann-Whitney test.

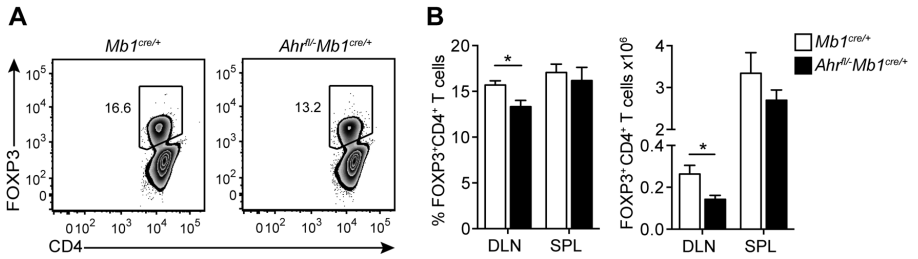

Figure 5.3. *Ahr$^{fl/-}$Mb1$^{cre/+}$* mice have reduced numbers of FOXP3^{+} Tregs in the DLN. **(A)** Representative flow cytometry plots and (**B**) bar charts showing respectively the percentage and number of FOXP3^{+}CD4^{+} T cells in the spleens and DLNs of *Mb1$^{cre/+}$* and *Ahr$^{fl/-}$Mb1$^{cre/+}$* mice (*n*=7). All experiments were performed at day 7 post IA-injection. Data representative of at least 3 independent experiments with biological replicates. For figure **B,** data are expressed as mean±sem. **p*<0.05. **B,** two-way ANOVA.

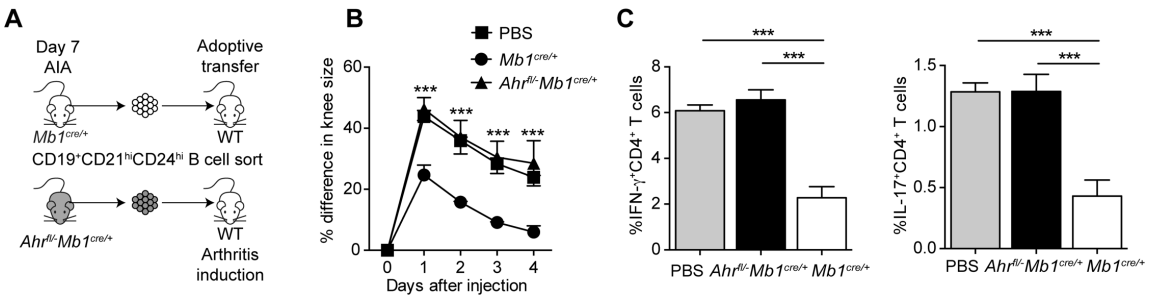

Figure 5.4. Adoptive transfer of AHR-deficient CD19^{+}CD21^{hi}CD24^{hi} B cells fails to ameliorate arthritis in recipient mice. (**A**) Schematic showing the experimental design of the adoptive transfer system. (**B**) Mean clinical score of C57BL/6 mice following adoptive transfer of CD19^{+}CD21^{hi}CD24^{hi} B cells purified from *Mb1$^{cre/+}$* and *Ahr$^{fl/-}$Mb1$^{cre/+}$* mice, administered on the day of disease onset. Control (no transfer) group received PBS (*n*=5). (**C**) Bar charts showing respectively the percentage of IFN-γ^{+}CD4^{+} T cells and IL-17^{+}CD4^{+} T cells in the spleens of WT recipient mice, following an adoptive transfer of *Mb1$^{cre/+}$* and *Ahr$^{fl/-}$Mb1$^{cre/+}$* CD19^{+}CD21^{hi}CD24^{hi} B cells, or a PBS control (*n*=5). All experiments were performed at day 7 post IA-injection. Data representative of at least 3 independent experiments with biological replicates. Figures **B and C,** data are expressed as mean±sem. **p*<0.05, ***p*<0.01. **B,** two-way ANOVA; **C,** one -way ANOVA.

5.2 *Ahr*$^{fl/-}$*Mb1*$^{cre/+}$ mice do not have a defect in B cell development, but present with a reduced frequency and number of Bregs

To establish that the increase in disease severity and the impact on the T cell compartment was due to the lack of AHR-expressing Bregs, rather than a consequence of abnormal B cell development, we next compared the frequencies of pro, pro-pre, pre, immature, transitional (T), early and late mature B cells in the bone marrow or T1 or FO B cells in the spleens of *Ahr*$^{fl/-}$*Mb1*$^{cre/+}$ and *Mb1*$^{cre/+}$ mice. We observed no differences in these populations, suggesting that the increase in arthritis severity and in pro-inflammatory T cells was indeed due to a reduction of CD19^{+}CD21^{hi}CD24^{hi} Bregs, rather than a consequence of abnormal B cell development (Figures 5.5A-B, Figures 5.6A-H). In line with previous findings showing that AHR represses differentiation of B cells into plasma cells [606], we found increased frequencies of splenic plasma cells (Figures 5.7A-B) and increased *Prdm1* mRNA expression in *Ahr*$^{fl/-}$*Mb1*$^{cre/+}$ B cells relative to *Mb1*$^{cre/+}$ B cells (Figure 5.7C). Despite changes in the frequency of plasma cells in the spleens there were no differences in the amount of secreted IgG, IgM and IgA in the serum of arthritic *Ahr*$^{fl/-}$*Mb1*$^{cre/+}$ versus *Mb1*$^{cre/+}$ mice (Figure 5.7D).

While there were no differences in the number of splenic CD19^{+}CD21^{hi}CD24^{hi} B cells between the two groups, *Ahr*$^{fl/-}$*Mb1*$^{cre/+}$CD21^{hi}CD24^{hi} B cells secreted significantly less IL-10 than *Mb1*$^{cre/+}$CD19^{+}CD21^{hi}CD24^{hi} B cells, following stimulation with LPS+anti-IgM (Figure 5.8). IL-10 production by *Ahr*$^{fl/-}$*Mb1*$^{cre/+}$ CD19^{+} B cells was significantly reduced in response to TLR9 stimulation (Figures 5.9A-C). Comparable levels of *Ebi3* and *Il12a* were present in B cells from *Ahr*$^{fl/-}$ *Mb1*$^{cre/+}$ mice and *Mb1*$^{cre/+}$ mice (Figures 5.10A-B). These results together with our previous findings showing a redundant effect of IL-35 in Bregs in this model[695], excluded that Bregs were non-functional because of a lack of IL-35 production, in the absence of AHR.

The observed IL-10 reduction was not due to impaired B cell proliferation, since an equivalent expression of Ki-67 in *Mb1*$^{cre/+}$ and *Ahr*$^{fl/-}$*Mb1*$^{cre/+}$ CD19^{+}CD21^{hi}CD24^{hi} B cells was observed both directly *ex vivo* after AIA and after stimulation with LPS+anti-IgM (Figures 5.11A-D). No difference in genes related to the cell cycle was observed, including *Ccno*, previously shown to be regulated by AHR in splenic B cells[615], between *Mb1*$^{cre/+}$ and *Ahr*$^{fl/-}$*Mb1*$^{cre/+}$ CD19^{+}CD21^{hi}CD24^{hi} B cells (Figure

5.11E), suggesting that there was no impairment in BCR-driven regulation of B cell entry into the cell cycle[696].

Mesenteric lymph nodes (MLNs) are important sites for the licensing of Breg development, through exposure to microbiota-driven induction of the pro-inflammatory cytokines IL-1β and IL-6[323]. Fewer $CD19^{+}CD21^{hi}CD24^{hi}$ B cells, and a decreased amount of B cell derived IL-10 after *in vitro* polarisation with LPS+anti-IgM, were observed in the MLN of $Ahr^{fl/-}Mb1^{cre/+}$ mice compared to control $Mb1^{cre/+}$ mice (Figures 5.12A-C). Of interest, no difference in the gut-homing integrin α4β7 expression was observed in splenic or MLN-derived $CD19^{+}CD21^{hi}CD24^{hi}$ B cells between $Ahr^{fl/-}Mb1^{cre/+}$ and $Mb1^{cre/+}$ mice, suggesting the reduction of Bregs observed in the MLN of $Ahr^{fl/-}Mb1^{cre/+}$ mice is α4β7-independent (Figures 5.13A-C). We can exclude that the decreased frequency of Bregs was the consequence of a reduction in monocyte-derived IL-1β and IL-6 produced in the spleens or in the MLNs, as equivalent amounts of these cytokines were produced by these cells in both $Ahr^{fl/-}Mb1^{cre/+}$ and $Mb1^{cre/+}$ mice (Figures 5.14A-D). Thus, our results collectively show that mice lacking AHR expression in B cells phenocopy the results that we have previously observed in mice with $Il10^{-/-}$ B cells[354] and show that AHR influences $IL\text{-}10^{+}CD19^{+}CD21^{hi}CD24^{hi}$ Breg differentiation in a cell intrinsic manner.

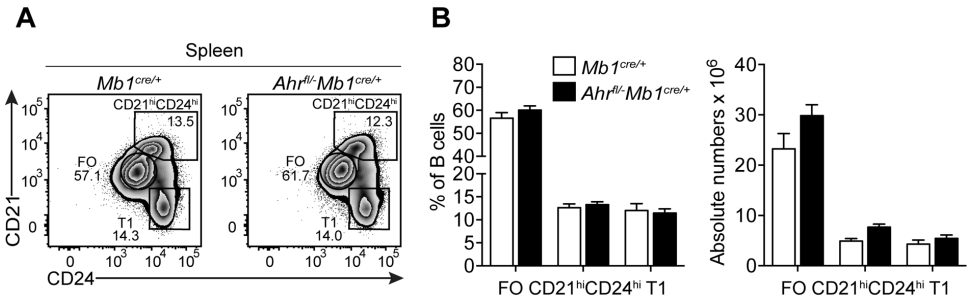

Figure 5.5. B cell subset numbers are unaffected in the absence of AHR expression in B cells. AIA was induced in *Mb1*$^{cre/+}$ and *Ahr*$^{fl/-}$*Mb1*$^{cre/+}$ mice. (**A**) Representative flow cytometry plots showing percentage and (**B**) bar charts showing the percentages and absolute numbers of CD19^{+}CD21^{-}CD24^{hi} (T1), CD19^{+}CD21^{hi}CD24^{hi} and FO B cells in the spleens of *Mb1*$^{cre/+}$ and *Ahr*$^{fl/-}$*Mb1*$^{cre/+}$ mice (*n*=7). All experiments were performed at day 7 post IA-injection. Data representative of at least 2 independent experiments with biological replicates. For figure **B,** data are expressed as mean±sem. **B,** Two-way ANOVA.

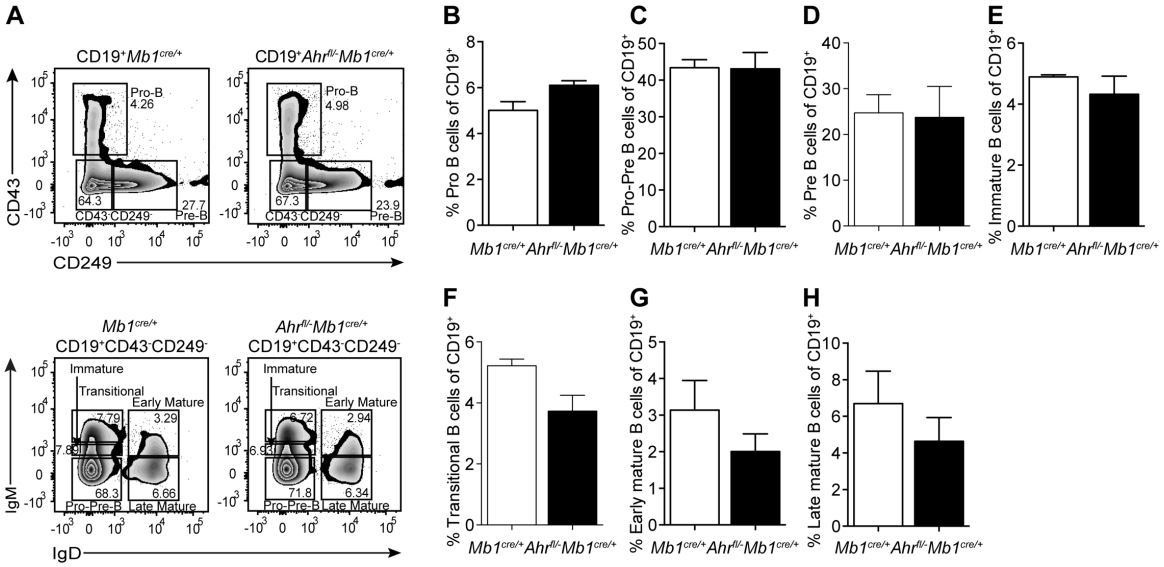

Figure 5.6. AHR plays a redundant role in early B cell development in the bone marrow. (**A**) Representative flow cytometry plots showing *Mb1*$^{cre/+}$ and *Ahr*$^{fl/-}$*Mb1*$^{cre/+}$ B cell subsets in the bone marrow. **B-H,** Bar charts showing the frequencies of (**B**) pro, (**C**) pro-pre, (**D**) pre, (**E**) immature, (**F**) transitional (**G**) early mature and (**H**) late mature B cells, as a percentage of total CD19^{+} B cells in the bone marrow for *Mb1*$^{cre/+}$ and *Ahr*$^{fl/-}$*Mb1*$^{cre/+}$ mice (n=3 per genotype). All experiments were carried out at day 7 post IA-injection. Data representative of at least 2 independent experiments with biological replicates. Figures **B-H,** data are expressed as mean±sem. **B-H,** Mann-Whitney test.

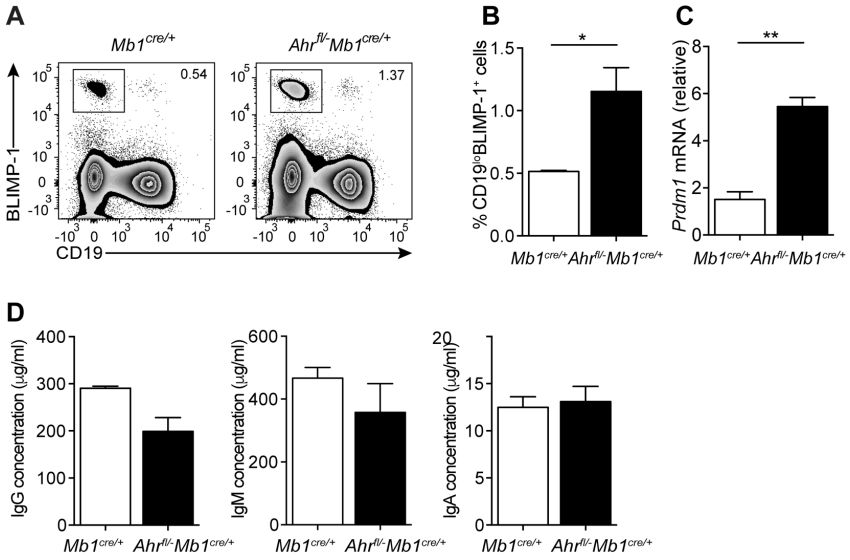

Figure 5.7. AHR represses plasma cell differentiation. (**A**) Representative flow cytometry plots and (**B**) bar chart showing the percentage of splenic BLIMP-1^{+} B cells from *Mb1*$^{cre/+}$ and *Ahr*$^{fl/-}$*Mb1*$^{cre/+}$ mice (n=3). (**C**) Total splenic B cells were isolated from *Mb1*$^{cre/+}$ and *Ahr*$^{fl/-}$*Mb1*$^{cre/+}$ mice and *Prdm1* mRNA levels were analysed *ex-vivo* (n=3). (**D**) Serum concentrations of total IgG, IgM and IgA from *Mb1*$^{cre/+}$ and *Ahr*$^{fl/-}$*Mb1*$^{cre/+}$ mice were measured by ELISA. For qPCR, gene expression was calculated normalizing to *β-Actin*. All experiments were carried out at day 7 post IA-injection. Data representative of at least 2 independent experiments with biological replicates. Figures **B-D,** data are expressed as mean±sem. **p*<0.05, ***p*<0.01. **B-D,** Student's t test.

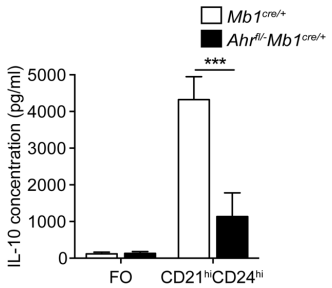

Figure 5.8. CD19^{+}CD21^{hi}CD24^{hi} B cells in *Ahr$^{fl/-}$Mb1$^{cre/+}$* mice are less able to differentiate into Bregs. AIA was induced in *Mb1$^{cre/+}$* and *Ahr$^{fl/-}$Mb1$^{cre/+}$* mice. CD19^{+}CD21^{hi}CD24^{hi} or FO B cells were sorted from *Mb1$^{cre/+}$* and *Ahr$^{fl/-}$Mb1$^{cre/+}$* mice and stimulated with LPS+anti-IgM for 48h. IL-10 production, as measured by ELISA (n=4 per group). All experiments were performed at day 7 post IA-injection. Data representative of at 2 independent experiments with biological replicates. Data are expressed as mean±sem. *p<0.05, **p<0.01, ***p<0.01, two-way ANOVA.

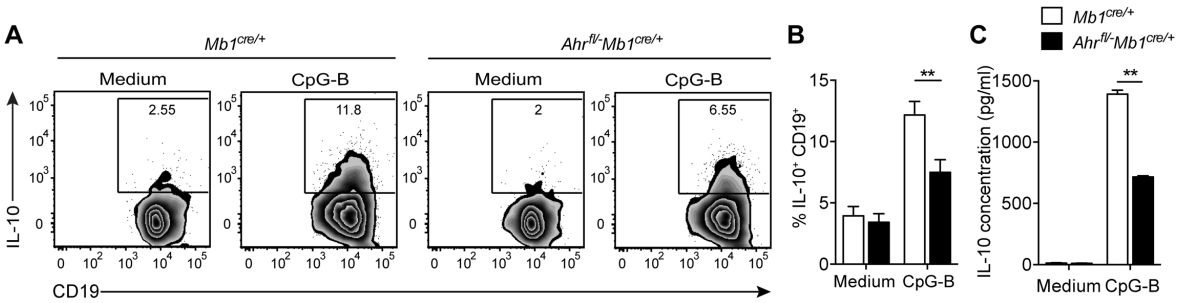

Figure 5.9. AHR is required for IL-10 production by B cells *in vitro*. Representative flow cytometry plots (**A**) and bar chart (**B**) showing the percentage of IL-10-expressing CD19$^+$ B cells from *Mb1*$^{cre/+}$ and *Ahr*$^{fl/-}$*Mb1*$^{cre/+}$ mice, after 48h stimulation with CpG-B (n=3). (**C**) IL-10 production, as measured by ELISA (n=3). All experiments were carried out at day 7 post IA-injection. All data representative of at least 2 independent experiments, with biological replicates. Figures **B-C,** data expressed as mean±sem. **p<0.01. **B-C,** two-way ANOVA.

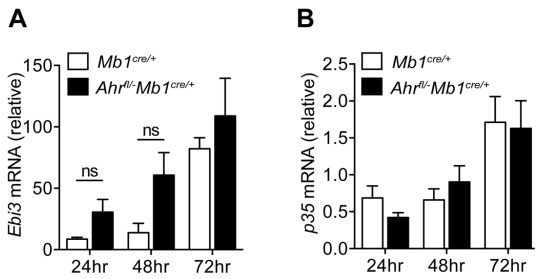

Figure 5.10. AHR does not control IL-35 production by B cells. Splenic B cells were isolated from *Mb1*$^{cre/+}$ and *Ahr*$^{fl/-}$*Mb1*$^{cre/+}$ mice and stimulated with LPS for the indicated times and (**A**) *Ebi3* and (**B**) *p35* mRNA levels were analysed (n=3). All experiments were carried out at day 7 post IA-injection. For qPCR gene expression was calculated normalising to *β-Actin*. All data representative of at least 2 independent experiments, with biological replicates. Figures **A-B,** data expressed as mean±sem. **A-B,** two-way ANOVA.

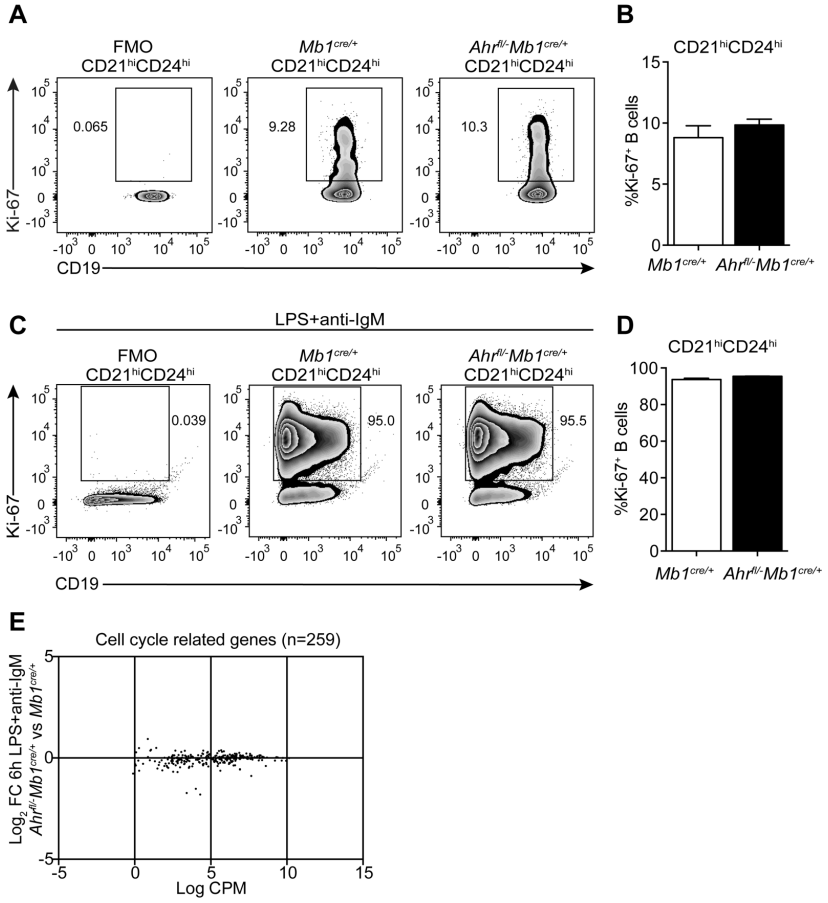

Figure 5.11. AHR does not affect the proliferation of CD19^{+}CD21^{hi}CD24^{hi} B cells in arthritic mice. (**A**) Representative flow cytometry plots and (**B**) bar graphs summarising Ki-67 expression in CD19^{+}CD21^{hi}CD24^{hi} B cells from *Mb1$^{cre/+}$* and *Ahr$^{fl/-}$Mb1$^{cre/+}$* mice *ex vivo* after day 7 AIA and (**C-D**) after 48h stimulation with LPS+anti-IgM (n=3). (**E**) Volcano plot (RNA-seq analysis) showing log_2 fold changes between 6h LPS+anti-IgM stimulated CD19^{+}CD21^{hi}CD24^{hi} B cells from *Ahr$^{fl/-}$Mb1$^{cre/+}$* versus *Mb1$^{cre/+}$* mice, plotted against average log counts per million (CPM; across all samples) for cell cycle related genes (n=259). All experiments were carried out at day 7 post IA-injection. All data representative of at least 2 independent experiments, with biological replicates. Figures **B and D**, data expressed as mean±sem. **B and D,** Mann-Whitney.

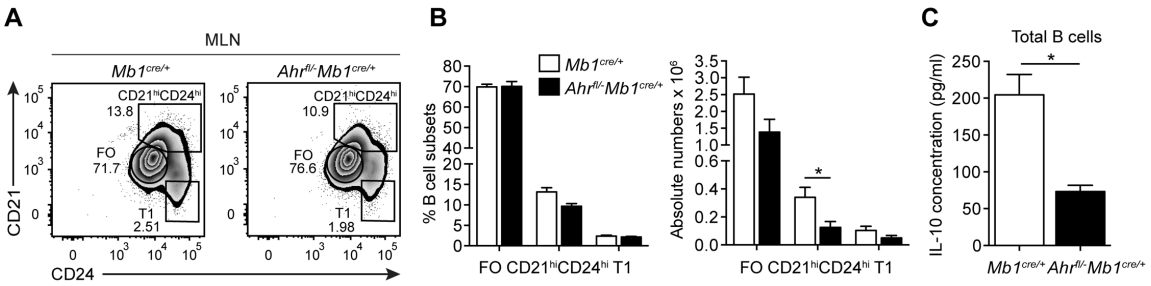

Figure 5.12 CD19^{+}CD21^{hi}CD24^{hi} B cells in *Ahr$^{fl/-}$Mb1$^{cre/+}$* mice are less able to differentiate into Bregs in the MLNs. AIA was induced in *Mb1$^{cre/+}$* and *Ahr$^{fl/-}$Mb1$^{cre/+}$* mice. (**A**) Representative flow cytometry plots showing percentage and (**B**) bar charts showing the percentages and absolute numbers of CD19^{+}CD21^{-}CD24^{hi} (T1), CD19^{+}CD21^{hi}CD24^{hi} and FO B cells in the MLNs of *Mb1$^{cre/+}$* and *Ahr$^{fl/-}$Mb1$^{cre/+}$* mice (n=7). (**C**) CD19^{+}B cells were sorted from *Mb1$^{cre/+}$* and *Ahr$^{fl/-}$Mb1$^{cre/+}$* mice and stimulated with LPS+anti-IgM for 48h. IL-10 production, as measured by ELISA (n=3). All experiments were performed at day 7 post IA-injection. Data representative of at least 2 independent experiments with biological replicates. Figures **B-C,** data are expressed as mean±sem. *p<0.05. **B,** two-way ANOVA; **C,** Mann-Whitney .

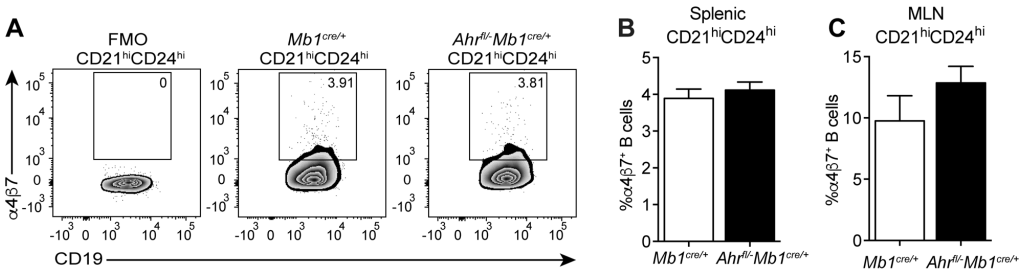

Figure 5.13. α4β7 is not differentially expressed between *Mb1*$^{cre/+}$ and *Ahr*$^{fl/-}$*Mb1*$^{cre/+}$ CD19^{+}CD21^{hi}CD24^{hi} B cells. (**A**) Representative flow cytometry plots of splenic α4β7 expression in CD19^{+}CD21^{hi}CD24^{hi} B cells from *Mb1*$^{cre/+}$ and *Ahr*$^{fl/-}$*Mb1*$^{cre/+}$ mice. **B-C,** Bar charts showing the frequencies of α4β7-expressing CD19^{+}CD21^{hi}CD24^{hi} B cells in the (**B**) spleen and (**C**) MLNs of *Mb1*$^{cre/+}$ and *Ahr*$^{fl/-}$*Mb1*$^{cre/+}$ mice (n=6). All experiments were carried out at day 7 post IA-injection. All data representative of at least 2 independent experiments, with biological replicates. Figures **B-C**, data expressed as mean±sem. **B-C,** Mann-Whitney.

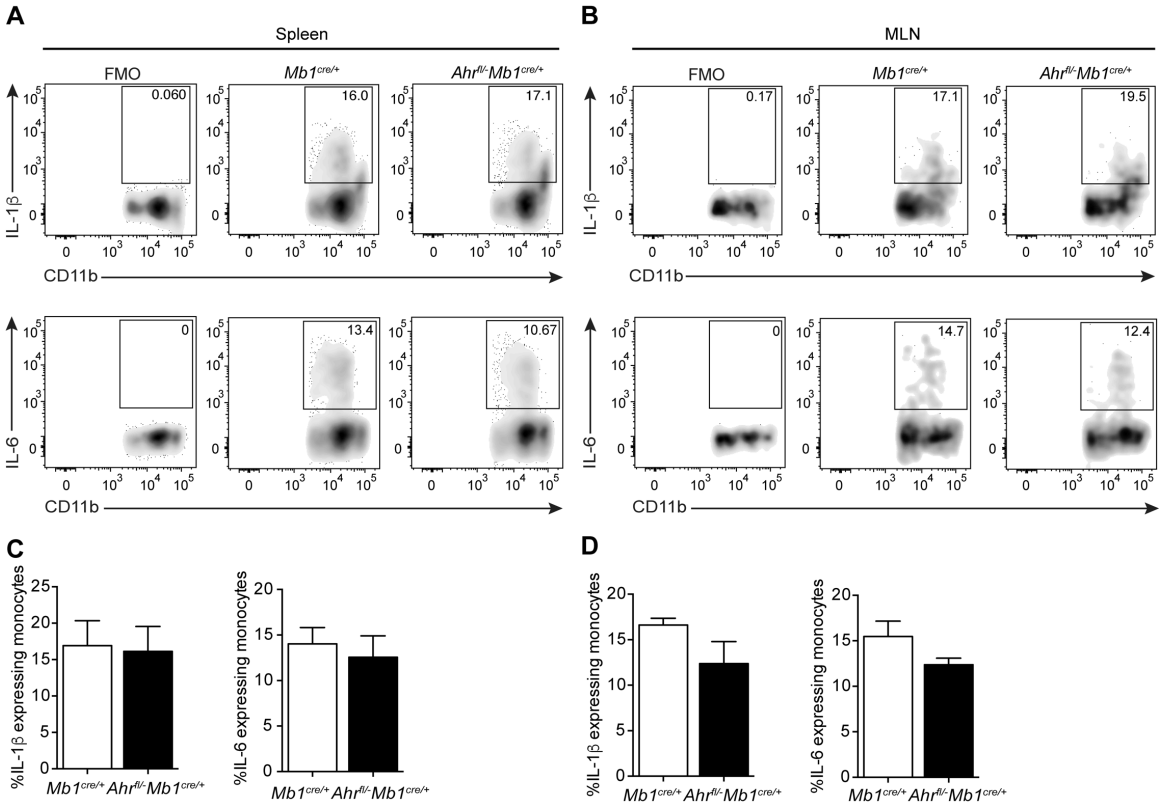

Figure 5.14. No difference in monocyte IL-1β and IL-6 expression is observed between *Mb1*$^{cre/+}$ and *Ahr*$^{fl/-}$*Mb1*$^{cre/+}$ mice. Total splenocytes or MLN cells were cultured for 6h with LPS. **A-D,** Representative flow cytometry plots and bar charts showing respectively the percentage of (**A,C**) splenic and (**B,D**) MLN IL-1β and IL-6-expressing monocytes (n=5). All data representative of at least 2 independent experiments with biological replicates. Figures **C-D,** data expressed as mean±sem. **C-D,** Mann Whitney.

5.3 AHR deficient CD19^{+}CD21^{hi}CD24^{hi} B cells are unable to differentiate into Bregs *in vivo*

To test if there was a defect in Breg differentiation *in vivo*, we followed the fate of adoptively transferred CD19^{+}CD21^{hi}CD24^{hi} B cells from WT and *Ahr*$^{-/-}$ mice into immunized CD45.1 recipient mice. An equal frequency of donor CD45.2^{+}CD19^{+}CD21^{hi}CD24^{hi} B cells from WT and *Ahr*$^{-/-}$ mice were identified 48 hours post-transfer. However, a significant decrease in the frequency of *Ahr*$^{-/-}$ CD45.2^{+}CD19^{+}CD21^{hi}CD24^{hi} B cells that differentiated into IL-10^{+} Bregs was observed when compared to WT CD45.2^{+}CD19^{+}CD21^{hi}CD24^{hi} B cells, indicating that B cell intrinsic AHR is required for the differentiation of IL-10^{+} Bregs *in vivo* (Figures 5.15A-D). One caveat of assaying B cells from *Ahr*$^{-/-}$ mice and then comparing it to WT mice is that the former develops exacerbated disease, which could influence the results due to the increase in inflammation. To demonstrate that the reduced frequency of IL-10 producing B cells was due to the lack of AHR and not a reflection of the pro-inflammatory environment from which the cells were isolated, we generated mixed bone-marrow chimeric mice, where lethally irradiated host mice were reconstituted with a 1:1 mixture of congenic CD45.1 WT and CD45.2 *Ahr*$^{-/-}$ bone marrow. We noted that CD45.2 *Ahr*$^{-/-}$ derived CD19^{+}CD21^{hi}CD24^{hi} B cells expressed significantly lower levels of IL-10 compared to WT-derived CD19^{+}CD21^{hi}CD24^{hi} B cells in the spleen of arthritic mice (Figures 5.15E-F). Our results demonstrate that AHR directly influences the differentiation of CD19^{+}CD21^{hi}CD24^{hi} B cells into IL-10^{+} Bregs *in vivo* and the defect in Breg differentiation is not a consequence of increased inflammation seen in *Ahr*$^{-/-}$ mice.

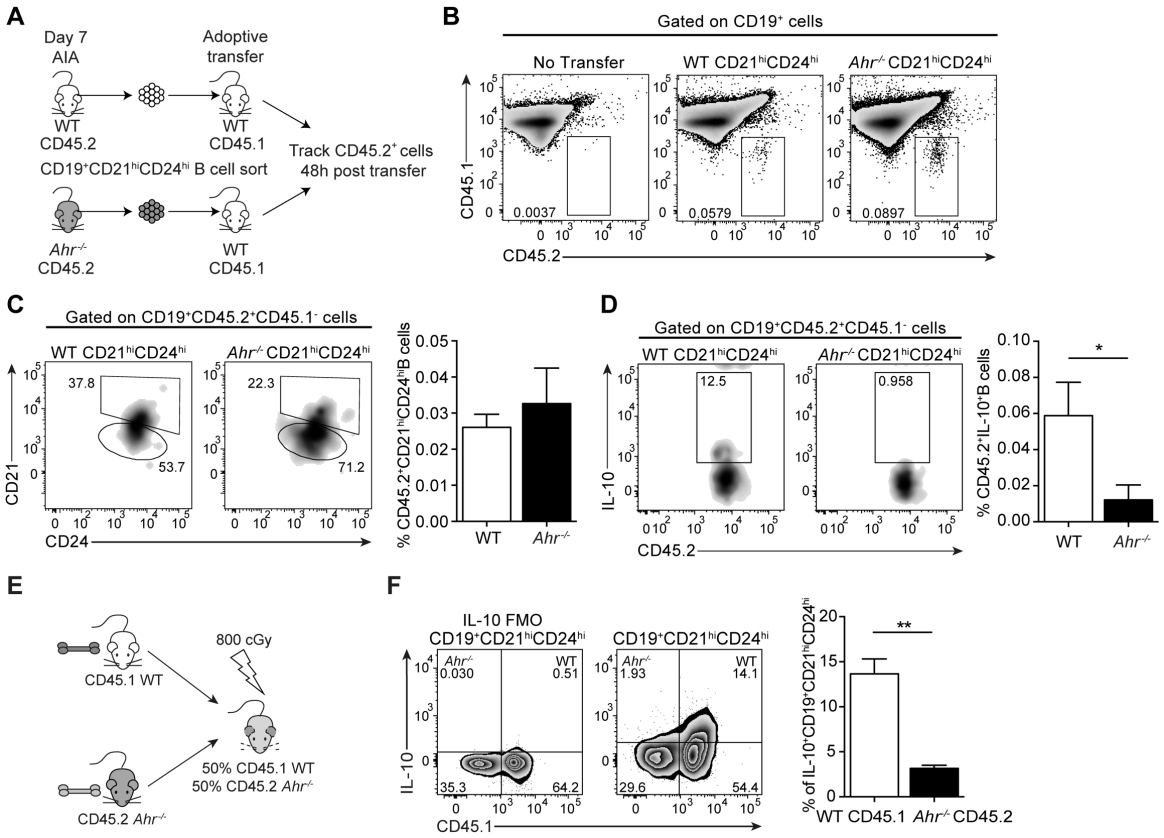

Figure 5.15. AHR is required for the differentiation of IL-10$^+$ Bregs *in vivo*. AIA was induced in WT and *Ahr*$^{-/-}$ mice. (**A**) Schematic showing the experimental design of the congenic adoptive transfer system. (**B**) Representative flow cytometry plots showing the frequency of adoptively transferred CD45.2$^+$ B cells from WT and *Ahr*$^{-/-}$ mice into CD45.1 recipient mice. (**C**) Representative flow cytometry plots and bar chart showing the frequency of CD45.2$^+$CD19$^+$CD21^{hi}CD24^{hi} B cells from WT and *Ahr*$^{-/-}$ mice. (**D**) Representative flow cytometry and bar chart showing the frequency of CD45.2$^+$IL-10$^+$ B cells from WT and *Ahr*$^{-/-}$ mice (n=4). (**E**) Schematic showing the experimental design of mixed bone marrow chimera reconstitution. (**F**) Representative flow cytometry plots and bar chart showing the percentages of IL-10$^+$CD19$^+$CD21^{hi}CD24^{hi} B cells in a mixed 50:50 bone marrow chimera of WT CD45.1 and *Ahr*$^{-/-}$ CD45.2 cells (n=5). All experiments were performed at day 7 post IA-injection. Data representative of at 2 independent experiments with biological replicates. Figures **C-D and F,** data are expressed as mean±sem. *p<0.05, **p<0.01. **C, D and F,** Mann-Whitney. Experiments performed in collaboration with Elizabeth Rosser.

Chapter VI: Results IV

The results in this chapter were carried out in collaboration with Elizabeth Rosser and form part of a manuscript, which is included here in Appendix V[697]. Due to the collaborative nature of the experiments I helped process the samples and jointly run the flow cytometry samples. Due to my specialty in AHR, my contribution was geared towards the experiments performed around AHR and the molecular biology side of the project (PCR's, western blot, RNA-seq and ATAC-seq analysis) and I carried out the breeding and maintenance of the AHR strains. 16s rDNA sequencing was carried out by Nigel Klein (Institute of Child Health, UCL). Michael Orford and Simon Eaton (Institute of Child Health, UCL) performed HPLC assay design and analysis. Where experiments were performed in collaboration, the respective authors are indicated in the figure legends.

We have so far shown that AHR controls Breg differentiation and function by directly regulating IL-10 expression and by suppressing a pro-inflammatory programme in $CD19^{+}CD21^{hi}CD24^{hi}$ B cells, after activation with inflammatory stimuli. The endogenous ligands of AHR in B cells remain poorly characterised. Given the abundance of dietary AHR ligands found in the gut[698] and that we have previously shown that inflammatory signals in the gut-associated lymphoid tissue (GALT), promote the suppressive function and differentiation of Bregs[323], we aimed to investigate whether signals through AHR from gut derived metabolites can drive Breg differentiation.

As discussed in the introduction, the microbiota-derived SCFAs are a potent class of immune-modulatory compounds with the capacity to modulate Treg, Th17 cells, and macrophage differentiation in the gut and periphery[647, 650, 699]. We show here that supplementing mice with butyrate can suppress arthritis severity and this is dependent on having fully functional Bregs. Moreover, we show that butyrate inhibits the differentiation of GC B cells and plasma cells, whilst maintaining Breg numbers and promoting the suppressive function of Bregs.

It has previously been described that butyrate acts as an AHR ligand in an intestinal epithelial cell line[561]. Therefore, we aimed to investigate whether the suppression of arthritis by butyrate supplementation was a consequence of signals through AHR. We show that the suppression of arthritis by butyrate is dependent on the

expression of AHR by B cells. Addition of butyrate to AHR-sufficient *Mb1*$^{cre/+}$ mice inhibited B cell maturation, whilst also promoting the differentiation of CD19^{+}CD21^{hi}CD24^{hi} B cells into IL-10^{+}Bregs *in vivo*. Analysis of the transcriptional and epigenetic profiles of *Mb1*$^{cre/+}$ and *Ahr*$^{fl/-}$*Mb1*$^{cre/+}$ CD19^{+}CD21^{hi}CD24^{hi} B cells revealed that butyrate downregulated the expression of several key transcription factors required for B cell differentiation, including *Bcl6* and *Prdm1*, in an AHR-dependent manner. We validated these findings *in vivo* by congenic transfer of *WT* and *Ahr*$^{-/-}$ CD19^{+}CD21^{hi}CD24^{hi} B cells into WT recipient mice. These data revealed that CD19^{+}CD21^{hi}CD24^{hi} B cells from butyrate treated WT mice readily differentiated into IL-10^{+} Bregs *in vivo* compared to the control-treated WT counterparts. Butyrate did not control the differentiation of Bregs in the absence of AHR, suggesting that AHR was needed for butyrate to enhance Breg differentiation.

We rule out butyrate as a direct ligand of AHR, instead showing that butyrate alters the gut microflora composition to favour the growth of bacterial genera, which promote the metabolism of tryptophan to the serotonin metabolite 5-HIAA. Lastly, we demonstrate that supplementation with 5-HIAA suppresses arthritis, only in B cell AHR-sufficient *Mb1*$^{cre/+}$ mice and show that 5-HIAA is a direct ligand of AHR. Thus collectively, these results highlight that butyrate increases the availability of the AHR ligand 5-HIAA, which in turn activates AHR and promotes Breg mediated suppression of arthritis.

6.1 Butyrate supplementation suppression of experimental arthritis Is Breg dependent

We have recently shown that low-grade inflammatory signals that drive the differentiation of immature B cells into Bregs are provided in the gut-associated lymphoid tissue (GALT) as a result of the interaction between the gut microbiota and the innate immune system[323]. The question of whether inflammatory signals produced in response to the microbiota control Breg development alone or whether microbial factors also play a direct role remains unanswered. Among different gut-microbiota-derived metabolites, the most well-characterized are the end products of dietary fibre fermentation, the short-chain fatty acids (SCFAs). To investigate how the levels of butyrate change during the course of arthritis, we utilized the antigen-induced model of arthritis (AIA) and measured stool levels of butyrate, pre-arthritis and during the acute and remission phases of arthritis. We found that butyrate levels were reduced during the acute and remission phases of arthritis compared to pre-arthritic mice (Figure 6.1A). These results suggest that the observed defect in butyrate production in arthritic mice, once established, cannot be reversed in spite of the reduced inflammation observed during disease remission. In line with reduced SCFAs, the bacterial families *Lactobacillaceae*, *Rikenellaceae*, and *Bacteroidaceae* were reduced in the stool of arthritic mice compared to naive mice (Figure 6.1B). Members of these bacterial families form a common functional group of bacteria that metabolize non-digestible carbohydrates into the immunogenic SCFA[700]. Conversely, we detected an increase in *Desulfovibrionaceae*, *Deferribacteraceae*, *Sutterellaceae*, and *Prevotellaceae* families in the stool of arthritic versus naive mice (Figure 6.1B).

Previously published research has demonstrated that supplementation with SCFAs, and in particular butyrate, has an immunosuppressive effect in diseases including diabetes and colitis[660, 701]. To evaluate the contribution of butyrate in controlling the severity of arthritis and to determine the possible role of B cells in mediating suppression, butyrate was supplemented in the drinking water of wild-type (WT) mice and B-cell-deficient (μMT) mice prior to disease induction. Control mice for both genotypes received drinking water that was salt and pH balanced (hereafter referred to as the control group). Supplementation with butyrate reduced arthritis in WT mice compared to control mice (Figure 6.1C). Butyrate supplementation failed to suppress disease in B-cell-deficient mice (μMT) (Figure

6.1C), demonstrating that under these experimental conditions, B cells are key in mediating the beneficial effects of butyrate supplementation. Furthermore, butyrate supplementation failed to suppress disease in mixed bone marrow chimeric mice lacking IL-10-producing B cells (Figure 6.1D), pinpointing the requirement of Bregs in the butyrate-mediated suppression of arthritis.

To investigate the effect of butyrate supplementation on both pro-arthritogenic cells and Bregs, we next took advantage of IL-10eGFP reporter mice, allowing the visualization of B cells actively transcribing IL-10[372]. Amelioration of disease in butyrate-supplemented IL-10eGFP reporter mice was similar to WT mice (Figures 6.1E-F respectively showing clinical score and histological changes of the joints). We next assessed the effect of butyrate supplementation on the differentiation of Bregs, identified here as IL-10eGFP^{+}CD19^{+}CD21^{hi}CD24^{hi} B cells[702]. We found that IL10eGFP^{+}CD19^{+}CD21^{hi}CD24^{hi} Breg number and frequency were similar between butyrate-supplemented and control mice (Figure 6.2A). There was no difference in the frequency and/or number of splenic follicular (FO) B cells, transitional-1 (T1) B cells, or total CD19^{+}CD21^{hi}CD24^{hi} B cells (Figures 6.2B-E). However, there was a significant reduction of CD19^{+}CD138^{+}BLIMP-1^{+} plasmablast and CD19^{+}CD95^{+}GL7^{+} GC B cell frequency and number between butyrate-supplemented and control mice (Figures 6.3A+C). Blinded histological analyses further confirmed a reduction in the number of GCs per B cell follicle and in the size of GCs in the spleens of butyrate-supplemented versus control mice (Figure 6.3E). Thus, butyrate supplementation had increased the ratio of IL-10eGFP^{+}CD19^{+}CD21^{hi}CD24^{hi} Bregs to plasmablasts and IL-10eGFP^{+}CD19^{+}CD21^{hi}CD24^{hi} Bregs to GC B cells compared to control mice (Figures 6.3B+D).

To determine whether butyrate supplementation affects the immunosuppressive function of Bregs, an equal number of IL-10eGFP^{+}CD19^{+}CD21^{hi}CD24^{hi} Bregs was isolated from butyrate-supplemented or control IL-10eGFP reporter mice and transferred into syngeneic arthritic hosts. IL-10eGFP^{+}CD19^{+}CD21^{hi}CD24^{hi} Bregs from butyrate-supplemented mice displayed enhanced suppressive capacity upon adoptive transfer compared to IL-10eGFP^{+}CD19^{+}CD21^{hi}CD24^{hi} Bregs from control mice (Figure 6.3F). These results demonstrated that butyrate supplementation

concurrently increases Breg suppressive capacity and limits GC B cell and plasmablast differentiation.

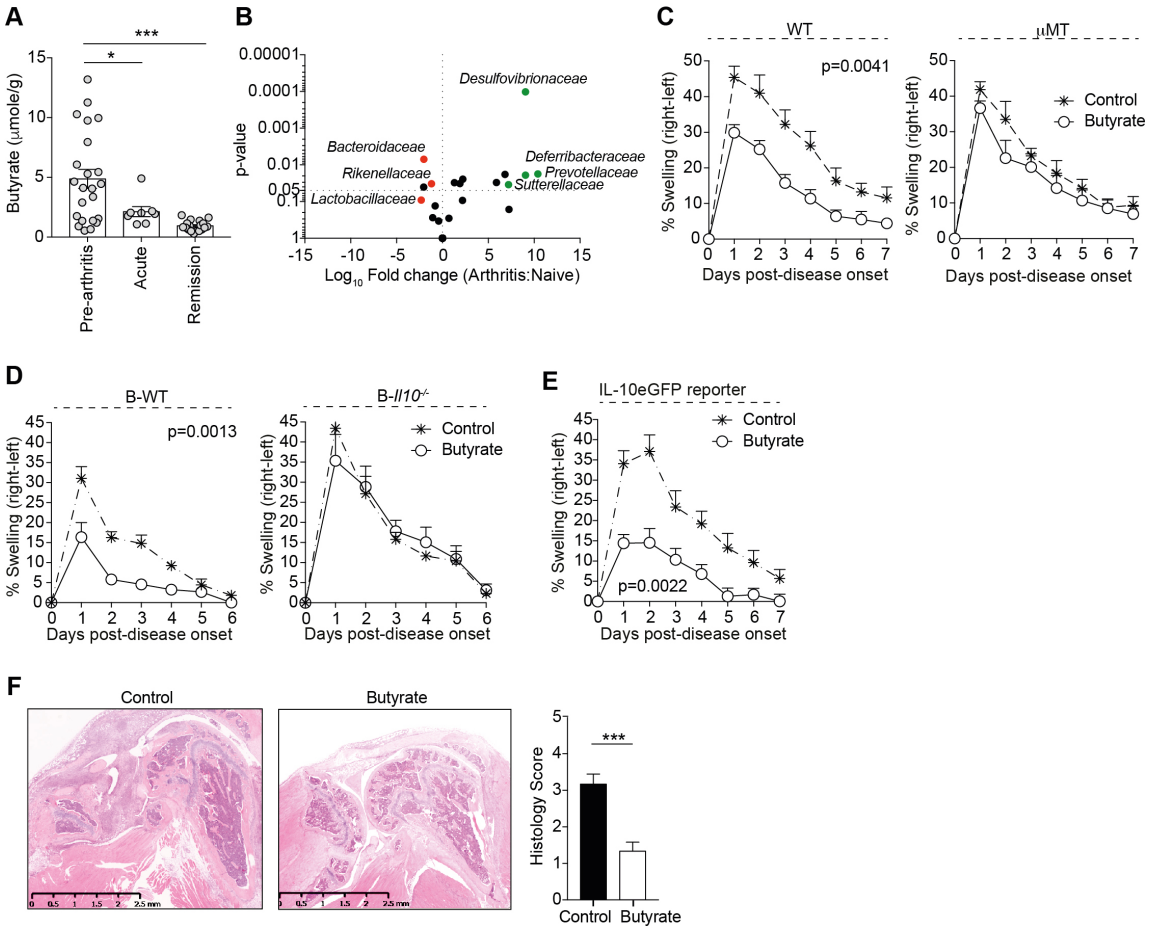

Figure 6.1. Suppression of arthritis by butyrate supplementation requires IL-10-expressing B cells. (**A**) Stool butyrate levels in WT mice pre-arthritis (n=23), with acute arthritis (n=8), and in remission from arthritis (n=18) as measured by high-performance liquid chromatography (cumulative data are shown). (**B**) Volcano plot shows fold change between bacterial families in the faeces of naïve mice compared to arthritic mice at day 3 post-disease onset (n=4 per group). (**C**) Mean clinical score of control (cumulative n=25) and butyrate-supplemented WT mice (cumulative n=24) (one representative experiment of six experiments is shown) or μMT mice (control, cumulative n=7; butyrate, cumulative n=9). (**D**) Mean clinical score of control (cumulative n=25) and butyrate-supplemented B-WT chimeric mice or B-*Il10*$^{-/-}$chimeric mice (n=8 per group) (one representative experiment of two experiments is shown); y axis shows percentage swelling in antigen-injected knee compared to control knee. (**E**) Mean clinical score of control (cumulative n=15) and butyrate-supplemented IL-10eGFP reporter mice (cumulative n=13); y axis shows percentage swelling in antigen-injected knee compared to control knee (one representative experiment of two experiments is shown). (**F**) Representative H&E staining of knee joints from control and butyrate-supplemented IL-10eGFP reporter mice (left) and blinded histology scores (right) of joint damage. Figures **A and C-F,** data are expressed as mean±sem. **p*<0.05, ***p*<0.01, ****p*<0.001. **A,** one-way ANOVA; **B-E,** two-way ANOVA; **F,** Student's t test.

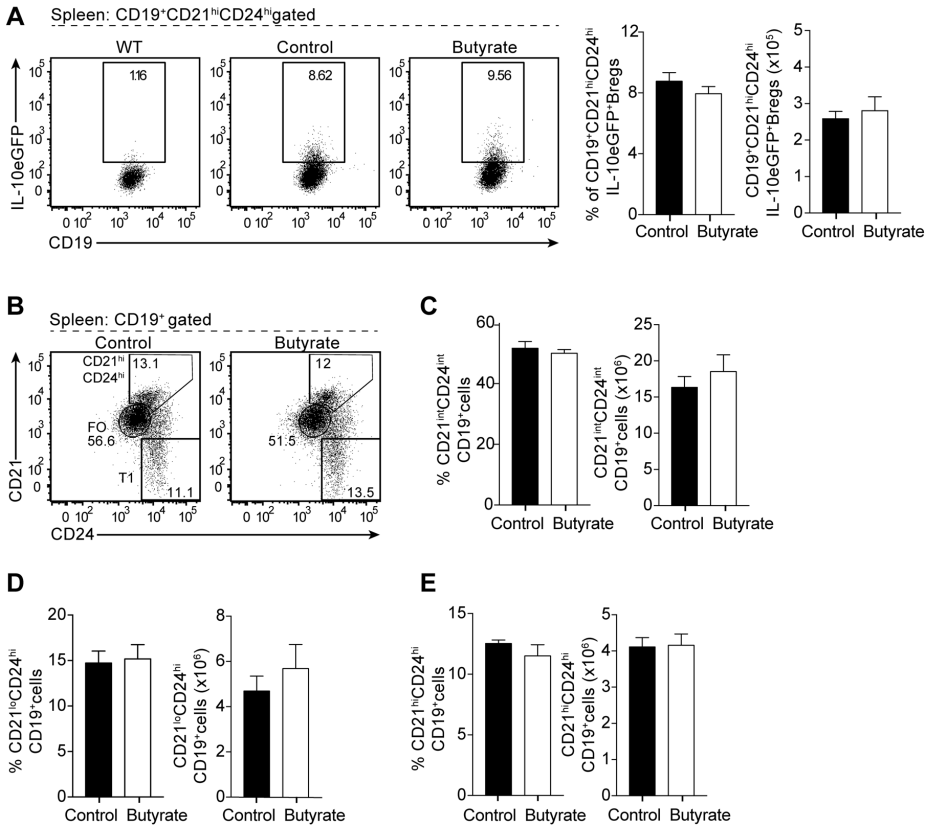

Figure 6.2. The number of IL-10^{+}CD19^{+}CD21^{hi}CD24^{hi}Bregs is maintained following butyrate supplementation. (**A**) Representative flow cytometry plots (left) and bar charts (right) showing CD19^{+}CD21^{hi}CD24^{hi}IL-10eGFP^{+} Breg frequency and number in control (cumulative n=15) and butyrate-supplemented mice (cumulative n=13) (one representative experiment of three experiments is shown). (**B**) Representative plots showing the percentage of CD19^{+}CD21^{int}CD24^{int} (FO) B cells, CD19^{+}CD21^{lo}CD24^{hi} (T1) B cells, and CD19^{+}CD21^{hi}CD24^{hi} B cells in the spleen at day 7 post-disease onset. Bar charts showing the percentage and number of (**C**) CD19^{+}CD21^{int}CD24^{int} B cells, (**D**) CD19^{+}CD21^{lo}CD24^{hi} B cells, and (**E**) CD19^{+}CD21^{hi}CD24^{hi} B cells. (Control, cumulative n=15; Butyrate cumulative n=13; one representative experiment of three experiments is shown. Figures **A-E,** data are expressed as mean±sem. **A-E,** Student's t test.

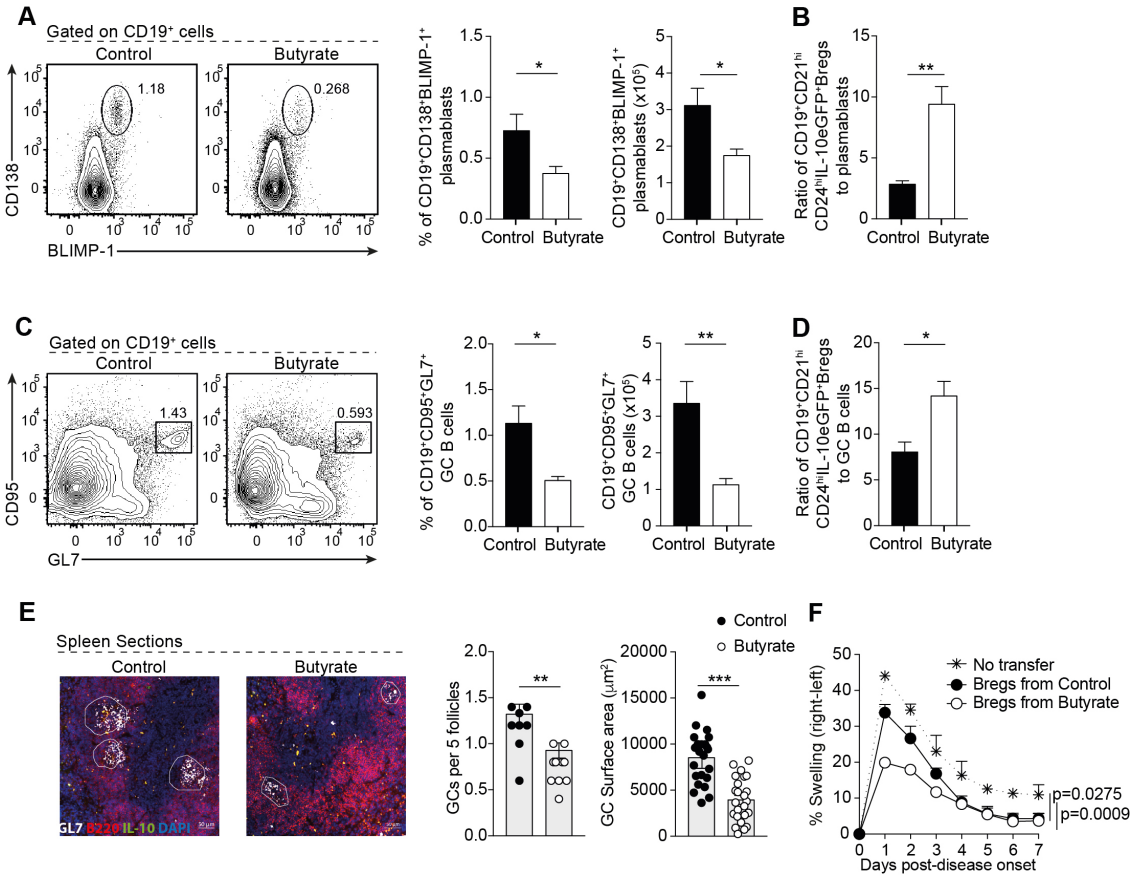

Figure 6.3. Butyrate suppresses the numbers of plasmablasts and GC B cells. (**A**) Representative flow cytometry plots (left) and bar charts (right) showing $CD19^+CD138^+BLIMP\text{-}1^+$ plasmablast frequency and number in control and butyrate-supplemented mice (cumulative n=11 per group, one representative experiment of two experiments is shown). (**B**) Bar chart showing the ratio of $CD19^+CD21^{hi}CD24^{hi}IL\text{-}10eGFP^+$ Bregs to plasmablasts in control and butyrate-supplemented mice (cumulative n=11 per group, one representative experiment of two experiments is shown). (**C**) Representative flow cytometry plots (left) and bar chart (right) shows the percentage and number of $CD19^+CD95^+GL7^+$ germinal center (GC) B cells in control and butyrate-supplemented mice (cumulative n=11 per group, one representative experiment of three experiments is shown). (**D**) Bar chart shows ratio of $CD19^+CD21^{hi}CD24^{hi}IL\text{-}10eGFP^+$ Bregs to GC B cells in control and butyrate-supplemented mice (cumulative n=11, one representative experiment of two experiments is shown). (**E**) Representative immunofluorescence blinded histological analysis of the number and size of GC control and butyrate-supplemented mice (original magnification 203, n=3). (**F**) Mean clinical score following transfer of $CD19^+CD21^{hi}CD24^{hi}IL\text{-}10eGFP^+$ Bregs from control (cumulative n=6) or butyrate-supplemented mice (cumulative n=6), a control group that did not receive a transfer; y axis shows percentage swelling in antigen-injected knee compared to control knee (cumulative n=8) (one representative experiment of two experiments is shown). Cells were isolated at day 7 post-disease onset. Figures **A-F,** data are expressed as mean±sem. *p<0.05, **p<0.01, ***p<0.001. **A-E,** Student's t test; **F,** two-way ANOVA.

6.2 Suppression of disease by butyrate supplementation requires B cell expression of AHR

We have demonstrated that there is higher expression of AHR in IL-10eGFP^{+}CD19^{+}CD21^{hi}CD24^{hi} Bregs and that activation of AHR contributes to the induction of a transcriptional program that controls IL-10^{+}CD19^{+}CD21^{hi}CD24^{hi} Breg suppressive function. These data, taken together with our previous findings demonstrating that butyrate suppresses arthritis by enhancing Breg function, led us to hypothesise that butyrate required AHR for its immunomodulatory role in arthritis. In line with this hypothesis, the expression of *Cyp1a1*, a prototypical reporter gene of AHR activation, was significantly upregulated in B cells isolated from butyrate-supplemented mice compared to control mice (Figure 6.4A). To confirm a role for AHR in the immunomodulatory effect of butyrate supplementation on the B cell compartment and arthritis severity, we supplemented *Ahr$^{fl/-}$Mb1$^{cre/+}$* and *Mb1$^{cre/+}$* mice with butyrate and assessed arthritis severity. Butyrate supplementation suppressed arthritis severity and IL-17^{+}CD4^{+} T cell frequency only in AHR-sufficient *Mb1$^{cre/+}$* mice but not in *Ahr$^{fl/-}$Mb1$^{cre/+}$* mice (Figures 6.4B-C). Confirming the results from the previous chapters, B cells from *Ahr$^{fl/-}$Mb1$^{cre/+}$* mice released less IL-10 compared to those isolated from *Mb1$^{cre/+}$* mice. Whilst butyrate maintained IL-10 production in B cells from *Mb1$^{cre/+}$* mice, butyrate supplementation further decreased IL-10 production in B cells from *Ahr$^{fl/-}$Mb1$^{cre/+}$* mice (Figure 6.5A).

Butyrate supplementation did not alter CD19^{+}CD21^{hi}CD24^{hi} B cell frequency or number in *Mb1$^{cre/+}$* or *Ahr$^{fl/-}$Mb1$^{cre/+}$* mice compared to control groups (Figure 6.5B). Butyrate supplementation reduced CD19^{+}CD138^{+}BLIMP-1^{+} plasmablast and CD19^{+}CD95^{+}GL7^{+} GC B cell frequency and number in *Mb1$^{cre/+}$* mice, but failed to suppress CD19^{+}CD138^{+}BLIMP-1^{+} plasmablast and CD19^{+}CD95^{+}GL7^{+} GC B cell frequency and number in *Ahrfl/-Mb1$^{cre/+}$* mice (Figures 6.5C-D). Although Treg frequency and number were unaffected by butyrate supplementation (Figures 6.6A-B), CD4^{+}CD25^{+} Tregs isolated from butyrate-supplemented *Mb1$^{cre/+}$* mice displayed enhanced suppressive capacity upon adoptive transfer into WT mice (Figure 6.6C). In contrast, Tregs isolated from both control and butyrate-supplemented *Ahr$^{fl/-}$Mb1$^{cre/+}$* mice failed to suppress disease on adoptive transfer (Figure 6.6C). As inflammation is a driver of Breg differentiation and function, and because *Ahr$^{fl/-}$Mb1$^{cre/+}$* mice develop an exacerbated arthritic inflammation

compared to *Mb1*$^{cre/+}$ mice, we next tested the effect of butyrate supplementation in chimeric mice reconstituted with a 1:1 mix of bone marrow cells from CD45.1 WT and CD45.2 *Ahr*$^{-/-}$ mice (Figure 6.7A). Under these conditions, WT and *Ahr*$^{-/-}$ B cells are exposed to identical inflammatory signals following arthritis induction. The frequency and number of WT CD45.1^{+}CD45.2^{-}IL-10^{+}CD19^{+}CD21^{hi}CD24^{hi} Bregs was unaffected by butyrate supplementation, whereas *Ahr*$^{-/-}$CD45.1^{-} CD45.2^{+}CD19^{+}CD21^{hi}CD24^{hi} B cells failed to differentiate into IL-10^{+}CD19^{+}CD21^{hi}CD24^{hi} Bregs in both control and butyrate-supplemented mice (Figure 6.7B). In addition, butyrate supplementation reduced the frequency and number of plasmablasts and GC B cells within CD45.1 WT-derived cells but not in CD45.2 *Ahr*$^{-/-}$ derived cells (Figures 6.7C-D).

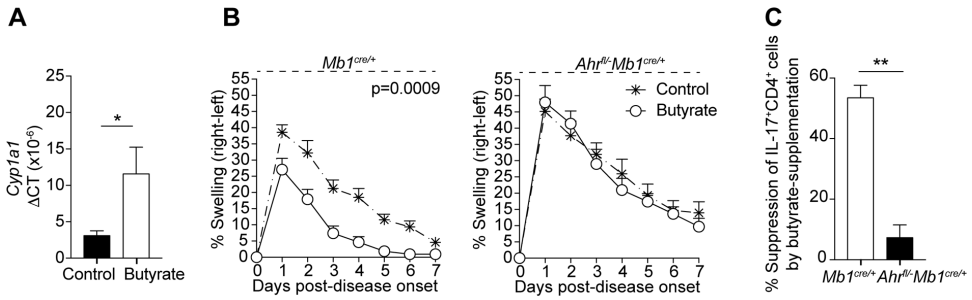

Figure 6.4. Suppression of arthritis by butyrate supplementation depends upon AHR expression in B cells. (**A**) Bar chart shows expression of *Cyp1a1* relative to *β-actin* in splenic B cells isolated from control or butyrate-supplemented mice (cumulative n=5, one representative experiment of two experiments is shown). (**B**) Mean clinical score of control and butyrate-supplemented $Mb1^{cre/+}$ mice or $Ahr^{fl/-}Mb1^{cre/+}$ mice; y axis shows percentage swelling in antigen-injected knee compared to control knee (cumulative n=15 per group, one representative experiment of five experiments is shown). (**C**) Bar chart showing the suppression of IL-$17^{+}CD4^{+}$ T cells in $Mb1^{cre/+}$ mice or $Ahr^{fl/-}Mb1^{cre/+}$ mice that received butyrate-supplementation compared to control $Mb1^{cre/+}$ mice or $Ahr^{fl/-}Mb1^{cre/+}$ mice (cumulative n=6 per group, one representative experiment of two experiments is shown). Figures **A-C,** data are expressed as mean±sem. *p<0.05. **A and C,** Student's t test; **B,** two-way ANOVA.

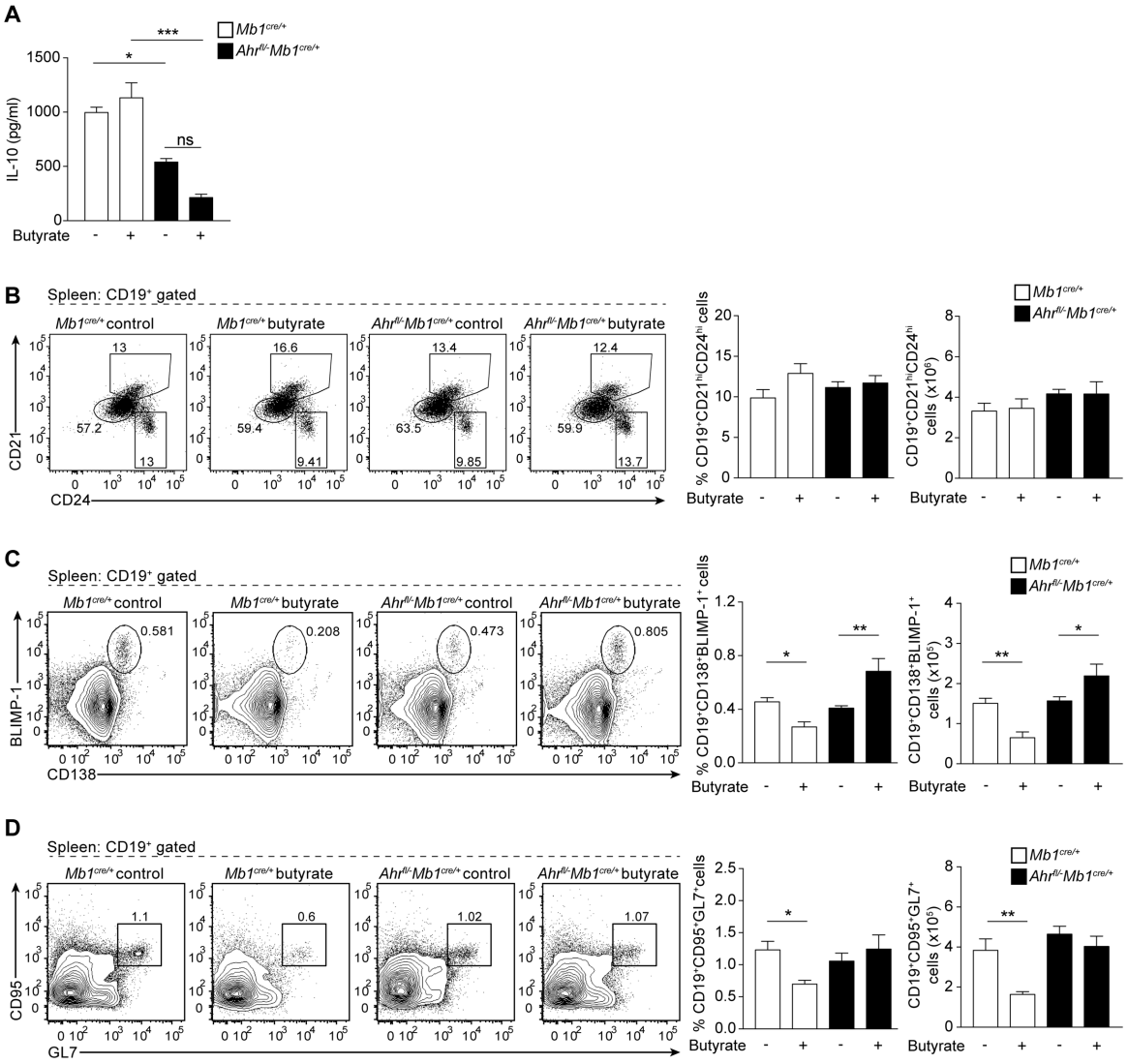

Figure 6.5. Butyrate suppresses plasmablast and GC differentiation whilst maintaining Bregs in an AHR dependent mechanism. (**A**) IL-10 production by splenic B cells isolated from control *Mb1*$^{cre/+}$ mice, butyrate-supplemented *Mb1*$^{cre/+}$ mice, control *Ahr*$^{fl/-}$*Mb1*$^{cre/+}$ mice, and butyrate-supplemented *Ahr*$^{fl/-}$*Mb1*$^{cre/+}$ mice at day 7 post-disease onset as measured by ELISA (n=3 per group). (**B**) Representative flow cytometry plots and bar charts showing the frequency and number of CD19^{+}CD21^{hi}CD24^{hi} B cells in control *Mb1*$^{cre/+}$ mice (cumulative n=8), butyrate-supplemented *Mb1*$^{cre/+}$ mice (cumulative n=5), control *Ahr*$^{fl/-}$*Mb1*$^{cre/+}$ mice (n=7), and butyrate-supplemented *Ahr*$^{fl/-}$*Mb1*$^{cre/+}$ mice (cumulative n=6) at day 7 post-disease onset (cumulative data are shown). (**C**) Representative flow cytometry plots and bar charts showing the frequency and number of CD19^{+}CD138^{+}BLIMP-1^{+} B cells in control *Mb1*$^{cre/+}$ mice (cumulative n=8), butyrate-supplemented *Mb1*$^{cre/+}$ mice (cumulative n=5), control *Ahr*$^{fl/-}$*Mb1*$^{cre/+}$ mice (cumulative n=7), and butyrate-supplemented *Ahr*$^{fl/-}$*Mb1*$^{cre/+}$ mice (cumulative n=6) (cumulative data are shown). (**D**) Representative flow cytometry plots and bar charts showing the frequency and number of CD19^{+}CD95^{+}GL7^{+} B cells in control *Mb1*$^{cre/+}$ mice (cumulative n=8), butyrate-supplemented *Mb1*$^{cre/+}$ mice (cumulative n=5), control *Ahr*$^{fl/-}$*Mb1*$^{cre/+}$ mice (cumulative n=7), and butyrate-supplemented *Ahr*$^{fl/-}$*Mb1*$^{cre/+}$ mice (cumulative n=6) (cumulative data are shown). Cells were isolated at day 7 post-disease onset. Figures **A-D,** data are expressed as mean±sem. *p<0.05, **p<0.01, ***p<0.001. **A-D,** one-way ANOVA.

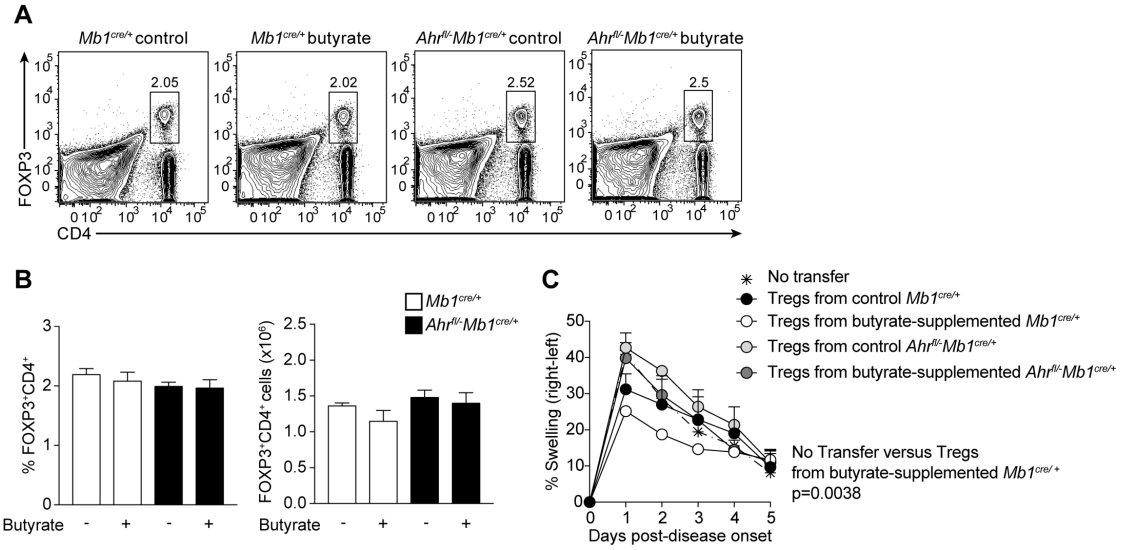

Figure 6.6. Expression of AHR in B cells is fundamental for modulation of T cell function after butyrate-supplementation. (**A**) Representative plots (**B**) and bar charts showing the percentage and number of FOXP3^{+}CD4^{+} T cells in *Mb1*$^{cre/+}$ or *Ahr*$^{fl/-}$*Mb1*$^{cre/+}$ mice that received butyrate-supplementation (n=6 and n=7 respectively) compared to control *Mb1*$^{cre/+}$ or *Ahr*$^{fl/-}$*Mb1*$^{cre/+}$ mice (n=8 and n=9 respectively) cumulative data are shown). (**C**) Mean clinical score following transfer of Tregs from control or butyrate supplemented *Mb1*$^{cre/+}$ and control or butyrate supplemented *Ahr*$^{fl/-}$*Mb1*$^{cre/+}$, a control group that did not receive transfer; y axis shows percentage swelling in antigen-injected knee compared to control knee (n=3 per group). Figures **B-C,** data are expressed as mean±sem. **B,** one-way ANOVA; **C,** two-way ANOVA.

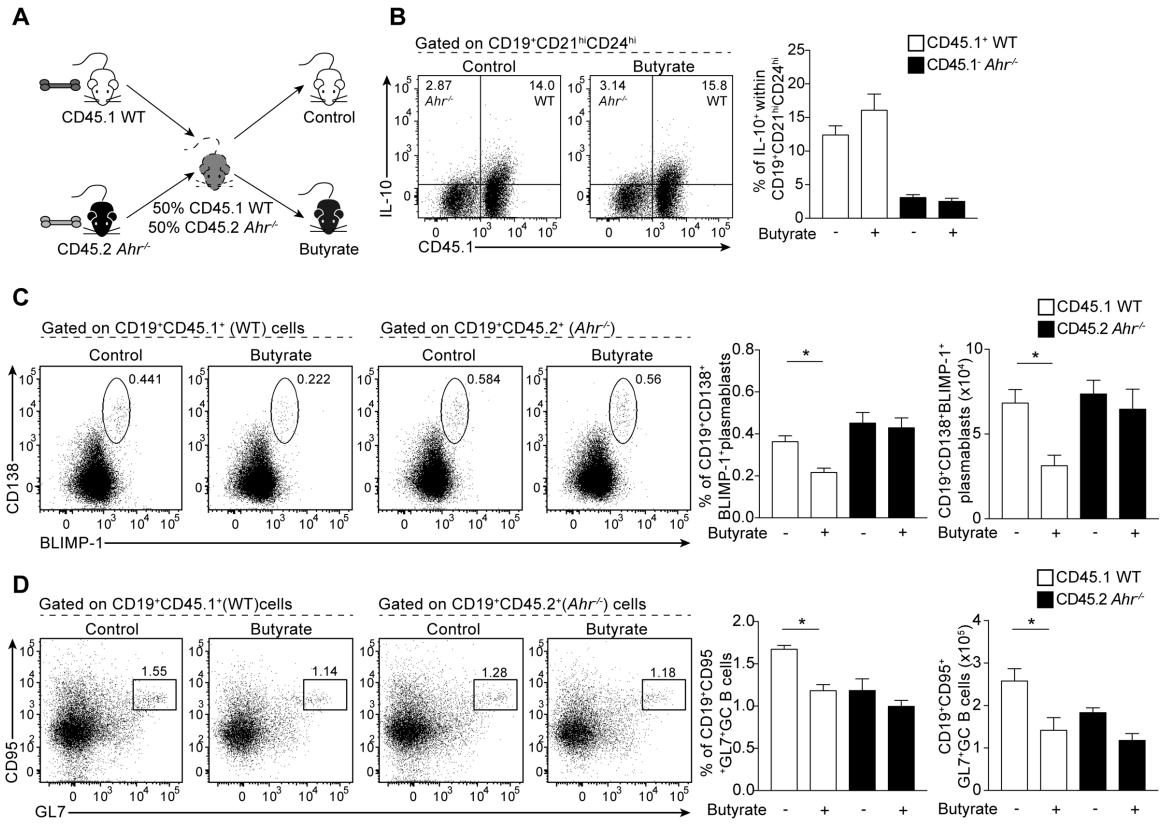

Figure 6.7. Butyrate-supplementation suppresses B cell maturation through activation of AHR. (**A**) Schematic showing experimental design for competitive congenic bone marrow chimeric experiment. (**B**) Representative flow cytometry plots (left) and bar charts (right) showing the frequency and number of CD45.1$^+$ IL-10$^+$CD21^{hi}CD24^{hi} B cells or CD45.1$^-$IL-10$^+$CD21^{hi}CD24^{hi} B cells in butyrate-supplemented or control chimeric mice (cumulative n=4 per group). (**C**) Representative flow cytometry plots (left) and bar charts showing the frequency and number of plasmablasts within CD45.1$^+$WT or CD45.2$^+$*Ahr*$^{-/-}$ derived cells in butyrate-supplemented or control chimeric mice (cumulative n=4 per group). (**D**) Representative flow cytometry plots (left) and bar charts (right) showing the frequency and number of GC B cells within CD45.1$^+$WT or CD45.2$^+$*Ahr*$^{-/-}$ derived cells in butyrate-supplemented or control chimeric mice (cumulative n=4 per group). Figures **B-D,** data are expressed as mean±sem. *p<0.05. **B-D,** one-way ANOVA.

6.3 Butyrate supplementation supports Breg suppressive function and controls B cell differentiation partly via an AHR-dependent transcriptional programme

To understand how butyrate supports Breg suppressive function and suppresses GC B cell and plasmablast differentiation, we compared the gene expression profiles and chromatin accessibility of $CD19^{+}CD21^{hi}CD24^{hi}$ B cells isolated from butyrate-supplemented and control $Mb1^{cre/+}$ and $Ahr^{fl/-}Mb1^{cre/+}$ mice. There were 412 significant differentially expressed genes (DEGs) between control and butyrate-supplemented $Mb1^{cre/+}$ $CD19^{+}CD21^{hi}CD24^{hi}$ B cells (Figure 6.8A). There were more changes (566 significant DEGs) in butyrate-supplemented versus control $Ahr^{fl/-}Mb1^{cre/+}$ $CD19^{+}CD21^{hi}CD24^{hi}$ B cells. This suggests that, as well as being necessary to mediate some of butyrate's effects on gene expression, AHR also modulates the expression of a number of genes that would otherwise be altered by butyrate treatment (Figure 6.8A). Signaling pathway impact analysis (SPIA) revealed that the ''protein processing in the endoplasmic reticulum'' pathway, previously associated with the differentiation of B cells into plasma cells[703], was significantly downregulated by butyrate supplementation in $Mb1^{cre/+}$ $CD19^{+}CD21^{hi}CD24^{hi}$ B cells and significantly upregulated in $Ahr^{fl/-}Mb1^{cre/+}$ $CD19^{+}CD21^{hi}CD24^{hi}$ B cells (Figure 6.8B). Based on this observation, we interrogated DEGs in the B cell differentiation Gene Ontology term (GO:0030183) and compared the effect of butyrate supplementation on gene expression in both genotypes. B cell lymphoma 6 protein (BCL6), a master regulator of GC B cell differentiation, and the orphan G protein-coupled receptor (GPR183), important in extrafollicular plasmablast differentiation[192], were among the genes reduced in $CD19^{+}CD21^{hi}CD24^{hi}$ B cells from $Mb1^{cre/+}$ mice compared to $Ahr^{fl/-}Mb1^{cre/+}$ mice after butyrate supplementation (Figure 6.8C). Conversely, the expression of ID2, a negative regulator of B cell maturation[704], was upregulated in $CD19^{+}CD21^{hi}CD24^{hi}$ B cells from $Mb1^{cre/+}$ mice, but not from $Ahr^{fl/-}Mb1^{cre/+}$ mice after butyrate supplementation (Figure 6.8C). To investigate whether there was an AHR-independent mechanism in the Breg-mediated regulation of arthritis by butyrate supplementation, we performed a four-way comparison analysis among all the groups (Figure 6.8D). This analysis also highlights the baseline transcriptional changes between control $Mb1^{cre/+}$ versus $Ahr^{fl/-}Mb1^{cre/+}$ mice. We found that 71 significantly DEGs were regulated in both $Mb1^{cre/+}$ versus $Ahr^{fl/-}Mb1^{cre/+}$ mice by butyrate supplementation (Figure 6.5D; Appendix II). There were 195 significantly

DEGs observed only in *Mb1*$^{cre/+}$ mice but not *Ahr*$^{fl/-}$*Mb1*$^{cre/+}$ mice following butyrate supplementation after genotype confounding genes had been removed; the majority of these genes were structural proteins (Figure 6.8D; Appendix III).

Similarly to the baseline transcriptional changes between *Mb1*$^{cre/+}$ versus *Ahr*$^{fl/-}$*Mb1*$^{cre/+}$ mice observed during the transcriptome analysis, there were clear differences in chromatin accessibility as measured by ATAC-seq between control *Mb1*$^{cre/+}$ mice and *Ahr*$^{fl/-}$*Mb1*$^{cre/+}$ mice (Figure 6.9A). However, corroborating the results in Figure 6.8C, there was decreased accessibility in several B cell maturation genes, including the *Bcl6* and *Gpr183* loci, upon butyrate supplementation exclusively in *Mb1*$^{cre/+}$ CD19^{+}CD21^{hi}CD24^{hi} B cells (Figure 6.9B). ATAC-seq analysis also revealed that butyrate supplementation did not alter accessibility of the AHR:ARNT specific binding motifs[705], but did increase accessibility at binding motifs for transcription factors that have been identified to function alongside the AHR:ARNT heterodimer, including ESRRA (estrogen receptor alpha), CREB1, and RARB/RARG (Retinoic acid receptor) (Figure 6.9C)[706]. We confirmed that, similarly to Tregs and monocytes[647, 650], butyrate acted as a histone deacetylase inhibitor (HDACi) on splenic B cells *in vitro*, providing a partial explanation of its effect on the transcriptional and epigenetic landscape of CD19^{+}CD21^{hi}CD24^{hi} B cells (Figure 6.9D).

To investigate whether changes in the epigenetic and transcriptional profile of AHR^{+}CD19^{+}CD21^{hi}CD24^{hi} B cells and AHR^{-}CD19^{+}CD21^{hi}CD24^{hi} B cells following butyrate supplementation had altered their stability and ability to differentiate into IL-10 competent Bregs, we followed the fate of adoptively transferred CD19^{+}CD21^{hi}CD24^{hi} B cells isolated from butyrate-supplemented and control WT or global *Ahr*$^{-/-}$ in congenic CD45.1 recipient WT mice. A higher number of donor CD45.2^{+}CD19^{+}CD21^{hi}CD24^{hi} B cells were recovered post-transfer, and more transferred cells were IL-10^{+} when cells were isolated from butyrate-supplemented WT mice compared to control WT mice (Figures 6.10A–E). The rate of cell recovery was not altered by butyrate supplementation when cells were isolated from *Ahr*$^{-/-}$ mice and there was a failure of CD45.2^{+}CD19^{+}CD21^{hi}CD24^{hi} B cells to differentiate into IL-10^{+} Bregs (Figures 6.10A–E).

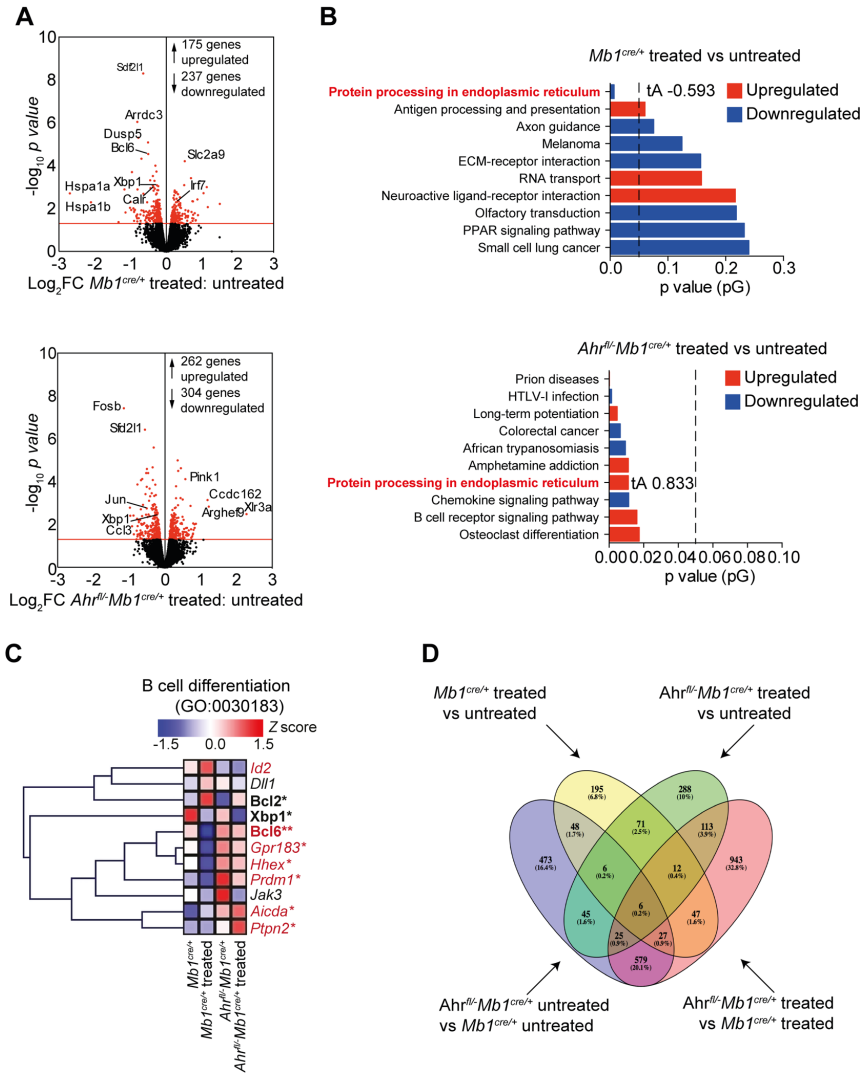

Figure 6.8. Butyrate supplementation modulates the transcriptional profile of CD19^{+}CD21^{hi}CD24^{hi} B cells in an AHR-dependent Manner. (A) Volcano plots shows $\log_2$ fold change (FC) in gene expression between CD19^{+}CD21^{hi}CD24^{hi} B cells isolated from butyrate-supplemented *Mb1$^{cre/+}$* mice compared to control *Mb1$^{cre/+}$* mice (top plot) and between butyrate supplemented *Ahr$^{fl/-}$Mb1$^{cre/+}$* compared to control *Ahr$^{fl/-}$Mb1$^{cre/+}$* mice (bottom plot). Red dots represent significant DEG, with the red line denoting a cut off *p* value of < 0.05. (**B)** Signaling pathway impact analysis (SPIA) ranked on significance (pG) comparing the pathways over-represented (red) and under-represented (blue) pathways in butyrate supplemented compared to control CD19^{+}CD21^{hi}CD24^{hi} B cells from *Mb1$^{cre/+}$* mice (top graph) and *Ahr$^{fl/-}$Mb1$^{cre/+}$* mice (bottom graph). The total perturbation accumulation of these pathways (tA) score is listed for the 'protein processing in endoplasmic reticulum' pathway. **(C)** Heat map shows the expression of B cell differentiation genes in CD19^{+}CD21^{hi}CD24^{hi} B cells isolated from control *Mb1$^{cre/+}$* mice, butyrate-supplemented *Mb1$^{cre/+}$* mice, control *Ahr$^{fl/-}$Mb1$^{cre/+}$* mice, and butyrate-supplemented *Ahr$^{fl/-}$Mb1$^{cre/+}$* mice. Mean z scores were calculated from log CPM values. Samples highlighted in red are significantly differentially expressed between CD19^{+}CD21^{hi}CD24^{hi} B cells isolated from butyrate-supplemented *Mb1$^{cre/+}$* mice compared to butyrate-supplemented *Ahr$^{fl/-}$Mb1$^{cre/+}$* mice. Samples highlighted in bold are significantly differentially expressed between CD19^{+}CD21^{hi}CD24^{hi} B cells isolated from butyrate-supplemented *Mb1$^{cre/+}$* mice compared to control *Mb1$^{cre/+}$* mice. (**D**) Venn diagram indicating the number of significant ($p < 0.05$) DEG across all 4 comparisons and the number of overlapping genes between each comparison. For RNA-seq data, n=3 per group. Cells were isolated at day 7 post-disease onset.

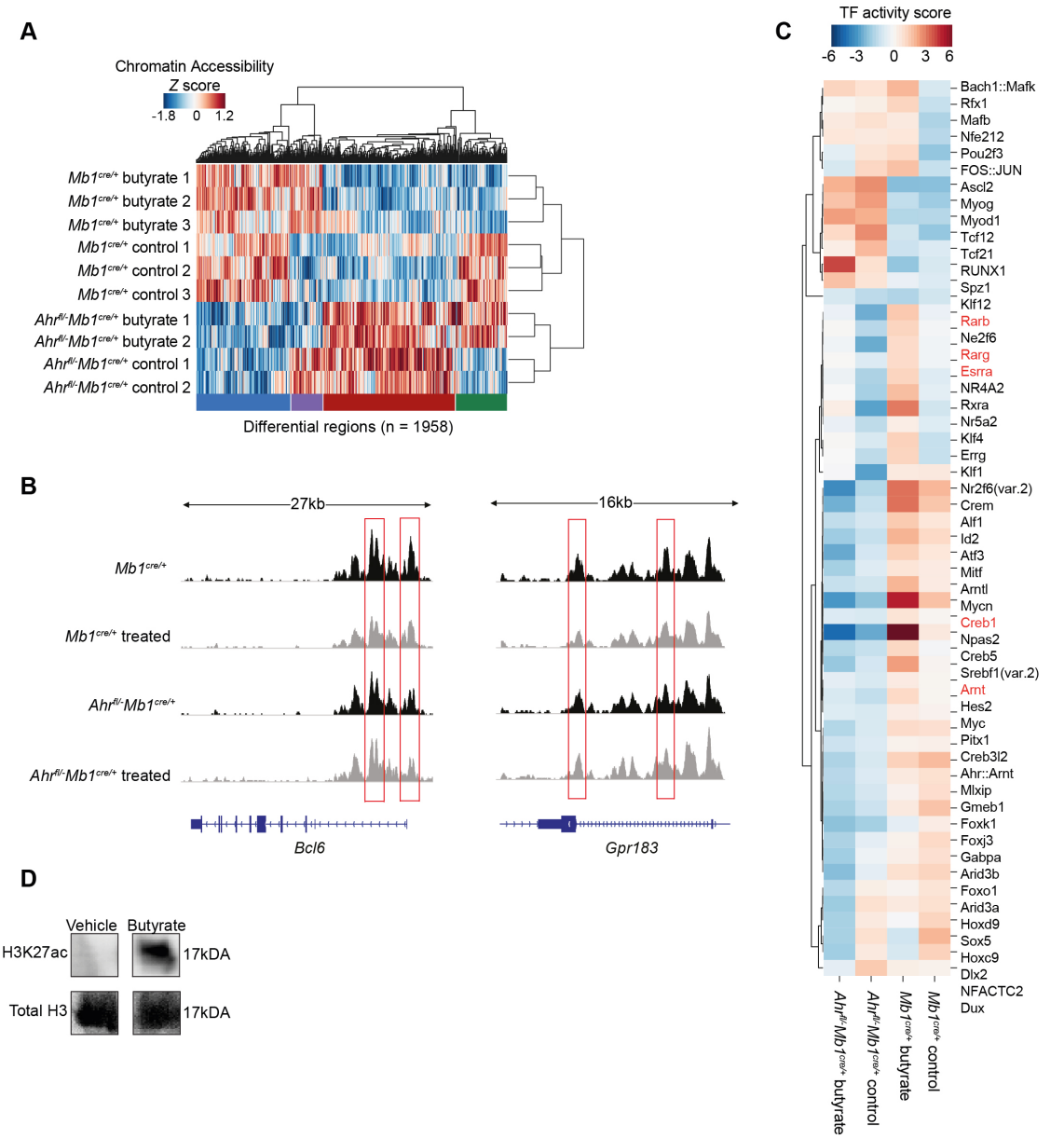

Figure 6.9. Butyrate supplementation modulates the epigenetic profile of CD19^{+}CD21^{hi}CD24^{hi} B cells in an AHR-dependent manner by increasing histone acetylation. (**A**) Heatmap shows differentially regulated regions of chromatin in CD19^{+}CD21^{hi}CD24^{hi} B cells isolated from control *Mb1*$^{cre/+}$ mice, butyrate-supplemented *Mb1*$^{cre/+}$ mice, control *Ahr*$^{fl/-}$*Mb1*$^{cre/+}$ mice, and butyrate-supplemented *Ahr*$^{fl/-}$*Mb1*$^{cre/+}$ mice as measured by ATAC-seq. (**B**) Representative ATAC-seq tracks for the *Bcl6* and *Gpr183* loci in CD19^{+}CD21^{hi}CD24^{hi} B cells from butyrate-supplemented or control *Mb1*$^{cre/+}$ and *Ahr*$^{fl/-}$*Mb1*$^{cre/+}$ mice (n=3). Track heights between samples are normalized through group autoscaling. (**C**) Heatmap shows inferred transcription factor activity scores based on accessibility at transcription factor binding motifs in CD19^{+}CD21^{hi}CD24^{hi} B cells isolated from control *Mb1*$^{cre/+}$ mice, butyrate-supplemented *Mb1*$^{cre/+}$ mice, control *Ahr*$^{fl/-}$*Mb1*$^{cre/+}$ mice, and butyrate-supplemented *Ahr*$^{fl/-}$*Mb1*$^{cre/+}$ mice as measured by ATAC-seq. AHR co-factors are highlighted in red. (**D**) Total splenic B cells were isolated from WT mice and treated either with a vehicle control or 500μM butyrate for 18h and analysed for H3K27ac by Western blot. Total H3 was used as a control. The numbers indicate the size of the protein bands in kDA. One of two representative experiments shown. For ATAC-seq data, n=3 for *Mb1*$^{cre/+}$ mice and n=2 for *Ahr*$^{fl/-}$*Mb1*$^{cre/+}$ mice. For figures **A and C**, experiments performed in collaboration with Andre Rendeiro.

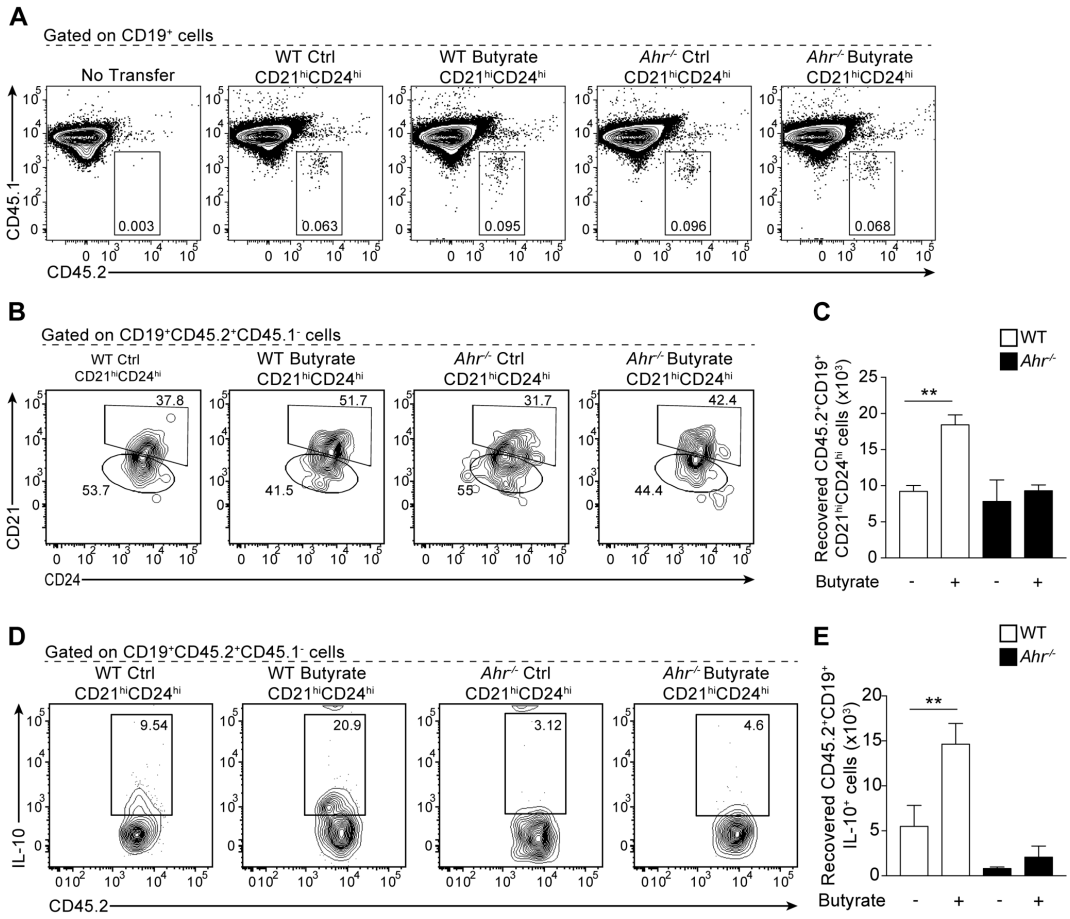

Figure 6.10. CD45.2$^+$CD19$^+$CD21^{hi}CD24^{hi} B cells from butyrate-supplemented WT but not *Ahr*$^{-/-}$ mice retain their phenotype and differentiate into IL-10$^+$ Bregs upon adoptive transfer. (**A-B**) Representative flow cytometry plots show (**A**) CD45.2$^+$CD19$^+$ B cell and (**B**) CD45.2$^+$CD19$^+$CD21^{hi}CD24^{hi} B cell frequency in CD45.1 congenic WT mice that had received a transfer of CD19$^+$CD21^{hi}CD24^{hi} B cells isolated from control or butyrate-supplemented WT or *Ahr*$^{-/-}$ mice. (**C**) Bar chart shows number of CD45.2$^+$CD19$^+$CD21^{hi}CD24^{hi} B cells recovered post-transfer from CD45.1 congenic WT mice that had received a transfer of CD19$^+$CD21^{hi}CD24^{hi} B cells isolated from control or butyrate-supplemented WT or *Ahr*$^{-/-}$ mice (cumulative n=3 per group, cumulative data are shown). (**D**) Representative flow cytometry plots and bar charts show CD45.2$^+$CD19$^+$IL-10$^+$ B cell frequency in CD45.1 congenic WT mice that had received a transfer of CD19$^+$CD21^{hi}CD24^{hi} B cells isolated from control or butyrate-supplemented WT or *Ahr*$^{-/-}$ mice. (**E**) Bar chart shows number of CD45.2$^+$CD19$^+$IL-10$^+$ B cells recovered post-transfer from CD45.1 congenic WT mice that had received a transfer of control or butyrate-supplemented WT or *Ahr*$^{-/-}$ mice. Cells were isolated at 48 h post-transfer (cumulative n=3 per group, cumulative data are shown). Figures **C and E,** data are expressed as mean±sem. ***p*<0.01. **C and E,** one-way ANOVA.

6.4 Butyrate changes the availability of microbiota-induced AHR ligands

The microbiota is an important contributor to the pool of endogenous AHR ligands, and we and others have previously shown that changes in the composition of the gut microbiota alters the differentiation of $CD19^{+}CD21^{hi}CD24^{hi}$ B cells into functionally suppressive Bregs[323, 707]. Having excluded a direct effect for butyrate in activating AHR, as butyrate did not upregulate the marker of AHR activation *Cyp1a1* compared to vehicle-treated B cells *in vitro* (Figure 6.11A), we investigated whether the endogenous microbiota or their metabolites are important in the butyrate-mediated suppression of arthritis and Breg maintenance. To address this, broad-spectrum antibiotic (ABX)-treated mice were given butyrate by oral gavage; this combination of antibiotics is known to ablate the majority of the gut microbiota[323, 708]. We found that the suppressive activity of butyrate depended upon the presence of the endogenous gut microbiota, as butyrate supplementation was ineffective at suppressing arthritis in ABX-treated mice (Figure 6.11B). In support of our previously published results showing that commensal microbiota is important in Breg differentiation, B cells isolated from ABX-treated mice expressed less *Il10* mRNA compared to untreated controls[323], and this defect was not recovered after butyrate supplementation (Figure 6.11C).

Having established that commensal microbes are required for butyrate to suppress arthritis, we compared the relative abundance of bacteria phyla in the stool of naive, control, and butyrate-supplemented arthritic mice using 16S rDNA amplicon sequencing. Butyrate supplementation induced a shift in the stool microbiota of arthritic mice, favoring a profile that was more similar to naive mice (Figure 6.12A). A detailed analysis of the bacterial composition revealed an increase in the abundance of the bacterial genera *Allobaculum*, *Bifidobacterium*, and *Rhodosprillaceae_unclassified* in butyrate-supplemented versus control mice (Figure 6.12B). Members of these bacteria genera have a previously described role in influencing the generation of tryptophan-derived metabolites, a family of ligands implicated in the activation of AHR[709]. To understand whether changes in bacterial composition following butyrate supplementation altered the level of tryptophan-derived metabolites, we measured these metabolites in the stool of butyrate-supplemented and control mice. There were no differences in the amount of tryptophan, tryptamine, indole, and L-kynurenine in stool samples from butyrate-supplemented compared to control mice (Figures 6.12C-D). Indole-3-acetate and

Indole-3-propionate levels were also measured but found to be below the limit of detection in all samples. There was, however, a significant increase in 5-HIAA, the main metabolite of serotonin (Figure 6.12E), and a significant reduction in the level of the kynurenine-derived metabolite kynurenic acid (KYNA) (Figure 6.12D).

To directly address how the changes in 5-HIAA and KYNA levels affect AHR-dependent gene transcription in B cells, WT B cells were isolated from naive mice and stimulated with 5-HIAA and KYNA *in vitro*. Unlike KYNA, which only induced *Cyp1a1* induction in B cells, 5-HIAA increased both *Cyp1a1* and *Il10* expression in B cells compared to vehicle-control-treated B cells (Figure 6.13A). Most importantly, treatment of WT mice with these AHR ligands *in vivo* demonstrated that 5-HIAA, but not KYNA, suppressed arthritis development and increased both *Cyp1a1* and *Il10* transcription in B cells *ex vivo* (Figures 6.13B-C). To examine the role for AHR in the immunosuppressive effect of 5-HIAA, we gavaged $Mb1^{cre/+}$ mice and $Ahr^{fl/-}Mb1^{cre/+}$ mice with 5-HIAA. 5-HIAA suppressed arthritis in $Mb1^{cre/+}$ mice but not in $Ahr^{fl/-}Mb1^{cre/+}$ mice (Figure 6.13D). Finally, to explore the role of 5-HIAA in the ability of butyrate supplementation to suppress arthritis, mice were treated with the tryptophan hydrolase (TPH) inhibitor L-para-chlorophenylalanine (PCPA), which is known to reduce 5-HIAA and serotonin biosynthesis[710]. In mice treated with PCPA, butyrate supplementation lost its ability to suppress arthritis when compared to vehicle-treated control mice (Figure 6.13E). Collectively, these data demonstrate that butyrate supplementation increases the production of 5-HIAA, a newly identified AHR ligand in B cells, which mediates the suppressive effect of butyrate supplementation *in vivo*.

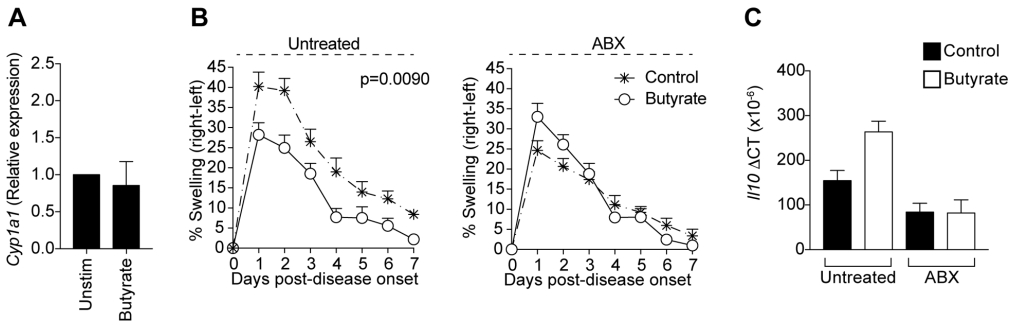

Figure 6.11. The suppression of arthritis by butyrate is dependent on the gut microbiota. (**A**) Bar chart shows relative expression of *Cyp1a1* following 6 hours culture with butyrate (cumulative n=5). (**B**) Mean clinical score of control and butyrate-supplemented ABX-treated or untreated mice; y axis shows percentage swelling in antigen-injected knee compared to control knee (cumulative n=8 per group, one representative experiment of two experiments is shown). (**C**) Bar chart shows expression of *Il10* relative to *β-actin* in splenic B cells isolated from ABX-treated WT or untreated mice (cumulative n=3 per group). Figures **A-C,** data are expressed as mean±sem. **A,** Student's t test; **B,** two-way ANOVA; **C,** one-way ANOVA.

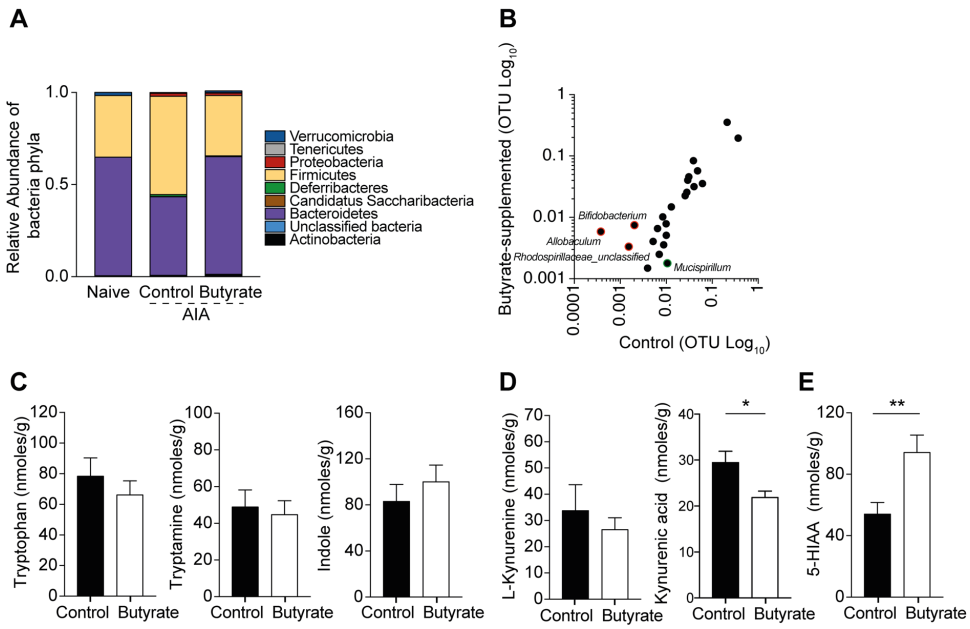

Figure 6.12. Butyrate supplementation increases the availability of AHR ligands. (**A**) Bar chart shows relative abundance of bacterial phyla in the stool of naive, control arthritic, or butyrate-supplemented arthritic mice (n=4 per group). (**B**) XY graph shows operational taxonomic units (OTUs) of bacterial genera in butyrate-supplemented and control arthritic mice (n=4 per group). (**C-E**) Bar charts shows levels of (**C**) tryptophan, tryptamine, indole, (**D**) L-Kynurenine, Kynurenic Acid (KYNA) and (**E**) 5-HIAA in the stool of control arthritic WT and butyrate-supplemented arthritic mice (cumulative n=5 per group). Figures **C-E,** data are expressed as mean±sem. **p*<0.05, ***p*<0.01. **C and E,** Student's t test. For figures **A-B,** experiments performed in collaboration with Nigel Klein.

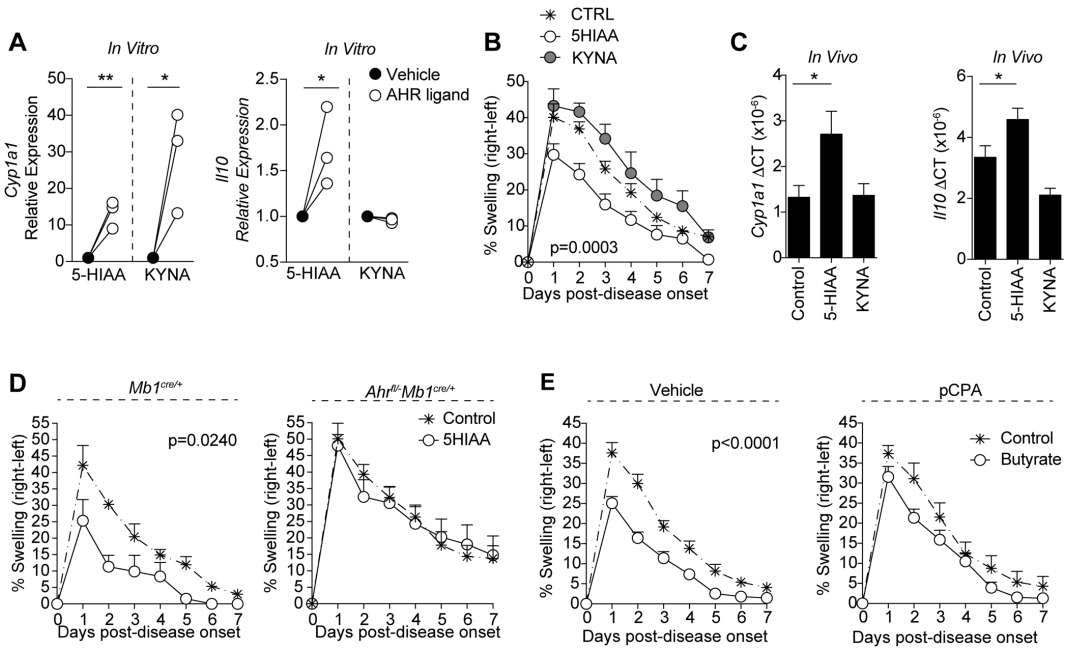

Figure 6.13. Hydroxyindole-3-acetic acid increases *Il10* transcription by B cells *in vivo* and *in vitro* by acting as a ligand for AHR. (**A**) Relative expression of *Cyp1a1* and *Il10* in total splenic B cells following 6h culture with 5-HIAA or kynurenic acid (KYNA) compared to vehicle alone (cumulative n=3 per group). (**B**) Mean clinical score of control, 5-HIAA-gavaged, or KYNA-gavaged mice; y axis shows percentage swelling in antigen-injected knee compared to control knee (cumulative n=8 per group, one representative experiment of two experiments is shown). (**C**) Bar charts show expression of *Cyp1a1* and *Il10* relative to *β-actin* in splenic B cells isolated from control, 5-HIAA-gavaged, or KYNA-gavaged mice (cumulative n=3 per group). (**D**) Mean clinical score of control or 5-HIAA-gavaged $Mb1^{cre/+}$ mice or $Ahr^{fl/-}Mb1^{cre/+}$ mice; y axis shows percentage swelling in antigen-injected knee compared to control knee (cumulative n=8 per group, one representative experiment of two experiments is shown). (**E**) Mean clinical score of control and butyrate-supplemented L-para-chlorophenylalanine (PCPA)-treated (tryptophanase inhibitor, TPH) or vehicle-treated mice; y axis shows percentage swelling in antigen-injected knee compared to control knee (cumulative n=10 per group, one representative experiment of two experiments is shown). Figures **A-E,** data are expressed as mean±sem. **p*<0.05, ***p*<0.01. **A,** Student's t test; **B and D-E,** two-way ANOVA; **C,** one-way ANOVA.

Chapter VII: Discussion

7.1 AHR defines Breg identity

Bregs are generated in the periphery in response to a variety of "homeostatic" inflammatory stimuli including activation through TLRs and by pro-inflammatory cytokines[286]. The transcriptional programme, which governs the differentiation and function of IL-10^{+}CD19^{+}CD21^{hi}CD24^{hi} Bregs remains virtually unknown. Here, we show that AHR contributes to the differentiation of CD19^{+}CD21^{hi}CD24^{hi} B cells into functionally suppressive IL-10^{+}CD19^{+}CD21^{hi}CD24^{hi} Bregs, by regulating their IL-10 production and by repressing the transcription of pro-inflammatory mediators. The importance of IL-10 in mediating the suppressive effect of Bregs is well established and its role is corroborated by *in vivo* results showing that mice lacking IL-10-producing B cells develop exacerbated autoimmunity[354]. Similarly, AHR deficiency restricted to B cells impairs IL-10^{+}CD19^{+}CD21^{hi}CD24^{hi} Breg differentiation and function, resulting in an increase of IFN-γ and IL-17-expressing CD4^{+} T cells, a decrease in Tregs, and the development of an exacerbated arthritis.

AHR plays a pleiotropic role in the regulation of several immune responses[445], most notably, in the differentiation of CD4^{+} T cells where AHR influences both the differentiation and activation of Th17 cells, which are known to play a major role in the pathogenesis of several autoimmune diseases[711], and the differentiation of CD4^{+} T cells into Tr1 cells[422]. Immune suppression was one of the earliest known observations of AHR function. 2,3,7,8-tetrachlorodibenzo-ρ-dioxin (TCDD), an environmental contaminant and potent AHR agonist, was found to suppress DTH responses to tuberculin[594]. More recently, it has become apparent that AHR has a conserved role in the regulation of IL-10 across the innate and adaptive immune system, controlling IL-10 production in NK cells[712], peritoneal[482] and bone marrow derived macrophages[713] and in Tr1 cells, where AHR binding to the *Il10* promoter region has been described[422]. We demonstrate that in IL-10^{+} B cells, AHR binds upstream of the *Il10* transcription start site, to a different genomic region than in Tr1 cells, suggesting that there are cell-context and cell-signal specific epigenetic differences in the regulation of *Il10*[714].

An interesting finding in our study was the discovery that AHR controls the differentiation of CD19^{+}CD21^{hi}CD24^{hi} B cells into a polarized IL-10^{+}CD19^{+}CD21^{hi}CD24^{hi} Breg population that produces only IL-10, by contributing

to IL-10 induction and by suppressing the transcription of several pro-inflammatory cytokines, such as *Il2*, *Il6* and *Tnf*. AHR has been previously shown to inhibit pro-inflammatory IL-17 and IFN-γ cytokine production in T cells and to induce Tr1 cell differentiation in the gut[686]. In addition, in the absence of AHR in macrophages, mice are more susceptible to LPS-induced endotoxic shock and present with an increase in pro-inflammatory IL-6 expression[482]. AHR deletion in microglial cells led to the upregulation of *Ccl2*, *Il1b*, *Nos2* and *Vegfb* gene expression, factors known to be involved in inflammation and neurodegeneration[685]. Our data reveals that AHR preserves the immunosuppressive function of splenic IL-10^{+}CD19^{+}CD21^{hi}CD24^{hi} Bregs by silencing a pro-inflammatory transcriptional programme. Whether AHR complexes bind to XRE on the loci of pro-inflammatory cytokines and directly inhibit their expression in B cells, or if AHR co-ordinates the suppression of pro-inflammatory immune responses through interaction with other transcription factors in B cells warrants further study.

Our adoptive transfer results suggest that the predominant effect of a lack of AHR in B cells is the loss of IL-10. We have previously shown that adoptive transfer of *Il10*$^{-/-}$ B cells are unable to suppress arthritis[297, 354]. Here we show that WT mice do not get worse disease than the PBS control injected mice upon adoptive transfer of AHR^{-}CD19^{+}CD21^{hi}CD24^{hi} B cells. Equally, AHR^{-}CD19^{+}CD21^{hi}CD24^{hi} B cells do not suppress disease onset in the recipient mice, unlike the transfer of control AHR^{+}CD19^{+}CD21^{hi}CD24^{hi} B cells. These data therefore suggest that the deleterious effects observed in AIA is the consequence of the reduced amount of IL-10. However, we cannot rule out the possibility that, *in vivo,* AHR-deficient B cells contribute to overall inflammation through the upregulation of pro-inflammatory cytokines and chemokines or indirectly through the recruitment of other cell types.

We have recently reported that AHR deletion rather than impairing the capacity of B cells to proliferate compromised their ability to commence the cell cycle. Indeed, there was reduction in *Ccno* mRNA expression in splenic B cells isolated from naïve *Ahr*$^{fl/-}$*Mb1*$^{cre/+}$ compared to *Mb1*$^{cre/+}$ mice[615]. Here we show that this defect, unlike in the steady state, is overcome during an arthritogenic response, as no change in Ki-67 expression or in genes regulating the cell cycle, including *Ccno*, were observed between *Mb1*$^{cre/+}$ and *Ahr*$^{fl/-}$*Mb1*$^{cre/+}$ CD19^{+}CD21^{hi}CD24^{hi} B cells

taken directly from arthritic mice. Furthermore, no difference was observed in Ki-67 expression between *Mb1*$^{cre/+}$ and *Ahr*$^{fl/-}$*Mb1*$^{cre/+}$ CD19^{+}CD21^{hi}CD24^{hi} B cells after restimulation with LPS+anti-IgM. Although, in the latter, we used purified CD19^{+}CD21^{hi}CD24^{hi} B cells instead of total splenic B cells and used different stimuli to activate this population, which together might account for the differences observed in this study. Therefore, these data confirmed that the phenotype observed in the absence of AHR expression in B cells is not due to impaired B cell proliferation, but instead is due to the reduced ability of B cells to differentiate into Bregs and reduction in the production of IL-10.

Our results show that while the loss of B cell AHR expression reduces IL-10^{+}CD19^{+}CD21^{hi}CD24^{hi} Breg frequency and leads to an expansion of plasma cells, it does not affect the frequencies or absolute numbers of B cell populations up to a mature naïve B cell stage. Taken together with previous findings showing that AHR is expressed by B cells from the immature B cell stage in the bone marrow[615, 616, 715], we suggest that B cell AHR expression is important primarily for the control of IL-10^{+}CD19^{+}CD21^{hi}CD24^{hi} Breg immune-regulatory transcriptional programming and restricting plasma cell development, but is dispensable for homeostatic early B cell development.

We report that *Ahr*$^{fl/-}$*Mb1*$^{cre/+}$ mice have increased frequencies of splenic plasma cells compared to control *Mb1*$^{cre/+}$ mice and these results are in line with those showing that both prototypic AHR agonists (polycyclic aromatic and planar halogenated hydrocarbons) affect terminal differentiation of B cells and humoral immune responses, by inhibiting plasma cell differentiation and reducing the production of IgM[217, 606, 619]. We find increased levels of *Prdm1* mRNA expression in B cells lacking AHR, consistent with previous findings showing that the suppression of terminal differentiation is mediated through AHR increasing BACH2 expression[620]. BACH2 in turn represses the expression of BLIMP-1, a key transcription factor that controls B cell differentiation into immunoglobulin-producing plasma cells[716]. We have extended the significance of these results to an inflammatory model and showed that early B cell development and maturation of B cells is not affected by B cell AHR expression, but that AHR is required for the differentiation of IL-10^{+}CD19^{+}CD21^{hi}CD24^{hi} Bregs. It is tantalizing to propose that the increase in plasma cells observed in mice lacking AHR is due to the impaired

function of Bregs. We have previously shown that, at least in humans, IL-10 produced by Bregs directly inhibits T helper cell differentiation which prevents plasma cell differentiation[350].

Here we have shown that AHR, in response to inflammatory signals, plays an important role in the homeostatic maintenance of Breg function by acting as a molecular brake, preventing the differentiation of Bregs into effector B cells producing pro-inflammatory mediators. In addition to identifying that AHR regulates IL-10 expression in Bregs, our data highlight an additional mechanism by which AHR restrains inflammatory responses. These results add to a growing body of evidence supporting AHR as a key modulator of immune tolerance, and therefore, a potential therapeutic target in autoimmunity.

7.2 Establishing a link between gut microbiota and Breg differentiation

Bregs are generated in the periphery in response to bacterial-derived metabolites and inflammatory signals. Whereas more is understood regarding how inflammation and inflammatory cytokines drive Breg differentiation[312, 323, 717, 718], the participation of microbiota in Breg biology is poorly understood. We have previously shown that low-grade inflammatory signals that drive the differentiation of immature B cells into Bregs are provided in the gut-associated lymphoid tissue, as a result of the interaction between the gut microbiota and the innate immune system[323]. Mice depleted of endogenous bacteria following administration of broad-spectrum antibiotics do not develop arthritis or Bregs, suggesting an intricate relationship between microbiota, inflammation, and Breg differentiation[323]. We hypothesised that signals through AHR in B cells in the GALT, prime B cells to differentiate into Bregs. Here we establish a link between the dietary SCFA butyrate and AHR-driven differentiation of Bregs. Butyrate-supplementation attenuates arthritis severity in mice by supporting AHR^+ Breg function and suppressing mature B cell subset differentiation. We show that butyrate is not a direct ligand of AHR in B cells, but indirectly supports Breg differentiation in an AHR-dependent manner by increasing the levels of the newly identified AHR ligand 5-HIAA; a downstream metabolite of serotonin.

Recent literature has demonstrated that butyrate can alter the function of a wide variety of immune cells[632]. In agreement with this, we found that butyrate-

supplementation of arthritic mice enhanced Treg suppressive function upon adoptive transfer. Butyrate has been shown to induce FOXP3$^+$ Tregs both directly, by acting as a histone deacetylase inhibitor (HDACi)[650], and indirectly, by promoting anti-inflammatory properties in macrophages and DC by engaging G protein coupled receptors GPR43 and GPR109A[648, 649]. Building on these findings, we found that Tregs only displayed enhanced suppressive function when isolated from butyrate-supplemented mice with a fully functional Breg compartment. This supports published data demonstrating that Treg homeostasis is altered in mice lacking IL-10 producing B cells[354].

Here, we also describe a previously unappreciated role for butyrate in altering B cell differentiation and function in mice with arthritic disease. Interrogation of the interaction between butyrate and B cells using a murine model of arthritis demonstrated a sophisticated system whereby butyrate alters AHR-dependent gene transcription, including key B cell differentiation genes and immunoregulatory genes serving to support Breg suppressive function and inhibit B cell maturation. Notably, we found that μMT mice, which lack both regulatory and inflammatory (e.g. GC B cells and plasmablasts) B cells have equivalent disease severity to WT mice in this model of arthritis but that chimeric mice, which exclusively lack IL-10 producing B cells, develop exacerbated disease compared to chimeric mice with WT B cells [354]. This demonstrates a fundamental role for IL-10 producing B cells in suppressing arthritic severity following butyrate-supplementation in this model. These data demonstrate for the first time that a microbial-derived metabolite can control the balance between regulatory and mature B cell subsets. Notably, we found that, only in AHR-sufficient B cells, butyrate enforces a developmental programme, which promotes and maintains Breg differentiation, whilst inhibiting mature B cell differentiation. These data demonstrate for the first time that a microbial-derived metabolite can control the balance between regulatory and mature B cell subsets and supports the previously described role of AHR in inhibiting the terminal differentiation of B cells[614].

Our data determined that butyrate-supplementation requires a fully competent endogenous microbiota to exert its anti-arthritogenic capabilities on the B cell compartment. Butyrate-supplementation shifted the microbiota to increase relative abundance of *Allobaculum*, *Bifidobacterium* and *Rhodosprillaceae_unclassified*,

genera which have been shown to influence tryptophan metabolism[709, 719, 720, 721]. One possible explanation for this shift is that butyrate possesses antimicrobial activity that targets pathobionts, creating a niche for the growth of tryptophan-metabolizing species. In the agricultural industry, butyrate is an established component of chicken feeds used to control the growth of pathogenic bacteria[722]. In addition to a direct bactericidal effect, butyrate enhances the microbicidal function of macrophages, by altering their metabolism and by eliciting the production of anti-microbial peptides, which may control out-growth of pathogenic components of the gut-microbiota[647]. Another complementary explanation justifying the observed shift in bacterial communities is that butyrate acts as a nutrient for beneficial bacteria. At present, we cannot exclude that changes observed in the gut microbiota following butyrate-supplementation could be the result of reduced inflammation. Unfortunately, due to the intertwined response between microbiota and inflammation it is difficult to extricate whether the butyrate effect on bacteria is direct, mediated by cells, or by other anti-inflammatory mediators. Future studies will be performed to investigate if the effect reported here is due to changes in inflammation or due to direct effect on the microbiota. Our findings support the notion that prebiotics supplementation could be used to restrain inflammation in systemic autoimmune disease with no obvious gut-related pathogenesis.

The diversity of endogenous AHR ligands have started to be well characterised in recent years[698]. However, determining the physiologically relevant ligands in immune cell function and examining if these ligands have differing roles in directing cell function has been harder to establish. Endogenous AHR ligands can be generated by host cells, microbiota, and through metabolism of dietary compounds[698]. Amongst the microbiota-derived ligands for AHR, an important family are tryptophan-derived metabolites. For example, it has been previously demonstrated that tryptophan is endogenously metabolized into tryptamine and indole-3-acetic acid, which directly binds to AHR[506, 683]. More recently, expression of tryptophanase by certain microbiota species has been shown to process tryptophan into indoles and its 3-substituted derivatives, which also act as agonists for AHR[723]. In addition, L-kynurenine and kynurenic acid which are produced following metabolism of tryptophan by indoleamine 2,3-dioxygenase (IDO) can also activate AHR in immune cells[581, 724]. In this study, we did not detect any

variation in the levels of tryptophan, tryptamine, L-kynurenine or indole, yet we observed a reduction in kynurenic acid (KYNA). We also found the levels of indole-3-substituted derivatives to be below the limit of detection suggesting that these pathways are unaffected by butyrate-supplementation. Rather our data suggests an additional mechanism by which 5-Hydroxyindole-3-acetic acid (5-HIAA), the main metabolite of serotonin (5-HT), activates AHR in B cells following butyrate-supplementation. Similarly to T cells, where it has been shown that different AHR ligands drive either Treg or Th17 differentiation[581], we show that both KYNA and 5-HIAA can activate AHR-dependent gene transcription in B cells, but only 5-HIAA and not KYNA upregulates *Il10* transcription in B cells in an AHR-dependent manner.

The production of the tryptophan-derived neurotransmitter 5-HT in the gut is intimately connected with the presence and species of the gut microbiota[725]. As well as regulating diverse physiological processes in both the brain and the gut, 5-HT also has a proposed immune-modulatory function, including the promotion of B cell proliferation, induction of cytokine release by monocytes, and changing in capabilities of dendritic cells to present antigen and activate T cells[726, 727]. Here we determine that 5-HT's main metabolite 5-HIAA activates AHR in B cells and drives the transcription of both *Cyp1a1* and *Il10* transcription in B cells and show that 5-HIAA is immunoregulatory in arthritis. Our data supports a recently established link between the serotonergic and AHR pathways, showing the efficacy of 5-HT in inducing *Cyp1a1* expression via AHR in an intestinal epithelial cell line[507]. It also adds to accumulating evidence that butyrate can induce 5-HT release by neural enterochromaffin cells in the gut[728]. We suggest that as well as regulating gut homeostasis and peristalsis, the butyrate-serotonin-AHR axis also acts to influence Breg homeostasis.

The data in this study suggest that gut-microbiota derived metabolites control many aspects of B cell development and Breg function. Moreover, it suggests that the threshold for Breg induction in response to inflammatory stimuli could potentially be lowered in AHR ligand rich environments. We show that butyrate increases the availability of the AHR agonist 5-HIAA and thus enforces an AHR-dependent transcriptional programme which promotes the generation of Bregs, whilst inhibiting terminal differentiation of B cells (Figure 7.1). To date, due to the

heterogenous nature of the Breg response, researchers have been unable to ascertain how to harness the suppressive function of Bregs. These results, in part, address this gap and reveal that supplementation of microbial end products like butyrate could be used for therapeutic intervention in autoimmune disease.

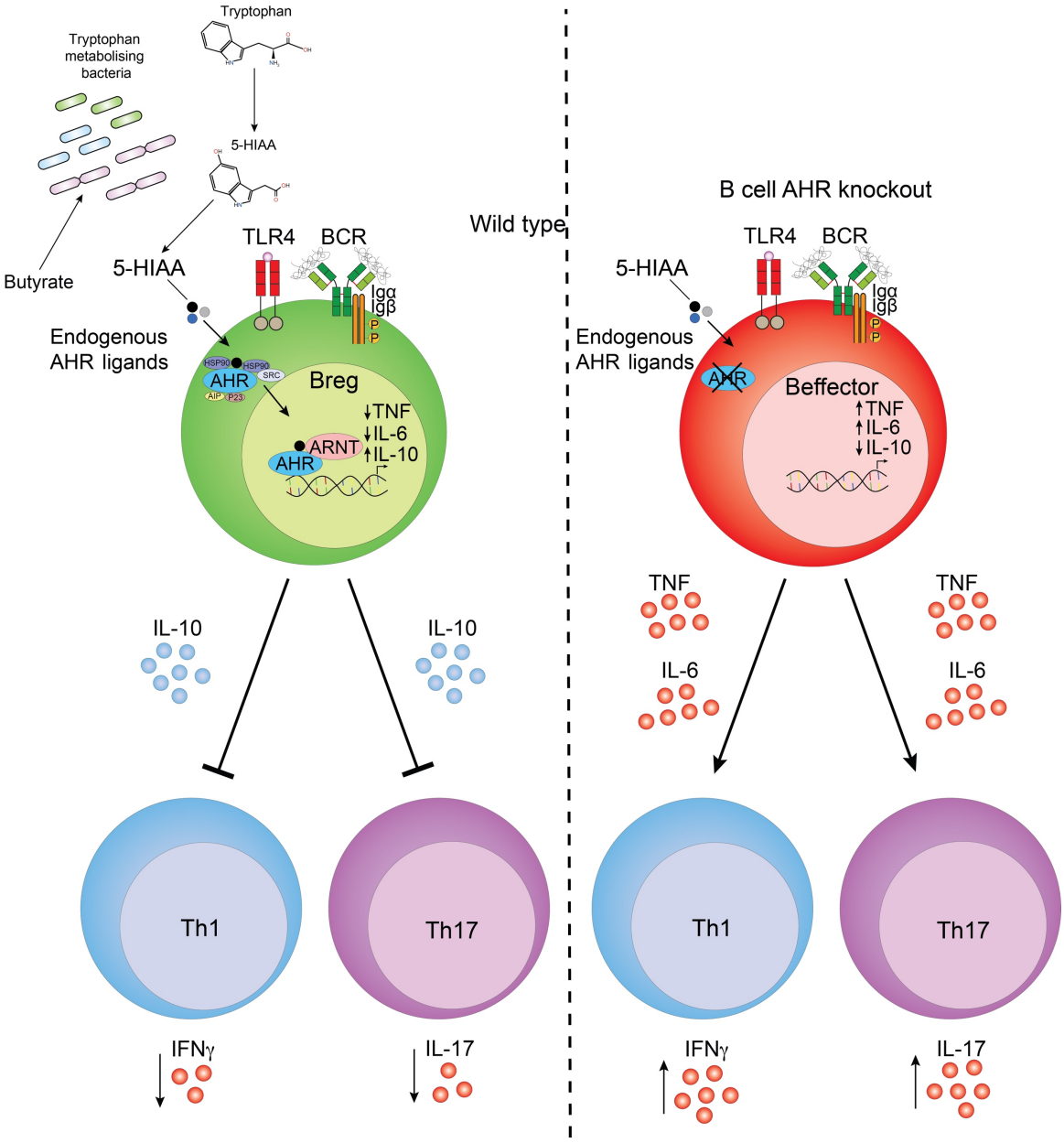

Figure 7.1. Working model of the role of butyrate and AHR in Breg differentiation and function. Butyrate promotes the growth of tryptophan metabolising bacteria, which metabolise tryptophan to 5-HIAA. 5-HIAA acts as an AHR ligand, which induces Breg differentiation by upregulating IL-10 and suppressing pro-inflammatory cytokine gene expression. $AHR^{+}IL\text{-}10^{+}$ Bregs then suppress pathogenic T cell responses in AIA.

References

1. LeBien, T.W. & Tedder, T.F. B lymphocytes: how they develop and function. *Blood* **112**, 1570-1580 (2008).

2. Jackson, K.J., Kidd, M.J., Wang, Y. & Collins, A.M. The shape of the lymphocyte receptor repertoire: lessons from the B cell receptor. *Front Immunol* **4**, 263 (2013).

3. Moore, M.A. & Metcalf, D. Ontogeny of the haemopoietic system: yolk sac origin of in vivo and in vitro colony forming cells in the developing mouse embryo. *Br J Haematol* **18**, 279-296 (1970).

4. Johnson, G.R. & Moore, M.A. Role of stem cell migration in initiation of mouse foetal liver haemopoiesis. *Nature* **258**, 726-728 (1975).

5. Mikkola, H.K. & Orkin, S.H. The journey of developing hematopoietic stem cells. *Development* **133**, 3733-3744 (2006).

6. Cheshier, S.H., Morrison, S.J., Liao, X. & Weissman, I.L. In vivo proliferation and cell cycle kinetics of long-term self-renewing hematopoietic stem cells. *Proc Natl Acad Sci U S A* **96**, 3120-3125 (1999).

7. Cumano, A. *et al.* New Molecular Insights into Immune Cell Development. *Annu Rev Immunol* **37**, 497-519 (2019).

8. Sawai, C.M. *et al.* Hematopoietic Stem Cells Are the Major Source of Multilineage Hematopoiesis in Adult Animals. *Immunity* **45**, 597-609 (2016).

9. Mackarehtschian, K. *et al.* Targeted disruption of the flk2/flt3 gene leads to deficiencies in primitive hematopoietic progenitors. *Immunity* **3**, 147-161 (1995).

10. Sitnicka, E. *et al.* Key role of flt3 ligand in regulation of the common lymphoid progenitor but not in maintenance of the hematopoietic stem cell pool. *Immunity* **17**, 463-472 (2002).

11. Rothenberg, E.V. Transcriptional control of early T and B cell developmental choices. *Annu Rev Immunol* **32**, 283-321 (2014).

12. Bajoghli, B. *et al.* Evolution of genetic networks underlying the emergence of thymopoiesis in vertebrates. *Cell* **138**, 186-197 (2009).

13. Ng, S.Y., Yoshida, T., Zhang, J. & Georgopoulos, K. Genome-wide lineage-specific transcriptional networks underscore Ikaros-dependent lymphoid priming in hematopoietic stem cells. *Immunity* **30**, 493-507 (2009).

14. Iwasaki, H. *et al.* Distinctive and indispensable roles of PU.1 in maintenance of hematopoietic stem cells and their differentiation. *Blood* **106**, 1590-1600 (2005).

15. Semerad, C.L., Mercer, E.M., Inlay, M.A., Weissman, I.L. & Murre, C. E2A proteins maintain the hematopoietic stem cell pool and promote the maturation of myelolymphoid and myeloerythroid progenitors. *Proc Natl Acad Sci U S A* **106**, 1930-1935 (2009).

16. Yu, Y. *et al.* Bcl11a is essential for lymphoid development and negatively regulates p53. *J Exp Med* **209**, 2467-2483 (2012).

17. Spooner, C.J., Cheng, J.X., Pujadas, E., Laslo, P. & Singh, H. A recurrent network involving the transcription factors PU.1 and Gfi1 orchestrates innate and adaptive immune cell fates. *Immunity* **31**, 576-586 (2009).

18. Yao, Z. *et al.* Stat5a/b are essential for normal lymphoid development and differentiation. *Proc Natl Acad Sci U S A* **103**, 1000-1005 (2006).

19. Fahl, S.P., Crittenden, R.B., Allman, D. & Bender, T.P. c-Myb is required for pro-B cell differentiation. *J Immunol* **183**, 5582-5592 (2009).

20. Seo, W., Ikawa, T., Kawamoto, H. & Taniuchi, I. Runx1-Cbfbeta facilitates early B lymphocyte development by regulating expression of Ebf1. *J Exp Med* **209**, 1255-1262 (2012).

21. Zandi, S. *et al.* Single-cell analysis of early B-lymphocyte development suggests independent regulation of lineage specification and commitment in vivo. *Proc Natl Acad Sci U S A* **109**, 15871-15876 (2012).

22. Mansson, R. *et al.* B-lineage commitment prior to surface expression of B220 and CD19 on hematopoietic progenitor cells. *Blood* **112**, 1048-1055 (2008).

23. Reth, M. & Nielsen, P. Signaling circuits in early B-cell development. *Adv Immunol* **122**, 129-175 (2014).

24. Hardy, R.R., Carmack, C.E., Shinton, S.A., Kemp, J.D. & Hayakawa, K. Resolution and characterization of pro-B and pre-pro-B cell stages in normal mouse bone marrow. *J Exp Med* **173**, 1213-1225 (1991).

25. Nutt, S.L., Heavey, B., Rolink, A.G. & Busslinger, M. Commitment to the B-lymphoid lineage depends on the transcription factor Pax5. *Nature* **401**, 556-562 (1999).

26. Fuxa, M. & Busslinger, M. Reporter gene insertions reveal a strictly B lymphoid-specific expression pattern of Pax5 in support of its B cell identity function. *J Immunol* **178**, 8222-8228 (2007).

27. Barberis, A., Widenhorn, K., Vitelli, L. & Busslinger, M. A novel B-cell lineage-specific transcription factor present at early but not late stages of differentiation. *Genes Dev* **4**, 849-859 (1990).

28. Cobaleda, C., Schebesta, A., Delogu, A. & Busslinger, M. Pax5: the guardian of B cell identity and function. *Nat Immunol* **8**, 463-470 (2007).

29. Souabni, A., Cobaleda, C., Schebesta, M. & Busslinger, M. Pax5 promotes B lymphopoiesis and blocks T cell development by repressing Notch1. *Immunity* **17**, 781-793 (2002).

30. Cotta, C.V., Zhang, Z., Kim, H.G. & Klug, C.A. Pax5 determines B- versus T-cell fate and does not block early myeloid-lineage development. *Blood* **101**, 4342-4346 (2003).

31. Perlot, T. & Alt, F.W. Cis-regulatory elements and epigenetic changes control genomic rearrangements of the IgH locus. *Adv Immunol* **99**, 1-32 (2008).

32. Komori, T., Okada, A., Stewart, V. & Alt, F.W. Lack of N regions in antigen receptor variable region genes of TdT-deficient lymphocytes. *Science* **261**, 1171-1175 (1993).

33. Melchers, F. Checkpoints that control B cell development. *J Clin Invest* **125**, 2203-2210 (2015).

34. Mostoslavsky, R., Alt, F.W. & Rajewsky, K. The lingering enigma of the allelic exclusion mechanism. *Cell* **118**, 539-544 (2004).

35. Sakaguchi, N. & Melchers, F. Lambda 5, a new light-chain-related locus selectively expressed in pre-B lymphocytes. *Nature* **324**, 579-582 (1986).

36. Kudo, A. & Melchers, F. A second gene, VpreB in the lambda 5 locus of the mouse, which appears to be selectively expressed in pre-B lymphocytes. *EMBO J* **6**, 2267-2272 (1987).

37. Winkler, T.H. & Martensson, I.L. The Role of the Pre-B Cell Receptor in B Cell Development, Repertoire Selection, and Tolerance. *Front Immunol* **9**, 2423 (2018).

38. Jung, D., Giallourakis, C., Mostoslavsky, R. & Alt, F.W. Mechanism and control of V(D)J recombination at the immunoglobulin heavy chain locus. *Annu Rev Immunol* **24**, 541-570 (2006).

39. Melchers, F. The pre-B-cell receptor: selector of fitting immunoglobulin heavy chains for the B-cell repertoire. *Nat Rev Immunol* **5**, 578-584 (2005).

40. Hardy, R.R. & Hayakawa, K. B cell development pathways. *Annu Rev Immunol* **19**, 595-621 (2001).

41. Pelanda, R. & Torres, R.M. Central B-cell tolerance: where selection begins. *Cold Spring Harb Perspect Biol* **4**, a007146 (2012).

42. Nemazee, D.A. & Burki, K. Clonal deletion of B lymphocytes in a transgenic mouse bearing anti-MHC class I antibody genes. *Nature* **337**, 562-566 (1989).

43. Hartley, S.B. *et al.* Elimination from peripheral lymphoid tissues of self-reactive B lymphocytes recognizing membrane-bound antigens. *Nature* **353**, 765-769 (1991).

44. Hartley, S.B. *et al.* Elimination of self-reactive B lymphocytes proceeds in two stages: arrested development and cell death. *Cell* **72**, 325-335 (1993).

45. Nemazee, D. Mechanisms of central tolerance for B cells. *Nat Rev Immunol* **17**, 281-294 (2017).

46. Grandien, A., Fucs, R., Nobrega, A., Andersson, J. & Coutinho, A. Negative selection of multireactive B cell clones in normal adult mice. *Eur J Immunol* **24**, 1345-1352 (1994).

47. Wardemann, H. *et al.* Predominant autoantibody production by early human B cell precursors. *Science* **301**, 1374-1377 (2003).

48. Mouquet, H. *et al.* Polyreactivity increases the apparent affinity of anti-HIV antibodies by heteroligation. *Nature* **467**, 591-595 (2010).

49. Herzog, S. *et al.* SLP-65 regulates immunoglobulin light chain gene recombination through the PI(3)K-PKB-Foxo pathway. *Nat Immunol* **9**, 623-631 (2008).

50. Hayashi, K., Nojima, T., Goitsuka, R. & Kitamura, D. Impaired receptor editing in the primary B cell repertoire of BASH-deficient mice. *J Immunol* **173**, 5980-5988 (2004).

51. Chen, C., Nagy, Z., Prak, E.L. & Weigert, M. Immunoglobulin heavy chain gene replacement: a mechanism of receptor editing. *Immunity* **3**, 747-755 (1995).

52. Duong, B.H. *et al.* Negative selection by IgM superantigen defines a B cell central tolerance compartment and reveals mutations allowing escape. *J Immunol* **187**, 5596-5605 (2011).

53. Wardemann, H., Hammersen, J. & Nussenzweig, M.C. Human autoantibody silencing by immunoglobulin light chains. *J Exp Med* **200**, 191-199 (2004).

54. Fulcher, D.A. & Basten, A. Reduced life span of anergic self-reactive B cells in a double-transgenic model. *J Exp Med* **179**, 125-134 (1994).

55. Cyster, J.G., Hartley, S.B. & Goodnow, C.C. Competition for follicular niches excludes self-reactive cells from the recirculating B-cell repertoire. *Nature* **371**, 389-395 (1994).

56. Hao, Z. & Rajewsky, K. Homeostasis of peripheral B cells in the absence of B cell influx from the bone marrow. *J Exp Med* **194**, 1151-1164 (2001).

57. Jones, D.D., Wilmore, J.R. & Allman, D. Cellular Dynamics of Memory B Cell Populations: IgM+ and IgG+ Memory B Cells Persist Indefinitely as Quiescent Cells. *J Immunol* **195**, 4753-4759 (2015).

58. Young, F. *et al.* Influence of immunoglobulin heavy- and light-chain expression on B-cell differentiation. *Genes Dev* **8**, 1043-1057 (1994).

59. Reichman-Fried, M., Hardy, R.R. & Bosma, M.J. Development of B-lineage cells in the bone marrow of scid/scid mice following the introduction of functionally rearranged immunoglobulin transgenes. *Proc Natl Acad Sci U S A* **87**, 2730-2734 (1990).

60. Tze, L.E. *et al.* Basal immunoglobulin signaling actively maintains developmental stage in immature B cells. *PLoS Biol* **3**, e82 (2005).

61. Monroe, J.G. ITAM-mediated tonic signalling through pre-BCR and BCR complexes. *Nat Rev Immunol* **6**, 283-294 (2006).

62. Schmitz, R., Baumann, G. & Gram, H. Catalytic specificity of phosphotyrosine kinases Blk, Lyn, c-Src and Syk as assessed by phage display. *J Mol Biol* **260**, 664-677 (1996).

63. Tedder, T.F., Inaoki, M. & Sato, S. The CD19-CD21 complex regulates signal transduction thresholds governing humoral immunity and autoimmunity. *Immunity* **6**, 107-118 (1997).

64. Thomas, M.L. & Brown, E.J. Positive and negative regulation of Src-family membrane kinases by CD45. *Immunol Today* **20**, 406-411 (1999).

65. Nitschke, L. The role of CD22 and other inhibitory co-receptors in B-cell activation. *Curr Opin Immunol* **17**, 290-297 (2005).

66. Srinivasan, L. *et al.* PI3 kinase signals BCR-dependent mature B cell survival. *Cell* **139**, 573-586 (2009).

67. Lam, K.P., Kuhn, R. & Rajewsky, K. In vivo ablation of surface immunoglobulin on mature B cells by inducible gene targeting results in rapid cell death. *Cell* **90**, 1073-1083 (1997).

68. Allman, D. *et al.* Resolution of three nonproliferative immature splenic B cell subsets reveals multiple selection points during peripheral B cell maturation. *J Immunol* **167**, 6834-6840 (2001).

69. Chu, V.T., Enghard, P., Riemekasten, G. & Berek, C. In vitro and in vivo activation induces BAFF and APRIL expression in B cells. *J Immunol* **179**, 5947-5957 (2007).

70. Smulski, C.R. & Eibel, H. BAFF and BAFF-Receptor in B Cell Selection and Survival. *Front Immunol* **9**, 2285 (2018).

71. Mackay, F. & Schneider, P. Cracking the BAFF code. *Nat Rev Immunol* **9**, 491-502 (2009).

72. Claudio, E., Brown, K., Park, S., Wang, H. & Siebenlist, U. BAFF-induced NEMO-independent processing of NF-kappa B2 in maturing B cells. *Nat Immunol* **3**, 958-965 (2002).

73. Kayagaki, N. *et al.* BAFF/BLyS receptor 3 binds the B cell survival factor BAFF ligand through a discrete surface loop and promotes processing of NF-kappaB2. *Immunity* **17**, 515-524 (2002).

74. Schiemann, B. *et al.* An essential role for BAFF in the normal development of B cells through a BCMA-independent pathway. *Science* **293**, 2111-2114 (2001).

75. Hoek, K.L., Carlesso, G., Clark, E.S. & Khan, W.N. Absence of mature peripheral B cell populations in mice with concomitant defects in B cell receptor and BAFF-R signaling. *J Immunol* **183**, 5630-5643 (2009).

76. Vincent, F.B., Saulep-Easton, D., Figgett, W.A., Fairfax, K.A. & Mackay, F. The BAFF/APRIL system: emerging functions beyond B cell biology and autoimmunity. *Cytokine Growth Factor Rev* **24**, 203-215 (2013).

77. Hsu, B.L., Harless, S.M., Lindsley, R.C., Hilbert, D.M. & Cancro, M.P. Cutting edge: BLyS enables survival of transitional and mature B cells through distinct mediators. *J Immunol* **168**, 5993-5996 (2002).

78. Mihalcik, S.A., Huddleston, P.M., 3rd, Wu, X. & Jelinek, D.F. The structure of the TNFRSF13C promoter enables differential expression of BAFF-R during B cell ontogeny and terminal differentiation. *J Immunol* **185**, 1045-1054 (2010).

79. Smith, S.H. & Cancro, M.P. Cutting edge: B cell receptor signals regulate BLyS receptor levels in mature B cells and their immediate progenitors. *J Immunol* **170**, 5820-5823 (2003).

80. Rowland, S.L., Leahy, K.F., Halverson, R., Torres, R.M. & Pelanda, R. BAFF receptor signaling aids the differentiation of immature B cells into transitional B cells following tonic BCR signaling. *J Immunol* **185**, 4570-4581 (2010).

81. Batten, M. *et al.* BAFF mediates survival of peripheral immature B lymphocytes. *J Exp Med* **192**, 1453-1466 (2000).

82. Castigli, E. *et al.* TACI and BAFF-R mediate isotype switching in B cells. *J Exp Med* **201**, 35-39 (2005).

83. Royston, I., Majda, J.A., Baird, S.M., Meserve, B.L. & Griffiths, J.C. Human T cell antigens defined by monoclonal antibodies: the 65,000-dalton antigen of T cells

(T65) is also found on chronic lymphocytic leukemia cells bearing surface immunoglobulin. *J Immunol* **125**, 725-731 (1980).

84. Wang, C.Y., Good, R.A., Ammirati, P., Dymbort, G. & Evans, R.L. Identification of a p69,71 complex expressed on human T cells sharing determinants with B-type chronic lymphatic leukemic cells. *J Exp Med* **151**, 1539-1544 (1980).

85. Lanier, L.L., Warner, N.L., Ledbetter, J.A. & Herzenberg, L.A. Expression of Lyt-1 antigen on certain murine B cell lymphomas. *J Exp Med* **153**, 998-1003 (1981).

86. Hayakawa, K., Hardy, R.R., Parks, D.R. & Herzenberg, L.A. The "Ly-1 B" cell subpopulation in normal immunodefective, and autoimmune mice. *J Exp Med* **157**, 202-218 (1983).

87. Kantor, A.B., Stall, A.M., Adams, S., Herzenberg, L.A. & Herzenberg, L.A. Differential development of progenitor activity for three B-cell lineages. *Proc Natl Acad Sci U S A* **89**, 3320-3324 (1992).

88. Stall, A.M., Adams, S., Herzenberg, L.A. & Kantor, A.B. Characteristics and development of the murine B-1b (Ly-1 B sister) cell population. *Ann N Y Acad Sci* **651**, 33-43 (1992).

89. Haas, K.M., Poe, J.C., Steeber, D.A. & Tedder, T.F. B-1a and B-1b cells exhibit distinct developmental requirements and have unique functional roles in innate and adaptive immunity to S. pneumoniae. *Immunity* **23**, 7-18 (2005).

90. Wells, S.M., Kantor, A.B. & Stall, A.M. CD43 (S7) expression identifies peripheral B cell subsets. *J Immunol* **153**, 5503-5515 (1994).

91. Baumgarth, N. A Hard(y) Look at B-1 Cell Development and Function. *J Immunol* **199**, 3387-3394 (2017).

92. Stall, A.M., Wells, S.M. & Lam, K.P. B-1 cells: unique origins and functions. *Semin Immunol* **8**, 45-59 (1996).

93. Kantor, A.B., Merrill, C.E., Herzenberg, L.A. & Hillson, J.L. An unbiased analysis of V(H)-D-J(H) sequences from B-1a, B-1b, and conventional B cells. *J Immunol* **158**, 1175-1186 (1997).

94. Hardy, R.R., Carmack, C.E., Shinton, S.A., Riblet, R.J. & Hayakawa, K. A single VH gene is utilized predominantly in anti-BrMRBC hybridomas derived from purified Ly-1 B cells. Definition of the VH11 family. *J Immunol* **142**, 3643-3651 (1989).

95. Hayakawa, K., Carmack, C.E., Hyman, R. & Hardy, R.R. Natural autoantibodies to thymocytes: origin, VH genes, fine specificities, and the role of Thy-1 glycoprotein. *J Exp Med* **172**, 869-878 (1990).

96. Wong, J.B. *et al.* B-1a cells acquire their unique characteristics by bypassing the pre-BCR selection stage. *Nat Commun* **10**, 4768 (2019).

97. Kitamura, D. *et al.* A critical role of lambda 5 protein in B cell development. *Cell* **69**, 823-831 (1992).

98. Wasserman, R. *et al.* A novel mechanism for B cell repertoire maturation based on response by B cell precursors to pre-B receptor assembly. *J Exp Med* **187**, 259-264 (1998).

99. Keenan, R.A. *et al.* Censoring of autoreactive B cell development by the pre-B cell receptor. *Science* **321**, 696-699 (2008).

100. Briles, D.E., Forman, C., Hudak, S. & Claflin, J.L. Anti-phosphorylcholine antibodies of the T15 idiotype are optimally protective against Streptococcus pneumoniae. *J Exp Med* **156**, 1177-1185 (1982).

101. Boes, M., Prodeus, A.P., Schmidt, T., Carroll, M.C. & Chen, J. A critical role of natural immunoglobulin M in immediate defense against systemic bacterial infection. *J Exp Med* **188**, 2381-2386 (1998).

102. Gil-Cruz, C. *et al.* The porin OmpD from nontyphoidal Salmonella is a key target for a protective B1b cell antibody response. *Proc Natl Acad Sci U S A* **106**, 9803-9808 (2009).

103. Choi, Y.S. & Baumgarth, N. Dual role for B-1a cells in immunity to influenza virus infection. *J Exp Med* **205**, 3053-3064 (2008).

104. Colombo, M.J. & Alugupalli, K.R. Complement factor H-binding protein, a putative virulence determinant of Borrelia hermsii, is an antigenic target for protective B1b lymphocytes. *J Immunol* **180**, 4858-4864 (2008).

105. Baumgarth, N. B-1 Cell Heterogeneity and the Regulation of Natural and Antigen-Induced IgM Production. *Front Immunol* **7**, 324 (2016).

106. O'Garra, A. *et al.* Ly-1 B (B-1) cells are the main source of B cell-derived interleukin 10. *Eur J Immunol* **22**, 711-717 (1992).

107. Arcanjo, A.F. *et al.* B-1 cells modulate the murine macrophage response to Leishmania major infection. *World J Biol Chem* **8**, 151-162 (2017).

108. Gonzaga, W.F., Xavier, V., Vivanco, B.C., Lopes, J.D. & Xander, P. B-1 cells contribute to susceptibility in experimental infection with Leishmania (Leishmania) chagasi. *Parasitology* **142**, 1506-1515 (2015).

109. Jacobsen, K. & Osmond, D.G. Microenvironmental organization and stromal cell associations of B lymphocyte precursor cells in mouse bone marrow. *Eur J Immunol* **20**, 2395-2404 (1990).

110. Loder, F. *et al.* B cell development in the spleen takes place in discrete steps and is determined by the quality of B cell receptor-derived signals. *J Exp Med* **190**, 75-89 (1999).

111. Carsetti, R., Rosado, M.M. & Wardmann, H. Peripheral development of B cells in mouse and man. *Immunol Rev* **197**, 179-191 (2004).

112. Carsetti, R., Kohler, G. & Lamers, M.C. Transitional B cells are the target of negative selection in the B cell compartment. *J Exp Med* **181**, 2129-2140 (1995).

113. Su, T.T. & Rawlings, D.J. Transitional B lymphocyte subsets operate as distinct checkpoints in murine splenic B cell development. *J Immunol* **168**, 2101-2110 (2002).

114. Petro, J.B. *et al.* Transitional type 1 and 2 B lymphocyte subsets are differentially responsive to antigen receptor signaling. *J Biol Chem* **277**, 48009-48019 (2002).

115. Teague, B.N. *et al.* Cutting edge: Transitional T3 B cells do not give rise to mature B cells, have undergone selection, and are reduced in murine lupus. *J Immunol* **178**, 7511-7515 (2007).

116. Merrell, K.T. *et al.* Identification of anergic B cells within a wild-type repertoire. *Immunity* **25**, 953-962 (2006).

117. Srivastava, B., Lindsley, R.C., Nikbakht, N. & Allman, D. Models for peripheral B cell development and homeostasis. *Semin Immunol* **17**, 175-182 (2005).

118. Pillai, S., Cariappa, A. & Moran, S.T. Positive selection and lineage commitment during peripheral B-lymphocyte development. *Immunol Rev* **197**, 206-218 (2004).

119. Bronte, V. & Pittet, M.J. The spleen in local and systemic regulation of immunity. *Immunity* **39**, 806-818 (2013).

120. Mebius, R.E. & Kraal, G. Structure and function of the spleen. *Nat Rev Immunol* **5**, 606-616 (2005).

121. Hendricks, J., Bos, N.A. & Kroese, F.G.M. Heterogeneity of Memory Marginal Zone B Cells. *Crit Rev Immunol* **38**, 145-158 (2018).

122. N, A.G. *et al.* The nuclear receptor LXRalpha controls the functional specialization of splenic macrophages. *Nat Immunol* **14**, 831-839 (2013).

123. Cariappa, A., Chase, C., Liu, H., Russell, P. & Pillai, S. Naive recirculating B cells mature simultaneously in the spleen and bone marrow. *Blood* **109**, 2339-2345 (2007).

124. Lindsley, R.C., Thomas, M., Srivastava, B. & Allman, D. Generation of peripheral B cells occurs via two spatially and temporally distinct pathways. *Blood* **109**, 2521-2528 (2007).

125. Forster, R. *et al.* A putative chemokine receptor, BLR1, directs B cell migration to defined lymphoid organs and specific anatomic compartments of the spleen. *Cell* **87**, 1037-1047 (1996).

126. Pillai, S. & Cariappa, A. The follicular versus marginal zone B lymphocyte cell fate decision. *Nat Rev Immunol* **9**, 767-777 (2009).

127. Arnon, T.I., Horton, R.M., Grigorova, I.L. & Cyster, J.G. Visualization of splenic marginal zone B-cell shuttling and follicular B-cell egress. *Nature* **493**, 684-688 (2013).

128. Cinamon, G. *et al.* Sphingosine 1-phosphate receptor 1 promotes B cell localization in the splenic marginal zone. *Nat Immunol* **5**, 713-720 (2004).

129. Xiong, Y., Yang, P., Proia, R.L. & Hla, T. Erythrocyte-derived sphingosine 1-phosphate is essential for vascular development. *J Clin Invest* **124**, 4823-4828 (2014).

130. Pappu, R. *et al.* Promotion of lymphocyte egress into blood and lymph by distinct sources of sphingosine-1-phosphate. *Science* **316**, 295-298 (2007).

131. Venkataraman, K. *et al.* Vascular endothelium as a contributor of plasma sphingosine 1-phosphate. *Circ Res* **102**, 669-676 (2008).

132. Pham, T.H. *et al.* Lymphatic endothelial cell sphingosine kinase activity is required for lymphocyte egress and lymphatic patterning. *J Exp Med* **207**, 17-27 (2010).

133. Lu, T.T. & Cyster, J.G. Integrin-mediated long-term B cell retention in the splenic marginal zone. *Science* **297**, 409-412 (2002).

134. Girkontaite, I. *et al.* The sphingosine-1-phosphate (S1P) lysophospholipid receptor S1P3 regulates MAdCAM-1+ endothelial cells in splenic marginal sinus organization. *J Exp Med* **200**, 1491-1501 (2004).

135. Liu, Y.J., Zhang, J., Lane, P.J., Chan, E.Y. & MacLennan, I.C. Sites of specific B cell activation in primary and secondary responses to T cell-dependent and T cell-independent antigens. *Eur J Immunol* **21**, 2951-2962 (1991).

136. Cinamon, G., Zachariah, M.A., Lam, O.M., Foss, F.W., Jr. & Cyster, J.G. Follicular shuttling of marginal zone B cells facilitates antigen transport. *Nat Immunol* **9**, 54-62 (2008).

137. King, I.L. *et al.* Invariant natural killer T cells direct B cell responses to cognate lipid antigen in an IL-21-dependent manner. *Nat Immunol* **13**, 44-50 (2011).

138. Wen, L. *et al.* Evidence of marginal-zone B cell-positive selection in spleen. *Immunity* **23**, 297-308 (2005).

139. Cerutti, A., Cols, M. & Puga, I. Marginal zone B cells: virtues of innate-like antibody-producing lymphocytes. *Nat Rev Immunol* **13**, 118-132 (2013).

140. Martin, F., Oliver, A.M. & Kearney, J.F. Marginal zone and B1 B cells unite in the early response against T-independent blood-borne particulate antigens. *Immunity* **14**, 617-629 (2001).

141. Guinamard, R., Okigaki, M., Schlessinger, J. & Ravetch, J.V. Absence of marginal zone B cells in Pyk-2-deficient mice defines their role in the humoral response. *Nat Immunol* **1**, 31-36 (2000).

142. Puga, I. *et al.* B cell-helper neutrophils stimulate the diversification and production of immunoglobulin in the marginal zone of the spleen. *Nat Immunol* **13**, 170-180 (2011).

143. Weller, S. *et al.* Human blood IgM "memory" B cells are circulating splenic marginal zone B cells harboring a prediversified immunoglobulin repertoire. *Blood* **104**, 3647-3654 (2004).

144. Spencer, J., Finn, T., Pulford, K.A., Mason, D.Y. & Isaacson, P.G. The human gut contains a novel population of B lymphocytes which resemble marginal zone cells. *Clin Exp Immunol* **62**, 607-612 (1985).

145. Dono, M. *et al.* Heterogeneity of tonsillar subepithelial B lymphocytes, the splenic marginal zone equivalents. *J Immunol* **164**, 5596-5604 (2000).

146. Tierens, A., Delabie, J., Michiels, L., Vandenberghe, P. & De Wolf-Peeters, C. Marginal-zone B cells in the human lymph node and spleen show somatic hypermutations and display clonal expansion. *Blood* **93**, 226-234 (1999).

147. Dunn-Walters, D.K., Isaacson, P.G. & Spencer, J. Analysis of mutations in immunoglobulin heavy chain variable region genes of microdissected marginal zone (MGZ) B cells suggests that the MGZ of human spleen is a reservoir of memory B cells. *J Exp Med* **182**, 559-566 (1995).

148. Seifert, M. & Kuppers, R. Molecular footprints of a germinal center derivation of human IgM+(IgD+)CD27+ B cells and the dynamics of memory B cell generation. *J Exp Med* **206**, 2659-2669 (2009).

149. Berkowska, M.A. *et al.* Human memory B cells originate from three distinct germinal center-dependent and -independent maturation pathways. *Blood* **118**, 2150-2158 (2011).

150. Pal Singh, S., Dammeijer, F. & Hendriks, R.W. Role of Bruton's tyrosine kinase in B cells and malignancies. *Mol Cancer* **17**, 57 (2018).

151. Khan, W.N. *et al.* Defective B cell development and function in Btk-deficient mice. *Immunity* **3**, 283-299 (1995).

152. Hardy, R.R., Hayakawa, K., Parks, D.R. & Herzenberg, L.A. Demonstration of B-cell maturation in X-linked immunodeficient mice by simultaneous three-colour immunofluorescence. *Nature* **306**, 270-272 (1983).

153. Kurosaki, T. *et al.* Regulation of the phospholipase C-gamma2 pathway in B cells. *Immunol Rev* **176**, 19-29 (2000).

154. Hikida, M., Johmura, S., Hashimoto, A., Takezaki, M. & Kurosaki, T. Coupling between B cell receptor and phospholipase C-gamma2 is essential for mature B cell development. *J Exp Med* **198**, 581-589 (2003).

155. Wen, R. *et al.* Phospholipase Cgamma2 provides survival signals via Bcl2 and A1 in different subpopulations of B cells. *J Biol Chem* **278**, 43654-43662 (2003).

156. Pani, G., Siminovitch, K.A. & Paige, C.J. The motheaten mutation rescues B cell signaling and development in CD45-deficient mice. *J Exp Med* **186**, 581-588 (1997).

157. Cariappa, A. *et al.* The follicular versus marginal zone B lymphocyte cell fate decision is regulated by Aiolos, Btk, and CD21. *Immunity* **14**, 603-615 (2001).

158. Wang, J.H. *et al.* Aiolos regulates B cell activation and maturation to effector state. *Immunity* **9**, 543-553 (1998).

159. Samardzic, T. *et al.* Reduction of marginal zone B cells in CD22-deficient mice. *Eur J Immunol* **32**, 561-567 (2002).

160. Cariappa, A. *et al.* B cell antigen receptor signal strength and peripheral B cell development are regulated by a 9-O-acetyl sialic acid esterase. *J Exp Med* **206**, 125-138 (2009).

161. Kaisho, T. *et al.* IkappaB kinase alpha is essential for mature B cell development and function. *J Exp Med* **193**, 417-426 (2001).

162. Senftleben, U. *et al.* Activation by IKKalpha of a second, evolutionary conserved, NF-kappa B signaling pathway. *Science* **293**, 1495-1499 (2001).

163. Cariappa, A., Liou, H.C., Horwitz, B.H. & Pillai, S. Nuclear factor kappa B is required for the development of marginal zone B lymphocytes. *J Exp Med* **192**, 1175-1182 (2000).

164. Tanigaki, K. *et al.* Notch-RBP-J signaling is involved in cell fate determination of marginal zone B cells. *Nat Immunol* **3**, 443-450 (2002).

165. Saito, T. *et al.* Notch2 is preferentially expressed in mature B cells and indispensable for marginal zone B lineage development. *Immunity* **18**, 675-685 (2003).

166. Hammad, H. *et al.* Transitional B cells commit to marginal zone B cell fate by Taok3-mediated surface expression of ADAM10. *Nat Immunol* **18**, 313-320 (2017).

167. Oyama, T. *et al.* Mastermind-1 is required for Notch signal-dependent steps in lymphocyte development in vivo. *Proc Natl Acad Sci U S A* **104**, 9764-9769 (2007).

168. Wu, L., Maillard, I., Nakamura, M., Pear, W.S. & Griffin, J.D. The transcriptional coactivator Maml1 is required for Notch2-mediated marginal zone B-cell development. *Blood* **110**, 3618-3623 (2007).

169. Hozumi, K. *et al.* Delta-like 1 is necessary for the generation of marginal zone B cells but not T cells in vivo. *Nat Immunol* **5**, 638-644 (2004).

170. Huang, Z., Nie, L., Xu, M. & Sun, X.H. Notch-induced E2A degradation requires CHIP and Hsc70 as novel facilitators of ubiquitination. *Mol Cell Biol* **24**, 8951-8962 (2004).

171. Newman, R. *et al.* Maintenance of the marginal-zone B cell compartment specifically requires the RNA-binding protein ZFP36L1. *Nat Immunol* **18**, 683-693 (2017).

172. Feng, J. *et al.* IFN regulatory factor 8 restricts the size of the marginal zone and follicular B cell pools. *J Immunol* **186**, 1458-1466 (2011).

173. Hart, G.T., Wang, X., Hogquist, K.A. & Jameson, S.C. Kruppel-like factor 2 (KLF2) regulates B-cell reactivity, subset differentiation, and trafficking molecule expression. *Proc Natl Acad Sci U S A* **108**, 716-721 (2011).

174. Winkelmann, R. *et al.* B cell homeostasis and plasma cell homing controlled by Kruppel-like factor 2. *Proc Natl Acad Sci U S A* **108**, 710-715 (2011).

175. Vu, T.T. *et al.* Impaired B cell development in the absence of Kruppel-like factor 3. *J Immunol* **187**, 5032-5042 (2011).

176. King, J.K. *et al.* Regulation of Marginal Zone B-Cell Differentiation by MicroRNA-146a. *Front Immunol* **7**, 670 (2016).

177. Kramer, N.J. *et al.* Altered lymphopoiesis and immunodeficiency in miR-142 null mice. *Blood* **125**, 3720-3730 (2015).

178. Belver, L., de Yebenes, V.G. & Ramiro, A.R. MicroRNAs prevent the generation of autoreactive antibodies. *Immunity* **33**, 713-722 (2010).

179. Taganov, K.D., Boldin, M.P., Chang, K.J. & Baltimore, D. NF-kappaB-dependent induction of microRNA miR-146, an inhibitor targeted to signaling proteins of innate immune responses. *Proc Natl Acad Sci U S A* **103**, 12481-12486 (2006).

180. Weigert, M.G., Cesari, I.M., Yonkovich, S.J. & Cohn, M. Variability in the lambda light chain sequences of mouse antibody. *Nature* **228**, 1045-1047 (1970).

181. Muramatsu, M. *et al.* Class switch recombination and hypermutation require activation-induced cytidine deaminase (AID), a potential RNA editing enzyme. *Cell* **102**, 553-563 (2000).

182. Eisen, H.N. & Siskind, G.W. Variations in Affinities of Antibodies during the Immune Response. *Biochemistry* **3**, 996-1008 (1964).

183. Allen, C.D., Okada, T. & Cyster, J.G. Germinal-center organization and cellular dynamics. *Immunity* **27**, 190-202 (2007).

184. Allen, C.D. *et al.* Germinal center dark and light zone organization is mediated by CXCR4 and CXCR5. *Nat Immunol* **5**, 943-952 (2004).

185. Bannard, O. *et al.* Germinal center centroblasts transition to a centrocyte phenotype according to a timed program and depend on the dark zone for effective selection. *Immunity* **39**, 912-924 (2013).

186. Mesin, L., Ersching, J. & Victora, G.D. Germinal Center B Cell Dynamics. *Immunity* **45**, 471-482 (2016).

187. Cyster, J.G. B cell follicles and antigen encounters of the third kind. *Nat Immunol* **11**, 989-996 (2010).

188. Heesters, B.A., Myers, R.C. & Carroll, M.C. Follicular dendritic cells: dynamic antigen libraries. *Nat Rev Immunol* **14**, 495-504 (2014).

189. Wang, X. *et al.* Follicular dendritic cells help establish follicle identity and promote B cell retention in germinal centers. *J Exp Med* **208**, 2497-2510 (2011).

190. Garin, A. *et al.* Toll-like receptor 4 signaling by follicular dendritic cells is pivotal for germinal center onset and affinity maturation. *Immunity* **33**, 84-95 (2010).

191. Heesters, B.A. *et al.* Endocytosis and recycling of immune complexes by follicular dendritic cells enhances B cell antigen binding and activation. *Immunity* **38**, 1164-1175 (2013).

192. Gatto, D., Paus, D., Basten, A., Mackay, C.R. & Brink, R. Guidance of B cells by the orphan G protein-coupled receptor EBI2 shapes humoral immune responses. *Immunity* **31**, 259-269 (2009).

193. Hannedouche, S. *et al.* Oxysterols direct immune cell migration via EBI2. *Nature* **475**, 524-527 (2011).

194. Pereira, J.P., Kelly, L.M., Xu, Y. & Cyster, J.G. EBI2 mediates B cell segregation between the outer and centre follicle. *Nature* **460**, 1122-1126 (2009).

195. Green, J.A. *et al.* The sphingosine 1-phosphate receptor S1P(2) maintains the homeostasis of germinal center B cells and promotes niche confinement. *Nat Immunol* **12**, 672-680 (2011).

196. Garside, P. *et al.* Visualization of specific B and T lymphocyte interactions in the lymph node. *Science* **281**, 96-99 (1998).

197. Cyster, J.G. & Allen, C.D.C. B Cell Responses: Cell Interaction Dynamics and Decisions. *Cell* **177**, 524-540 (2019).

198. Till, K.J., Pettitt, A.R. & Slupsky, J.R. Expression of functional sphingosine-1 phosphate receptor-1 is reduced by B cell receptor signaling and increased by inhibition of PI3 kinase delta but not SYK or BTK in chronic lymphocytic leukemia cells. *J Immunol* **194**, 2439-2446 (2015).

199. Crotty, S. T follicular helper cell differentiation, function, and roles in disease. *Immunity* **41**, 529-542 (2014).

200. Stebegg, M. *et al.* Regulation of the Germinal Center Response. *Front Immunol* **9**, 2469 (2018).

201. Paus, D. *et al.* Antigen recognition strength regulates the choice between extrafollicular plasma cell and germinal center B cell differentiation. *J Exp Med* **203**, 1081-1091 (2006).

202. Kurosaki, T., Kometani, K. & Ise, W. Memory B cells. *Nat Rev Immunol* **15**, 149-159 (2015).

203. Zaretsky, I. *et al.* ICAMs support B cell interactions with T follicular helper cells and promote clonal selection. *J Exp Med* **214**, 3435-3448 (2017).

204. Yusuf, I. *et al.* Germinal center T follicular helper cell IL-4 production is dependent on signaling lymphocytic activation molecule receptor (CD150). *J Immunol* **185**, 190-202 (2010).

205. Gonzalez, D.G. *et al.* Nonredundant Roles of IL-21 and IL-4 in the Phased Initiation of Germinal Center B Cells and Subsequent Self-Renewal Transitions. *J Immunol* **201**, 3569-3579 (2018).

206. Muramatsu, M. *et al.* Specific expression of activation-induced cytidine deaminase (AID), a novel member of the RNA-editing deaminase family in germinal center B cells. *J Biol Chem* **274**, 18470-18476 (1999).

207. Linterman, M.A. *et al.* IL-21 acts directly on B cells to regulate Bcl-6 expression and germinal center responses. *J Exp Med* **207**, 353-363 (2010).

208. Liu, D. *et al.* T-B-cell entanglement and ICOSL-driven feed-forward regulation of germinal centre reaction. *Nature* **517**, 214-218 (2015).

209. Shi, J. *et al.* PD-1 Controls Follicular T Helper Cell Positioning and Function. *Immunity* **49**, 264-274 e264 (2018).

210. Chung, Y. *et al.* Follicular regulatory T cells expressing Foxp3 and Bcl-6 suppress germinal center reactions. *Nat Med* **17**, 983-988 (2011).

211. Linterman, M.A. *et al.* Foxp3+ follicular regulatory T cells control the germinal center response. *Nat Med* **17**, 975-982 (2011).

212. Wing, J.B., Tekguc, M. & Sakaguchi, S. Control of Germinal Center Responses by T-Follicular Regulatory Cells. *Front Immunol* **9**, 1910 (2018).

213. Sage, P.T., Paterson, A.M., Lovitch, S.B. & Sharpe, A.H. The coinhibitory receptor CTLA-4 controls B cell responses by modulating T follicular helper, T follicular regulatory, and T regulatory cells. *Immunity* **41**, 1026-1039 (2014).

214. Wing, J.B., Ise, W., Kurosaki, T. & Sakaguchi, S. Regulatory T cells control antigen-specific expansion of Tfh cell number and humoral immune responses via the coreceptor CTLA-4. *Immunity* **41**, 1013-1025 (2014).

215. Victora, G.D. & Nussenzweig, M.C. Germinal centers. *Annu Rev Immunol* **30**, 429-457 (2012).

216. Pavri, R. *et al.* Activation-induced cytidine deaminase targets DNA at sites of RNA polymerase II stalling by interaction with Spt5. *Cell* **143**, 122-133 (2010).

217. Vaidyanathan, B. *et al.* The aryl hydrocarbon receptor controls cell-fate decisions in B cells. *J Exp Med* **214**, 197-208 (2017).

218. Kawabe, T. *et al.* The immune responses in CD40-deficient mice: impaired immunoglobulin class switching and germinal center formation. *Immunity* **1**, 167-178 (1994).

219. Snapper, C.M. & Mond, J.J. Towards a comprehensive view of immunoglobulin class switching. *Immunol Today* **14**, 15-17 (1993).

220. Klein, U. & Dalla-Favera, R. Germinal centres: role in B-cell physiology and malignancy. *Nat Rev Immunol* **8**, 22-33 (2008).

221. Roco, J.A. *et al.* Class-Switch Recombination Occurs Infrequently in Germinal Centers. *Immunity* **51**, 337-350 e337 (2019).

222. Kepler, T.B. & Perelson, A.S. Cyclic re-entry of germinal center B cells and the efficiency of affinity maturation. *Immunol Today* **14**, 412-415 (1993).

223. Schwickert, T.A. *et al.* In vivo imaging of germinal centres reveals a dynamic open structure. *Nature* **446**, 83-87 (2007).

224. Gitlin, A.D., Shulman, Z. & Nussenzweig, M.C. Clonal selection in the germinal centre by regulated proliferation and hypermutation. *Nature* **509**, 637-640 (2014).

225. Meyer-Hermann, M. *et al.* A theory of germinal center B cell selection, division, and exit. *Cell Rep* **2**, 162-174 (2012).

226. Batista, F.D. & Neuberger, M.S. B cells extract and present immobilized antigen: implications for affinity discrimination. *EMBO J* **19**, 513-520 (2000).

227. Victora, G.D. *et al.* Germinal center dynamics revealed by multiphoton microscopy with a photoactivatable fluorescent reporter. *Cell* **143**, 592-605 (2010).

228. Shulman, Z. *et al.* Dynamic signaling by T follicular helper cells during germinal center B cell selection. *Science* **345**, 1058-1062 (2014).

229. Gitlin, A.D. *et al.* HUMORAL IMMUNITY. T cell help controls the speed of the cell cycle in germinal center B cells. *Science* **349**, 643-646 (2015).

230. Goenka, R. *et al.* Local BLyS production by T follicular cells mediates retention of high affinity B cells during affinity maturation. *J Exp Med* **211**, 45-56 (2014).

231. Bannard, O. *et al.* Ubiquitin-mediated fluctuations in MHC class II facilitate efficient germinal center B cell responses. *J Exp Med* **213**, 993-1009 (2016).

232. Zhang, Y. *et al.* Germinal center B cells govern their own fate via antibody feedback. *J Exp Med* **210**, 457-464 (2013).

233. Chan, T.D. *et al.* Elimination of germinal-center-derived self-reactive B cells is governed by the location and concentration of self-antigen. *Immunity* **37**, 893-904 (2012).

234. Sabouri, Z. *et al.* Redemption of autoantibodies on anergic B cells by variable-region glycosylation and mutation away from self-reactivity. *Proc Natl Acad Sci U S A* **111**, E2567-2575 (2014).

235. Jacob, J., Kassir, R. & Kelsoe, G. In situ studies of the primary immune response to (4-hydroxy-3-nitrophenyl)acetyl. I. The architecture and dynamics of responding cell populations. *J Exp Med* **173**, 1165-1175 (1991).

236. Tas, J.M. *et al.* Visualizing antibody affinity maturation in germinal centers. *Science* **351**, 1048-1054 (2016).

237. Adachi, Y. *et al.* Distinct germinal center selection at local sites shapes memory B cell response to viral escape. *J Exp Med* **212**, 1709-1723 (2015).

238. Nutt, S.L., Hodgkin, P.D., Tarlinton, D.M. & Corcoran, L.M. The generation of antibody-secreting plasma cells. *Nat Rev Immunol* **15**, 160-171 (2015).

239. Krautler, N.J. *et al.* Differentiation of germinal center B cells into plasma cells is initiated by high-affinity antigen and completed by Tfh cells. *J Exp Med* **214**, 1259-1267 (2017).

240. Haniuda, K., Fukao, S., Kodama, T., Hasegawa, H. & Kitamura, D. Autonomous membrane IgE signaling prevents IgE-memory formation. *Nat Immunol* **17**, 1109-1117 (2016).

241. Todd, D.J. *et al.* XBP1 governs late events in plasma cell differentiation and is not required for antigen-specific memory B cell development. *J Exp Med* **206**, 2151-2159 (2009).

242. Taubenheim, N. *et al.* High rate of antibody secretion is not integral to plasma cell differentiation as revealed by XBP-1 deficiency. *J Immunol* **189**, 3328-3338 (2012).

243. Kallies, A. *et al.* Plasma cell ontogeny defined by quantitative changes in blimp-1 expression. *J Exp Med* **200**, 967-977 (2004).

244. Kallies, A. *et al.* Initiation of plasma-cell differentiation is independent of the transcription factor Blimp-1. *Immunity* **26**, 555-566 (2007).

245. Minnich, M. *et al.* Multifunctional role of the transcription factor Blimp-1 in coordinating plasma cell differentiation. *Nat Immunol* **17**, 331-343 (2016).

246. Sciammas, R. *et al.* Graded expression of interferon regulatory factor-4 coordinates isotype switching with plasma cell differentiation. *Immunity* **25**, 225-236 (2006).

247. Ochiai, K. *et al.* Transcriptional regulation of germinal center B and plasma cell fates by dynamical control of IRF4. *Immunity* **38**, 918-929 (2013).

248. Low, M.S.Y. *et al.* IRF4 Activity Is Required in Established Plasma Cells to Regulate Gene Transcription and Mitochondrial Homeostasis. *Cell Rep* **29**, 2634-2645 e2635 (2019).

249. Wang, Y. & Bhattacharya, D. Adjuvant-specific regulation of long-term antibody responses by ZBTB20. *J Exp Med* **211**, 841-856 (2014).

250. Nguyen, D.C., Joyner, C.J., Sanz, I. & Lee, F.E. Factors Affecting Early Antibody Secreting Cell Maturation Into Long-Lived Plasma Cells. *Front Immunol* **10**, 2138 (2019).

251. Wang, Y. *et al.* Germinal-center development of memory B cells driven by IL-9 from follicular helper T cells. *Nat Immunol* **18**, 921-930 (2017).

252. Kometani, K. *et al.* Repression of the transcription factor Bach2 contributes to predisposition of IgG1 memory B cells toward plasma cell differentiation. *Immunity* **39**, 136-147 (2013).

253. Toyama, H. *et al.* Memory B cells without somatic hypermutation are generated from Bcl6-deficient B cells. *Immunity* **17**, 329-339 (2002).

254. Weisel, F. & Shlomchik, M. Memory B Cells of Mice and Humans. *Annu Rev Immunol* **35**, 255-284 (2017).

255. Allie, S.R. *et al.* The establishment of resident memory B cells in the lung requires local antigen encounter. *Nat Immunol* **20**, 97-108 (2019).

256. Moran, I. *et al.* Memory B cells are reactivated in subcapsular proliferative foci of lymph nodes. *Nat Commun* **9**, 3372 (2018).

257. Tomayko, M.M., Steinel, N.C., Anderson, S.M. & Shlomchik, M.J. Cutting edge: Hierarchy of maturity of murine memory B cell subsets. *J Immunol* **185**, 7146-7150 (2010).

258. Zuccarino-Catania, G.V. *et al.* CD80 and PD-L2 define functionally distinct memory B cell subsets that are independent of antibody isotype. *Nat Immunol* **15**, 631-637 (2014).

259. Mesin, L. *et al.* Restricted Clonality and Limited Germinal Center Reentry Characterize Memory B Cell Reactivation by Boosting. *Cell* **180**, 92-106 e111 (2020).

260. Chen, X. & Jensen, P.E. The role of B lymphocytes as antigen-presenting cells. *Arch Immunol Ther Exp (Warsz)* **56**, 77-83 (2008).

261. Lanzavecchia, A. Receptor-mediated antigen uptake and its effect on antigen presentation to class II-restricted T lymphocytes. *Annu Rev Immunol* **8**, 773-793 (1990).

262. Gondre-Lewis, T.A., Moquin, A.E. & Drake, J.R. Prolonged antigen persistence within nonterminal late endocytic compartments of antigen-specific B lymphocytes. *J Immunol* **166**, 6657-6664 (2001).

263. Bosma, A., Abdel-Gadir, A., Isenberg, D.A., Jury, E.C. & Mauri, C. Lipid-antigen presentation by CD1d(+) B cells is essential for the maintenance of invariant natural killer T cells. *Immunity* **36**, 477-490 (2012).

264. Oleinika, K. *et al.* CD1d-dependent immune suppression mediated by regulatory B cells through modulations of iNKT cells. *Nat Commun* **9**, 684 (2018).

265. Shen, P. & Fillatreau, S. Antibody-independent functions of B cells: a focus on cytokines. *Nat Rev Immunol* **15**, 441-451 (2015).

266. Harris, D.P. *et al.* Reciprocal regulation of polarized cytokine production by effector B and T cells. *Nat Immunol* **1**, 475-482 (2000).

267. Paul, C.C., Keller, J.R., Armpriester, J.M. & Baumann, M.A. Epstein-Barr virus transformed B lymphocytes produce interleukin-5. *Blood* **75**, 1400-1403 (1990).

268. Fu, Y.X., Huang, G., Wang, Y. & Chaplin, D.D. B lymphocytes induce the formation of follicular dendritic cell clusters in a lymphotoxin alpha-dependent fashion. *J Exp Med* **187**, 1009-1018 (1998).

269. Endres, R. *et al.* Mature follicular dendritic cell networks depend on expression of lymphotoxin beta receptor by radioresistant stromal cells and of lymphotoxin beta and tumor necrosis factor by B cells. *J Exp Med* **189**, 159-168 (1999).

270. Gonzalez, M., Mackay, F., Browning, J.L., Kosco-Vilbois, M.H. & Noelle, R.J. The sequential role of lymphotoxin and B cells in the development of splenic follicles. *J Exp Med* **187**, 997-1007 (1998).

271. Wojciechowski, W. *et al.* Cytokine-producing effector B cells regulate type 2 immunity to H. polygyrus. *Immunity* **30**, 421-433 (2009).

272. Wang, J. *et al.* Transgenic expression of granulocyte-macrophage colony-stimulating factor induces the differentiation and activation of a novel dendritic cell population in the lung. *Blood* **95**, 2337-2345 (2000).

273. Weber, G.F. *et al.* Pleural innate response activator B cells protect against pneumonia via a GM-CSF-IgM axis. *J Exp Med* **211**, 1243-1256 (2014).

274. Hilgendorf, I. *et al.* Innate response activator B cells aggravate atherosclerosis by stimulating T helper-1 adaptive immunity. *Circulation* **129**, 1677-1687 (2014).

275. Karnowski, A. *et al.* B and T cells collaborate in antiviral responses via IL-6, IL-21, and transcriptional activator and coactivator, Oct2 and OBF-1. *J Exp Med* **209**, 2049-2064 (2012).

276. Barr, T.A. *et al.* B cell depletion therapy ameliorates autoimmune disease through ablation of IL-6-producing B cells. *J Exp Med* **209**, 1001-1010 (2012).

277. Molnarfi, N. *et al.* MHC class II-dependent B cell APC function is required for induction of CNS autoimmunity independent of myelin-specific antibodies. *J Exp Med* **210**, 2921-2937 (2013).

278. Bermejo, D.A. *et al.* Trypanosoma cruzi trans-sialidase initiates a program independent of the transcription factors RORgammat and Ahr that leads to IL-17 production by activated B cells. *Nat Immunol* **14**, 514-522 (2013).

279. Menten, P., Wuyts, A. & Van Damme, J. Macrophage inflammatory protein-1. *Cytokine Growth Factor Rev* **13**, 455-481 (2002).

280. Menard, L.C. *et al.* B cells amplify IFN-gamma production by T cells via a TNF-alpha-mediated mechanism. *J Immunol* **179**, 4857-4866 (2007).

281. Bystry, R.S., Aluvihare, V., Welch, K.A., Kallikourdis, M. & Betz, A.G. B cells and professional APCs recruit regulatory T cells via CCL4. *Nat Immunol* **2**, 1126-1132 (2001).

282. Schaniel, C. *et al.* Activated murine B lymphocytes and dendritic cells produce a novel CC chemokine which acts selectively on activated T cells. *J Exp Med* **188**, 451-463 (1998).

283. Andrew, D.P. *et al.* STCP-1 (MDC) CC chemokine acts specifically on chronically activated Th2 lymphocytes and is produced by monocytes on stimulation with Th2 cytokines IL-4 and IL-13. *J Immunol* **161**, 5027-5038 (1998).

284. Iellem, A. *et al.* Unique chemotactic response profile and specific expression of chemokine receptors CCR4 and CCR8 by CD4(+)CD25(+) regulatory T cells. *J Exp Med* **194**, 847-853 (2001).

285. Nakayama, T. *et al.* Selective induction of Th2-attracting chemokines CCL17 and CCL22 in human B cells by latent membrane protein 1 of Epstein-Barr virus. *J Virol* **78**, 1665-1674 (2004).

286. Rosser, E.C. & Mauri, C. Regulatory B cells: origin, phenotype, and function. *Immunity* **42**, 607-612 (2015).

287. Turk, J.L., Parker, D. & Poulter, L.W. Functional aspects of the selective depletion of lymphoid tissue by cyclophosphamide. *Immunology* **23**, 493-501 (1972).

288. Katz, S.I., Parker, D., Sommer, G. & Turk, J.L. Suppressor cells in normal immunisation as a basic homeostatic phenomenon. *Nature* **248**, 612-614 (1974).

289. Neta, R. & Salvin, S.B. Specific suppression of delayed hypersensitivity: the possible presence of a suppressor B cell in the regulation of delayed hypersensitivity. *J Immunol* **113**, 1716-1725 (1974).

290. Wolf, S.D., Dittel, B.N., Hardardottir, F. & Janeway, C.A., Jr. Experimental autoimmune encephalomyelitis induction in genetically B cell-deficient mice. *J Exp Med* **184**, 2271-2278 (1996).

291. Mizoguchi, A., Mizoguchi, E., Takedatsu, H., Blumberg, R.S. & Bhan, A.K. Chronic intestinal inflammatory condition generates IL-10-producing regulatory B cell subset characterized by CD1d upregulation. *Immunity* **16**, 219-230 (2002).

292. Fillatreau, S., Sweenie, C.H., McGeachy, M.J., Gray, D. & Anderton, S.M. B cells regulate autoimmunity by provision of IL-10. *Nat Immunol* **3**, 944-950 (2002).

293. Mauri, C., Gray, D., Mushtaq, N. & Londei, M. Prevention of arthritis by interleukin 10-producing B cells. *J Exp Med* **197**, 489-501 (2003).

294. Constantinescu, C.S., Farooqi, N., O'Brien, K. & Gran, B. Experimental autoimmune encephalomyelitis (EAE) as a model for multiple sclerosis (MS). *Br J Pharmacol* **164**, 1079-1106 (2011).

295. Goodnow, C.C. *et al.* Altered immunoglobulin expression and functional silencing of self-reactive B lymphocytes in transgenic mice. *Nature* **334**, 676-682 (1988).

296. Yanaba, K., Bouaziz, J.D., Matsushita, T., Tsubata, T. & Tedder, T.F. The development and function of regulatory B cells expressing IL-10 (B10 cells) requires antigen receptor diversity and TLR signals. *J Immunol* **182**, 7459-7472 (2009).

297. Evans, J.G. *et al.* Novel suppressive function of transitional 2 B cells in experimental arthritis. *J Immunol* **178**, 7868-7878 (2007).

298. Zhang, J. *et al.* Positive selection of B10 cells is determined by BCR specificity and signaling strength. *Cell Immunol* **304-305**, 27-34 (2016).

299. Okkenhaug, K. *et al.* Impaired B and T cell antigen receptor signaling in p110delta PI 3-kinase mutant mice. *Science* **297**, 1031-1034 (2002).

300. Kennedy, R.J. *et al.* Interleukin 10-deficient colitis: new similarities to human inflammatory bowel disease. *Br J Surg* **87**, 1346-1351 (2000).

301. Matsumoto, M. *et al.* The calcium sensors STIM1 and STIM2 control B cell regulatory function through interleukin-10 production. *Immunity* **34**, 703-714 (2011).

302. Roos, J. *et al.* STIM1, an essential and conserved component of store-operated Ca2+ channel function. *J Cell Biol* **169**, 435-445 (2005).

303. Yanaba, K. *et al.* A regulatory B cell subset with a unique CD1dhiCD5+ phenotype controls T cell-dependent inflammatory responses. *Immunity* **28**, 639-650 (2008).

304. Watanabe, R. *et al.* Regulatory B cells (B10 cells) have a suppressive role in murine lupus: CD19 and B10 cell deficiency exacerbates systemic autoimmunity. *J Immunol* **184**, 4801-4809 (2010).

305. Matsushita, T., Yanaba, K., Bouaziz, J.D., Fujimoto, M. & Tedder, T.F. Regulatory B cells inhibit EAE initiation in mice while other B cells promote disease progression. *J Clin Invest* **118**, 3420-3430 (2008).

306. Yanaba, K. *et al.* IL-10-producing regulatory B10 cells inhibit intestinal injury in a mouse model. *Am J Pathol* **178**, 735-743 (2011).

307. Elgueta, R. *et al.* Molecular mechanism and function of CD40/CD40L engagement in the immune system. *Immunol Rev* **229**, 152-172 (2009).

308. Bishop, G.A. & Hostager, B.S. The CD40-CD154 interaction in B cell-T cell liaisons. *Cytokine Growth Factor Rev* **14**, 297-309 (2003).

309. Mizoguchi, E., Mizoguchi, A., Preffer, F.I. & Bhan, A.K. Regulatory role of mature B cells in a murine model of inflammatory bowel disease. *Int Immunol* **12**, 597-605 (2000).

310. Richard, M.L. & Gilkeson, G. Mouse models of lupus: what they tell us and what they don't. *Lupus Sci Med* **5**, e000199 (2018).

311. Blair, P.A. *et al.* Selective targeting of B cells with agonistic anti-CD40 is an efficacious strategy for the generation of induced regulatory T2-like B cells and for the suppression of lupus in MRL/lpr mice. *J Immunol* **182**, 3492-3502 (2009).

312. Yoshizaki, A. *et al.* Regulatory B cells control T-cell autoimmunity through IL-21-dependent cognate interactions. *Nature* **491**, 264-268 (2012).

313. Greenwald, R.J., Freeman, G.J. & Sharpe, A.H. The B7 family revisited. *Annu Rev Immunol* **23**, 515-548 (2005).

314. Mann, M.K., Maresz, K., Shriver, L.P., Tan, Y. & Dittel, B.N. B cell regulation of CD4+CD25+ T regulatory cells and IL-10 via B7 is essential for recovery from experimental autoimmune encephalomyelitis. *J Immunol* **178**, 3447-3456 (2007).

315. Hua, Z. & Hou, B. TLR signaling in B-cell development and activation. *Cell Mol Immunol* **10**, 103-106 (2013).

316. Barr, T.A., Brown, S., Ryan, G., Zhao, J. & Gray, D. TLR-mediated stimulation of APC: Distinct cytokine responses of B cells and dendritic cells. *Eur J Immunol* **37**, 3040-3053 (2007).

317. Zhou, M. *et al.* Tumor-released autophagosomes induce IL-10-producing B cells with suppressive activity on T lymphocytes via TLR2-MyD88-NF-kappaB signal pathway. *Oncoimmunology* **5**, e1180485 (2016).

318. Sayi, A. *et al.* TLR-2-activated B cells suppress Helicobacter-induced preneoplastic gastric immunopathology by inducing T regulatory-1 cells. *J Immunol* **186**, 878-890 (2011).

319. Tian, J. *et al.* Lipopolysaccharide-activated B cells down-regulate Th1 immunity and prevent autoimmune diabetes in nonobese diabetic mice. *J Immunol* **167**, 1081-1089 (2001).

320. Parekh, V.V. *et al.* B cells activated by lipopolysaccharide, but not by anti-Ig and anti-CD40 antibody, induce anergy in CD8+ T cells: role of TGF-beta 1. *J Immunol* **170**, 5897-5911 (2003).

321. Buenafe, A.C. & Bourdette, D.N. Lipopolysaccharide pretreatment modulates the disease course in experimental autoimmune encephalomyelitis. *J Neuroimmunol* **182**, 32-40 (2007).

322. Wang, Z., Zhou, Y., Yu, Y., He, K. & Cheng, L.M. Lipopolysaccharide preconditioning increased the level of regulatory B cells in the spleen after acute ischaemia/reperfusion in mice. *Brain Res* **1701**, 46-57 (2018).

323. Rosser, E.C. *et al.* Regulatory B cells are induced by gut microbiota-driven interleukin-1beta and interleukin-6 production. *Nat Med* **20**, 1334-1339 (2014).

324. Neves, P. *et al.* Signaling via the MyD88 adaptor protein in B cells suppresses protective immunity during Salmonella typhimurium infection. *Immunity* **33**, 777-790 (2010).

325. Lampropoulou, V. *et al.* TLR-activated B cells suppress T cell-mediated autoimmunity. *J Immunol* **180**, 4763-4773 (2008).

326. Bankoti, R., Gupta, K., Levchenko, A. & Stager, S. Marginal zone B cells regulate antigen-specific T cell responses during infection. *J Immunol* **188**, 3961-3971 (2012).

327. Khan, A.R. *et al.* Ligation of TLR7 on CD19(+) CD1d(hi) B cells suppresses allergic lung inflammation via regulatory T cells. *Eur J Immunol* **45**, 1842-1854 (2015).

328. Liu, B.S., Cao, Y., Huizinga, T.W., Hafler, D.A. & Toes, R.E. TLR-mediated STAT3 and ERK activation controls IL-10 secretion by human B cells. *Eur J Immunol* **44**, 2121-2129 (2014).

329. Piper, C.J.M. *et al.* CD19(+)CD24(hi)CD38(hi) B Cells Are Expanded in Juvenile Dermatomyositis and Exhibit a Pro-Inflammatory Phenotype After Activation Through Toll-Like Receptor 7 and Interferon-alpha. *Front Immunol* **9**, 1372 (2018).

330. Miles, K. *et al.* A tolerogenic role for Toll-like receptor 9 is revealed by B-cell interaction with DNA complexes expressed on apoptotic cells. *Proc Natl Acad Sci U S A* **109**, 887-892 (2012).

331. Gantner, F. *et al.* CD40-dependent and -independent activation of human tonsil B cells by CpG oligodeoxynucleotides. *Eur J Immunol* **33**, 1576-1585 (2003).

332. Zhang, X. *et al.* Type I interferons protect neonates from acute inflammation through interleukin 10-producing B cells. *J Exp Med* **204**, 1107-1118 (2007).

333. Sun, C.M., Deriaud, E., Leclerc, C. & Lo-Man, R. Upon TLR9 signaling, CD5+ B cells control the IL-12-dependent Th1-priming capacity of neonatal DCs. *Immunity* **22**, 467-477 (2005).

334. Gray, M., Miles, K., Salter, D., Gray, D. & Savill, J. Apoptotic cells protect mice from autoimmune inflammation by the induction of regulatory B cells. *Proc Natl Acad Sci U S A* **104**, 14080-14085 (2007).

335. Hamann, A., Andrew, D.P., Jablonski-Westrich, D., Holzmann, B. & Butcher, E.C. Role of alpha 4-integrins in lymphocyte homing to mucosal tissues in vivo. *J Immunol* **152**, 3282-3293 (1994).

336. Spolski, R. & Leonard, W.J. Interleukin-21: a double-edged sword with therapeutic potential. *Nat Rev Drug Discov* **13**, 379-395 (2014).

337. Xiao, S., Brooks, C.R., Sobel, R.A. & Kuchroo, V.K. Tim-1 is essential for induction and maintenance of IL-10 in regulatory B cells and their regulation of tissue inflammation. *J Immunol* **194**, 1602-1608 (2015).

338. Lindner, S. *et al.* Interleukin 21-induced granzyme B-expressing B cells infiltrate tumors and regulate T cells. *Cancer Res* **73**, 2468-2479 (2013).

339. Banko, Z. *et al.* Induction and Differentiation of IL-10-Producing Regulatory B Cells from Healthy Blood Donors and Rheumatoid Arthritis Patients. *J Immunol* **198**, 1512-1520 (2017).

340. Yang, M. *et al.* Novel function of B cell-activating factor in the induction of IL-10-producing regulatory B cells. *J Immunol* **184**, 3321-3325 (2010).

341. Zhang, Y. *et al.* The Unknown Aspect of BAFF: Inducing IL-35 Production by a CD5(+)CD1d(hi)FcgammaRIIb(hi) Regulatory B-Cell Subset in Lupus. *J Invest Dermatol* **137**, 2532-2543 (2017).

342. Saulep-Easton, D. *et al.* The BAFF receptor TACI controls IL-10 production by regulatory B cells and CLL B cells. *Leukemia* **30**, 163-172 (2016).

343. Hua, C. *et al.* A proliferation inducing ligand (APRIL) promotes IL-10 production and regulatory functions of human B cells. *J Autoimmun* **73**, 64-72 (2016).

344. Fehres, C.M. *et al.* APRIL Induces a Novel Subset of IgA(+) Regulatory B Cells That Suppress Inflammation via Expression of IL-10 and PD-L1. *Front Immunol* **10**, 1368 (2019).

345. Sattler, S. *et al.* IL-10-producing regulatory B cells induced by IL-33 (Breg(IL-33)) effectively attenuate mucosal inflammatory responses in the gut. *J Autoimmun* **50**, 107-122 (2014).

346. Zhu, J.F. *et al.* IL-33 Protects Mice against DSS-Induced Chronic Colitis by Increasing Both Regulatory B Cell and Regulatory T Cell Responses as Well as Decreasing Th17 Cell Response. *J Immunol Res* **2018**, 1827901 (2018).

347. Wang, R.X. *et al.* Interleukin-35 induces regulatory B cells that suppress autoimmune disease. *Nat Med* **20**, 633-641 (2014).

348. Lundy, S.K. Killer B lymphocytes: the evidence and the potential. *Inflamm Res* **58**, 345-357 (2009).

349. Klinker, M.W., Reed, T.J., Fox, D.A. & Lundy, S.K. Interleukin-5 supports the expansion of fas ligand-expressing killer B cells that induce antigen-specific apoptosis of CD4(+) T cells and secrete interleukin-10. *PLoS One* **8**, e70131 (2013).

350. Menon, M., Blair, P.A., Isenberg, D.A. & Mauri, C. A Regulatory Feedback between Plasmacytoid Dendritic Cells and Regulatory B Cells Is Aberrant in Systemic Lupus Erythematosus. *Immunity* **44**, 683-697 (2016).

351. Mauri, C. & Menon, M. Human regulatory B cells in health and disease: therapeutic potential. *J Clin Invest* **127**, 772-779 (2017).

352. Sarvaria, A., Madrigal, J.A. & Saudemont, A. B cell regulation in cancer and anti-tumor immunity. *Cell Mol Immunol* **14**, 662-674 (2017).

353. van den Berg, W.B., Joosten, L.A. & van Lent, P.L. Murine antigen-induced arthritis. *Methods Mol Med* **136**, 243-253 (2007).

354. Carter, N.A. *et al.* Mice lacking endogenous IL-10-producing regulatory B cells develop exacerbated disease and present with an increased frequency of Th1/Th17 but a decrease in regulatory T cells. *J Immunol* **186**, 5569-5579 (2011).

355. Mauri, C. & Menon, M. The expanding family of regulatory B cells. *Int Immunol* **27**, 479-486 (2015).

356. Mangan, N.E. *et al.* Helminth infection protects mice from anaphylaxis via IL-10-producing B cells. *J Immunol* **173**, 6346-6356 (2004).

357. Mangan, N.E., van Rooijen, N., McKenzie, A.N. & Fallon, P.G. Helminth-modified pulmonary immune response protects mice from allergen-induced airway hyperresponsiveness. *J Immunol* **176**, 138-147 (2006).

358. Chaudhry, M.S. & Karadimitris, A. Role and regulation of CD1d in normal and pathological B cells. *J Immunol* **193**, 4761-4768 (2014).

359. Miles, K. *et al.* Immune Tolerance to Apoptotic Self Is Mediated Primarily by Regulatory B1a Cells. *Front Immunol* **8**, 1952 (2017).

360. Lee, C.C. & Kung, J.T. Marginal zone B cell is a major source of Il-10 in Listeria monocytogenes susceptibility. *J Immunol* **189**, 3319-3327 (2012).

361. Bjarnadottir, K. *et al.* B cell-derived transforming growth factor-beta1 expression limits the induction phase of autoimmune neuroinflammation. *Sci Rep* **6**, 34594 (2016).

362. Maseda, D. *et al.* Regulatory B10 cells differentiate into antibody-secreting cells after transient IL-10 production in vivo. *J Immunol* **188**, 1036-1048 (2012).

363. Matsushita, T., Horikawa, M., Iwata, Y. & Tedder, T.F. Regulatory B cells (B10 cells) and regulatory T cells have independent roles in controlling experimental autoimmune encephalomyelitis initiation and late-phase immunopathogenesis. *J Immunol* **185**, 2240-2252 (2010).

364. Ronet, C. *et al.* Regulatory B cells shape the development of Th2 immune responses in BALB/c mice infected with Leishmania major through IL-10 production. *J Immunol* **184**, 886-894 (2010).

365. Horikawa, M. *et al.* Regulatory B cell (B10 Cell) expansion during Listeria infection governs innate and cellular immune responses in mice. *J Immunol* **190**, 1158-1168 (2013).

366. Popi, A.F., Lopes, J.D. & Mariano, M. Interleukin-10 secreted by B-1 cells modulates the phagocytic activity of murine macrophages in vitro. *Immunology* **113**, 348-354 (2004).

367. Velupillai, P., Secor, W.E., Horauf, A.M. & Harn, D.A. B-1 cell (CD5+B220+) outgrowth in murine schistosomiasis is genetically restricted and is largely due to activation by polylactosamine sugars. *J Immunol* **158**, 338-344 (1997).

368. Lundy, S.K. & Boros, D.L. Fas ligand-expressing B-1a lymphocytes mediate CD4(+)-T-cell apoptosis during schistosomal infection: induction by interleukin 4 (IL-4) and IL-10. *Infect Immun* **70**, 812-819 (2002).

369. Nakashima, H. *et al.* CD22 expression mediates the regulatory functions of peritoneal B-1a cells during the remission phase of contact hypersensitivity reactions. *J Immunol* **184**, 4637-4645 (2010).

370. Clark, E.A. & Giltiay, N.V. CD22: A Regulator of Innate and Adaptive B Cell Responses and Autoimmunity. *Front Immunol* **9**, 2235 (2018).

371. Shimomura, Y. *et al.* Regulatory role of B-1 B cells in chronic colitis. *Int Immunol* **20**, 729-737 (2008).

372. Madan, R. *et al.* Nonredundant roles for B cell-derived IL-10 in immune counter-regulation. *J Immunol* **183**, 2312-2320 (2009).

373. Hess, J., Ladel, C., Miko, D. & Kaufmann, S.H. Salmonella typhimurium aroA- infection in gene-targeted immunodeficient mice: major role of CD4+ TCR-alpha beta cells and IFN-gamma in bacterial clearance independent of intracellular location. *J Immunol* **156**, 3321-3326 (1996).

374. Conlan, J.W. Neutrophils prevent extracellular colonization of the liver microvasculature by Salmonella typhimurium. *Infect Immun* **64**, 1043-1047 (1996).

375. Matsumoto, M. *et al.* Interleukin-10-producing plasmablasts exert regulatory function in autoimmune inflammation. *Immunity* **41**, 1040-1051 (2014).

376. Tedder, T.F., Steeber, D.A. & Pizcueta, P. L-selectin-deficient mice have impaired leukocyte recruitment into inflammatory sites. *J Exp Med* **181**, 2259-2264 (1995).

377. Shalapour, S. *et al.* Immunosuppressive plasma cells impede T-cell-dependent immunogenic chemotherapy. *Nature* **521**, 94-98 (2015).

378. Lino, A.C. *et al.* LAG-3 Inhibitory Receptor Expression Identifies Immunosuppressive Natural Regulatory Plasma Cells. *Immunity* **49**, 120-133 e129 (2018).

379. Huang, C.T. *et al.* Role of LAG-3 in regulatory T cells. *Immunity* **21**, 503-513 (2004).

380. Shen, P. *et al.* IL-35-producing B cells are critical regulators of immunity during autoimmune and infectious diseases. *Nature* **507**, 366-370 (2014).

381. Collison, L.W. *et al.* The inhibitory cytokine IL-35 contributes to regulatory T-cell function. *Nature* **450**, 566-569 (2007).

382. Niedbala, W. *et al.* IL-35 is a novel cytokine with therapeutic effects against collagen-induced arthritis through the expansion of regulatory T cells and suppression of Th17 cells. *Eur J Immunol* **37**, 3021-3029 (2007).

383. Rafei, M. *et al.* A granulocyte-macrophage colony-stimulating factor and interleukin-15 fusokine induces a regulatory B cell population with immune suppressive properties. *Nat Med* **15**, 1038-1045 (2009).

384. Du, P., Xiong, R., Li, X. & Jiang, J. Immune Regulation and Antitumor Effect of TIM-1. *J Immunol Res* **2016**, 8605134 (2016).

385. Xiao, S. *et al.* Differential engagement of Tim-1 during activation can positively or negatively costimulate T cell expansion and effector function. *J Exp Med* **204**, 1691-1702 (2007).

386. Ueno, T. *et al.* The emerging role of T cell Ig mucin 1 in alloimmune responses in an experimental mouse transplant model. *J Clin Invest* **118**, 742-751 (2008).

387. Ding, Q. *et al.* Regulatory B cells are identified by expression of TIM-1 and can be induced through TIM-1 ligation to promote tolerance in mice. *J Clin Invest* **121**, 3645-3656 (2011).

388. Yeung, M.Y. *et al.* TIM-1 signaling is required for maintenance and induction of regulatory B cells. *Am J Transplant* **15**, 942-953 (2015).

389. Xiao, S. *et al.* Defect in regulatory B-cell function and development of systemic autoimmunity in T-cell Ig mucin 1 (Tim-1) mucin domain-mutant mice. *Proc Natl Acad Sci U S A* **109**, 12105-12110 (2012).

390. Kaku, H., Cheng, K.F., Al-Abed, Y. & Rothstein, T.L. A novel mechanism of B cell-mediated immune suppression through CD73 expression and adenosine production. *J Immunol* **193**, 5904-5913 (2014).

391. Blair, P.A. *et al.* CD19(+)CD24(hi)CD38(hi) B cells exhibit regulatory capacity in healthy individuals but are functionally impaired in systemic Lupus Erythematosus patients. *Immunity* **32**, 129-140 (2010).

392. Mavropoulos, A. *et al.* Breg Cells Are Numerically Decreased and Functionally Impaired in Patients With Systemic Sclerosis. *Arthritis Rheumatol* **68**, 494-504 (2016).

393. Flores-Borja, F. *et al.* CD19+CD24hiCD38hi B cells maintain regulatory T cells while limiting TH1 and TH17 differentiation. *Sci Transl Med* **5**, 173ra123 (2013).

394. Todd, S.K. *et al.* Regulatory B cells are numerically but not functionally deficient in anti-neutrophil cytoplasm antibody-associated vasculitis. *Rheumatology (Oxford)* **53**, 1693-1703 (2014).

395. Knippenberg, S. *et al.* Reduction in IL-10 producing B cells (Breg) in multiple sclerosis is accompanied by a reduced naive/memory Breg ratio during a relapse but not in remission. *J Neuroimmunol* **239**, 80-86 (2011).

396. Wang, W.W. *et al.* CD19+CD24hiCD38hiBregs involved in downregulate helper T cells and upregulate regulatory T cells in gastric cancer. *Oncotarget* **6**, 33486-33499 (2015).

397. Iwata, Y. *et al.* Characterization of a rare IL-10-competent B-cell subset in humans that parallels mouse regulatory B10 cells. *Blood* **117**, 530-541 (2011).

398. Saze, Z. *et al.* Adenosine production by human B cells and B cell-mediated suppression of activated T cells. *Blood* **122**, 9-18 (2013).

399. Chesneau, M. *et al.* Tolerant Kidney Transplant Patients Produce B Cells with Regulatory Properties. *J Am Soc Nephrol* **26**, 2588-2598 (2015).

400. Vidarsson, G., Dekkers, G. & Rispens, T. IgG subclasses and allotypes: from structure to effector functions. *Front Immunol* **5**, 520 (2014).

401. van de Veen, W. *et al.* IgG4 production is confined to human IL-10-producing regulatory B cells that suppress antigen-specific immune responses. *J Allergy Clin Immunol* **131**, 1204-1212 (2013).

402. Dumonde, D.C. & Glynn, L.E. The production of arthritis in rabbits by an immunological reaction to fibrin. *Br J Exp Pathol* **43**, 373-383 (1962).

403. Brackertz, D., Mitchell, G.F. & Mackay, I.R. Antigen-induced arthritis in mice. I. Induction of arthritis in various strains of mice. *Arthritis Rheum* **20**, 841-850 (1977).

404. Brackertz, D., Mitchell, G.F., Vadas, M.A. & Mackay, I.R. Studies on antigen-induced arthritis in mice. III. Cell and serum transfer experiments. *J Immunol* **118**, 1645-1648 (1977).

405. Petrow, P.K., Thoss, K., Katenkamp, D. & Brauer, R. Adoptive transfer of susceptibility to antigen-induced arthritis into severe combined immunodeficient (SCID) mice: role of CD4+ and CD8+ T cells. *Immunol Invest* **25**, 341-353 (1996).

406. Lens, J.W., van den Berg, W.B. & van de Putte, L.B. Flare-up of antigen-induced arthritis in mice after challenge with intravenous antigen: studies on the characteristics of and mechanisms involved in the reaction. *Clin Exp Immunol* **55**, 287-294 (1984).

407. Lens, J.W., van den Berg, W.B., van de Putte, L.B., Berden, J.H. & Lems, S.P. Flare-up of antigen-induced arthritis in mice after challenge with intravenous antigen: effects of pre-treatment with cobra venom factor and anti-lymphocyte serum. *Clin Exp Immunol* **57**, 520-528 (1984).

408. Lens, J.W., van den Berg, W.B., van de Putte, L.B. & Zwarts, W.A. Flare of antigen-induced arthritis in mice after intravenous challenge. Kinetics of antigen in the circulation and localization of antigen in the arthritic and noninflamed joint. *Arthritis Rheum* **29**, 665-674 (1986).

409. Nissler, K. *et al.* Anti-CD4 monoclonal antibody treatment in acute and early chronic antigen induced arthritis: influence on macrophage activation. *Ann Rheum Dis* **63**, 1470-1477 (2004).

410. van de Loo, A.A. *et al.* Role of interleukin 1 in antigen-induced exacerbations of murine arthritis. *Am J Pathol* **146**, 239-249 (1995).

411. Ouyang, W. & O'Garra, A. IL-10 Family Cytokines IL-10 and IL-22: from Basic Science to Clinical Translation. *Immunity* **50**, 871-891 (2019).

412. Fiorentino, D.F., Bond, M.W. & Mosmann, T.R. Two types of mouse T helper cell. IV. Th2 clones secrete a factor that inhibits cytokine production by Th1 clones. *J Exp Med* **170**, 2081-2095 (1989).

413. Saraiva, M. & O'Garra, A. The regulation of IL-10 production by immune cells. *Nat Rev Immunol* **10**, 170-181 (2010).

414. Cao, S., Liu, J., Song, L. & Ma, X. The protooncogene c-Maf is an essential transcription factor for IL-10 gene expression in macrophages. *J Immunol* **174**, 3484-3492 (2005).

415. Ananieva, O. *et al.* The kinases MSK1 and MSK2 act as negative regulators of Toll-like receptor signaling. *Nat Immunol* **9**, 1028-1036 (2008).

416. Cao, S., Zhang, X., Edwards, J.P. & Mosser, D.M. NF-kappaB1 (p50) homodimers differentially regulate pro- and anti-inflammatory cytokines in macrophages. *J Biol Chem* **281**, 26041-26050 (2006).

417. Brightbill, H.D., Plevy, S.E., Modlin, R.L. & Smale, S.T. A prominent role for Sp1 during lipopolysaccharide-mediated induction of the IL-10 promoter in macrophages. *J Immunol* **164**, 1940-1951 (2000).

418. Iyer, S.S. & Cheng, G. Role of interleukin 10 transcriptional regulation in inflammation and autoimmune disease. *Crit Rev Immunol* **32**, 23-63 (2012).

419. Shoemaker, J., Saraiva, M. & O'Garra, A. GATA-3 directly remodels the IL-10 locus independently of IL-4 in CD4+ T cells. *J Immunol* **176**, 3470-3479 (2006).

420. Wang, Z.Y. *et al.* Regulation of IL-10 gene expression in Th2 cells by Jun proteins. *J Immunol* **174**, 2098-2105 (2005).

421. Karwacz, K. *et al.* Critical role of IRF1 and BATF in forming chromatin landscape during type 1 regulatory cell differentiation. *Nat Immunol* **18**, 412-421 (2017).

422. Apetoh, L. *et al.* The aryl hydrocarbon receptor interacts with c-Maf to promote the differentiation of type 1 regulatory T cells induced by IL-27. *Nat Immunol* **11**, 854-861 (2010).

423. Meng, X. *et al.* Hypoxia-inducible factor-1alpha is a critical transcription factor for IL-10-producing B cells in autoimmune disease. *Nat Commun* **9**, 251 (2018).

424. Geng, X. *et al.* Transcriptional regulation of hypoxia inducible factors alpha (HIF-alpha) and their inhibiting factor (FIH-1) of channel catfish (Ictalurus punctatus) under hypoxia. *Comp Biochem Physiol B Biochem Mol Biol* **169**, 38-50 (2014).

425. Liu, M. *et al.* Transcription factor c-Maf is essential for IL-10 gene expression in B cells. *Scand J Immunol* **88**, e12701 (2018).

426. Bhattacharyya, S. *et al.* NFATc1 affects mouse splenic B cell function by controlling the calcineurin--NFAT signaling network. *J Exp Med* **208**, 823-839 (2011).

427. Alrefai, H. *et al.* NFATc1 supports imiquimod-induced skin inflammation by suppressing IL-10 synthesis in B cells. *Nat Commun* **7**, 11724 (2016).

428. Rangaswamy, U.S. & Speck, S.H. Murine gammaherpesvirus M2 protein induction of IRF4 via the NFAT pathway leads to IL-10 expression in B cells. *PLoS Pathog* **10**, e1003858 (2014).

429. Ziegler-Heitbrock, L. *et al.* IFN-alpha induces the human IL-10 gene by recruiting both IFN regulatory factor 1 and Stat3. *J Immunol* **171**, 285-290 (2003).

430. Kuhn, R., Lohler, J., Rennick, D., Rajewsky, K. & Muller, W. Interleukin-10-deficient mice develop chronic enterocolitis. *Cell* **75**, 263-274 (1993).

431. Steinbrink, K. *et al.* Interleukin-10-treated human dendritic cells induce a melanoma-antigen-specific anergy in CD8(+) T cells resulting in a failure to lyse tumor cells. *Blood* **93**, 1634-1642 (1999).

432. Yue, F.Y. *et al.* Interleukin-10 is a growth factor for human melanoma cells and down-regulates HLA class-I, HLA class-II and ICAM-1 molecules. *Int J Cancer* **71**, 630-637 (1997).

433. Stoecklin, G. *et al.* Genome-wide analysis identifies interleukin-10 mRNA as target of tristetraprolin. *J Biol Chem* **283**, 11689-11699 (2008).

434. Wang, Q. *et al.* Tristetraprolin inhibits macrophage IL-27-induced activation of antitumour cytotoxic T cell responses. *Nat Commun* **8**, 867 (2017).

435. Shaw, G. & Kamen, R. A conserved AU sequence from the 3' untranslated region of GM-CSF mRNA mediates selective mRNA degradation. *Cell* **46**, 659-667 (1986).

436. Kontoyiannis, D., Pasparakis, M., Pizarro, T.T., Cominelli, F. & Kollias, G. Impaired on/off regulation of TNF biosynthesis in mice lacking TNF AU-rich elements: implications for joint and gut-associated immunopathologies. *Immunity* **10**, 387-398 (1999).

437. Lykke-Andersen, J. & Wagner, E. Recruitment and activation of mRNA decay enzymes by two ARE-mediated decay activation domains in the proteins TTP and BRF-1. *Genes Dev* **19**, 351-361 (2005).

438. Wahid, F., Shehzad, A., Khan, T. & Kim, Y.Y. MicroRNAs: synthesis, mechanism, function, and recent clinical trials. *Biochim Biophys Acta* **1803**, 1231-1243 (2010).

439. Wang, H., Xu, W., Shao, Q. & Ding, Q. miR-21 silencing ameliorates experimental autoimmune encephalomyelitis by promoting the differentiation of IL-10-producing B cells. *Oncotarget* **8**, 94069-94079 (2017).

440. Jia, X. *et al.* MiR-15a/16-1 deficiency induces IL-10-producing CD19(+) TIM-1(+) cells in tumor microenvironment. *J Cell Mol Med* **23**, 1343-1353 (2019).

441. Zheng, Y. *et al.* miR-155 Regulates IL-10-Producing CD24(hi)CD27(+) B Cells and Impairs Their Function in Patients with Crohn's Disease. *Front Immunol* **8**, 914 (2017).

442. Landeira, D. *et al.* Jarid2 is a PRC2 component in embryonic stem cells required for multi-lineage differentiation and recruitment of PRC1 and RNA Polymerase II to developmental regulators. *Nat Cell Biol* **12**, 618-624 (2010).

443. Tonon, S. *et al.* IL-10-producing B cells are characterized by a specific methylation signature. *Eur J Immunol* **49**, 1213-1225 (2019).

444. Hahn, M.E., Karchner, S.I., Shapiro, M.A. & Perera, S.A. Molecular evolution of two vertebrate aryl hydrocarbon (dioxin) receptors (AHR1 and AHR2) and the PAS family. *Proc Natl Acad Sci U S A* **94**, 13743-13748 (1997).

445. Stockinger, B., Di Meglio, P., Gialitakis, M. & Duarte, J.H. The aryl hydrocarbon receptor: multitasking in the immune system. *Annu Rev Immunol* **32**, 403-432 (2014).

446. Pongratz, I., Antonsson, C., Whitelaw, M.L. & Poellinger, L. Role of the PAS domain in regulation of dimerization and DNA binding specificity of the dioxin receptor. *Mol Cell Biol* **18**, 4079-4088 (1998).

447. Swanson, H.I., Chan, W.K. & Bradfield, C.A. DNA binding specificities and pairing rules of the Ah receptor, ARNT, and SIM proteins. *J Biol Chem* **270**, 26292-26302 (1995).

448. Yao, E.F. & Denison, M.S. DNA sequence determinants for binding of transformed Ah receptor to a dioxin-responsive enhancer. *Biochemistry* **31**, 5060-5067 (1992).

449. Reyes, H., Reisz-Porszasz, S. & Hankinson, O. Identification of the Ah receptor nuclear translocator protein (Arnt) as a component of the DNA binding form of the Ah receptor. *Science* **256**, 1193-1195 (1992).

450. Berg, P. & Pongratz, I. Two parallel pathways mediate cytoplasmic localization of the dioxin (aryl hydrocarbon) receptor. *J Biol Chem* **277**, 32310-32319 (2002).

451. Carver, L.A. & Bradfield, C.A. Ligand-dependent interaction of the aryl hydrocarbon receptor with a novel immunophilin homolog in vivo. *J Biol Chem* **272**, 11452-11456 (1997).

452. Meyer, B.K., Pray-Grant, M.G., Vanden Heuvel, J.P. & Perdew, G.H. Hepatitis B virus X-associated protein 2 is a subunit of the unliganded aryl hydrocarbon receptor core complex and exhibits transcriptional enhancer activity. *Mol Cell Biol* **18**, 978-988 (1998).

453. Meyer, B.K. & Perdew, G.H. Characterization of the AhR-hsp90-XAP2 core complex and the role of the immunophilin-related protein XAP2 in AhR stabilization. *Biochemistry* **38**, 8907-8917 (1999).

454. Enan, E. & Matsumura, F. Evidence for a second pathway in the action mechanism of 2,3,7,8-tetrachlorodibenzo-p-dioxin (TCDD). Significance of Ah-receptor mediated activation of protein kinase under cell-free conditions. *Biochem Pharmacol* **49**, 249-261 (1995).

455. Enan, E. & Matsumura, F. Identification of c-Src as the integral component of the cytosolic Ah receptor complex, transducing the signal of 2,3,7,8-tetrachlorodibenzo-p-dioxin (TCDD) through the protein phosphorylation pathway. *Biochem Pharmacol* **52**, 1599-1612 (1996).

456. Grenert, J.P. *et al.* The amino-terminal domain of heat shock protein 90 (hsp90) that binds geldanamycin is an ATP/ADP switch domain that regulates hsp90 conformation. *J Biol Chem* **272**, 23843-23850 (1997).

457. Nair, S.C. *et al.* A pathway of multi-chaperone interactions common to diverse regulatory proteins: estrogen receptor, Fes tyrosine kinase, heat shock transcription factor Hsf1, and the aryl hydrocarbon receptor. *Cell Stress Chaperones* **1**, 237-250 (1996).

458. Antonsson, C., Whitelaw, M.L., McGuire, J., Gustafsson, J.A. & Poellinger, L. Distinct roles of the molecular chaperone hsp90 in modulating dioxin receptor function via the basic helix-loop-helix and PAS domains. *Mol Cell Biol* **15**, 756-765 (1995).

459. Coumailleau, P., Poellinger, L., Gustafsson, J.A. & Whitelaw, M.L. Definition of a minimal domain of the dioxin receptor that is associated with Hsp90 and maintains

wild type ligand binding affinity and specificity. *J Biol Chem* **270**, 25291-25300 (1995).

460. Pongratz, I., Mason, G.G. & Poellinger, L. Dual roles of the 90-kDa heat shock protein hsp90 in modulating functional activities of the dioxin receptor. Evidence that the dioxin receptor functionally belongs to a subclass of nuclear receptors which require hsp90 both for ligand binding activity and repression of intrinsic DNA binding activity. *J Biol Chem* **267**, 13728-13734 (1992).

461. Petrulis, J.R., Kusnadi, A., Ramadoss, P., Hollingshead, B. & Perdew, G.H. The hsp90 Co-chaperone XAP2 alters importin beta recognition of the bipartite nuclear localization signal of the Ah receptor and represses transcriptional activity. *J Biol Chem* **278**, 2677-2685 (2003).

462. Kazlauskas, A., Sundstrom, S., Poellinger, L. & Pongratz, I. The hsp90 chaperone complex regulates intracellular localization of the dioxin receptor. *Mol Cell Biol* **21**, 2594-2607 (2001).

463. Kazlauskas, A., Poellinger, L. & Pongratz, I. The immunophilin-like protein XAP2 regulates ubiquitination and subcellular localization of the dioxin receptor. *J Biol Chem* **275**, 41317-41324 (2000).

464. Pappas, B. *et al.* p23 protects the human aryl hydrocarbon receptor from degradation via a heat shock protein 90-independent mechanism. *Biochem Pharmacol* **152**, 34-44 (2018).

465. Ikuta, T. *et al.* Nucleocytoplasmic shuttling of the aryl hydrocarbon receptor. *J Biochem* **127**, 503-509 (2000).

466. Ikuta, T., Eguchi, H., Tachibana, T., Yoneda, Y. & Kawajiri, K. Nuclear localization and export signals of the human aryl hydrocarbon receptor. *J Biol Chem* **273**, 2895-2904 (1998).

467. McGuire, J., Whitelaw, M.L., Pongratz, I., Gustafsson, J.A. & Poellinger, L. A cellular factor stimulates ligand-dependent release of hsp90 from the basic helix-loop-helix dioxin receptor. *Mol Cell Biol* **14**, 2438-2446 (1994).

468. Hoffman, E.C. *et al.* Cloning of a factor required for activity of the Ah (dioxin) receptor. *Science* **252**, 954-958 (1991).

469. Swanson, H.I. & Yang, J.H. The aryl hydrocarbon receptor interacts with transcription factor IIB. *Mol Pharmacol* **54**, 671-677 (1998).

470. Wang, S., Ge, K., Roeder, R.G. & Hankinson, O. Role of mediator in transcriptional activation by the aryl hydrocarbon receptor. *J Biol Chem* **279**, 13593-13600 (2004).

471. Tian, Y., Ke, S., Chen, M. & Sheng, T. Interactions between the aryl hydrocarbon receptor and P-TEFb. Sequential recruitment of transcription factors and differential phosphorylation of C-terminal domain of RNA polymerase II at cyp1a1 promoter. *J Biol Chem* **278**, 44041-44048 (2003).

472. Marshall, N.F. & Price, D.H. Purification of P-TEFb, a transcription factor required for the transition into productive elongation. *J Biol Chem* **270**, 12335-12338 (1995).

473. Wang, S. & Hankinson, O. Functional involvement of the Brahma/SWI2-related gene 1 protein in cytochrome P4501A1 transcription mediated by the aryl hydrocarbon receptor complex. *J Biol Chem* **277**, 11821-11827 (2002).

474. Schnekenburger, M., Peng, L. & Puga, A. HDAC1 bound to the Cyp1a1 promoter blocks histone acetylation associated with Ah receptor-mediated trans-activation. *Biochim Biophys Acta* **1769**, 569-578 (2007).

475. DiNatale, B.C., Schroeder, J.C., Francey, L.J., Kusnadi, A. & Perdew, G.H. Mechanistic insights into the events that lead to synergistic induction of interleukin 6 transcription upon activation of the aryl hydrocarbon receptor and inflammatory signaling. *J Biol Chem* **285**, 24388-24397 (2010).

476. Beischlag, T.V. *et al.* Recruitment of the NCoA/SRC-1/p160 family of transcriptional coactivators by the aryl hydrocarbon receptor/aryl hydrocarbon receptor nuclear translocator complex. *Mol Cell Biol* **22**, 4319-4333 (2002).

477. Rothhammer, V. & Quintana, F.J. The aryl hydrocarbon receptor: an environmental sensor integrating immune responses in health and disease. *Nat Rev Immunol* **19**, 184-197 (2019).

478. Vogel, C.F. *et al.* RelB, a new partner of aryl hydrocarbon receptor-mediated transcription. *Mol Endocrinol* **21**, 2941-2955 (2007).

479. Vogel, C.F., Sciullo, E. & Matsumura, F. Involvement of RelB in aryl hydrocarbon receptor-mediated induction of chemokines. *Biochem Biophys Res Commun* **363**, 722-726 (2007).

480. Kim, D.W. *et al.* The RelA NF-kappaB subunit and the aryl hydrocarbon receptor (AhR) cooperate to transactivate the c-myc promoter in mammary cells. *Oncogene* **19**, 5498-5506 (2000).

481. Chen, P.H., Chang, H., Chang, J.T. & Lin, P. Aryl hydrocarbon receptor in association with RelA modulates IL-6 expression in non-smoking lung cancer. *Oncogene* **31**, 2555-2565 (2012).

482. Kimura, A. *et al.* Aryl hydrocarbon receptor in combination with Stat1 regulates LPS-induced inflammatory responses. *J Exp Med* **206**, 2027-2035 (2009).

483. Wilson, S.R., Joshi, A.D. & Elferink, C.J. The tumor suppressor Kruppel-like factor 6 is a novel aryl hydrocarbon receptor DNA binding partner. *J Pharmacol Exp Ther* **345**, 419-429 (2013).

484. Puga, A. *et al.* Aromatic hydrocarbon receptor interaction with the retinoblastoma protein potentiates repression of E2F-dependent transcription and cell cycle arrest. *J Biol Chem* **275**, 2943-2950 (2000).

485. Ohtake, F. *et al.* Modulation of oestrogen receptor signalling by association with the activated dioxin receptor. *Nature* **423**, 545-550 (2003).

486. Cui, G. *et al.* Liver X receptor (LXR) mediates negative regulation of mouse and human Th17 differentiation. *J Clin Invest* **121**, 658-670 (2011).

487. Wang, L. *et al.* The aryl hydrocarbon receptor interacts with nuclear factor erythroid 2-related factor 2 to mediate induction of NAD(P)H:quinoneoxidoreductase 1 by 2,3,7,8-tetrachlorodibenzo-p-dioxin. *Arch Biochem Biophys* **537**, 31-38 (2013).

488. Hankinson, O. Role of coactivators in transcriptional activation by the aryl hydrocarbon receptor. *Arch Biochem Biophys* **433**, 379-386 (2005).

489. Ohtake, F. *et al.* Dioxin receptor is a ligand-dependent E3 ubiquitin ligase. *Nature* **446**, 562-566 (2007).

490. Luecke-Johansson, S. *et al.* A Molecular Mechanism To Switch the Aryl Hydrocarbon Receptor from a Transcription Factor to an E3 Ubiquitin Ligase. *Mol Cell Biol* **37** (2017).

491. Mejia-Garcia, A. *et al.* Activation of AHR mediates the ubiquitination and proteasome degradation of c-Fos through the induction of Ubcm4 gene expression. *Toxicology* **337**, 47-57 (2015).

492. Bunaciu, R.P. & Yen, A. Activation of the aryl hydrocarbon receptor AhR Promotes retinoic acid-induced differentiation of myeloblastic leukemia cells by restricting expression of the stem cell transcription factor Oct4. *Cancer Res* **71**, 2371-2380 (2011).

493. Dominguez-Acosta, O. *et al.* Activation of aryl hydrocarbon receptor regulates the LPS/IFNgamma-induced inflammatory response by inducing ubiquitin-proteosomal and lysosomal degradation of RelA/p65. *Biochem Pharmacol* **155**, 141-149 (2018).

494. Kawajiri, K. *et al.* Aryl hydrocarbon receptor suppresses intestinal carcinogenesis in ApcMin/+ mice with natural ligands. *Proc Natl Acad Sci U S A* **106**, 13481-13486 (2009).

495. Denison, M.S. & Nagy, S.R. Activation of the aryl hydrocarbon receptor by structurally diverse exogenous and endogenous chemicals. *Annu Rev Pharmacol Toxicol* **43**, 309-334 (2003).

496. Poland, A. & Knutson, J.C. 2,3,7,8-tetrachlorodibenzo-p-dioxin and related halogenated aromatic hydrocarbons: examination of the mechanism of toxicity. *Annu Rev Pharmacol Toxicol* **22**, 517-554 (1982).

497. Consonni, D. *et al.* Mortality in a population exposed to dioxin after the Seveso, Italy, accident in 1976: 25 years of follow-up. *Am J Epidemiol* **167**, 847-858 (2008).

498. Poland, A., Glover, E. & Kende, A.S. Stereospecific, high affinity binding of 2,3,7,8-tetrachlorodibenzo-p-dioxin by hepatic cytosol. Evidence that the binding species is receptor for induction of aryl hydrocarbon hydroxylase. *J Biol Chem* **251**, 4936-4946 (1976).

499. Srogi, K. Monitoring of environmental exposure to polycyclic aromatic hydrocarbons: a review. *Environ Chem Lett* **5**, 169-195 (2007).

500. Nguyen, L.P. & Bradfield, C.A. The search for endogenous activators of the aryl hydrocarbon receptor. *Chem Res Toxicol* **21**, 102-116 (2008).

501. Li, Y. *et al.* Exogenous stimuli maintain intraepithelial lymphocytes via aryl hydrocarbon receptor activation. *Cell* **147**, 629-640 (2011).

502. Shertzer, H.G. & Senft, A.P. The micronutrient indole-3-carbinol: implications for disease and chemoprevention. *Drug Metabol Drug Interact* **17**, 159-188 (2000).

503. Ross, J.A. & Kasum, C.M. Dietary flavonoids: bioavailability, metabolic effects, and safety. *Annu Rev Nutr* **22**, 19-34 (2002).

504. Badawy, A.A. Kynurenine Pathway of Tryptophan Metabolism: Regulatory and Functional Aspects. *Int J Tryptophan Res* **10**, 1178646917691938 (2017).

505. Aoki, R., Aoki-Yoshida, A., Suzuki, C. & Takayama, Y. Indole-3-Pyruvic Acid, an Aryl Hydrocarbon Receptor Activator, Suppresses Experimental Colitis in Mice. *J Immunol* **201**, 3683-3693 (2018).

506. Vikstrom Bergander, L., Cai, W., Klocke, B., Seifert, M. & Pongratz, I. Tryptamine serves as a proligand of the AhR transcriptional pathway whose activation is dependent of monoamine oxidases. *Mol Endocrinol* **26**, 1542-1551 (2012).

507. Manzella, C. *et al.* Serotonin is an endogenous regulator of intestinal CYP1A1 via AhR. *Sci Rep* **8**, 6103 (2018).

508. Mezrich, J.D. *et al.* An interaction between kynurenine and the aryl hydrocarbon receptor can generate regulatory T cells. *J Immunol* **185**, 3190-3198 (2010).

509. Lowe, M.M. *et al.* Identification of cinnabarinic acid as a novel endogenous aryl hydrocarbon receptor ligand that drives IL-22 production. *PLoS One* **9**, e87877 (2014).

510. Frericks, M., Meissner, M. & Esser, C. Microarray analysis of the AHR system: tissue-specific flexibility in signal and target genes. *Toxicol Appl Pharmacol* **220**, 320-332 (2007).

511. Wincent, E. *et al.* The suggested physiologic aryl hydrocarbon receptor activator and cytochrome P4501 substrate 6-formylindolo[3,2-b]carbazole is present in humans. *J Biol Chem* **284**, 2690-2696 (2009).

512. Rannug, A. *et al.* Certain photooxidized derivatives of tryptophan bind with very high affinity to the Ah receptor and are likely to be endogenous signal substances. *J Biol Chem* **262**, 15422-15427 (1987).

513. Di Meglio, P. *et al.* Activation of the aryl hydrocarbon receptor dampens the severity of inflammatory skin conditions. *Immunity* **40**, 989-1001 (2014).

514. Osborne, R. & Greenlee, W.F. 2,3,7,8-Tetrachlorodibenzo-p-dioxin (TCDD) enhances terminal differentiation of cultured human epidermal cells. *Toxicol Appl Pharmacol* **77**, 434-443 (1985).

515. Sutter, C.H. *et al.* EGF receptor signaling blocks aryl hydrocarbon receptor-mediated transcription and cell differentiation in human epidermal keratinocytes. *Proc Natl Acad Sci U S A* **106**, 4266-4271 (2009).

516. Rannug, A. & Fritsche, E. The aryl hydrocarbon receptor and light. *Biol Chem* **387**, 1149-1157 (2006).

517. Bohonowych, J.E. & Denison, M.S. Persistent binding of ligands to the aryl hydrocarbon receptor. *Toxicol Sci* **98**, 99-109 (2007).

518. Poland, A., Clover, E., Kende, A.S., DeCamp, M. & Giandomenico, C.M. 3,4,3',4'-Tetrachloro azoxybenzene and azobenzene: potent inducers of aryl hydrocarbon hydroxylase. *Science* **194**, 627-630 (1976).

519. Gregoraszczuk, E.L., Barc, J. & Falandysz, J. Differences in the action of lower and higher chlorinated polychlorinated naphthalene (PCN) congeners on estrogen dependent breast cancer cell line viability and apoptosis, and its correlation with Ahr and CYP1A1 expression. *Toxicology* **366-367**, 53-59 (2016).

520. Kim, H., Reddy, S. & Novak, R.F. 3-Methylcholanthrene and pyridine effects on CYP1A1 and CYP1A2 expression in rat renal tissue. *Drug Metab Dispos* **23**, 818-824 (1995).

521. Zhang, W. *et al.* PCB 126 and other dioxin-like PCBs specifically suppress hepatic PEPCK expression via the aryl hydrocarbon receptor. *PLoS One* **7**, e37103 (2012).

522. Shimizu, Y. *et al.* Benzo[a]pyrene carcinogenicity is lost in mice lacking the aryl hydrocarbon receptor. *Proc Natl Acad Sci U S A* **97**, 779-782 (2000).

523. MacDonald, C.J., Ciolino, H.P. & Yeh, G.C. Dibenzoylmethane modulates aryl hydrocarbon receptor function and expression of cytochromes P50 1A1, 1A2, and 1B1. *Cancer Res* **61**, 3919-3924 (2001).

524. Daujat, M. *et al.* Induction of CYP1A1 gene by benzimidazole derivatives during Caco-2 cell differentiation. Evidence for an aryl-hydrocarbon receptor-mediated mechanism. *Eur J Biochem* **237**, 642-652 (1996).

525. Lawrence, B.P. *et al.* Activation of the aryl hydrocarbon receptor is essential for mediating the anti-inflammatory effects of a novel low-molecular-weight compound. *Blood* **112**, 1158-1165 (2008).

526. DuSell, C.D. *et al.* Regulation of aryl hydrocarbon receptor function by selective estrogen receptor modulators. *Mol Endocrinol* **24**, 33-46 (2010).

527. McDougal, A., Wormke, M., Calvin, J. & Safe, S. Tamoxifen-induced antitumorigenic/antiestrogenic action synergized by a selective aryl hydrocarbon receptor modulator. *Cancer Res* **61**, 3902-3907 (2001).

528. Berg, J. *et al.* The immunomodulatory effect of laquinimod in CNS autoimmunity is mediated by the aryl hydrocarbon receptor. *J Neuroimmunol* **298**, 9-15 (2016).

529. Mahiout, S. *et al.* In vitro toxicity and in silico docking analysis of two novel selective AH-receptor modulators. *Toxicol In Vitro* **52**, 178-188 (2018).

530. Prokopec, S.D., Pohjanvirta, R., Mahiout, S., Pettersson, L. & Boutros, P.C. Transcriptomic Impact of IMA-08401, a Novel AHR Agonist Resembling Laquinimod, on Rat Liver. *Int J Mol Sci* **20** (2019).

531. Punj, S. *et al.* Benzimidazoisoquinolines: a new class of rapidly metabolized aryl hydrocarbon receptor (AhR) ligands that induce AhR-dependent Tregs and prevent murine graft-versus-host disease. *PLoS One* **9**, e88726 (2014).

532. O'Donnell, E.F. *et al.* The anti-inflammatory drug leflunomide is an agonist of the aryl hydrocarbon receptor. *PLoS One* **5** (2010).

533. Knockaert, M. *et al.* Independent actions on cyclin-dependent kinases and aryl hydrocarbon receptor mediate the antiproliferative effects of indirubins. *Oncogene* **23**, 4400-4412 (2004).

534. Hoagland, M.S., Hoagland, E.M. & Swanson, H.I. The p53 inhibitor pifithrin-alpha is a potent agonist of the aryl hydrocarbon receptor. *J Pharmacol Exp Ther* **314**, 603-610 (2005).

535. Kramer, H.J. *et al.* Malassezin, a novel agonist of the aryl hydrocarbon receptor from the yeast Malassezia furfur, induces apoptosis in primary human melanocytes. *Chembiochem* **6**, 860-865 (2005).

536. Magiatis, P. *et al.* Malassezia yeasts produce a collection of exceptionally potent activators of the Ah (dioxin) receptor detected in diseased human skin. *J Invest Dermatol* **133**, 2023-2030 (2013).

537. Phelan, D., Winter, G.M., Rogers, W.J., Lam, J.C. & Denison, M.S. Activation of the Ah receptor signal transduction pathway by bilirubin and biliverdin. *Arch Biochem Biophys* **357**, 155-163 (1998).

538. Schaldach, C.M., Riby, J. & Bjeldanes, L.F. Lipoxin A4: a new class of ligand for the Ah receptor. *Biochemistry* **38**, 7594-7600 (1999).

539. Seidel, S.D. *et al.* Activation of the Ah receptor signaling pathway by prostaglandins. *J Biochem Mol Toxicol* **15**, 187-196 (2001).

540. Chiaro, C.R., Morales, J.L., Prabhu, K.S. & Perdew, G.H. Leukotriene A4 metabolites are endogenous ligands for the Ah receptor. *Biochemistry* **47**, 8445-8455 (2008).

541. Chiaro, C.R., Patel, R.D. & Perdew, G.H. 12(R)-Hydroxy-5(Z),8(Z),10(E),14(Z)-eicosatetraenoic acid [12(R)-HETE], an arachidonic acid derivative, is an activator of the aryl hydrocarbon receptor. *Mol Pharmacol* **74**, 1649-1656 (2008).

542. Adachi, J. *et al.* Indirubin and indigo are potent aryl hydrocarbon receptor ligands present in human urine. *J Biol Chem* **276**, 31475-31478 (2001).

543. Abdullah, A. *et al.* Activation of aryl hydrocarbon receptor signaling by a novel agonist ameliorates autoimmune encephalomyelitis. *PLoS One* **14**, e0215981 (2019).

544. Tong, B. *et al.* Norisoboldine, an isoquinoline alkaloid, acts as an aryl hydrocarbon receptor ligand to induce intestinal Treg cells and thereby attenuate arthritis. *Int J Biochem Cell Biol* **75**, 63-73 (2016).

545. Miller, C.A., 3rd. Expression of the human aryl hydrocarbon receptor complex in yeast. Activation of transcription by indole compounds. *J Biol Chem* **272**, 32824-32829 (1997).

546. Song, J. *et al.* A ligand for the aryl hydrocarbon receptor isolated from lung. *Proc Natl Acad Sci U S A* **99**, 14694-14699 (2002).

547. Bjeldanes, L.F., Kim, J.Y., Grose, K.R., Bartholomew, J.C. & Bradfield, C.A. Aromatic hydrocarbon responsiveness-receptor agonists generated from indole-3-carbinol in vitro and in vivo: comparisons with 2,3,7,8-tetrachlorodibenzo-p-dioxin. *Proc Natl Acad Sci U S A* **88**, 9543-9547 (1991).

548. Ciolino, H.P., Daschner, P.J., Wang, T.T. & Yeh, G.C. Effect of curcumin on the aryl hydrocarbon receptor and cytochrome P450 1A1 in MCF-7 human breast carcinoma cells. *Biochem Pharmacol* **56**, 197-206 (1998).

549. Ciolino, H.P., Wang, T.T. & Yeh, G.C. Diosmin and diosmetin are agonists of the aryl hydrocarbon receptor that differentially affect cytochrome P450 1A1 activity. *Cancer Res* **58**, 2754-2760 (1998).

550. Hanieh, H. *et al.* Novel Aryl Hydrocarbon Receptor Agonist Suppresses Migration and Invasion of Breast Cancer Cells. *PLoS One* **11**, e0167650 (2016).

551. Ronnekleiv-Kelly, S.M. *et al.* Aryl hydrocarbon receptor-dependent apoptotic cell death induced by the flavonoid chrysin in human colorectal cancer cells. *Cancer Lett* **370**, 91-99 (2016).

552. Ciolino, H.P. & Yeh, G.C. The flavonoid galangin is an inhibitor of CYP1A1 activity and an agonist/antagonist of the aryl hydrocarbon receptor. *Br J Cancer* **79**, 1340-1346 (1999).

553. Zhang, S., Qin, C. & Safe, S.H. Flavonoids as aryl hydrocarbon receptor agonists/antagonists: effects of structure and cell context. *Environ Health Perspect* **111**, 1877-1882 (2003).

554. DiNatale, B.C. *et al.* Kynurenic acid is a potent endogenous aryl hydrocarbon receptor ligand that synergistically induces interleukin-6 in the presence of inflammatory signaling. *Toxicol Sci* **115**, 89-97 (2010).

555. Bittinger, M.A., Nguyen, L.P. & Bradfield, C.A. Aspartate aminotransferase generates proagonists of the aryl hydrocarbon receptor. *Mol Pharmacol* **64**, 550-556 (2003).

556. Jin, U.H. *et al.* Microbiome-derived tryptophan metabolites and their aryl hydrocarbon receptor-dependent agonist and antagonist activities. *Mol Pharmacol* **85**, 777-788 (2014).

557. Weems, J.M. & Yost, G.S. 3-Methylindole metabolites induce lung CYP1A1 and CYP2F1 enzymes by AhR and non-AhR mechanisms, respectively. *Chem Res Toxicol* **23**, 696-704 (2010).

558. Zelante, T. *et al.* Tryptophan catabolites from microbiota engage aryl hydrocarbon receptor and balance mucosal reactivity via interleukin-22. *Immunity* **39**, 372-385 (2013).

559. Schroeder, J.C. *et al.* The uremic toxin 3-indoxyl sulfate is a potent endogenous agonist for the human aryl hydrocarbon receptor. *Biochemistry* **49**, 393-400 (2010).

560. Smith, S.H. *et al.* Tapinarof Is a Natural AhR Agonist that Resolves Skin Inflammation in Mice and Humans. *J Invest Dermatol* **137**, 2110-2119 (2017).

561. Marinelli, L. *et al.* Identification of the novel role of butyrate as AhR ligand in human intestinal epithelial cells. *Sci Rep* **9**, 643 (2019).

562. Ciolino, H.P., Daschner, P.J. & Yeh, G.C. Dietary flavonols quercetin and kaempferol are ligands of the aryl hydrocarbon receptor that affect CYP1A1 transcription differentially. *Biochem J* **340 (Pt 3)**, 715-722 (1999).

563. Beedanagari, S.R., Bebenek, I., Bui, P. & Hankinson, O. Resveratrol inhibits dioxin-induced expression of human CYP1A1 and CYP1B1 by inhibiting recruitment of the aryl hydrocarbon receptor complex and RNA polymerase II to the regulatory regions of the corresponding genes. *Toxicol Sci* **110**, 61-67 (2009).

564. Zhao, B., Degroot, D.E., Hayashi, A., He, G. & Denison, M.S. CH223191 is a ligand-selective antagonist of the Ah (Dioxin) receptor. *Toxicol Sci* **117**, 393-403 (2010).

565. Boitano, A.E. *et al.* Aryl hydrocarbon receptor antagonists promote the expansion of human hematopoietic stem cells. *Science* **329**, 1345-1348 (2010).

566. Fang, Z.Z. *et al.* In vivo effects of the pure aryl hydrocarbon receptor antagonist GNF-351 after oral administration are limited to the gastrointestinal tract. *Br J Pharmacol* **171**, 1735-1746 (2014).

567. Henry, E.C. *et al.* Flavone antagonists bind competitively with 2,3,7, 8-tetrachlorodibenzo-p-dioxin (TCDD) to the aryl hydrocarbon receptor but inhibit nuclear uptake and transformation. *Mol Pharmacol* **55**, 716-725 (1999).

568. Liu, Y. *et al.* Blockade of IDO-kynurenine-AhR metabolic circuitry abrogates IFN-gamma-induced immunologic dormancy of tumor-repopulating cells. *Nat Commun* **8**, 15207 (2017).

569. Bock, K.W. & Kohle, C. Ah receptor: dioxin-mediated toxic responses as hints to deregulated physiologic functions. *Biochem Pharmacol* **72**, 393-404 (2006).

570. Delescluse, C., Lemaire, G., de Sousa, G. & Rahmani, R. Is CYP1A1 induction always related to AHR signaling pathway? *Toxicology* **153**, 73-82 (2000).

571. Fujisawa-Sehara, A., Sogawa, K., Yamane, M. & Fujii-Kuriyama, Y. Characterization of xenobiotic responsive elements upstream from the drug-metabolizing cytochrome P-450c gene: a similarity to glucocorticoid regulatory elements. *Nucleic Acids Res* **15**, 4179-4191 (1987).

572. Bergander, L. *et al.* Metabolic fate of the Ah receptor ligand 6-formylindolo[3,2-b]carbazole. *Chem Biol Interact* **149**, 151-164 (2004).

573. Ito, S., Chen, C., Satoh, J., Yim, S. & Gonzalez, F.J. Dietary phytochemicals regulate whole-body CYP1A1 expression through an arylhydrocarbon receptor nuclear translocator-dependent system in gut. *J Clin Invest* **117**, 1940-1950 (2007).

574. Miniero, R., De Felip, E., Ferri, F. & di Domenico, A. An overview of TCDD half-life in mammals and its correlation to body weight. *Chemosphere* **43**, 839-844 (2001).

575. Mimura, J., Ema, M., Sogawa, K. & Fujii-Kuriyama, Y. Identification of a novel mechanism of regulation of Ah (dioxin) receptor function. *Genes Dev* **13**, 20-25 (1999).

576. Davarinos, N.A. & Pollenz, R.S. Aryl hydrocarbon receptor imported into the nucleus following ligand binding is rapidly degraded via the cytosplasmic proteasome following nuclear export. *J Biol Chem* **274**, 28708-28715 (1999).

577. Ma, Q. & Baldwin, K.T. 2,3,7,8-tetrachlorodibenzo-p-dioxin-induced degradation of aryl hydrocarbon receptor (AhR) by the ubiquitin-proteasome pathway. Role of the transcription activaton and DNA binding of AhR. *J Biol Chem* **275**, 8432-8438 (2000).

578. Bekesi, J.G. *et al.* Lymphocyte function of Michigan dairy farmers exposed to polybrominated biphenyls. *Science* **199**, 1207-1209 (1978).

579. Cella, M. & Colonna, M. Aryl hydrocarbon receptor: Linking environment to immunity. *Semin Immunol* **27**, 310-314 (2015).

580. Sun, Y.V., Boverhof, D.R., Burgoon, L.D., Fielden, M.R. & Zacharewski, T.R. Comparative analysis of dioxin response elements in human, mouse and rat genomic sequences. *Nucleic Acids Res* **32**, 4512-4523 (2004).

581. Quintana, F.J. *et al.* Control of T(reg) and T(H)17 cell differentiation by the aryl hydrocarbon receptor. *Nature* **453**, 65-71 (2008).

582. Veldhoen, M. *et al.* The aryl hydrocarbon receptor links TH17-cell-mediated autoimmunity to environmental toxins. *Nature* **453**, 106-109 (2008).

583. Veldhoen, M., Hirota, K., Christensen, J., O'Garra, A. & Stockinger, B. Natural agonists for aryl hydrocarbon receptor in culture medium are essential for optimal differentiation of Th17 T cells. *J Exp Med* **206**, 43-49 (2009).

584. Ramirez, J.M. *et al.* Activation of the aryl hydrocarbon receptor reveals distinct requirements for IL-22 and IL-17 production by human T helper cells. *Eur J Immunol* **40**, 2450-2459 (2010).

585. Trifari, S., Kaplan, C.D., Tran, E.H., Crellin, N.K. & Spits, H. Identification of a human helper T cell population that has abundant production of interleukin 22 and is distinct from T(H)-17, T(H)1 and T(H)2 cells. *Nat Immunol* **10**, 864-871 (2009).

586. Mascanfroni, I.D. *et al.* Metabolic control of type 1 regulatory T cell differentiation by AHR and HIF1-alpha. *Nat Med* **21**, 638-646 (2015).

587. Yeste, A. *et al.* IL-21 induces IL-22 production in CD4+ T cells. *Nat Commun* **5**, 3753 (2014).

588. Yasuda, K., Takeuchi, Y. & Hirota, K. The pathogenicity of Th17 cells in autoimmune diseases. *Semin Immunopathol* **41**, 283-297 (2019).

589. McGeachy, M.J. *et al.* TGF-beta and IL-6 drive the production of IL-17 and IL-10 by T cells and restrain T(H)-17 cell-mediated pathology. *Nat Immunol* **8**, 1390-1397 (2007).

590. McGeachy, M.J. GM-CSF: the secret weapon in the T(H)17 arsenal. *Nat Immunol* **12**, 521-522 (2011).

591. Ghoreschi, K. *et al.* Generation of pathogenic T(H)17 cells in the absence of TGF-beta signalling. *Nature* **467**, 967-971 (2010).

592. Gagliani, N. *et al.* Th17 cells transdifferentiate into regulatory T cells during resolution of inflammation. *Nature* **523**, 221-225 (2015).

593. Longhi, M.S. *et al.* Bilirubin suppresses Th17 immunity in colitis by upregulating CD39. *JCI Insight* **2** (2017).

594. Vos, J.G., Moore, J.A. & Zinkl, J.G. Effect of 2,3,7,8-tetrachlorodibenzo-p-dioxin on the immune system of laboratory animals. *Environ Health Perspect* **5**, 149-162 (1973).

595. Funatake, C.J., Marshall, N.B., Steppan, L.B., Mourich, D.V. & Kerkvliet, N.I. Cutting edge: activation of the aryl hydrocarbon receptor by 2,3,7,8-tetrachlorodibenzo-p-dioxin generates a population of CD4+ CD25+ cells with characteristics of regulatory T cells. *J Immunol* **175**, 4184-4188 (2005).

596. Lv, Q. *et al.* Norisoboldine, a natural AhR agonist, promotes Treg differentiation and attenuates colitis via targeting glycolysis and subsequent NAD(+)/SIRT1/SUV39H1/H3K9me3 signaling pathway. *Cell Death Dis* **9**, 258 (2018).

597. Gandhi, R. *et al.* Activation of the aryl hydrocarbon receptor induces human type 1 regulatory T cell-like and Foxp3(+) regulatory T cells. *Nat Immunol* **11**, 846-853 (2010).

598. Tousa, S. *et al.* Activin-A co-opts IRF4 and AhR signaling to induce human regulatory T cells that restrain asthmatic responses. *Proc Natl Acad Sci U S A* **114**, E2891-E2900 (2017).

599. Singh, N.P. *et al.* Activation of aryl hydrocarbon receptor (AhR) leads to reciprocal epigenetic regulation of FoxP3 and IL-17 expression and amelioration of experimental colitis. *PLoS One* **6**, e23522 (2011).

600. Kim, H.P. & Leonard, W.J. CREB/ATF-dependent T cell receptor-induced FoxP3 gene expression: a role for DNA methylation. *J Exp Med* **204**, 1543-1551 (2007).

601. Sulentic, C.E. & Kaminski, N.E. The long winding road toward understanding the molecular mechanisms for B-cell suppression by 2,3,7,8-tetrachlorodibenzo-p-dioxin. *Toxicol Sci* **120 Suppl 1**, S171-191 (2011).

602. Vecchi, A. *et al.* Effect of acute exposure to 2,3,7,8-tetrachlorodibenzo-p-dioxin on humoral antibody production in mice. *Chem Biol Interact* **30**, 337-342 (1980).

603. Vecchi, A. *et al.* The effect of acute administration of 2,3,7,8-tetrachlorodibenzo-p-dioxin (TCDD) on humoral antibody production and cell-mediated activities in mice. *Arch Toxicol Suppl* **4**, 163-165 (1980).

604. Holsapple, M.P., Dooley, R.K., McNerney, P.J. & McCay, J.A. Direct suppression of antibody responses by chlorinated dibenzodioxins in cultured spleen cells from (C57BL/6 x C3H)F1 and DBA/2 mice. *Immunopharmacology* **12**, 175-186 (1986).

605. Dooley, R.K. & Holsapple, M.P. Elucidation of cellular targets responsible for tetrachlorodibenzo-p-dioxin (TCDD)-induced suppression of antibody responses: I. The role of the B lymphocyte. *Immunopharmacology* **16**, 167-180 (1988).

606. Tucker, A.N., Vore, S.J. & Luster, M.I. Suppression of B cell differentiation by 2,3,7,8-tetrachlorodibenzo-p-dioxin. *Mol Pharmacol* **29**, 372-377 (1986).

607. Morris, D.L., Karras, J.G. & Holsapple, M.P. Direct effects of 2,3,7,8-tetrachlorodibenzo-p-dioxin (TCDD) on responses to lipopolysaccharide (LPS) by isolated murine B-cells. *Immunopharmacology* **26**, 105-112 (1993).

608. Sulentic, C.E., Holsapple, M.P. & Kaminski, N.E. Putative link between transcriptional regulation of IgM expression by 2,3,7,8-tetrachlorodibenzo-p-dioxin and the aryl hydrocarbon receptor/dioxin-responsive enhancer signaling pathway. *J Pharmacol Exp Ther* **295**, 705-716 (2000).

609. Henseler, R.A., Romer, E.J. & Sulentic, C.E. Diverse chemicals including aryl hydrocarbon receptor ligands modulate transcriptional activity of the 3'immunoglobulin heavy chain regulatory region. *Toxicology* **261**, 9-18 (2009).

610. Madisen, L. & Groudine, M. Identification of a locus control region in the immunoglobulin heavy-chain locus that deregulates c-myc expression in plasmacytoma and Burkitt's lymphoma cells. *Genes Dev* **8**, 2212-2226 (1994).

611. Yoo, B.S. *et al.* 2,3,7,8-Tetrachlorodibenzo-p-dioxin (TCDD) alters the regulation of Pax5 in lipopolysaccharide-activated B cells. *Toxicol Sci* **77**, 272-279 (2004).

612. Lieberson, R., Ong, J., Shi, X. & Eckhardt, L.A. Immunoglobulin gene transcription ceases upon deletion of a distant enhancer. *EMBO J* **14**, 6229-6238 (1995).

613. Pinaud, E. *et al.* Localization of the 3' IgH locus elements that effect long-distance regulation of class switch recombination. *Immunity* **15**, 187-199 (2001).

614. Sherr, D.H. & Monti, S. The role of the aryl hydrocarbon receptor in normal and malignant B cell development. *Semin Immunopathol* **35**, 705-716 (2013).

615. Villa, M. *et al.* Aryl hydrocarbon receptor is required for optimal B-cell proliferation. *EMBO J* **36**, 116-128 (2017).

616. Yamaguchi, K. *et al.* Induction of PreB cell apoptosis by 7,12-dimethylbenz[a]anthracene in long-term primary murine bone marrow cultures. *Toxicol Appl Pharmacol* **147**, 190-203 (1997).

617. Near, R.I. *et al.* Regulation of preB cell apoptosis by aryl hydrocarbon receptor/transcription factor-expressing stromal/adherent cells. *Proc Soc Exp Biol Med* **221**, 242-252 (1999).

618. Allan, L.L. & Sherr, D.H. Disruption of human plasma cell differentiation by an environmental polycyclic aromatic hydrocarbon: a mechanistic immunotoxicological study. *Environ Health* **9**, 15 (2010).

619. Schneider, D., Manzan, M.A., Yoo, B.S., Crawford, R.B. & Kaminski, N. Involvement of Blimp-1 and AP-1 dysregulation in the 2,3,7,8-Tetrachlorodibenzo-p-dioxin-mediated suppression of the IgM response by B cells. *Toxicol Sci* **108**, 377-388 (2009).

620. De Abrew, K.N., Phadnis, A.S., Crawford, R.B., Kaminski, N.E. & Thomas, R.S. Regulation of Bach2 by the aryl hydrocarbon receptor as a mechanism for suppression of B-cell differentiation by 2,3,7,8-tetrachlorodibenzo-p-dioxin. *Toxicol Appl Pharmacol* **252**, 150-158 (2011).

621. Sidwell, T. & Kallies, A. Bach2 is required for B cell and T cell memory differentiation. *Nat Immunol* **17**, 744-745 (2016).

622. Nera, K.P. *et al.* Loss of Pax5 promotes plasma cell differentiation. *Immunity* **24**, 283-293 (2006).

623. Ikuta, T., Ohba, M., Zouboulis, C.C., Fujii-Kuriyama, Y. & Kawajiri, K. B lymphocyte-induced maturation protein 1 is a novel target gene of aryl hydrocarbon receptor. *J Dermatol Sci* **58**, 211-216 (2010).

624. Zhang, Q. *et al.* All-or-none suppression of B cell terminal differentiation by environmental contaminant 2,3,7,8-tetrachlorodibenzo-p-dioxin. *Toxicol Appl Pharmacol* **268**, 17-26 (2013).

625. Lawrence, B.P. & Vorderstrasse, B.A. Activation of the aryl hydrocarbon receptor diminishes the memory response to homotypic influenza virus infection but does not impair host resistance. *Toxicol Sci* **79**, 304-314 (2004).

626. Marcus, R.S., Holsapple, M.P. & Kaminski, N.E. Lipopolysaccharide activation of murine splenocytes and splenic B cells increased the expression of aryl hydrocarbon receptor and aryl hydrocarbon receptor nuclear translocator. *J Pharmacol Exp Ther* **287**, 1113-1118 (1998).

627. Allan, L.L. & Sherr, D.H. Constitutive activation and environmental chemical induction of the aryl hydrocarbon receptor/transcription factor in activated human B lymphocytes. *Mol Pharmacol* **67**, 1740-1750 (2005).

628. Tan, J. *et al.* The role of short-chain fatty acids in health and disease. *Adv Immunol* **121**, 91-119 (2014).

629. Russo, E. *et al.* Immunomodulating Activity and Therapeutic Effects of Short Chain Fatty Acids and Tryptophan Post-biotics in Inflammatory Bowel Disease. *Front Immunol* **10**, 2754 (2019).

630. Hoverstad, T. & Midtvedt, T. Short-chain fatty acids in germfree mice and rats. *J Nutr* **116**, 1772-1776 (1986).

631. Riviere, A., Selak, M., Lantin, D., Leroy, F. & De Vuyst, L. Bifidobacteria and Butyrate-Producing Colon Bacteria: Importance and Strategies for Their Stimulation in the Human Gut. *Front Microbiol* **7**, 979 (2016).

632. Correa-Oliveira, R., Fachi, J.L., Vieira, A., Sato, F.T. & Vinolo, M.A. Regulation of immune cell function by short-chain fatty acids. *Clin Transl Immunology* **5**, e73 (2016).

633. Le Poul, E. *et al.* Functional characterization of human receptors for short chain fatty acids and their role in polymorphonuclear cell activation. *J Biol Chem* **278**, 25481-25489 (2003).

634. Thangaraju, M. *et al.* GPR109A is a G-protein-coupled receptor for the bacterial fermentation product butyrate and functions as a tumor suppressor in colon. *Cancer Res* **69**, 2826-2832 (2009).

635. Miyauchi, S., Gopal, E., Fei, Y.J. & Ganapathy, V. Functional identification of SLC5A8, a tumor suppressor down-regulated in colon cancer, as a Na(+)-coupled transporter for short-chain fatty acids. *J Biol Chem* **279**, 13293-13296 (2004).

636. Licciardi, P.V., Ververis, K. & Karagiannis, T.C. Histone deacetylase inhibition and dietary short-chain Fatty acids. *ISRN Allergy* **2011**, 869647 (2011).

637. Kelly, C.J. *et al.* Crosstalk between Microbiota-Derived Short-Chain Fatty Acids and Intestinal Epithelial HIF Augments Tissue Barrier Function. *Cell Host Microbe* **17**, 662-671 (2015).

638. Donohoe, D.R. *et al.* The Warburg effect dictates the mechanism of butyrate-mediated histone acetylation and cell proliferation. *Mol Cell* **48**, 612-626 (2012).

639. Vinolo, M.A., Hirabara, S.M. & Curi, R. G-protein-coupled receptors as fat sensors. *Curr Opin Clin Nutr Metab Care* **15**, 112-116 (2012).

640. Fellows, R. *et al.* Microbiota derived short chain fatty acids promote histone crotonylation in the colon through histone deacetylases. *Nat Commun* **9**, 105 (2018).

641. Tan, M. *et al.* Identification of 67 histone marks and histone lysine crotonylation as a new type of histone modification. *Cell* **146**, 1016-1028 (2011).

642. White, N.R., Mulligan, P., King, P.J. & Sanderson, I.R. Sodium butyrate-mediated Sp3 acetylation represses human insulin-like growth factor binding protein-3 expression in intestinal epithelial cells. *J Pediatr Gastroenterol Nutr* **42**, 134-141 (2006).

643. Pesavento, J.J., Yang, H., Kelleher, N.L. & Mizzen, C.A. Certain and progressive methylation of histone H4 at lysine 20 during the cell cycle. *Mol Cell Biol* **28**, 468-486 (2008).

644. Mathew, O.P., Ranganna, K. & Yatsu, F.M. Butyrate, an HDAC inhibitor, stimulates interplay between different posttranslational modifications of histone H3 and differently alters G1-specific cell cycle proteins in vascular smooth muscle cells. *Biomed Pharmacother* **64**, 733-740 (2010).

645. de Haan, J.B., Gevers, W. & Parker, M.I. Effects of sodium butyrate on the synthesis and methylation of DNA in normal cells and their transformed counterparts. *Cancer Res* **46**, 713-716 (1986).

646. Chang, P.V., Hao, L., Offermanns, S. & Medzhitov, R. The microbial metabolite butyrate regulates intestinal macrophage function via histone deacetylase inhibition. *Proc Natl Acad Sci U S A* **111**, 2247-2252 (2014).

647. Schulthess, J. *et al.* The Short Chain Fatty Acid Butyrate Imprints an Antimicrobial Program in Macrophages. *Immunity* **50**, 432-445 e437 (2019).

648. Gurav, A. *et al.* Slc5a8, a Na+-coupled high-affinity transporter for short-chain fatty acids, is a conditional tumour suppressor in colon that protects against colitis and colon cancer under low-fibre dietary conditions. *Biochem J* **469**, 267-278 (2015).

649. Singh, N. *et al.* Activation of Gpr109a, receptor for niacin and the commensal metabolite butyrate, suppresses colonic inflammation and carcinogenesis. *Immunity* **40**, 128-139 (2014).

650. Arpaia, N. *et al.* Metabolites produced by commensal bacteria promote peripheral regulatory T-cell generation. *Nature* **504**, 451-455 (2013).

651. Furusawa, Y. *et al.* Commensal microbe-derived butyrate induces the differentiation of colonic regulatory T cells. *Nature* **504**, 446-450 (2013).

652. Trompette, A. *et al.* Gut microbiota metabolism of dietary fiber influences allergic airway disease and hematopoiesis. *Nat Med* **20**, 159-166 (2014).

653. Park, J. *et al.* Short-chain fatty acids induce both effector and regulatory T cells by suppression of histone deacetylases and regulation of the mTOR-S6K pathway. *Mucosal Immunol* **8**, 80-93 (2015).

654. Waickman, A.T. & Powell, J.D. mTOR, metabolism, and the regulation of T-cell differentiation and function. *Immunol Rev* **249**, 43-58 (2012).

655. Kim, M., Qie, Y., Park, J. & Kim, C.H. Gut Microbial Metabolites Fuel Host Antibody Responses. *Cell Host Microbe* **20**, 202-214 (2016).

656. Wu, W. *et al.* Microbiota metabolite short-chain fatty acid acetate promotes intestinal IgA response to microbiota which is mediated by GPR43. *Mucosal Immunol* **10**, 946-956 (2017).

657. Sanchez, H.N. *et al.* B cell-intrinsic epigenetic modulation of antibody responses by dietary fiber-derived short-chain fatty acids. *Nat Commun* **11**, 60 (2020).

658. Jin, U.H. *et al.* Short Chain Fatty Acids Enhance Aryl Hydrocarbon (Ah) Responsiveness in Mouse Colonocytes and Caco-2 Human Colon Cancer Cells. *Sci Rep* **7**, 10163 (2017).

659. Madan, R. *et al.* Nonredundant roles for B cell-derived IL-10 in immune counter-regulation. *Journal of immunology* **183**, 2312-2320 (2009).

660. Smith, P.M. *et al.* The microbial metabolites, short-chain fatty acids, regulate colonic Treg cell homeostasis. *Science* **341**, 569-573 (2013).

661. Denaes, T. *et al.* The Cannabinoid Receptor 2 Protects Against Alcoholic Liver Disease Via a Macrophage Autophagy-Dependent Pathway. *Sci Rep* **6**, 28806 (2016).

662. Hao, S. *et al.* Critical role of CCL22/CCR4 axis in the maintenance of immune homeostasis during apoptotic cell clearance by splenic CD8alpha(+) CD103(+) dendritic cells. *Immunology* **148**, 174-186 (2016).

663. Torii, T. *et al.* Measurement of short-chain fatty acids in human faeces using high-performance liquid chromatography: specimen stability. *Ann Clin Biochem* **47**, 447-452 (2010).

664. Kozich, J.J., Westcott, S.L., Baxter, N.T., Highlander, S.K. & Schloss, P.D. Development of a dual-index sequencing strategy and curation pipeline for analyzing amplicon sequence data on the MiSeq Illumina sequencing platform. *Appl Environ Microbiol* **79**, 5112-5120 (2013).

665. Schloss, P.D. *et al.* Introducing mothur: open-source, platform-independent, community-supported software for describing and comparing microbial communities. *Appl Environ Microbiol* **75**, 7537-7541 (2009).

666. Rognes, T., Flouri, T., Nichols, B., Quince, C. & Mahe, F. VSEARCH: a versatile open source tool for metagenomics. *PeerJ* **4**, e2584 (2016).

667. Quast, C. *et al.* The SILVA ribosomal RNA gene database project: improved data processing and web-based tools. *Nucleic Acids Res* **41**, D590-596 (2013).

668. McClintick, J.N. & Edenberg, H.J. Effects of filtering by Present call on analysis of microarray experiments. *BMC Bioinformatics* **7**, 49 (2006).

669. Kauffmann, A., Gentleman, R. & Huber, W. arrayQualityMetrics--a bioconductor package for quality assessment of microarray data. *Bioinformatics* **25**, 415-416 (2009).

670. Ritchie, M.E. *et al.* limma powers differential expression analyses for RNA-sequencing and microarray studies. *Nucleic acids research* (2015).

671. Dobin, A. *et al.* STAR: ultrafast universal RNA-seq aligner. *Bioinformatics* **29**, 15-21 (2013).

672. Anders, S., Pyl, P.T. & Huber, W. HTSeq--a Python framework to work with high-throughput sequencing data. *Bioinformatics* **31**, 166-169 (2015).

673. Bray, N.L., Pimentel, H., Melsted, P. & Pachter, L. Near-optimal probabilistic RNA-seq quantification. *Nat Biotechnol* **34**, 525-527 (2016).

674. Robinson, M.D., McCarthy, D.J. & Smyth, G.K. edgeR: a Bioconductor package for differential expression analysis of digital gene expression data. *Bioinformatics* **26**, 139-140 (2010).

675. Robinson, M.D. & Smyth, G.K. Small-sample estimation of negative binomial dispersion, with applications to SAGE data. *Biostatistics* **9**, 321-332 (2008).

676. Tarca, A.L. *et al.* A novel signaling pathway impact analysis. *Bioinformatics* **25**, 75-82 (2009).

677. Kanehisa, M., Sato, Y., Kawashima, M., Furumichi, M. & Tanabe, M. KEGG as a reference resource for gene and protein annotation. *Nucleic Acids Res* **44**, D457-462 (2016).

678. Rendeiro, A.F. *et al.* Chromatin accessibility maps of chronic lymphocytic leukaemia identify subtype-specific epigenome signatures and transcription regulatory networks. *Nat Commun* **7**, 11938 (2016).

679. Saeed, A.I. *et al.* TM4: a free, open-source system for microarray data management and analysis. *Biotechniques* **34**, 374-378 (2003).

680. Brummel, R. & Lenert, P. Activation of marginal zone B cells from lupus mice with type A(D) CpG-oligodeoxynucleotides. *J Immunol* **174**, 2429-2434 (2005).

681. Imai, T. *et al.* Selective recruitment of CCR4-bearing Th2 cells toward antigen-presenting cells by the CC chemokines thymus and activation-regulated chemokine and macrophage-derived chemokine. *Int Immunol* **11**, 81-88 (1999).

682. Mohan, K. & Issekutz, T.B. Blockade of chemokine receptor CXCR3 inhibits T cell recruitment to inflamed joints and decreases the severity of adjuvant arthritis. *J Immunol* **179**, 8463-8469 (2007).

683. Heath-Pagliuso, S. *et al.* Activation of the Ah receptor by tryptophan and tryptophan metabolites. *Biochemistry* **37**, 11508-11515 (1998).

684. Khan, A. *et al.* JASPAR 2018: update of the open-access database of transcription factor binding profiles and its web framework. *Nucleic Acids Res* **46**, D260-D266 (2018).

685. Rothhammer, V. *et al.* Microglial control of astrocytes in response to microbial metabolites. *Nature* **557**, 724-728 (2018).

686. Ye, J. *et al.* The Aryl Hydrocarbon Receptor Preferentially Marks and Promotes Gut Regulatory T Cells. *Cell Rep* **21**, 2277-2290 (2017).

687. Szekanecz, Z. *et al.* Temporal expression of inflammatory cytokines and chemokines in rat adjuvant-induced arthritis. *Arthritis Rheum* **43**, 1266-1277 (2000).

688. Kasama, T. *et al.* Interleukin-10 expression and chemokine regulation during the evolution of murine type II collagen-induced arthritis. *J Clin Invest* **95**, 2868-2876 (1995).

689. Thornton, S., Duwel, L.E., Boivin, G.P., Ma, Y. & Hirsch, R. Association of the course of collagen-induced arthritis with distinct patterns of cytokine and chemokine messenger RNA expression. *Arthritis Rheum* **42**, 1109-1118 (1999).

690. Ruth, J.H. *et al.* CXCL16-mediated cell recruitment to rheumatoid arthritis synovial tissue and murine lymph nodes is dependent upon the MAPK pathway. *Arthritis Rheum* **54**, 765-778 (2006).

691. Feige, U. *et al.* Anti-interleukin-1 and anti-tumor necrosis factor-alpha synergistically inhibit adjuvant arthritis in Lewis rats. *Cell Mol Life Sci* **57**, 1457-1470 (2000).

692. Ohshima, S. *et al.* Interleukin 6 plays a key role in the development of antigen-induced arthritis. *Proc Natl Acad Sci U S A* **95**, 8222-8226 (1998).

693. Thornton, S., Boivin, G.P., Kim, K.N., Finkelman, F.D. & Hirsch, R. Heterogeneous effects of IL-2 on collagen-induced arthritis. *J Immunol* **165**, 1557-1563 (2000).

694. De Abrew, K.N., Kaminski, N.E. & Thomas, R.S. An integrated genomic analysis of aryl hydrocarbon receptor-mediated inhibition of B-cell differentiation. *Toxicol Sci* **118**, 454-469 (2010).

695. Vasconcellos, R., Carter, N.A., Rosser, E.C. & Mauri, C. IL-12p35 subunit contributes to autoimmunity by limiting IL-27-driven regulatory responses. *J Immunol* **187**, 3402-3412 (2011).

696. Richards, S., Watanabe, C., Santos, L., Craxton, A. & Clark, E.A. Regulation of B-cell entry into the cell cycle. *Immunol Rev* **224**, 183-200 (2008).

697. Rosser, E.C. *et al.* Microbiota-Derived Metabolites Suppress Arthritis by Amplifying Aryl-Hydrocarbon Receptor Activation in Regulatory B Cells. *Cell Metab* **31**, 837-851 e810 (2020).

698. Shinde, R. & McGaha, T.L. The Aryl Hydrocarbon Receptor: Connecting Immunity to the Microenvironment. *Trends Immunol* **39**, 1005-1020 (2018).

699. Chen, L. *et al.* Microbiota Metabolite Butyrate Differentially Regulates Th1 and Th17 Cells' Differentiation and Function in Induction of Colitis. *Inflamm Bowel Dis* **25**, 1450-1461 (2019).

700. Basson, A., Trotter, A., Rodriguez-Palacios, A. & Cominelli, F. Mucosal Interactions between Genetics, Diet, and Microbiome in Inflammatory Bowel Disease. *Front Immunol* **7**, 290 (2016).

701. Marino, E. *et al.* Gut microbial metabolites limit the frequency of autoimmune T cells and protect against type 1 diabetes. *Nat Immunol* **18**, 552-562 (2017).

702. Piper, C.J.M. *et al.* Aryl Hydrocarbon Receptor Contributes to the Transcriptional Program of IL-10-Producing Regulatory B Cells. *Cell Rep* **29**, 1878-1892 e1877 (2019).

703. Iwakoshi, N.N. *et al.* Plasma cell differentiation and the unfolded protein response intersect at the transcription factor XBP-1. *Nat Immunol* **4**, 321-329 (2003).

704. Becker-Herman, S., Lantner, F. & Shachar, I. Id2 negatively regulates B cell differentiation in the spleen. *J Immunol* **168**, 5507-5513 (2002).

705. Abel, J. & Haarmann-Stemmann, T. An introduction to the molecular basics of aryl hydrocarbon receptor biology. *Biol Chem* **391**, 1235-1248 (2010).

706. Jackson, D.P., Joshi, A.D. & Elferink, C.J. Ah Receptor Pathway Intricacies; Signaling Through Diverse Protein Partners and DNA-Motifs. *Toxicol Res (Camb)* **4**, 1143-1158 (2015).

707. Alhabbab, R. *et al.* Diversity of gut microflora is required for the generation of B cell with regulatory properties in a skin graft model. *Sci Rep* **5**, 11554 (2015).

708. Rakoff-Nahoum, S., Paglino, J., Eslami-Varzaneh, F., Edberg, S. & Medzhitov, R. Recognition of commensal microflora by toll-like receptors is required for intestinal homeostasis. *Cell* **118**, 229-241 (2004).

709. Gao, J. *et al.* Impact of the Gut Microbiota on Intestinal Immunity Mediated by Tryptophan Metabolism. *Front Cell Infect Microbiol* **8**, 13 (2018).

710. Welford, R.W. *et al.* Serotonin biosynthesis as a predictive marker of serotonin pharmacodynamics and disease-induced dysregulation. *Sci Rep* **6**, 30059 (2016).

711. Stockinger, B. & Omenetti, S. The dichotomous nature of T helper 17 cells. *Nat Rev Immunol* **17**, 535-544 (2017).

712. Wagage, S. *et al.* The aryl hydrocarbon receptor promotes IL-10 production by NK cells. *J Immunol* **192**, 1661-1670 (2014).

713. Shinde, R. *et al.* Apoptotic cell-induced AhR activity is required for immunological tolerance and suppression of systemic lupus erythematosus in mice and humans. *Nat Immunol* **19**, 571-582 (2018).

714. Saraiva, M. *et al.* Identification of a macrophage-specific chromatin signature in the IL-10 locus. *J Immunol* **175**, 1041-1046 (2005).

715. Yamaguchi, K. *et al.* Activation of the aryl hydrocarbon receptor/transcription factor and bone marrow stromal cell-dependent preB cell apoptosis. *J Immunol* **158**, 2165-2173 (1997).

716. Turner, C.A., Jr., Mack, D.H. & Davis, M.M. Blimp-1, a novel zinc finger-containing protein that can drive the maturation of B lymphocytes into immunoglobulin-secreting cells. *Cell* **77**, 297-306 (1994).

717. Mizoguchi, A., Mizoguchi, E., Smith, R.N., Preffer, F.I. & Bhan, A.K. Suppressive role of B cells in chronic colitis of T cell receptor alpha mutant mice. *J Exp Med* **186**, 1749-1756 (1997).

718. Menon, M., Blair, P.A., Isenberg, D.A. & Mauri, C. A Regulatory Feedback between Plasmacytoid Dendritic Cells and Regulatory B Cells Is Aberrant in Systemic Lupus Erythematosus. *Immunity* **44**, 683-697 (2016).

719. Mujahid, M., Sasikala, C. & Ramana Ch, V. Aniline-induced tryptophan production and identification of indole derivatives from three purple bacteria. *Curr Microbiol* **61**, 285-290 (2010).

720. Desbonnet, L., Garrett, L., Clarke, G., Bienenstock, J. & Dinan, T.G. The probiotic Bifidobacteria infantis: An assessment of potential antidepressant properties in the rat. *J Psychiatr Res* **43**, 164-174 (2008).

721. Lamas, B. *et al.* CARD9 impacts colitis by altering gut microbiota metabolism of tryptophan into aryl hydrocarbon receptor ligands. *Nature Medicine* **22**, 598-+ (2016).

722. Vahjen, W., Glaser, K., Schafer, K. & Simon, O. Influence of xylanase-supplemented feed on the development of selected bacterial groups in the intestinal tract of broiler chicks. *J Agr Sci* **130**, 489-+ (1998).

723. Rasmussen, M.K., Balaguer, P., Ekstrand, B., Daujat-Chavanieu, M. & Gerbal-Chaloin, S. Skatole (3-Methylindole) Is a Partial Aryl Hydrocarbon Receptor Agonist and Induces CYP1A1/2 and CYP1B1 Expression in Primary Human Hepatocytes. *PLoS One* **11**, e0154629 (2016).

724. Seok, S.H. *et al.* Trace derivatives of kynurenine potently activate the aryl hydrocarbon receptor (AHR). *J Biol Chem* **293**, 1994-2005 (2018).

725. Yano, J.M. *et al.* Indigenous bacteria from the gut microbiota regulate host serotonin biosynthesis. *Cell* **161**, 264-276 (2015).

726. Idzko, M. *et al.* The serotoninergic receptors of human dendritic cells: identification and coupling to cytokine release. *J Immunol* **172**, 6011-6019 (2004).

727. O'Connell, P.J. *et al.* A novel form of immune signaling revealed by transmission of the inflammatory mediator serotonin between dendritic cells and T cells. *Blood* **107**, 1010-1017 (2006).

728. Reigstad, C.S. *et al.* Gut microbes promote colonic serotonin production through an effect of short-chain fatty acids on enterochromaffin cells. *FASEB J* **29**, 1395-1403 (2015).

List of publications arising from this thesis

Piper CJM, Rosser EC, Oleinika K, Nistala K, Krausgruber T, Rendeiro AF, Banos A, Drozdov I, Villa M, Thomson S, Xanthou G, Bock C, Stockinger B, Mauri C. 2019. Aryl hydrocarbon receptor contributes to the transcriptional programme of IL-10-producing regulatory B cells. *Cell Reports* 29: 1878-1892. doi: 10.1016/j.celrep.2019.10.018

Rosser EC, **Piper CJM**, Matei DM, Blair P, Rendeiro AF, Orford M, Alber DG, Krausgruber T, Catalan D, Klein N, Manson JJ, Drozdov I, , Bock C, Wedderburn LR, Eaton S, Mauri C. 2020. Microbiota-Derived Metabolites Suppress Arthritis by Amplifying Aryl-Hydrocarbon Receptor Activation in Regulatory B Cells. *Cell Metabolism* 31: 837-851 e10. doi: 10.1016/j.cmet.2020.03.003

Piper CJM, Wilkinson MGLl, Deakin CT, Otto GW, Dowle S, Duurland CL, Adams S, Marasco E, Rosser EC, Radziszewska A, Carsetti R, Ioannou Y, Beales PL, Kelberman D, Isenberg DA, Mauri C, Nistala K, Wedderburn LR. 2018. $CD19^{+}CD24^{hi}CD38^{hi}$ B Cells Are Expanded in Juvenile Dermatomyositis and Exhibit a Pro-Inflammatory Phenotype After Activation Through Toll-Like Receptor 7 and Interferon-α. *Frontiers in Immunology* 9:1372. doi: 10.3389/fimmu.2018.01372.

Appendices

Appendix I: Table AI. Transcription factors differentially expressed between GFP^+ and GFP^- populations.

Appendix II: Table AII. AHR independent butyrate regulated genes.

Appendix III: Table AIII. AHR-dependent butyrate regulated genes.

Symbol	Name	Function	FC ($CD21^{hi}CD24^{hi}$ pos vs $CD21^{hi}CD24^{hi}$ neg)	adj.P.Val ($CD21^{hi}CD24^{hi}$ pos vs $CD21^{hi}CD24^{hi}$ neg)	FC ($CD21^{hi}CD24^{hi}$ pos vs FO)	adj.P.Val ($CD21^{hi}CD24^{hi}$ pos vs FO)
Ahr	Aryl-hydrocarbon receptor	DNA binding	1.869114565	5.05135E-05	5.183739908	1.73543E-08
E2f8	E2F transcription factor 8	Core promoter binding	3.524122031	8.24144E-05	9.937468163	1.16556E-07
Bhlhe41	Basic helix-loop-helix family, member e41	RNA polymerase II core promoter proximal region sequence-specific DNA binding	3.151182551	5.20865E-05	5.070827978	2.34121E-07
Pim1	Proviral integration site 1	Nucleotide binding	1.43710652	0.000803313	1.536952061	5.28079E-05
Tacc3	Transforming, acidic coiled-coil containing protein 3	Protein binding	1.754219566	0.000237504	2.612848846	1.13543E-06
E2f7	E2F transcription factor 7	Core promoter binding	1.569164933	0.000491558	2.089170639	3.35506E-06
Dnmt1	DNA methyltransferase (cytosine-5) 1	DNA binding	1.525927763	0.001016079	1.542642041	0.000192334
Zbtb32	Zinc finger and BTB domain containing 32	Nucleic acid binding	1.564102074	0.00060818	1.599906949	8.54549E-05
Zfpm1	Zinc finger protein, multitype 1	RNA polymerase II core promoter binding transcription factor activity	1.635156815	0.000956596	2.073406035	1.36055E-05
Pmf1	Polyamine-modulated factor 1	Transcription coactivator activity	1.613117282	0.000743998	2.03500123	9.61821E-06
C1qbp	C1q binding protein	Complement component C1q binding	1.49365815	0.002166338	1.796509212	4.16981E-05
Foxm1	Forkhead box M1	DNA binding	1.457277204	0.00190059	2.20317842	3.01442E-06
Cenpf	Centromere protein F	Protein C-terminus binding	1.922637351	0.008852351	3.81234672	2.613E-05

Pdlim1	PDZ and LIM domain 1 (elfin)	Transcription coactivator activity	1.538439454	0.001738439	1.372627344	0.00277832
Setd8	SET domain containing (lysine methyltransferase) 8	P53 binding	1.481768428	0.005872492	1.58624982	0.000660724
E2f1	E2F transcription factor 1	Core promoter binding	1.27720107	0.005234129	1.799717751	4.40902E-06
Hes6	Hairy and enhancer of split 6	DNA binding	1.26830407	0.004558499	1.367381679	0.000227666
Smarca4	SWI/SNF related, matrix associated, actin dependent regulator of chromatin	Nucleotide binding	1.335143927	0.011950492	1.398775214	0.00168523
Dip2c	DIP2 disco-interacting protein 2 homolog C (Drosophila)	Unknown	1.258003811	0.02122796	1.734098658	2.86597E-05
Skil	SKI-like	Chromatin binding	-1.201268078	0.022180352	-1.54986752	3.18895E-05
Hhex	Hematopoietically expressed homeobox	DNA binding	-1.235422164	0.026407274	-1.511651527	0.000170022
Rbpms	RNA binding protein gene with multiple splicing	Nucleotide binding	-1.326003662	0.040745097	-1.992794467	7.70317E-05
Hist1h4k	Histone Cluster 1 H4 Family Member K	Unknown	1.274	0.019929	1.5213	0.00027

Table AI: Transcription factors differentially expressed between GFP^+ and GFP^- populations. List of 23 candidate genes differentially expressed between $CD21^{hi}CD24^{hi}$IL-10eGFP^+ and GFP^- populations. Abbreviations: FC – fold change, FO – Follicular.

Gene set – AHR independent butyrate regulated genes					
Adamdec1	*Casc4*	*Hip1*	*Mtfr1l*	*Pomt1*	*Tbxa2r*
Ahdc1	*Cbfa2t3*	*Hpse*	*Mtmr4*	*Ppcdc*	*Tecpr2*
Anks1	*Ddx11*	*Hsp90b1*	*Nfya*	*R3hdm1*	*Tmc4*
Ano10	*Ece1*	*Hyou1*	*Pafah2*	*Rpgrip1l*	*Tmcc3*
Ano8	*Fahd2a*	*L3mbtl3*	*Patz1*	*Sdf2l1*	*Tmem129*
Asl	*Fam173b*	*Lamc1*	*Pdia3*	*Slc16a6*	*Tnfrsf4*
Bcl2	*Fbxl5*	*Lman2l*	*Pdia6*	*Slc2a9*	*Unc119b*
Bcl9	*Fkbp2*	*Magt1*	*Piga*	*Slc37a2*	*Usp31*
Bicd2	*Flnb*	*Manf*	*Pik3r5*	*Smg7*	*Vti1a*
Calr	*Fuca1*	*Med16*	*Plod1*	*Sorbs3*	*Xbp1*
Canx	*Gprasp1*	*Mib2*	*Plxna1*	*St13*	*Znhit1*
Capn5	*Guca1b*	*Mrpl1*	*Poln*	*Tbc1d19*	

Table AII. AHR independent butyrate regulated genes. 71 identified genes which are significantly differentially expressed after butyrate-supplementation in both $Mb1^{cre/+}$ and $Ahr^{fl/-}$ $Mb1^{cre/+}$ mice.

Gene Set – AHR-dependent butyrate regulated genes					
1110065P20Rik	*Cchcr1*	*Gfod1*	*Nacc1*	*Rab26os*	*Top3a*
1700048O20Rik	*Cd180*	*Haghl*	*Nek1*	*Rala*	*Tpst1*
1810014B01Rik	*Cep104*	*Haus2*	*Nfe2l2*	*Recql*	*Trmt10b*
1810024B03Rik	*Cep162*	*Hdac11*	*Nfkbiz*	*Rnase12*	*Trmt2b*
2010111I01Rik	*Cep78*	*Hist1h4d*	*Noa1*	*Rpl12*	*Tsc22d1*
2500004C02Rik	*Cers4*	*Ift74*	*Nod1*	*Rpl37*	*Ttc13*
3110009E18Rik	*Cgrrf1*	*Ints3*	*Nt5c2*	*Rpn1*	*Unc119*
4632415L05Rik	*Chid1*	*Ints9*	*Oplah*	*Rps19-ps3*	*Urb1*
4833418N02Rik	*Creld1*	*Ipmk*	*Ovgp1*	*Rundc3b*	*Utp4*
4930402H24Rik	*Creld2*	*Ipp*	*Oxsm*	*Sel1l3*	*Vmac*
6030419C18Rik	*Cwc27*	*Itga10*	*P2rx7*	*Selenoi*	*Vps37b*
A430033K04Rik	*Cyp4v3*	*Kcnk13*	*Pacs2*	*Slamf1*	*Wdr62*
A530072M11Rik	*Dbp*	*Kctd1*	*Pcgf3*	*Slc12a3*	*Xpnpep3*
Adam15	*Dcxr*	*Kctd17*	*Pde6d*	*Slc12a5*	*Xrn2*
AI504432	*Dedd2*	*Kifc5b*	*Pde8a*	*Slc17a9*	*Zc3h12b*
Aldh1l2	*Dip2a*	*Ldhd*	*Pfkfb1*	*Slc25a1*	*Zdhhc20*
Arid3b	*Dirc2*	*Lrp11*	*Pfkfb4*	*Slc2a8*	*Zdhhc7*
Arl6ip4	*Dnajb11*	*Lrpap1*	*Pgp*	*Slc30a4*	*Zfp112*
Asphd1	*Dqx1*	*Lta*	*Pi4k2a*	*Spast*	*Zfp128*
Atg10	*Dscr3*	*Mapre3*	*Pik3ip1*	*Spata24*	*Zfp229*
Atp9a	*Eif2b4*	*Marf1*	*Plk2*	*Ssbp2*	*Zfp236*
Atrn	*Emsy*	*Mccc2*	*Ppard*	*St3gal1*	*Zfp280c*
Atxn2	*Ergic1*	*Med26*	*Ppm1d*	*Stxbp4*	*Zfp292*
Baiap2	*Evi5*	*Mettl22*	*Ppm1l*	*Susd2*	*Zfp39*
BC051142	*Fam120c*	*Mettl23*	*Ppp1r35*	*Suv39h2*	*Zfp438*
Begain	*Fam241a*	*Mfsd1*	*Ppp2r1b*	*Taf3*	*Zfp446*
Bloc1s4	*Fbf1*	*Mfsd2a*	*Praf2*	*Tbl1x*	*Zfp568*
Bmt2	*Fchsd1*	*Mlkl*	*Prelid3b*	*Tfcp2*	*Zfp729a*
Btbd18	*Flot1*	*Mrpl33*	*Prkar2a*	*Timd2*	*Zfp943*
Camk2a	*Fndc10*	*Mterf3*	*Prmt6*	*Tmem165*	*Zfyve21*
Cars	*Gabbr1*	*Mturn*	*Psph*	*Tmem71*	*Znrf1*
Ccdc85b	*Galnt7*	*Mzt2*	*Ptger1*	*Tomm6os*	*Zscan22*
	Gfm2		*Pycr1*		*Zscan26*

Table AIII. AHR-dependent butyrate regulated genes. 195 identified genes which were significantly differentially expressed after butyrate-supplementation in *Mb1*$^{cre/+}$ mice, once baseline transcriptional changes between control *Mb1*$^{cre/+}$ mice versus *Ahr*$^{fl/-}$*Mb1*$^{cre/+}$ mice had been removed.